BNL 19302, VOL. II
ENDF-202

CROSS SECTION EVALUATION WORKING GROUP BENCHMARK SPECIFICATIONS

VOLUME II

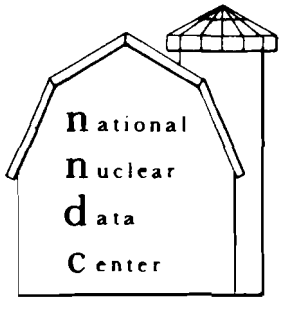

BNL 19302
(ENDF-202)

ENDF-202

CROSS SECTION EVALUATION WORKING GROUP

BENCHMARK SPECIFICATIONS

November 1974

NATIONAL NEUTRON CROSS SECTION CENTER

BROOKHAVEN NATIONAL LABORATORY

ASSOCIATED UNIVERSITIES, INC.

UNDER CONTRACT NO. AT(30-1)-16 WITH THE

UNITED STATES ATOMIC ENERGY COMMISSION

Research supported by the United States Atomic Energy Commission.

NOTICE

Printed in the United States of America

November 1974 600 copies

CROSS SECTION EVALUATION WORKING GROUP DOSIMETRY BENCHMARK COMPILATION

by

CSEWG Shielding Subcommittee

Special Applications File Subcommittee

September 1982

DOSIMETRY BENCHMARK CONTENTS

1. CFRMF

DOSIMETRY BENCHMARK NO. 1

A. Benchmark Name and Type: CFRMF (Coupled Fast Reactivity Measurements Facility), a zoned-core critical assembly with a fast neutron spectrum zone in the center of an enriched ^{235}U, water-moderated, thermal driver.

B. System Description

The CFRMF is a zoned-core critical assembly with a fast-neutron spectrum zone in the center of an enriched ^{235}U, water-moderated, thermal driver. The core is contained in a large pool about 4.5 m beneath the surface. A pictorial diagram of the CFRMF is shown in Fig. 1. Conventional plate type elements of 93.16% enriched ^{235}U clad in aluminum comprise the fuel elements in the thermal driver zone. There are 15 plates in each fuel element and 32 fuel elements in the core. Each element is 8.283 cm square and the fueled portion of the core is 60.96 cm long. Accounting for the water annulus around each fuel element, the cross sectional area occupied by each fuel element is 69.4512 cm^2. Total fuel loading is 5698.9 gm ^{235}U. The total cross sectional area of the four cruciform-shaped safety rods is 86.2837 cm^2.

The fast-filter assembly consists primarily of a large depleted uranium block (14.52 cm square x 60.96 cm long, weighing approximately 217 kg) surrounded by 0.635-cm-thick 50 wt % boral side and end plates and sealed in a 0.317-cm-thick stainless steel housing. The solid metal ^{238}U block has a 5.395-cm-diameter hole drilled through its axial center and aligned vertically with the core fuel. Concentric annular sleeves of ^{10}B and ^{235}U are slipfitted into the axial hole in the ^{238}U block. The boron sleeve has a 0.635-cm thick annulus of 90% enriched ^{10}B crystalline powder vibrocompacted to a density of 1.355 g/cm^3 and weighing 437.05 g. The enriched uranium sleeve has a 0.0889-cm-thick solid metal annulus of 93.16% enriched ^{235}U

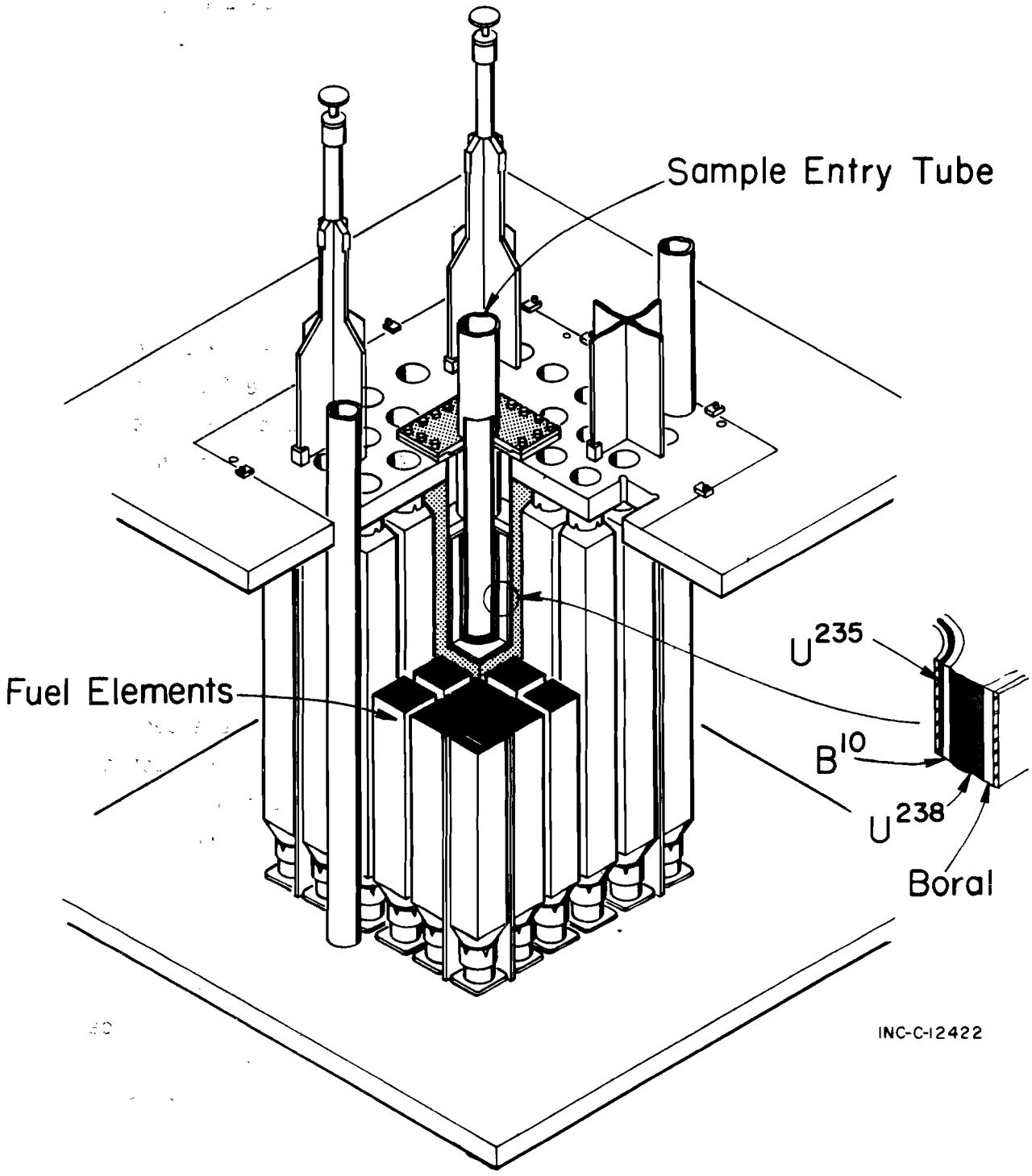

Fig. 1 Cutaway pictorial diagram showing general assembly of the CFRMF.

which weighs 1494.7 g. Both sleeves are clad with 0.0305-cm-thick stainless steel. The stainless steel access tube, with 0.147-cm-thick walls in the core region, slip fits inside the ^{235}U annulus and will accept objects with effective diameters up to 3.78 cm.

C. Model Description

1. One-Dimensional Model

A full core one-dimensional cylindrical model has been developed to represent the CFRMF. Although many features of the fast-zone assembly are rectangular in shape the cylindrical model has been found to adequately represent the CFRMF for calculation of the central neutron spectrum. Details of the one-dimensional cylindrical model are given in Table 1. A vacuum boundary condition should be applied at the outer boundary. Various regions of the model are based on conservation of material mass and the midplane areas of the CFRMF's components.

The fast filter assembly (regions 1 through 16) is represented more or less explicitly. However, details of the water reflected thermal driver (regions 17 through 22) have been substantially homogenized. The ^{10}B sleeve (regions 5 through 7) and the boral thermal neutron filter were divided in the manner shown to reduce the number of mesh points required. The region widths and mesh spacing used allow for a sufficient reduction of the flux in the peripheral regions so that any erratic flux behavior which might develop in the interior regions would have a small influence on the fluxes outside these heavily self-shielded regions. The depleted uranium block has been split into four regions so that spatially dependent cross sections can be used.

The recommended mode of calculation is one dimensional S_n transport theory using n=6. An axial buckling of 0.001769 for

TABLE 1. ONE-DIMENSIONAL CALCULATIONAL MODEL FOR THE CFRMF

Reg. No.	SCAMP Mtl. No.	Outer Radius (cm)	No. of Mesh Pts.	Material Description	Isotopes In Material	Atom Density (barn-cm)
1	1	1.91643	10	Void	--	--
2	2	2.12344	1	Dry Tube and Cladding; SSTL-304	Manganese Nickel Iron Chromium	1.7947 -3 8.1239 -3 5.80747-2 1.74285-2
3	3	2.21996	8	Uranium Sleeve; Enriched Uranium	^{235}Uranium ^{238}Uranium	4.53606-2 2.6310 -3
4	2	2.29997	1	Cladding; SSTL-304	Same as Region 2	
5	4	2.31497	10	Boron Sleeve; Enriched Boron	^{10}Boron ^{11}Boron	7.32773-2 6.8255 -3
6	4	2.63549	50	Boron Sleeve	Same as Region 5	
7	4	2.65049	10	Boron Sleeve	Same as Region 5	
8	2	2.69748	1	Cladding	Same as Region 2	
9	5	5.44437	6	Uranium Block; Depleted Uranium	^{235}Uranium ^{238}Uranium	9.334 -5 4.76476-2
10	6	6.36000	3	Uranium Block	Same as Region 9	
11	7	7.27563	3	Uranium Block	Same as Region 9	
12	8	8.19126	3	Uranium Block	Same as Region 9	

TABLE 1. (cont'd)

Reg. No.	SCAMP Mtl. No.	Outer Radius (cm)	No. of Mesh Pts.	Material Description	Isotopes In Material	Atom Density (barn-cm)
13	9	8.34126	10	Thermal Neutron Filter; Boral	Aluminum	3.61511-2
					^{10}Boron	6.95051-3
					^{11}Boron	2.81886-2
					Carbon	8.7848 -3
14	9	8.82084	10	Thermal Neutron Filter	Same as Region 13	
15	9	8.97084	10	Thermal Neutron Filter	Same as Region 13	
16	2	9.32910	1	Assembly Container; SSTL-304	Same as Region 2	
17	10	9.40362	1	Water (18°C)	Hydrogen	6.67621-2
					Oxygen	3.33810-2
18	11	9.96967	2	Side Plates and Reactor Fuel	Hydrogen	2.24398-2
					Oxygen	1.12199-2
					Aluminum	3.99175-2
					^{235}Uranium	5.64413-5
					^{238}Uranium	3.3542-6
19	12	18.80724	18	Homogenized Reactor Fuel	Hydrogen	4.25589-2
					Oxygen	2.12794-2
					Aluminum	2.16756-2
					^{235}Uranium	1.22423-4
					^{238}Uranium	7.2752 -6

TABLE 1. (cont'd)

Reg. No.	SCAMP Mtl. No.	Outer Radius (cm)	No. of Mesh Pts.	Material Description	Isotopes In Material	Atom Density (barn-cm)
20	13	27.10884	17	Homogenized Reactor Fuel and Control Rod Followers	Hydrogen	4.15815-2
					Oxygen	2.07907-2
					Aluminum	2.24869-2
					^{235}Uranium	1.02190-4
					^{238}Uranium	6.0735 -6
21	14	28.69351	3	Homogenized Reactor Fuel	Hydrogen	4.58562-2
					Oxygen	2.29281-2
					Aluminum	1.87558-2
					^{235}Uranium	8.08407-5
					^{238}Uranium	4.8051 -6
22	10	43.69351	15	Reflector; Water	Same as Region 17	

all regions and groups should be used. An energy sturcture with 0.25 lethargy spacing between 0.414 eV and 20.0 MeV is suitable for generation of multigroup representations of the central flux spectrum.

2. Two-Dimensional Model

A detailed description of a two-dimensional (r,z) model is given in references 2 and 5.

D. Experimental Data

1. Fission-Rate Ratios at Core Center

Reaction Nuclides	Fission-Rate Ratio
$^{232}Th/^{235}U$	0.0130 ± 3.0%
$^{238}U/^{235}U$	0.0490 ± 1.4%
$^{237}Np/^{235}U$	0.354 ± 2.3%
$^{239}Pu/^{235}U$	1.145 ± 1.5%

2. Spectrum-Averaged Cross Sections at Core Center

a. Non-Fission Dosimeters

Reaction	Integral Cross Section (mb)
$^{6}Li(n,He)$	942.1 ± 2.9%
$^{10}B(n,He)$	1850. ± 3.6%
$^{27}Al(n,p)^{24}Na$	0.863 ± 3.4%
$^{27}Al(n,\alpha)^{27}Mg$	0.1596 ± 3.0%
$^{45}Sc(n,\gamma)^{46}Sc$	23.2 ± 3.3%
$^{46}Ti(n,p)^{46}Sc$	2.58 ± 3.4%

a. Non-Fission Dosimeters (cont'd)

Reaction	Integral Cross Section (mb)
$^{47}Ti(n,p)^{47}Sc$	4.12 ± 4.8%
$^{48}Ti(n,p)^{48}Sc$	0.0680 ± 3.4%
$^{54}Fe(n,p)^{54}Mn$	17.2 ± 2.9%
$^{58}Fe(n,\gamma)^{59}Fe$	6.04 ± 3.1%
$^{59}Co(n,\gamma)^{60}Co$	90.4 ± 3.6%
$^{58}Ni(n,p)^{58}Co$	23.8 ± 2.9%
$^{63}Cu(n,\gamma)^{64}Cu$	43.3 ± 6.2%
$^{115}In(n,n')^{115m}In$	50.6 ± 3.9%
$^{115}In(n,\gamma)^{116m}In$	269. ± 3.7%
$^{197}Au(n,\gamma)^{198}Au$	419. ± 2.9%

b. Fissionable Dosimeters

Reaction	Integral Cross Section (mb)
$^{232}Th(n,f)$	19.6 ± 5.2%
$^{232}Th(n,\gamma)$	290. ± 3.8%
$^{235}U(n,f)$	1538. ± 3.1%
$^{238}U(n,f)$	75.1 ± 3.3%
$^{238}U(n,\gamma)$	217. ± 3.7%
$^{237}Np(n,f)$	548. ± 3.3%
$^{239}Pu(n,f)$	1792. ± 2.2%

c. Higher Actinides

Reaction	Integral Cross Section (mb)
$^{240}Pu(n,f)$	573. ± 4%
$^{242}Pu(n,\gamma)$	146 ± 15%

c. Higher Actinides (cont'd)

Reaction	Integral Cross Section (mb)
$^{242}Pu(n,f)$	557 ± 10%
$^{241}Am(n,\gamma)$	1550 ± 3.5%
$^{241}Am(n,f)$	450 ± 6.2%
$^{243}Am(n,\gamma)$	895 ± 4.8%
$^{243}Am(n,f)$	353 ± 6.1%

d. Fission-Product Nuclides: Neutron Capture

Nuclide	Integral Cross Section (mb)
^{87}Rb	12 ± 10%
^{98}Mo	56.4 ± 6.4%
^{100}Mo	55 ± 17%
^{99}Tc	267 ± 15%
^{102}Ru	88.9 ± 6.6%
^{104}Ru	82.6 ± 6.3%
^{108}Pd	144. ± 6.7%
^{107}Ag	380 ± 19%
^{109}Ag	507 ± 10%
^{121}Sb	251 ± 8.3%
^{123}Sb	154 ± 7.0%
^{127}I	298 ± 10%
^{129}I	184 ± 6.6%
^{132}Xe	43.9 ± 7.7%
^{134}Xe	14.6 ± 6.9%
^{133}Cs	276 ± 6.6%

d. Fission-Product Nuclides: Neutron Capture (cont'd)

Nuclide	Integral Cross Section (mb)
^{137}Cs	90 ± 25%
^{139}La	17.6 ± 5.2%
^{142}Ce	18.4 ± 7.4%
^{141}Pr	73 ± 15%
^{146}Nd	58 ± 6.5%
^{148}Nd	89 ± 14%
^{150}Nd	66.6 ± 12%
^{147}Pm	641 ± 13%
^{152}Sm	277 ± 6.4%
^{151}Eu	2390 ± 5.8%
^{153}Eu	1450 ± 7.0%

3. Central Neutron Flux Spectrum

a. ^{6}Li Spectrometry

Group Number	Lower Energy (keV)	Group† Flux	Group Number	Lower Energy (keV)	Group† Flux
1	3.36	0.01655	2	4.31	0.01655
3	5.53	0.01998	4	7.10	0.02290
5	9.12	0.02494	6	11.7	0.03457
7	15.0	0.03854	8	19.3	0.04479
9	24.8	0.05849	10	31.8	0.06549
11	40.9	0.06733	12	52.5	0.08846
13	67.4	0.1367	14	86.5	0.1503
15	111.	0.1913	16	143.	0.2093

† Group Flux: Values tabulated are relative group flux per unit lethargy.

a. ^{6}Li Spectrometry (cont'd)

Group Number	Lower Energy (keV)	Group Flux	Group Number	Lower Energy (keV)	Group Flux
17	183.	0.1737	18	235.	0.1882
19	302.	0.3178	20	388.	0.3716
21	498.	0.3717	22	639.	0.3358
23	821.	0.2460	24	1050	0.1741
25	1350	0.1349	26	1740	0.1157
27	2230	0.1038	28	2870	0.07754
29	3680	0.06068	30	4720	0.03865
31	6070	0.01553	32	7790	---

b. Proton-Recoil Spectrometry

Group Number	Lower Energy (keV)	Group† Flux	Group Number	Lower Energy (keV)	Group† Flux
1	64	0.1105	2	70	0.1196
3	75	0.1255	4	80	0.1244
5	85	0.1243	6	90	0.1333
7	95	0.1456	8	100	0.1546
9	110	0.1711	10	120	0.1919
11	130	0.1988	12	140	0.1987
13	150	0.2105	14	160	0.2254
15	170	0.2326	16	180	0.2395
17	190	0.2476	18	200	0.2559
19	210	0.2639	20	220	0.2721
21	230	0.2806	22	240	0.2875
23	250	0.2917	24	260	0.2949
25	270	0.2975	26	280	0.3003
27	290	0.3029	28	300	0.3071
29	320	0.3141	30	340	0.3220

† Group flux: Values tabulated are relative group flux per unit lethargy.

b. Proton-Recoil Spectrometry (cont'd)

Group Number	Lower Energy (keV)	Group Flux	Group Number	Lower Energy (keV)	Group Flux
31	360	0.3267	32	380	0.3262
33	400	0.3231	34	420	0.3204
35	440	0.3226	36	460	0.3295
37	480	0.3348	38	500	0.3343
39	550	0.3278	40	600	0.3173
41	650	0.3029	42	700	0.2853
43	750	0.2668	44	800	0.2482
45	850	0.2349	46	900	0.2248
47	950	0.2136	48	1000	0.2003
49	1100	0.1886	50	1200	0.1797
51	1300	0.1706	52	1400	0.1626
53	1500	0.1546	54	1600	0.1467
55	1700	0.1360	56	1800	0.1259
57	1900	0.1185	58	2000	---

E. Calculated Results

Comparisons of the measured integral cross sections tabulated here to integral cross sections calculated with ENDF/B-V nuclear data are given in Refs. 1-3.

F. Comments and Documentation

1. The CFRMF Facility

A detailed description of the CFRMF is found in Refs. 4 and 5. Capable of operation at 100 kW, the CFRMF has a maximum integrated neutron flux of approximately 10^{12} n/cm^2-s in the central fast zone irradiation location. The central neutron spectrum has a mean energy of 760 keV, a median energy of 375 keV and 95% of the neutrons between 4 keV and 4 MeV.

An extensive program of measurements and calculations has been undertaken to characterize the central neutron spectrum. Active neutron spectrometry has been done with proton-recoil detectors[4-6] and with ^{6}Li-semiconductor sandwich detectors.[7] The tabulated measured spectra in the specification D.3.a and D.3.b are based on the results in Refs. 6 and 7. From a neutronics calculational standpoint, transport, Monte Carlo and resonance theory techniques have been applied.[4,5,8] Details of most of the spectrum measurements and a comparison of those measurements to neutronics calculations with ENDF/B-III and ENDF/B-IV nuclear data are given in Refs. 4-6. A comparison of the measured spectra to a spectrum derived from a neutronics calculation with ENDF/B-V nuclear data is given in Ref. 1.

A sensitivity and uncertainty analysis has been done for the CFRMF. This work is documented in Refs. 9 and 10. In this study the AMPX[1] and FORSS[2] code systems were used to determine, for the central neutron spectrum, a flux covariance matrix related to uncertainties and correlations in the ENDF/B-V nuclear data for the materials which comprise the facility.

2. Measured Integral Data

a. Dosimeter Materials

The spectrum-averaged cross sections which are compiled in this specification were derived from integral reaction-rate measurements. Most of the dosimeter reaction-rate data were generated as part of the Interlaboratory Reaction-Rate (ILRR) Program.[13] Integral cross sections for the non-fission dosimeters (D.2.a), were derived from the updated measured integral data in Refs. 14-16 rather than from the earlier data in Refs. 17 and 18. Integral cross sections for the fissionable dosimeters (D.2.b) were

derived from the integral data in Ref. 19 for Th and in Ref. 20 for the remaining reactions.

Pertinent details concerning the derivation of these spectrum-averaged cross sections from the measured integral data are found in Ref. 1. It should be noted that the non-fission dosimeter integral cross sections include resonance self-shielding corrections as applied to the measured reaction-rate data reported in Refs. 14 and 15. The cross sections for ^{6}Li and ^{10}B helium production also include corrections for flux depression and scattering in the sample packets.[15] However, no intrinsic scattering corrections are included in the remaining non-fission reactions for the reasons given in Ref. 17. The integral cross-section derivation is based on a flux transfer using the $^{239}Pu(n,f)$ reaction and the NBS ^{252}Cf source as suggested by Grundl et al.[21] The flux transfer is based on a measured spectrum-averaged cross section of 1800 mb $\pm$ 2.2% for ^{239}Pu in the ^{252}Cf neutron field;[14] computed $^{239}Pu(n,f)$ integral cross sections of 1789 mb and 1781 mb in the ^{252}Cf and CFRMF neutrons fields, respectively;[14] and a measured integral reaction rate of ($14.23 \times 10^{-14} \pm$ 1.6%) fissions/sec-nucleus for $^{239}Pu(n,f)$ in the CFRMF HEDL-VI irradiation.[20] An integral flux value of 7.94×10^{10} n/cm^2-sec $\pm$ 2.7% was determined for the HEDL-VI irradiation.

Older compilations of spectrum-averaged cross sections for these dosimeter reactions are found in Refs. 22 and 23. Differences between the dosimeter integral cross sections in this specification and those in Refs. 22 and 23 are discussed in Ref. 1.

The core center fission-rate ratios (D.1) were taken from Ref. 24.

b. Fission-Product and Higher Actinide Materials

Spectrum-averaged cross sections for the fission products, as tabulated here under D.2.d, are based on the integral data reported in Ref. 25. This compilation[25] provides an update to the fission-product integral data reported in Ref. 8. The higher actinide integral cross sections tabulated here in D.2.c are based on the integral data reported in Refs. 26-27. The americium integral data in Ref. 27 update the preliminary results reported in Ref. 26.

REFERENCES

1. R. A. Anderl, D. A. Millsap, J W Rogers, Y. D. Harker, "INEL Integral Data Testing Report for ENDF/B-V Dosimeter Cross Sections," USDOE Report EGG-PHYS-5608, Idaho National Engineering Laboratory (October 1981).

2. R. A. Anderl, D. A. Millsap, J W Rogers, Y. D. Harker, "Addendum to Integral Data Testing Report for ENDF/B-V Dosimeter Cross Sections," to be published as USDOE Report EGG-PHYS-5668, Idaho National Engineering Laboratory (1982).

3. R. A. Anderl, "INEL Integral Data-Testing Report for ENDF/B-V Fission Product and Actinide Cross Sections," USDOE Report EGG-PHYS-5406, Idaho National Engineering Laboratory (April, 1980).

4. J W Rogers, D. A. Millsap and Y. D. Harker, "CFRMF Neutron Field Flux Spectral Characterization," Nucl. Tech. 25, 330 (1975).

5. J W Rogers, D. A. Millsap and Y. D. Harker, "The Coupled Fast Reactivity Measurements Facility (CFRMF)," in Proc. of IAEA Consultants Meeting on Integral Cross-Section Measurements for Reactor Dosimetry, IAEA, Vienna, Austria, November 15-19, 1976, IAEA-208, vol. II, 117 (1976).

6. J W Rogers et al., "Reactor Dosimetry Studies at the Coupled Fast Reactivity Measurements Facility (CFRMF)," in Proc. 2nd ASTM-EURATOM Symposium on Reactor Dosimetry, Palo Alto (1977), NUREG/CP-004, vol. 3, 1237 (1978).

7. G. Deleeuw-Gierts et al., "Neutron Spectrum Measurements in CFRMF by ^{6}Li Spectrometry," USDOE Report TREE-1358 (1979).

8. Y. D. Harker, J W Rogers and D. A. Millsap, "Fission-Product and Reactor Dosimetry Studies at Coupled Fast Reactivity Measurements Facility," USDOE Report TREE-1259, Idaho National Engineering Laboratory (1978).

9. J. M. Ryskamp, R. A. Anderl, B. L. Broadhead, W. E. Ford, III, J. L. Lucius, J. H. Marable, and J. J. Wagschal, "Sensitivity and a priori Uncertainty Analysis of the CFRMF Central Flux Spectrum," USDOE Report, EGG-PHYS-5243, Idaho National Engineering Laboratory (1980).

10. J. M. Ryskamp, R. A. Anderl, B. L. Broadhead, W. E. Ford III, J. L. Lucius, J. H. Marable, and J. J. Wagschal, "Sensitivity and Uncertainty Analysis of the CFRMF Central Flux Spectrum," accepted for publication in Nuclear Technology.

11. N. M. Green, W. E. Ford, III, et al., "AMPX: A Modular Code System for Generating Coupled Neutron-Gamma Libraries from ENDF/B," USDOE Report ORNL/TM-3706, Oak Ridge National Laboratory (1976).

12. J. L. Lucius, C. R. Weisbin, J. H. Marable, J. D. Drischler, R. Q. Wright, and J. E. White, "A User's Manual for the FORSS Sensitivity and Uncertainty Analysis Code System," USDOE Report, ORNL-5316, Oak Ridge National Laboratory (1977).

13. W. N. McElroy and L. S. Kellogg, "Fuels and Materials Reactor Dosimeter Data Development and Testing," Nuc. Tech. 25, 180 (1975).

14. R. C. Greenwood et al., "Radiometric Reaction-Rate Measurements in CFRMF and BIG-10," in Proc. 2nd ASTM-EURATOM Symposium on Reactor Dosimetry, Palo Alto (1977), NUREG/CP-004, Vol. 3, 1207 (1978).

15. H. Farrar IV, B. M. Oliver and E. P. Lippincott, "Helium Generation Reaction Rates for ^{6}Li and ^{10}B in Benchmark Facilities," in Dosimetry Methods for Fuels, Cladding and Structural Materials, H. Rottger, ed., Proc. Third ASTM-Euratom Symposium on Reactor Dosimetry, Ispra, Italy, October 1-5, 1979, EUR 6813 EN-FR, Vol. 1, pp. 552-570 (1980).

16. Private communication B. M. Oliver to E. P. Lippincott (November 20, 1981).

17. R. C. Greenwood et al., "Nonfission Reaction Rate Measurements," Nucl. Tech. 25, 274 (1975).

18. H. Farrar IV, W. N. McElroy, and E. P. Lippincott, "Helium Production Cross Section of Boron for Fast Reactor Neutron Spectra," Nuc. Tech. 25, 305 (1975).

19. R. A. Anderl and Y. D. Harker, "Measurement of the Integral Capture and Fission Cross Sections for ^{232}Th in the CFRMF," in Proc. International Conference on Nuclear Cross Sections for Technology, Knoxville, Tennessee, October 22-26, 1979, NBS Special Publication 594 (September, 1980) 475.

20. J. A. Grundl et al., "Measurement of Absolute Fission Rates," Nuc. Tech. 25, 237 (1975).

21. J. A. Grundl and C. M. Eisenhauer, "Fission Spectrum Neutrons for Cross Section Validation and Neutron Flux Transfer," in Proc. Conf. on Nuclear Cross Sections and Technology, NBS Special Publication 425, Vol I, p. 270 (1975).

22. A. Fabry et al., "Review of Microscopic Integral Cross-Section Data in Fundamental Reactor Dosimetry Benchmark Neutron Fields," in Proc. Consultants Meeting on Integral Cross-Section Measurement in Standard Neutron Fields for Reactor Dosimetry," International Atomic Energy Agency, Vienna (1976), IAEA-208, vol. 1, 233 (1976).

23. "Preliminary Recommendations by ILRR Program Participants," in Interlaboratory Reaction Rate Programs 12th Progress Report, HEDL-TME 79-58, p. HEDL-33 (1979).

24. D. M. Gilliam and J W Rogers, "Fission Cross-Section Ratios for U-233, Th-232, and Pu-240 in CFRMF and Preparation for Absolute Fission Counting at 100 kW," contribution to Interlaboratory Reaction Rate Program 12th Progress Report, HEDL-TME 79-58, pp. NBS-57 to NBS-68 (1979).

25. Y. D. Harker and R. A. Anderl, "Integral Cross-Section Measurements on Fission Products in Fast Neutron Fields," in Proc. Specialists' Meeting on Neutron Cross Sections of Fission Product Nuclei, Bologna, Italy, December 12-14, 1979, NEANDC(E)-209"L", 5 (1980).

26. Y. D. Harker, R. A. Anderl, E. H. Turk, and N. C. Schroeder, "Integral Measurements for Higher Actinides in CFRMF," in Proc. International Conference on Nuclear Cross Sections for Technology, Knoxville, Tennessee, October 22-26, 1979, NBS Special Publication 594 (September, 1980) 548.

27. R. A. Anderl and N. C. Schroeder, "Integral Capture and Fission Cross Sections for ^{241}Am and ^{243}Am in the CFRMF," to be published as USDOE Report EGG-PHYS-5691, Idaho National Engineering Laboratory (1982).

APPENDIX

This appendix to the benchmark specification for the CFRMF contains a tabulation of a point-wise, free-field spectrum for the central neutron field. The spectrum, tabulated according to the ENDF/B TAB1 format, corresponds to relative point-wise fluxes per eV for each of the 621 energy bounds of the 620-group energy structure. This fine-group spectrum was derived from a broad group spectrum which was generated by a transport calculation using a P1-S6 approximation and ENDF/B-V nuclear data in the filter assembly. Details about the broad-group neutronics calculation are given in Ref. 2 and details concerning the interpolation scheme for generating the fine-group spectrum are given in Ref. 1.

TABLE A-1. ENDF/B-V CENTRAL NEUTRON SPECTRUM FOR CFRMF, POINT FLUX PER EV, SAND-II 621 POINT ENERGY TABLE, ENDF/B TAB1 FORMAT.

1	4	1 621	1 2
1.0000E-04 0.	1.0500E-04 0.	1.1000E-04 0.	3
1.1500E-04 0.	1.2000E-04 0.	1.2750E-04 0.	4
1.3500E-04 0.	1.4250E-04 0.	1.5000E-04 0.	5
1.6000E-04 0.	1.7000E-04 0.	1.8000E-04 0.	6
1.9000E-04 0.	2.0000E-04 0.	2.1000E-04 0.	7
2.2000E-04 0.	2.3000E-04 0.	2.4000E-04 0.	8
2.5500E-04 0.	2.7000E-04 0.	2.8000E-04 0.	9
3.0000E-04 0.	3.2000E-04 0.	3.4000E-04 0.	10
3.6000E-04 0.	3.8000E-04 0.	4.0000E-04 0.	11
4.2500E-04 0.	4.5000E-04 0.	4.7500E-04 0.	12
5.0000E-04 0.	5.2500E-04 0.	5.5000E-04 0.	13
5.7500E-04 0.	6.0000E-04 0.	6.3000E-04 0.	14
6.6000E-04 0.	6.9000E-04 0.	7.2000E-04 0.	15
7.6000E-04 0.	8.0000E-04 0.	8.4000E-04 0.	16
8.8000E-04 0.	9.2000E-04 0.	9.6000E-04 0.	17
1.0000E-03 0.	1.0500E-03 0.	1.1000E-03 0.	18
1.1500E-03 0.	1.2000E-03 0.	1.2750E-03 0.	19
1.3500E-03 0.	1.4250E-03 0.	1.5000E-03 0.	20
1.6000E-03 0.	1.7000E-03 0.	1.8000E-03 0.	21
1.9000E-03 0.	2.0000E-03 0.	2.1000E-03 0.	22
2.2000E-03 0.	2.3000E-03 0.	2.4000E-03 0.	23
2.5500E-03 0.	2.7000E-03 0.	2.8000E-03 0.	24
3.0000E-03 0.	3.2000E-03 0.	3.4000E-03 0.	25
3.6000E-03 0.	3.8000E-03 0.	4.0000E-03 0.	26
4.2500E-03 0.	4.5000E-03 0.	4.7500E-03 0.	27
5.0000E-03 0.	5.2500E-03 0.	5.5000E-03 0.	28
5.7500E-03 0.	6.0000E-03 0.	6.3000E-03 0.	29
6.6000E-03 0.	6.9000E-03 0.	7.2000E-03 0.	30
7.6000E-03 0.	8.0000E-03 0.	8.4000E-03 0.	31
8.8000E-03 0.	9.2000E-03 0.	9.6000E-03 0.	32
1.0000E-02 0.	1.0500E-02 0.	1.1000E-02 0.	33
1.1500E-02 0.	1.2000E-02 0.	1.2750E-02 0.	34

TABLE A-1. (CONTINUED).

1.3500E-02	0.	1.4250E-02	0.	1.5000E-02	0.	35
1.6000E-02	0.	1.7000E-02	0.	1.8000E-02	0.	36
1.9000E-02	0.	2.0000E-02	0.	2.1000E-02	0.	37
2.2000E-02	0.	2.3000E-02	0.	2.4000E-02	0.	38
2.5500E-02	0.	2.7000E-02	0.	2.8000E-02	0.	39
3.0000E-02	0.	3.2000E-02	0.	3.4000E-02	0.	40
3.6000E-02	0.	3.8000E-02	0.	4.0000E-02	0.	41
4.2500E-02	0.	4.5000E-02	0.	4.7500E-02	0.	42
5.0000E-02	0.	5.2500E-02	0.	5.5000E-02	0.	43
5.7500E-02	0.	6.0000E-02	0.	6.3000E-02	0.	44
6.6000E-02	0.	6.9000E-02	0.	7.2000E-02	0.	45
7.6000E-02	0.	8.0000E-02	0.	8.4000E-02	0.	46
8.8000E-02	0.	9.2000E-02	0.	9.6000E-02	0.	47
1.0000E-01	3.2372E-11	1.0500E-01	3.1013E-11	1.1000E-01	2.9777E-11	48
1.1500E-01	2.8648E-11	1.2000E-01	2.7613E-11	1.2750E-01	2.6212E-11	49
1.3500E-01	2.4967E-11	1.4250E-01	2.3853E-11	1.5000E-01	2.2850E-11	50
1.6000E-01	2.1660E-11	1.7000E-01	2.0610E-11	1.8000E-01	1.9671E-11	51
1.9000E-01	1.8816E-11	2.0000E-01	1.8035E-11	2.1000E-01	1.7317E-11	52
2.2000E-01	1.6655E-11	2.3000E-01	1.6042E-11	2.4000E-01	1.5473E-11	53
2.5500E-01	1.4693E-11	2.7000E-01	1.3987E-11	2.8000E-01	1.3553E-11	54
3.0000E-01	1.2760E-11	3.2000E-01	1.2054E-11	3.4000E-01	1.1420E-11	55
3.6000E-01	1.0849E-11	3.8000E-01	1.0330E-11	4.0000E-01	9.8572E-12	56
4.2500E-01	9.3229E-12	4.5000E-01	8.8528E-12	4.7500E-01	8.4383E-12	57
5.0000E-01	8.0705E-12	5.2500E-01	7.7421E-12	5.5000E-01	7.4475E-12	58
5.7500E-01	7.1817E-12	6.0000E-01	6.9410E-12	6.3000E-01	6.6807E-12	59
6.6000E-01	6.4471E-12	6.9000E-01	6.2365E-12	7.2000E-01	6.0457E-12	60
7.6000E-01	5.8178E-12	8.0000E-01	5.6155E-12	8.4000E-01	5.4350E-12	61
8.8000E-01	5.2729E-12	9.2000E-01	5.1266E-12	9.6000E-01	4.9940E-12	62
1.0000E+00	4.8733E-12	1.0500E+00	3.8166E-12	1.1000E+00	1.1720E-11	63
1.1500E+00	3.7858E-11	1.2000E+00	5.7039E-11	1.2750E+00	7.0408E-11	64
1.3500E+00	8.4486E-11	1.4250E+00	1.8239E-10	1.5000E+00	3.1507E-10	65
1.6000E+00	3.3598E-10	1.7000E+00	3.7143E-10	1.8000E+00	6.9314E-10	66
1.9000E+00	1.4528E-09	2.0000E+00	1.6790E-09	2.1000E+00	1.6933E-09	67
2.2000E+00	2.1184E-09	2.3000E+00	2.8321E-09	2.4000E+00	5.5033E-09	68
2.5500E+00	8.8886E-09	2.7000E+00	7.6396E-09	2.8000E+00	7.7432E-09	69
3.0000E+00	1.2437E-08	3.2000E+00	2.3365E-08	3.4000E+00	2.2921E-08	70

TABLE A-1. (CONTINUED).

3.6000E+00	1.8212E-08	3.8000E+00	3.1324E-08	4.0000E+00	6.4261E-08	71
4.2500E+00	8.0710E-08	4.5000E+00	7.0204E-08	4.7500E+00	3.9424E-08	72
5.0000E+00	8.6142E-08	5.2500E+00	1.4951E-07	5.5000E+00	7.6311E-08	73
5.7500E+00	3.9607E-08	6.0000E+00	1.8429E-08	6.3000E+00	1.7385E-08	74
6.6000E+00	1.7408E-08	6.9000E+00	1.7820E-08	7.2000E+00	4.4964E-08	75
7.6000E+00	1.1977E-07	8.0000E+00	2.3012E-07	8.4000E+00	2.2585E-07	76
8.8000E+00	2.1200E-07	9.2000E+00	4.0528E-07	9.6000E+00	6.2558E-07	77
1.0000E+01	7.2121E-07	1.0500E+01	1.0769E-06	1.1000E+01	1.6769E-06	78
1.1500E+01	1.1661E-06	1.2000E+01	6.9650E-07	1.2750E+01	1.2715E-06	79
1.3500E+01	1.8945E-06	1.4250E+01	2.2919E-06	1.5000E+01	2.5665E-06	80
1.6000E+01	1.9220E-06	1.7000E+01	2.1320E-06	1.8000E+01	2.3776E-06	81
1.9000E+01	9.2511E-07	2.0000E+01	1.4097E-07	2.1000E+01	2.4477E-07	82
2.2000E+01	1.0029E-06	2.3000E+01	1.6432E-06	2.4000E+01	2.3015E-06	83
2.5500E+01	3.6307E-06	2.7000E+01	3.5633E-06	2.8000E+01	4.6307E-06	84
3.0000E+01	6.8692E-06	3.2000E+01	5.0028E-06	3.4000E+01	1.8405E-06	85
3.6000E+01	4.1162E-07	3.8000E+01	1.2077E-06	4.0000E+01	2.7733E-06	86
4.2500E+01	4.6825E-06	4.5000E+01	5.4549E-06	4.7500E+01	7.1473E-06	87
5.0000E+01	6.8452E-06	5.2500E+01	7.6196E-06	5.5000E+01	7.1061E-06	88
5.7500E+01	5.3387E-06	6.0000E+01	7.1023E-06	6.3000E+01	4.8427E-06	89
6.6000E+01	3.0064E-06	6.9000E+01	4.5586E-06	7.2000E+01	6.0319E-06	90
7.6000E+01	4.9729E-06	8.0000E+01	6.6283E-06	8.4000E+01	9.7944E-06	91
8.8000E+01	9.8045E-06	9.2000E+01	9.3943E-06	9.6000E+01	9.0865E-06	92
1.0000E+02	5.8045E-06	1.0500E+02	2.8664E-06	1.1000E+02	4.1630E-06	93
1.1500E+02	4.4017E-06	1.2000E+02	5.7912E-06	1.2750E+02	9.4492E-06	94
1.3500E+02	9.8558E-06	1.4250E+02	9.2593E-06	1.5000E+02	9.6223E-06	95
1.6000E+02	9.2968E-06	1.7000E+02	9.3532E-06	1.8000E+02	1.4908E-05	96
1.9000E+02	8.8519E-06	2.0000E+02	3.0714E-06	2.1000E+02	6.9054E-06	97
2.2000E+02	7.6586E-06	2.3000E+02	8.4695E-06	2.4000E+02	8.4070E-06	98
2.5500E+02	8.8264E-06	2.7000E+02	7.8993E-06	2.8000E+02	7.6640E-06	99
3.0000E+02	8.5618E-06	3.2000E+02	9.4282E-06	3.4000E+02	9.4896E-06	100
3.6000E+02	8.7083E-06	3.8000E+02	7.6413E-06	4.0000E+02	7.7116E-06	101
4.2500E+02	7.7593E-06	4.5000E+02	8.0873E-06	4.7500E+02	9.2560E-06	102
5.0000E+02	1.0173E-05	5.2500E+02	9.1774E-06	5.5000E+02	8.2516E-06	103
5.7500E+02	9.2448E-06	6.0000E+02	7.6480E-06	6.3000E+02	9.5464E-06	104
6.6000E+02	8.9961E-06	6.9000E+02	5.6378E-06	7.2000E+02	7.2932E-06	105
7.6000E+02	7.8425E-06	8.0000E+02	8.3301E-06	8.4000E+02	7.5926E-06	106

TABLE A-1. (CONTINUED).

8.8000E+02	6.4862E-06	9.2000E+02	9.0363E-06	9.6000E+02	9.0292E-06	107
1.0000E+03	5.7076E-06	1.0500E+03	4.9445E-06	1.1000E+03	6.6240E-06	108
1.1500E+03	6.2720E-06	1.2000E+03	5.5659E-06	1.2750E+03	6.2818E-06	109
1.3500E+03	6.1960E-06	1.4250E+03	5.8186E-06	1.5000E+03	6.4382E-06	110
1.6000E+03	6.1563E-06	1.7000E+03	5.7333E-06	1.8000E+03	5.0217E-06	111
1.9000E+03	7.0797E-06	2.0000E+03	6.3229E-06	2.1000E+03	4.7679E-06	112
2.2000E+03	5.0527E-06	2.3000E+03	3.1178E-06	2.4000E+03	4.9079E-06	113
2.5500E+03	4.6131E-06	2.7000E+03	3.6577E-06	2.8000E+03	4.0923E-06	114
3.0000E+03	3.7442E-06	3.2000E+03	3.8476E-06	3.4000E+03	4.2867E-06	115
3.6000E+03	4.3428E-06	3.8000E+03	3.8769E-06	4.0000E+03	3.4885E-06	116
4.2500E+03	3.2290E-06	4.5000E+03	3.1208E-06	4.7500E+03	3.0157E-06	117
5.0000E+03	2.9092E-06	5.2500E+03	2.8022E-06	5.5000E+03	2.6952E-06	118
5.7500E+03	2.5915E-06	6.0000E+03	2.4955E-06	6.3000E+03	2.3892E-06	119
6.6000E+03	2.2917E-06	6.9000E+03	2.2020E-06	7.2000E+03	2.1201E-06	120
7.6000E+03	2.0397E-06	8.0000E+03	1.9918E-06	8.4000E+03	1.9705E-06	121
8.8000E+03	1.9712E-06	9.2000E+03	1.9897E-06	9.6000E+03	2.0072E-06	122
1.0000E+04	2.0168E-06	1.0500E+04	2.0194E-06	1.1000E+04	2.0131E-06	123
1.1500E+04	1.9995E-06	1.2000E+04	1.9791E-06	1.2750E+04	1.9331E-06	124
1.3500E+04	1.8716E-06	1.4250E+04	1.7979E-06	1.5000E+04	1.7146E-06	125
1.6000E+04	1.6177E-06	1.7000E+04	1.5577E-06	1.8000E+04	1.5274E-06	126
1.9000E+04	1.5212E-06	2.0000E+04	1.5416E-06	2.1000E+04	1.6040E-06	127
2.2000E+04	1.7029E-06	2.3000E+04	1.8331E-06	2.4000E+04	2.0070E-06	128
2.5500E+04	3.5045E-06	2.7000E+04	2.3852E-06	2.8000E+04	7.4434E-07	129
3.0000E+04	1.3068E-06	3.2000E+04	1.4599E-06	3.4000E+04	1.4087E-06	130
3.6000E+04	1.4181E-06	3.8000E+04	1.4772E-06	4.0000E+04	1.5778E-06	131
4.2500E+04	1.7227E-06	4.5000E+04	1.7913E-06	4.7500E+04	1.7873E-06	132
5.0000E+04	1.7203E-06	5.2500E+04	1.5990E-06	5.5000E+04	1.4955E-06	133
5.7500E+04	1.4675E-06	6.0000E+04	1.5052E-06	6.3000E+04	1.6263E-06	134
6.6000E+04	1.8209E-06	6.9000E+04	2.0065E-06	7.2000E+04	1.8032E-06	135
7.6000E+04	1.6212E-06	8.0000E+04	2.0860E-06	8.4000E+04	1.2977E-06	136
8.8000E+04	1.1675E-06	9.2000E+04	1.3039E-06	9.6000E+04	1.3889E-06	137
1.0000E+05	1.4295E-06	1.0500E+05	1.4256E-06	1.1000E+05	1.3683E-06	138
1.1500E+05	1.3064E-06	1.2000E+05	1.3284E-06	1.2750E+05	1.4395E-06	139
1.3500E+05	1.4219E-06	1.4250E+05	1.1551E-06	1.5000E+05	1.0182E-06	140
1.6000E+05	1.1892E-06	1.7000E+05	1.2336E-06	1.8000E+05	1.1938E-06	141
1.9000E+05	1.1209E-06	2.0000E+05	1.1173E-06	2.1000E+05	1.1461E-06	142

TABLE A-1. (CONTINUED).

2.2000E+05	1.1280E-06	2.3000E+05	1.0856E-06	2.4000E+05	1.0866E-06	143
2.5500E+05	1.0998E-06	2.7000E+05	1.0203E-06	2.8000E+05	9.4224E-07	144
3.0000E+05	9.9305E-07	3.2000E+05	9.3573E-07	3.4000E+05	8.9734E-07	145
3.6000E+05	8.8680E-07	3.8000E+05	8.7237E-07	4.0000E+05	7.6862E-07	146
4.2500E+05	7.0628E-07	4.5000E+05	7.0290E-07	4.7500E+05	7.0283E-07	147
5.0000E+05	6.7460E-07	5.2500E+05	6.4242E-07	5.5000E+05	6.1667E-07	148
5.7500E+05	5.9326E-07	6.0000E+05	5.6967E-07	6.3000E+05	5.4133E-07	149
6.6000E+05	5.1283E-07	6.9000E+05	4.8292E-07	7.2000E+05	4.4618E-07	150
7.6000E+05	3.9321E-07	8.0000E+05	3.5228E-07	8.4000E+05	3.2251E-07	151
8.8000E+05	3.0088E-07	9.2000E+05	2.8367E-07	9.6000E+05	2.5438E-07	152
1.0000E+06	2.2744E-07	1.1000E+06	1.8896E-07	1.2000E+06	1.5724E-07	153
1.3000E+06	1.3303E-07	1.4000E+06	1.1736E-07	1.5000E+06	1.0282E-07	154
1.6000E+06	9.2043E-08	1.7000E+06	8.5010E-08	1.8000E+06	7.6343E-08	155
1.9000E+06	6.7859E-08	2.0000E+06	6.2535E-08	2.1000E+06	5.9215E-08	156
2.2000E+06	5.6958E-08	2.3000E+06	5.5704E-08	2.4000E+06	5.4723E-08	157
2.5000E+06	4.8312E-08	2.6000E+06	4.4091E-08	2.7000E+06	4.0692E-08	158
2.8000E+06	3.7889E-08	2.9000E+06	3.5501E-08	3.0000E+06	3.3250E-08	159
3.1000E+06	3.1088E-08	3.2000E+06	2.9027E-08	3.3000E+06	2.7072E-08	160
3.4000E+06	2.5228E-08	3.5000E+06	2.3494E-08	3.6000E+06	2.1869E-08	161
3.7000E+06	2.0351E-08	3.8000E+06	1.8967E-08	3.9000E+06	1.7714E-08	162
4.0000E+06	1.6571E-08	4.1000E+06	1.5521E-08	4.2000E+06	1.4553E-08	163
4.3000E+06	1.3654E-08	4.4000E+06	1.2818E-08	4.5000E+06	1.2036E-08	164
4.6000E+06	1.1303E-08	4.7000E+06	1.0615E-08	4.8000E+06	9.9654E-09	165
4.9000E+06	9.3464E-09	5.0000E+06	8.7580E-09	5.1000E+06	8.1998E-09	166
5.2000E+06	7.6713E-09	5.3000E+06	7.1718E-09	5.4000E+06	6.7003E-09	167
5.5000E+06	6.2560E-09	5.6000E+06	5.8379E-09	5.7000E+06	5.4449E-09	168
5.8000E+06	5.0759E-09	5.9000E+06	4.7297E-09	6.0000E+06	4.4054E-09	169
6.1000E+06	4.1017E-09	6.2000E+06	3.8184E-09	6.3000E+06	3.5540E-09	170
6.4000E+06	3.3075E-09	6.5000E+06	3.0776E-09	6.6000E+06	2.8632E-09	171
6.7000E+06	2.6633E-09	6.8000E+06	2.4769E-09	6.9000E+06	2.3032E-09	172
7.0000E+06	2.1413E-09	7.1000E+06	1.9904E-09	7.2000E+06	1.8498E-09	173
7.3000E+06	1.7188E-09	7.4000E+06	1.5968E-09	7.5000E+06	1.4832E-09	174
7.6000E+06	1.3775E-09	7.7000E+06	1.2791E-09	7.8000E+06	1.1875E-09	175
7.9000E+06	1.1023E-09	8.0000E+06	1.0231E-09	8.1000E+06	9.4945E-10	176
8.2000E+06	8.8101E-10	8.3000E+06	8.1739E-10	8.4000E+06	7.5827E-10	177
8.5000E+06	7.0333E-10	8.6000E+06	6.5228E-10	8.7000E+06	6.0485E-10	178

TABLE A-1. (CONTINUED).

8.8000E+06	5.6080E-10	8.9000E+06	5.1988E-10	9.0000E+06	4.8188E-10	179
9.1000E+06	4.4660E-10	9.2000E+06	4.1385E-10	9.3000E+06	3.8345E-10	180
9.4000E+06	3.5524E-10	9.5000E+06	3.2905E-10	9.6000E+06	3.0476E-10	181
9.7000E+06	2.8223E-10	9.8000E+06	2.6133E-10	9.9000E+06	2.4194E-10	182
1.0000E+07	2.2397E-10	1.0100E+07	2.0729E-10	1.0200E+07	1.9178E-10	183
1.0300E+07	1.7738E-10	1.0400E+07	1.6402E-10	1.0500E+07	1.5163E-10	184
1.0600E+07	1.4015E-10	1.0700E+07	1.2951E-10	1.0800E+07	1.1966E-10	185
1.0900E+07	1.1055E-10	1.1000E+07	1.0212E-10	1.1100E+07	9.4324E-11	186
1.1200E+07	8.7118E-11	1.1300E+07	8.0459E-11	1.1400E+07	7.4307E-11	187
1.1500E+07	6.8624E-11	1.1600E+07	6.3377E-11	1.1700E+07	5.8532E-11	188
1.1800E+07	5.4059E-11	1.1900E+07	4.9930E-11	1.2000E+07	4.6119E-11	189
1.2100E+07	4.2600E-11	1.2200E+07	3.9351E-11	1.2300E+07	3.6352E-11	190
1.2400E+07	3.3585E-11	1.2500E+07	3.1031E-11	1.2600E+07	2.8675E-11	191
1.2700E+07	2.6500E-11	1.2800E+07	2.4494E-11	1.2900E+07	2.2643E-11	192
1.3000E+07	2.0935E-11	1.3100E+07	1.9359E-11	1.3200E+07	1.7905E-11	193
1.3300E+07	1.6563E-11	1.3400E+07	1.5324E-11	1.3500E+07	1.4181E-11	194
1.3600E+07	1.3111E-11	1.3700E+07	1.2097E-11	1.3800E+07	1.1142E-11	195
1.3900E+07	1.0246E-11	1.4000E+07	9.4090E-12	1.4100E+07	8.6297E-12	196
1.4200E+07	7.9061E-12	1.4300E+07	7.2356E-12	1.4400E+07	6.6157E-12	197
1.4500E+07	6.0433E-12	1.4600E+07	5.5155E-12	1.4700E+07	5.0292E-12	198
1.4800E+07	4.5813E-12	1.4900E+07	4.1688E-12	1.5000E+07	3.7932E-12	199
1.5100E+07	3.4583E-12	1.5200E+07	3.1592E-12	1.5300E+07	2.8914E-12	200
1.5400E+07	2.6512E-12	1.5500E+07	2.4352E-12	1.5600E+07	2.2405E-12	201
1.5700E+07	2.0649E-12	1.5800E+07	1.9060E-12	1.5900E+07	1.7620E-12	202
1.6000E+07	1.6314E-12	1.6100E+07	1.5126E-12	1.6200E+07	1.4044E-12	203
1.6300E+07	1.3057E-12	1.6400E+07	1.2156E-12	1.6500E+07	1.1332E-12	204
1.6600E+07	1.0578E-12	1.6700E+07	9.8857E-13	1.6800E+07	9.2505E-13	205
1.6900E+07	8.6668E-13	1.7000E+07	8.1300E-13	1.7100E+07	7.6357E-13	206
1.7200E+07	7.1802E-13	1.7300E+07	6.7602E-13	1.7400E+07	6.3727E-13	207
1.7500E+07	6.0149E-13	1.7600E+07	5.6845E-13	1.7700E+07	5.3791E-13	208
1.7800E+07	5.0969E-13	1.7900E+07	4.8361E-13	1.8000E+07	4.5950E-13	209

FAST REACTOR BENCHMARK CONTENTS

I. INTRODUCTION

II. CONTRIBUTORS

III. BENCHMARK SPECIFICATION FORMAT

IV. FAST REACTOR BENCHMARKS

No. F1. JEZEBEL (Revised) 11/81

F 2. VERA-11A

F 3. ZPR-3-48

F 4. ZEBRA-3

F 5. GODIVA (Revised) 11/81

F 6. VERA-1B

F 7 ZPR-3-6F

F 8. ZPR-3-11

F 9. ZPR-3-12

F 10. ZEBRA-2

F 11. ZPPR-2

F 12. ZPR-6-7

F 13. ZPR-3-56B

14. SEFOR

15. ZPR-6-6A

16. SNEAK-7A

17. SNEAK-7B

18. ZPR-9-31

19. JEZEBEL-23

20. BIG TEN

21. JEZEBEL-PU 9/11/81

22. FLATTOP-25

23. FLATTOP-PU

24. FLATTOP-23

25. THOR

CSEWG FAST REACTOR BENCHMARK COMPILATION

June 1973

Contributors

H. Alter
R. B. Kidman
R. LaBauve
R. Protsik
B. A. Zolotar

I. INTRODUCTION

The utilization of integral experiments has been widely accepted by the CSEWG community as a mechanism for validation of the ENDF/B data files. Over the past half dozen years a number of fast integral experiments have been given recognizance as CSEWG Fast Reactor Benchmarks. These benchmarks have been specified at various times by various people. These efforts are recognized as having been very worthwhile.

This report represents an attempt by the CSEWG community to systematically present specifications for the currently accepted Fast Reactor Benchmarks. Specifications for these benchmarks conform to an agreed upon format. All accepted benchmarks have been reviewed for completeness and accuracy of the experimental information. It is anticipated that from time to time additional benchmarks will be generated from now available integral experiments. With the establishment and acceptance of a standard specification format, it is believed that the problems of passing from experiment to benchmark will be minimized.

II. CONTRIBUTORS

In 1971 E. M. Pennington, ANL and J. D. Jekins, ORNL, were assigned the task of producing an acceptable standard format for specifying CSEWG Fast Reactor Benchmarks. Their success is documented in Section III.

Upon acceptance of the above standard, members of the CSEWG Data Testing Subcommittee were assigned Fast Reactor Benchmarks for re-specification according to the accepted format, and to verify wherever possible, the accuracy of the given experimental data for these benchmarks. The responsible personnel, their affiliation and the benchmarks so specified are as follows:

CSEWG BENCHMARK ASSEMBLY	RESPONSIBILITY	
JEZEBEL GODIVA	R. LaBauve	LASL
VERA-11A ZEBRA-3 VERA-1B ZEBRA-2	H. Alter*	AI
ZPR-3-48 ZPR-6-7 ZPR-6-6A	B. A. Zolotar**	ANL
ZPR-3-6F ZPR-3-11 ZPR-3-56B	R. B. Kidman ***	HEDL
ZPR-3-12 ZPPR-2 SEFOR	R. Protsik	GE

New addresses:
*Divs. of Reactor Research & Development, USAEC, Washington, D. C. 20545
**Electric Power Research Institute, 3412 Hillview Avenue, Palo Alto, CA 94304
***Los Alamos Scientific Laboratory, P. O. Box 1663, Los Alamos, New Mexico 87544

III. BENCHMARK SPECIFICATION FORMAT

CSEWG benchmark problems are intended to allow the assessment of the validity of microscopic nuclear data by comparison of integral experiments and calculations. CSEWG benchmarks should therefore be selected for usefulness and ease of calculation and representation, and should be as free as possible from effects ascribable to computational techniques and modeling.

A CSEWG benchmark should provide a logically ordered description of the system which will allow the user to determine if the problem is of interest, to set up the problem in an unambiguous fashion with a reasonable amount of effort, to compare calculated results directly to the experiment with a minimum application of correction factors, and where such factors are unavoidable, to apply correction factors in an unambiguous and clearly described fashion. The benchmark description should contain sufficient information and suitable documentation to permit the user to form an independent assessment of the validity of the calculational models described. Benchmark descriptions lacking comments and documentation in this regard are unacceptable.

In accord with the broad requirements above, the following format for benchmark specifications is required:

A. Benchmark name and type., e.g., JEZEBEL - a bare sphere of plutonium; SEFOR Doppler benchmark.

B. System Description: This should be a description in English of the physical system and the general reasons for its selection as a benchmark. The section should include, for example, specific cross section and energy range sensitivities of the system.

C. Model Description:

1. One-Dimensional Model: If at all possible, the system should be described as a one-dimensional homogeneous model.

Such a prescription should include:

a. model dimensions and a figure;

b. boundary conditions;

c. atom densities in each region in units of atoms/barns cm;

d. the perpendicular bucklings, which may be energy - and region-dependent, if the geometry is not spherical;

e. the suggested geometrical mesh description;

f. the suggested calculational method, i.e., diffusion theory, S_n with n specified, etc.;

g. the suggested energy group structure;

h. details on special calculational techniques, i.e., if central worth data are available, then the size of the region over which such a calculation is to be effective might be specified, or if resonance shielding for a particular nuclide is important, then this fact might be noted;

i. an estimate of the suitability of the simple model to represent the actual system, with some estimated uncertainty in k_{eff} ascribable to the model.

2. Other more complicated models: Two- and three-dimensional models for the system may be prescribed as outlined above. Exact specifications can be useful for those wishing to perform Monte Carlo calculations.

D. Experimental Data:

Experimental data with error estimates should be presented for all available quantities of interest. Errors should be represented as one standard deviation and so described.

Experimental data should include:

a. measured eigenvalue with error estimates. It is permissible to give correction factors to be applied to the calculated eigenvalue to allow for heterogeneous-homogeneous, transport-diffusion, 2D-1D, etc., corrections.

b. experimental spectral indices at the core center with error estimates wherever possible. Correction factors may be required to allow for heterogeneity effects.

c. material worths at the core center including error estimates wherever possible. These should be given in units of $10^{-5}\Delta$ k/k/mole. It may be necessary to give correction factors to allow for the differences between the simplified one-dimensional and actual models.

d. other quantities for optional analysis such as central activation cross sections, Doppler effects, Rossi alpha, and leakage spectra should be included. Error estimates should be given if possible. Wherever corrections are necessary to relate calculated and experimental results, detailed instructions on their application should be given together with a numerical example.

E. Calculated Results:

An optional section giving CSEWG calculated results using version N data would be helpful in establishing both model validity and data trends. Individual results should be given for specific codes and calculational procedures rather than averaged results. This allows assessment of the merits of various codes. Comments on the committee's experience with the specific benchmark could be included here.

F. Comments and Documentation:

This section should contain sufficient information to allow the user first, to comprehend the approximations inherent in the benchmark representation and how they were resolved, and second, to trace back through references the detailed calculation basis for the model. In particular, this section should cover:

a. the method used for converting the actual three-dimensional geometry to one-dimensional geometry should be briefly described, and an error estimate should be given for the process.

b. a brief description should be presented of the method for converting from heterogeneous to homogeneous regions including an error estimate.

c. some discussion should be given of any corrections which were made to experimental spectral indices and central worths for flux depressions by fission chambers, sample size effects, etc. In the case of central worths, the values of inhours per $\%\Delta k/k$ used for converting the experimental measurements should be given, along with a reference to the delayed neutron parameters involved. The persons providing the benchmark description should be aware of the fact that central worths calculated for the simpllfied 1D-system may be considerably different from those of the actual system, and that calculations to investigate this fact should be made.

d. finally, the section must include references to the sources of information presented. The references should be to published documents or papers rather than internal memoranda.

G. Limitations:

The benchmark descriptions should not require any specifications which are pertinent only to individual multigroup cross-section production codes such as MC^2 or ETOX for example. Such specifications include weighting spectra within groups, ordinary or consistent P_1 or B_1 options, etc. However, generally applicable problem qualifications, i.e., order of S_n or broad group structure, may appear as suggestions in the model description, Section C.

FAST REACTOR BENCHMARK NO. 1

A. Benchmark Name and Type

JEZEBEL, a bare sphere of plutonium.

B. Systems Description

JEZEBEL is a bare sphere of plutonium metal. The single-region, simple geometry and uniform composition conveniently facilitate calculational testing, especially for the plutonium isotope cross sections in the fission source energy range.

C. Model Description

The spherical homogeneous model has a core radius of 6.385 cm and the following composition.[1]

Isotope	Density, nuclei/b-cm
^{239}Pu	0.03705
^{240}Pu	0.001751
^{241}Pu	0.000117
Ga	0.001375

The recommended mode of calculation is one-dimensional transport theory, S_{16}, with 40 mesh intervals in the core, a vacuum boundary condition on the core boundary (6.385 cm) and a 26 energy group structure with half-lethargy unit widths and an upper energy of 10 MeV.

D. Experimental Data

1. Measured Eigenvalue: $k = 1.000 \pm 0.002$

2. Spectral Indices at Core Center

a. Central Fission Ratios[2]

$\sigma_f(^{238}U)/\sigma_f(^{235}U)$	0.2137 ± 0.0023
$\sigma_f(^{233}U)/\sigma_f(^{235}U)$	1.578 ± 0.027
$\sigma_f(^{237}Np)/\sigma_f(^{235}U)$	0.962 ± 0.016
$\sigma_f(^{239}Pu)/\sigma_f(^{235}U)$	1.448 ± 0.029

b. Central Activation Ratios[3]

Isotope	$\sigma_{n,\gamma}/\sigma_f$ (^{235}U)	Thermal Normalization Value of $\sigma_{n,\gamma}$, barns
^{51}V	0.0023 ± 0.0003	4.88 ± 0.04
^{55}Mn	0.0024 ± 0.0003	13.3 ± 0.2
^{63}Cu	0.0100 ± 0.0006	4.5 ± 0.1
^{93}Nb	0.023 ± 0.002	1.15 ± 0.05
^{197}Au	0.083 ± 0.002	98.8 ± 0.3

3. Rossi Alpha [2]

$$\alpha = -\beta_{eff}/\ell^* = -(0.64 \pm 0.01) \times 10^6 \text{sec}^{-1}$$

4. Central Reactivity Worths[4]

Material	Central Worth, 10^{-5} Δk/k/mole
H	40 ± 20
Be	30 ± 2
^{10}B	-490 ± 10
C	-14 ± 2
N	-44 ± 2
O	-19 ± 2
F	-36 ± 2
Al	-28 ± 0.2

Material	Central Worth, 10^{-5} Δk/k/mole
Ti	-51 ± 2
V	-30 ± 2
Fe	-42 ± 2
Co	-48 ± 2
Ni	-94 ± 2
Zr	-70 ± 2
Mo	-86 ± 2
Ag	-183 ± 3
Ta	-197 ± 3
W	-143 ± 3
Au	-171 ± 3
Th	-127 ± 2
^{233}U	2687 ± 27
^{235}U	1580 ± 16
^{238}U	220 ± 4
^{237}Np	1630 ± 100
^{239}Pu	3154 ± 31
^{240}Pu	2050 ± 100
^{241}Am	2070 ± 170

5. Neutron Flux Spectrum

a. Leakage Spectrum[5]

The spectrum of neutrons emitting from the surface of the core is represented below in the 1/2 lethargy group structure (E_{max} = 10 MeV) with an arbitrary normalization to the value 20 in group 4. Uncertainties are based on counting statistics alone.

Energy Group	Lower Lethargy Limit	Relative Neutron Leakage
1	0.5	3.1 ± 0.5
2	1.0	11.7 ± 0.7
3	1.5	17.7 ± 0.7
4	2.0	20.0 ± 0.8
5	2.5	16.5 ± 0.7
6	3.0	13.6 ± 0.7
7	3.5	9.7 ± 0.7

b. Central Spectrum Relative to ^{239}Pu Fission Spectrum [2b]

Deviation of the central spectrum from the ^{239}Pu fission spectrum is characterized by the following ratios of central high-energy spectral indices to the corresponding indices for the ^{239}Pu fission spectrum.

Spectral Index	Ratio of Central values to Value for ^{239}Pu Fission Spectrum
$\sigma_f(^{238}U)/\sigma_{n,p}(^{31}P)$	1.015± 0.016
$\sigma_{n,p}(^{27}Al)/\sigma_{n,p}(^{31}P)$	1.016 ± 0.020
$\sigma_{n,p}(^{56}Fe)/\sigma_{n,p}(^{31}P)$	1.033 ± 0.015
$\sigma_{n,\alpha}(^{27}Al)/\sigma_{n,p}(^{31}P)$	1.043 ± 0.022
$\sigma_{n,2n}(^{63}Cu)/\sigma_{n,p}(^{31}P)$	1.050 ± 0.030

E. Calculated Results

Calculated results may be appended to these specifications.

F. Comments and Documentation

The composition and configuration specifications were taken from Ref. 1 which also gives the uncertainty in critical mass, at the specified composition and density, as ± 0.6%.

This translates to an uncertainty in eigenvalue, at the specified composition, density, and size, of ± 0.2%.

The most accurate fission ratios for Jezebel are obtained from recent absolute-ratio measurements in Flattop-25 and Big Ten and double-ratio measurements connecting these to Jezebel. These measurements are described below.

Measurement Location	Value	Double Ratio to Jezebel	Jezebel	Reference
$\sigma_f(^{238}U)/\sigma_f(^{235}U)$				
Flattop-25	0.1479(±1.5%)	1.436(±0.6%)	0.2124(±1.6%)	2c
Big Ten	0.0373(±1.7%)	5.73(±0.8%)	0.2137(±1.9%)	2d
Van de Graaff (E_n=2.43 MeV)	0.433(±1.5%)	0.497(±0.9%)	0.2152(±1.7%)	ENDF/B-IV
		Average:	0.2137(±1.1%)	
$\sigma_f(^{233}U)/\sigma_f(^{235}U)$				
Flattop-25	1.572(±1.5%)	0.988(±0.4%)	1.553(±1.6%)	2c
Topsy	1.65(±4%)	0.988(±0.4%)	1.630(±4%)	2e
Big Ten	1.61(±2.1%)	0.999(±0.5%)	1.608(±2.2%)	prelim. value from D.M.Gilliam (1979)
		Average:	1.578(±1.7%)	

Measurement Location	Value	Double Ratio to Jezebel	Jezebel	Reference
$\sigma_f(^{237}Np)/\sigma_f(^{235}U)$				
Topsy	0.760(±4%)	1.258(±0.8%)	0.956(±4.1%)	2e
Big Ten	0.317(±2.2%)	3.046(±1.1%)	0.966(±2.5%)	2d
Van de Graaff	1.328(±2%)	0.723(±1.3%)	0.960(±2.4%)	ENDF/B-IV
(E_n = 2.43 MeV)				
		Average:	0.962(±1.7%)	
$\sigma_f(^{239}Pu)/\sigma_f(^{235}U)$				
Flattop-25	1.349(±1.5%)	1.055(±1.0%)	1.423(±1.8%)	2c
Topsy	1.42(±4%)	1.055(±1.0%)	1.498(±4.1%)	2e
Big Ten	1.198(±1.5%)	1.224(±1.2%)	1.466(±1.9%)	2d
		Average:	1.448(±2.0%)	

The central activation cross section ratios were obtained from double ratio measurements, connecting the thermal column of the LASL water boiler to the center of Jezebel, and literature values for the thermal cross sections. The data for the central activation cross sections were reported in Ref. 3. Subsequently, the thermal normalization values, and consequently the activation cross sections, have been updated by LASL.

The measured central reactivity worths were taken from Ref. 4 Corrections for sample size effects have been reevaluated by 50 group transport calculations based on ENDF/B-IV. The conversion from dollars/ mole to $(\Delta k/k)$/mole uses the factor $\beta_{eff} = 0.00190$ (the surface mass increment between delayed and prompt critical gave 0.00189, the central void coefficient gave 0.00191, and ENDF/B-IV delayed neutron data gave 0.00186).

The data listed for the leakage spectrum were derived from Ref. 5. A finer energy mesh representation for the spectrum is given in this reference along with statistical uncertainties.

REFERENCES

1. G. E. Hansen and H. C. Paxton, "Reevaluated Critical Specifications of Some Los Alamos Fast-Neutron Systems," Los Alamos Scientific Laboratory report LA-4208 (1969).

2. (a) G.E. Hansen, "Status of Computational and Experimental Correlations for Los Alamos Fast Neutron Critical Assemblies," Proc. Seminar Physics of Fast and Intermediate Reactors, Vienna, August 3-11, 1961 (IAEA, Vienna, 1962) Vol. I, pp 445-455. (b) J. A. Grundl and G. E. Hansen, "Measurement of Average Cross Section Ratios in Fundamental Fast-Neutron Spectra, "Proc. Paris Conf. Nuclear Data for Reactors (IAEA, Vienna, 1967) Vol. I, pp 321-336. (c) P. I. Amundson, A. M. Broomfield, W. G. Davey, and J. M. Stevenson, "An International Comparison of Fission Detector Standards, "Proc. Intern. Conf. Fast Critical Experiments and Their Analysis, Argonne, October 10-13, 1966 (Argonne National Laboratory report ANL-7320) pp 679-687. (d) D. M. Gilliam, "Integral Measurement Results in Standard Fields,"Proc. Intern. Specialist's Symposium Neutron Standards and Applications, Gaithersburg, March 28-31, 1977 (NBS Special Publication 493, 1977) pp 293-303. (e) G.A. Linenberger and L. L. Lowry, "Neutron Detector Traverses in the Topsy and Godiva Critical Assemblies," Los Alamos Scientific Laboratory report LA-1653 (1953).

3. C. E. Byers, "Cross Sections of Various Materials in the Godiva and Jezebel Critical Assemblies, "Nucl. Sci. Eng. 8, 608-614 (1960).

4. L. B. Engle, G. E. Hansen, and H. C. Paxton, "Reactivity Contributions of Various Materials in Topsy, Godiva, and Jezebel," Nucl. Sci. Eng. 8, 543-569 (1960).

5. L. Stewart, "Leakage Neutron Spectrum from a Bare Pu-239 Critical Assembly, "Nucl. Sci. Eng. 8, 595-597 (1960).

FAST REACTOR BENCHMARK NO. 2

A. Benchmark Name and Type

VERA-11A, a plutonium-plus-graphite assembly.

B. System Description

VERA-11A was a cylindrically shaped critical assembly fueled with plutonium and diluted with graphite. Assembly core height was 21.7 cm and the effective core diameter was 26.9 cm. The core region was surrounded by a blanket consisting of depleted uranium and stainless steel. This assembly was designed to explore the accuracy of the plutonium 239 neutron cross section data.

C. Model Description

1. One-Dimensional Model Description

A one-dimensional spherical model of VERA-11A is given in Figure 1. A vacuum boundary condition should be applied at the outer reflector boundary. Material atom densities for the core and reflector regions are given in Table 1. The standard calculation mode is an S_8 transport theory calculation using a multigroup structure composed of 26 groups, each of lethargy width equal to 0.5 and with E_{max} set to 10 MeV. The number of mesh are 40 in the core and 40 in the reflector.

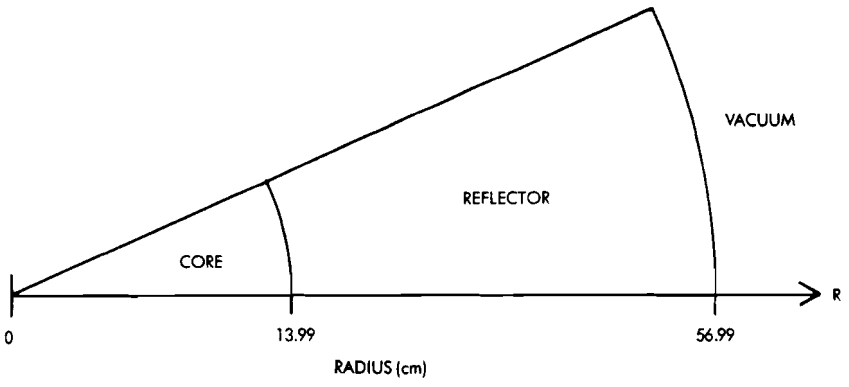

Figure 1. Spherical Model of VERA-11A Assembly

2. Two-Dimensional Model Description

A two-dimensional (R-Z) cylindrical model of the VERA-11A assembly is given in Figure 2. Zero return current boundary conditions should be applied to the top and the right side of the model; a symmetry boundary condition should be applied along the model bottom. It is suggested the assembly be calculated using a two-dimensional diffusion theory code. Suggested mesh is 40 radial and axial intervals in the core and 40 intervals for the reflector thickness.

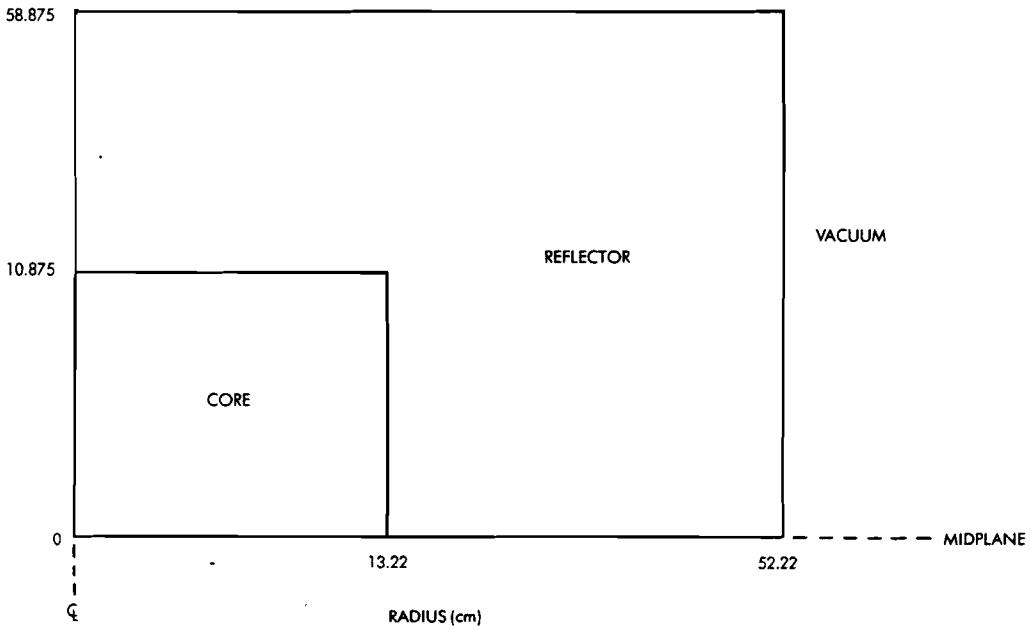

Figure 2. Two-Dimensional (R-Z) Model of VERA-11A Assembly

Table 1.

VERA-11A Region Compositions

(Atoms/Barn-cm)

Material	Core	Reflector*	
		(a)	(b)
Pu-239	0.007213	-	-
Pu-240	0.000370	-	-
Pu-241	0.000028	-	-
Ga	0.000449	-	-
C	0.046204	-	-
Fe	0.006084	0.0065	0.006582
Cr	0.001579	0.0017	0.001713
Ni	0.000665	0.00071	0.000721
Cu	0.007402	-	-
U-235	-	0.00025	0.00026
U-238	-	0.03440	0.03610
Pb	0.000035	-	-
Sn	0.000043	-	-

*Composition (a) should be used for calculations.

D. Experimental Data

1. Experimental Critical Mass — 33.81±0.06 Kg Pu-239

   Corrections for Edge Irregularities — -0.97±0.3

   Finite Fuel Plate Thickness — +1.37±0.3

   Homogeneous Cylinder Critical Mass — 34.2±0.4 Kg Pu-239

   Experimental Eigenvalue — 1.000±0.003

2. Experimental Spectral Indices at Core Center Relative to σ_f (U-235)

   σ_f (U-238) = 0.077±0.002

   σ_f (Pu-239) = 1.07±0.02

   σ_f (Pu-240) = 0.475±0.020

   σ_f (N_p-237) = 0.43±0.02

   σ_f (U-233) = 1.49±0.03

3. Material Worths at Core Center

The measured reactivity coefficients for U-235, U-238, and Pu-239 at the core center of VERA-11A were equated[3] to perturbation cross sections by normalizing to a value of 1.901 barns for U-235 calculated using the FD1 cross section library.

Material	Reactivity Coefficient, mb, (normalized to 1901 for U-235)
U-235	1901±20
U-238	24±1
Pu-239	3448±38

F. Comments and Documentations

VERA-11A was a cylindrical critical assembly fueled with plutonium and diluted with graphite. Detailed descriptions of the experimenta have not been published. Model specifications are those derived by McTaggart.[1]

The experimental critical mass is 33.81±0.06 Kg Pu-239. Corrections for edge irregularities (-0.97±0.3) and for finite fuel plate thickness (+1.37±0.3) produce a homogeneous cylindrical critical mass of 34.2±0.4 Kg Pu-239. Plates in the fuel elements in VERA-11A form continuous planes perpendicular to the axis of the cylindrical core. It was therefore possible to estimate corrections for heterogeneity ($\sim$ 1.0% in k) from infinite slab calculations. Applying a shape factor of 0.959 produces a homogeneous spherical critical mass of 32.8±0.5 Kg Pu-239, with the radius of the critical sphere equal to 13.99±0.07 cm. Experimental results were derived from results quoted by McTaggart, Baker[2] and Smith.[3] R. W. Smith[4] provided the following comment on the experiment: The correction for heterogeneity in VERA-11A is 1.37 Kg Pu-239, McTaggart of AWRE has pointed out that heterogeneity measurements on the current re-build of VERA-11A suggest a heterogeneity correction nearer 1.0 Kg Pu-239; the atom densities for lead and tin arise from the solder in the plutonium can; a figure of 95±15 p.p.m. of hydrogen in the graphite has been suggested to allow for possible moisture content in the graphite, the effect of this moisture or k_{eff} for VERA-11A is about +0.03% $\Delta k/k$.

The estimated correction to the S_8 eigenvalue for the "S_∞" is -0.0024. For example, if the transport theory, $k_{eff}(S_8)$, result was 0.9990, then the $k_{eff}(S_\infty)$ result would be 0.9990-0.0024 = 0.9876.

REFERENCES

1. M. H. McTaggart, Internal Report VERA/OP113, (January 1967).
2. A. R. Baker, "Comparative Studies of the Criticality of Fast Critical Assemblies," Proc. of International Conf. in Fast Critical Experiments and Their Analysis, ANL-7320 (1966)
3. R. D. Smith, et al, "Fast Reactor Physics Including Results from U. K. Zero Power Reactors," Proc. 3rd Int. Conf. Peaceful Uses of Atomic Energy, 6 pg 166, IAEA (1964)
4. Private Communication, R. W. Smith (UKAEA) to H. Alter, (Nov. 1970).

FAST REACTOR BENCHMARK NO. 3

A) ZPR-3 Assembly 48 - A Plutonium Fueled Fast Critical Assembly

B) System Description

The ZPR-3 consists of two halves, each a horizontal matrix of 2.2 in. square stainless steel tubes into which are loaded perforated stainless steel drawers containing fuel and diluent materials of various types. Assembly 48 was a small (400 liter) fast critical assembly with a soft spectrum and other characteristic representative of current LMFBR designs. The drawers contained plates of plutonium, Pu/U/Mo alloy, sodium, depleted uranium, and graphite. The atomic ratio of uranium to plutonium was approximately 4:1, with the ^{240}Pu isotopic fraction of 6%. The L/D ratio was approximately unity and the blanket was 12 in. of depleted uranium.[1] Figure 1 shows the loading of a core drawer as well as several other special drawers. Figures 2 and 3 show the cross sectional views of the as-built reference assembly, which had an excess reactivity of 61 Ih. The equivalent cylindricalized representation of the as-built reference assembly is shown in Fig. 4.

C) Model Description

1. One-Dimensional Model: A one-dimensional model with spherical geometry has been used in the analysis of many measurements in this assembly. The spherical homogeneous model was defined with reference to a two-dimensional finite cylindrical, heterogeneous model which will be described in Section C.2, and a spherical, heterogeneous model. The radius of the core in the spherical, heterogeneous model was chosen such that the multiplication constant was the same as for the two-dimensional model. The spherical, homogeneous model used the same core radius as the spherical heterogeneous model. The resulting core

radius and blanket thickness were 45.245 cm and 30.0 cm, respectively. The appropriate compositions for use with the spherical model are given in Table I.

An energy group structure with 27 energy groups, as given in Table II, is suggested. Such a structure has sufficient detail at low energies to afford accurate computations of material worths and Doppler effects.

Because of the simplicity of the two-region, homogeneous spherical model the macroscopic flux distributions across the reactor may be computed with diffusion theory, and a relatively coarse mesh of 2 cm should be adequate.

Central material reactivity worths and Doppler reactivity worths may be computed by perturbation theory. If the material sample is optically thin and if the material is contained in the core, the homogeneous core cross section for the material are fairly appropriate to the sample. If the material sample is optically thin and if the material is not contained in the core, then infinite dilution cross sections are appropriate for the sample.

The major flaw in the homogeneous spherical model for this geometrically simple system is in the neglect of heterogeneities in the unit cell. Sections D and F indicate the uncertainties arising from the use of homogeneous cross sections. The error in material worth or Doppler worth introduced by flux distortions depends strongly upon the nature of the sample.

2. Other More Complicated Models: A two-dimensional finite cylindrical representation of the system is closer to the physical configuration than a spherical representation. In defining the finite cylindrical

model, the as-built loading was corrected for excess reactivity, edge smoothing, spiking of the control and safety rods with extra fuel and for the stainless steel interface between the halves of the assembly. The resulting region dimensions and compositions for the zero-excess reactivity, heterogeneous, two-dimensional model are given in Tables III and IV, respectively.

D) Experimental Data

1. Measured Eigenvalues: The measured eigenvalue corresponding to the models of Section C is 1.000 ± 0.001. Calculations indicate a 0.0183 heterogeneity correction.[2]

2. Unit-Cell Reaction Rates: Foils of enriched uranium and depleted uranium were irradiated at the center of Assembly 48 to obtain ratios of capture and fission in ^{238}U to fission in ^{235}U. The foils, 0.39 in. in diam by 0.01 in. thick were wrapped in aluminum foil for placement between plates at 12 locations in the unit cell. The fission and capture activations were determined by radiochemical methods.[3]

Table V gives the cell-averaged values of the capture and fission ratios obtained from these measurements together with the heterogeneity correction. To be clear, these unit-cell reaction rate values correspond to the reactions actually taking place in the unit-cell in the assembly, and not, for example, to a cell-average defined as the value of the flux at every point in the cell multiplied by the cross section of the foil material. We use the term to refer to the flux and volume weighted reaction rates as they actually occur in the unit-cell. Hence, a per atom unit-cell reaction rate ratio is converted to the actual

ratio of the number of reactions taking place in the cell simply by multiplying the former ratio by the appropriate atom density ratio.

3. Material Worth at the Center of the Core: Central reactivity worths of several heavy and structural materials were measured in a small diameter (0.45 in.) steel carrier cylinder. The reactivity of the carrier with a sample as compared on empty carrier was obtained from the change in position of the autorod. The plutonium and uranium samples were clad annuli while the structural material samples were generally 0.42 in. cylinders. Table VI gives the experimental worths of several isotopes together with the results of calculations using the homogeneous, spherical model.

E) Calculated Results

The calculations described in this section were made using ENDF/B-III data and the standard one-dimensional, homogeneous spherical model of the assembly. The fundamental mode option of the SDX[4] code was used to compute homogeneous cross sections. This model yielded a multiplication constant of 0.9744 for the critical. The addition of the heterogeneity and the transport corrections gives a k_{eff} of 0.9999.

Table VII gives the comparison of the multiplication constant, reaction rate ratios and several central worths computed with several models. First-order perturbation theory was used in the central worth calculations.

F) Comments and Documentation

To assess the limitations of the homogeneous, spherical Benchmark model, the multiplication constant, reaction rate ratios and central reactivity worths

were calculated with a one-dimensional spherical heterogeneous model and with a two-dimensional finite cylindrical model. In this way, the errors arising from homogenization can be separated from the errors arising from the simplified geometric representation. The heterogeneous cross sections were computed with the plate unit cell option of the SDX code, which uses the NR approximation to obtain resonance cross sections and integral transport methods to obtain spatial weighting factors. The model used to represent the unit cell in these SDX problems as described in Ref. 5.

The results of calculations with the three models are compared in Table VII. The one-dimensional and the two-dimensional heterogeneous models are in good agreement. From comparison of the spherical homogeneous and heterogeneous results, heterogeneities account for a difference of about 1.8% in the multiplication constant and differences up to 10% in the central worths. For the central worth measurements, the conversion factor 1% $\Delta k/k$ = 981 Ih was used to convert the measured periods to the desired reactivity units. The delayed neutron data of Keepin[6] were used in computing this conversion factor.

References

1. A. M. Broomfield, A. L. Hess, P. I. Amundson, et al., "ZPR-3 Assemblies 48, 48A and 48B: The Study of a Dilute Plutonium-Fueled Assembly and Its Variants," ANL-7759 (1970).
2. B. A. Zolotar, E. M. Bohn, and K. D. Dance, "Benchmark Tests and Comparisons Using ENDF/B Version III Data," Applied Physics Division Annual Report, July 1, 1971 to June 30, 1972, ANL-8010 (in press).
3. R. J. Armani et al., "Improved Techniques for Low-Flux Measurements of Prompt-Neutron Lifetime, Conversion Ratio, and Fast Spectra," IAEA Symp. on Exponential and Critical Experiments, Vienna (1964).
4. W. M. Stacy, Jr., H. Henryson II, B. J. Toppel, and B. A. Zolotar, "MC^2-2/SDX Development - Part II," Applied Physics Division Annual Report, July 1, 1971 to June 30, 1972, ANL-8010 (in press).
5. J. E. Marshall, "The Unit-Cell Composition Model Developed for SDX Input Preparation and the Resulting Cell Specifications for the ZPR/ZPPR Benchmark Assemblies," Applied Physics Division Annual Report, July 1, 1971 to June 30, 1972, ANL-8010 (in press).
6. G. R. Keepin, "Physics of Nuclear Kinetics," Addison-Wesley, Reading, Mass. (1965), Table 4-7.

TABLE I. ZPR-3 Assembly 48 Spherical Model Atom Densities, atom/barn-cm

Isotope	Core Radius = 45.245 cm	Blanket Thickness = 30.0 cm
^{239}Pu	0.001645	-
^{240}Pu	0.000106	-
^{241}Pu	0.000011	-
^{242}Pu	0.0000004	-
^{235}U	0.000016	0.000083
^{238}U	0.007405	0.03969
C	0.02077	-
Na	0.006231	-
Fe	0.01018	0.004925
Cr	0.002531	0.001225
Ni	0.001119	0.000536
Mo	0.000206	-
Al	0.000109	-
Mn	0.000106	0.000051
Si	0.000124	0.000060

TABLE II. Specifications of 27-Group Structure

Group	ΔU	E_{upper}, keV	Group	ΔU	E_{upper}, keV
1	0.5	10000	14	0.5	15.034
2	0.5	6065.3	15	0.5	9.1188
3	0.5	3678.8	16	0.5	5.5308
4	0.5	2231.3	17	0.5	3.3546
5	0.5	1353.4	18	0.5	2.0347
6	0.5	820.85	19	0.5	1.2341
7	0.5	497.87	20	0.5	0.74851
8	0.5	301.97	21	0.5	0.45400
9	0.5	183.16	22	1	0.27536
10	0.5	111.09	23	1	0.10130
11	0.5	67.379	24	1	0.03727
12	0.5	40.868	25	1	0.01371
13	0.5	24.787	26	2	0.00504
			27	-	0.00068

TABLE III. Dimensions for the Zero-Excess Reactivity, Cylindrical Version of ZPR-3 Assembly 48

Core radius, cm	41.59
Core height, cm	76.352
Radial blanket thickness, cm	34.47
Radial blanket height, cm	137.16
Axial blanket thickness, cm	31.144
Core volume, liters	415

TABLE IV. Mean Atom Densities for the Zero-Excess Cylindrical Model of Assembly 48, atoms/barn-cm

	Core	Axial Blanket[(a)]	Radial Blanket
^{239}Pu	0.001645	-	-
^{240}Pu	0.000106	-	-
^{241}Pu	0.000011	-	-
^{242}Pu	0.0000004	-	-
^{235}U	0.000016	0.0000803	0.000083
^{238}U	0.007405	0.038497	0.03988
C	0.02077	-	-
Na	0.006231	-	-
Fe	0.01018	0.005871	0.004540
Cr	0.002531	0.001460	0.001129
Ni	0.001119	0.000639	0.000494
Mo	0.000206	-	-
Al	0.000109	-	-
Mn	0.000106	0.000061	0.000047
Si	0.000124	0.000072	0.000055

[(a)] These concentrations differ from data given in Ref. 1 due to inclusion of spring gap and spring in axial blanket (Ref. B.A. Zolotar, 1/75.).

TABLE V. Unit-Cell Reaction Rate Ratios in ZPR-3 Assembly 48

	Measurement[a]	Calculated Heterogeneity Correction Factors[b]
$^{28}c/^{25}f$	0.131 ± 0.007	1.057
$^{28}f/^{25}f$	0.0321 ± 0.0016	1.017

[a] Flux-weighted average of seven unit-cell locations.
[b] Homogeneous/heterogeneous.

TABLE VI. Central Reactivity Worths Measured in ZPR-3 Assembly 48, 10^{-5} Δk/k/mole

Isotope[a]	Measured Worth 1σ Inprecision[b]	Calculated Worth[c]
^{239}Pu	108.4 ± 1.0	138.06
^{235}U	80.0 ± 1.2	103.10
^{238}U	-5.72 ± 0.17	-6.894
^{23}Na	-0.148 ± 0.007	-0.2543
^{10}B	-90.96 ± 0.61	-93.57
Fe	-0.700 ± 0.023	
Cr	-0.652 ± 0.079	
Ni	-1.09 ± 0.01	
Mn	-1.28 ± 0.06	
Al	-0.432 ± 0.022	
Ta	-30.25 ± 0.92	
Mo	-4.24 ± 0.04	
C	-0.055 ± 0.015	

[a]See Table 35 of Ref. 1 for further description of samples.
[b]Measured period converted to reactivity with use of conversion factor 1% Δk/k = 981 Ih.
[c]FOP calculation based on ENDF/B-III data and central spherical, homogeneous fluxes.

TABLE VII. Comparison of Calculations for ZPR-3 Assembly 48 with Several Models

		1-Dimensional Homogeneous	1-Dimensional Heterogeneous	2-Dimensional Heterogeneous
	k_{eff}	0.9744	0.9927	0.9927
Reaction Rates	$^{28}c/^{25}f$	0.1359	0.1285	
	$^{28}f/^{25}f$	0.03187	0.03135	
Central Worths, 10^{-5} $\Delta k/k$/mole	^{239}Pu	138.06	136.38	134.95
	^{235}U	103.10	102.33	
	^{238}U	-6.894	-7.715	-7.654
	^{23}Na	-0.2543	-0.2522	-0.2482
	^{10}B	-93.57	-103.53	-102.61

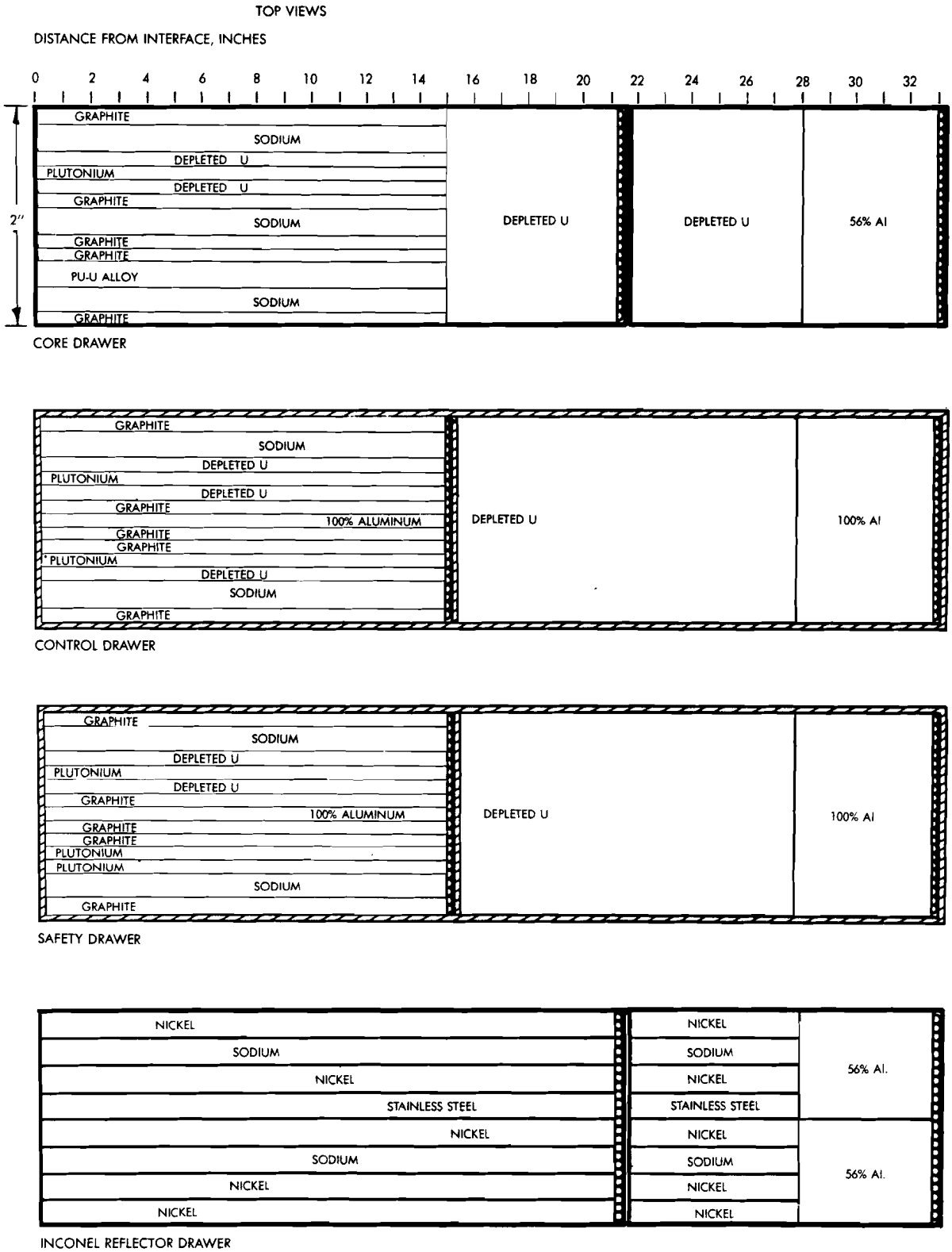

Figure 1. Basic Drawer Arrangements for Assemblies 48, 48A, and 48B

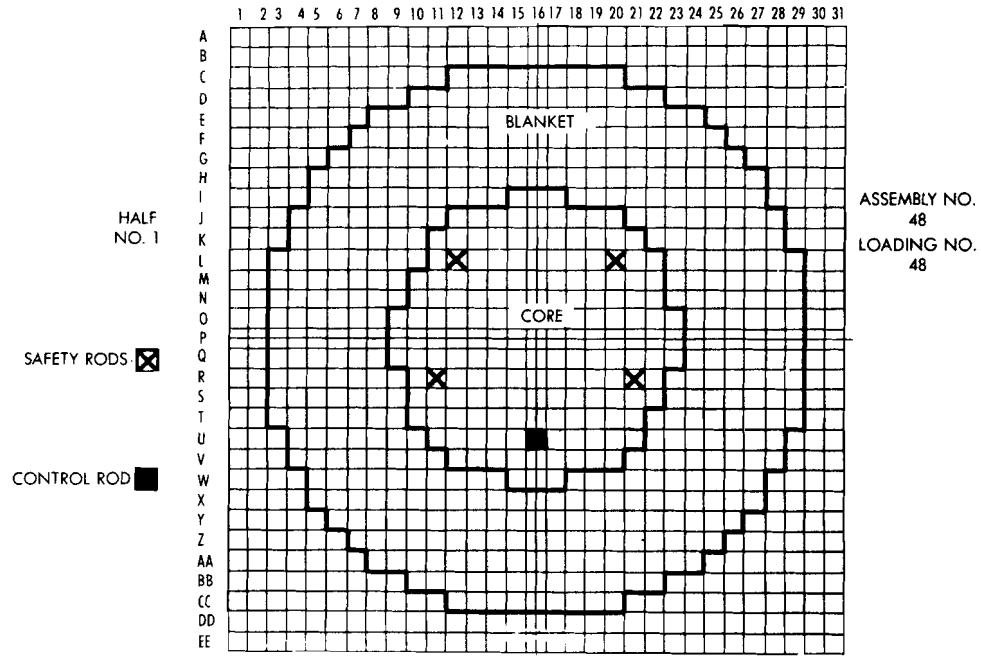

Figure 2. Assembly 48 Drawer Arrangement in Half No. 1

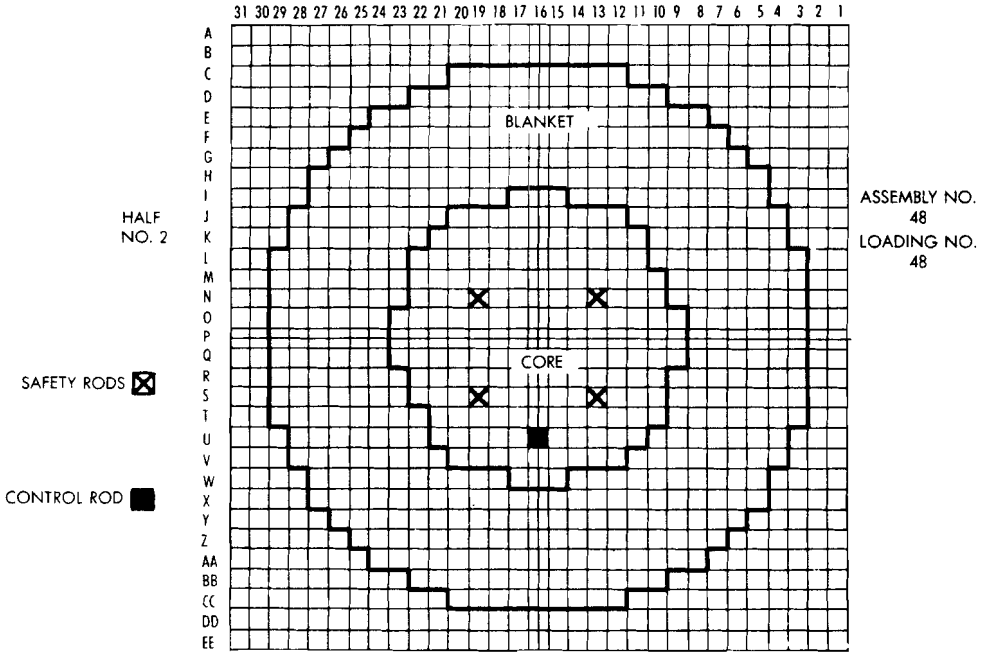

Figure 3. Assembly 48 Drawer Arrangement in Half No. 2

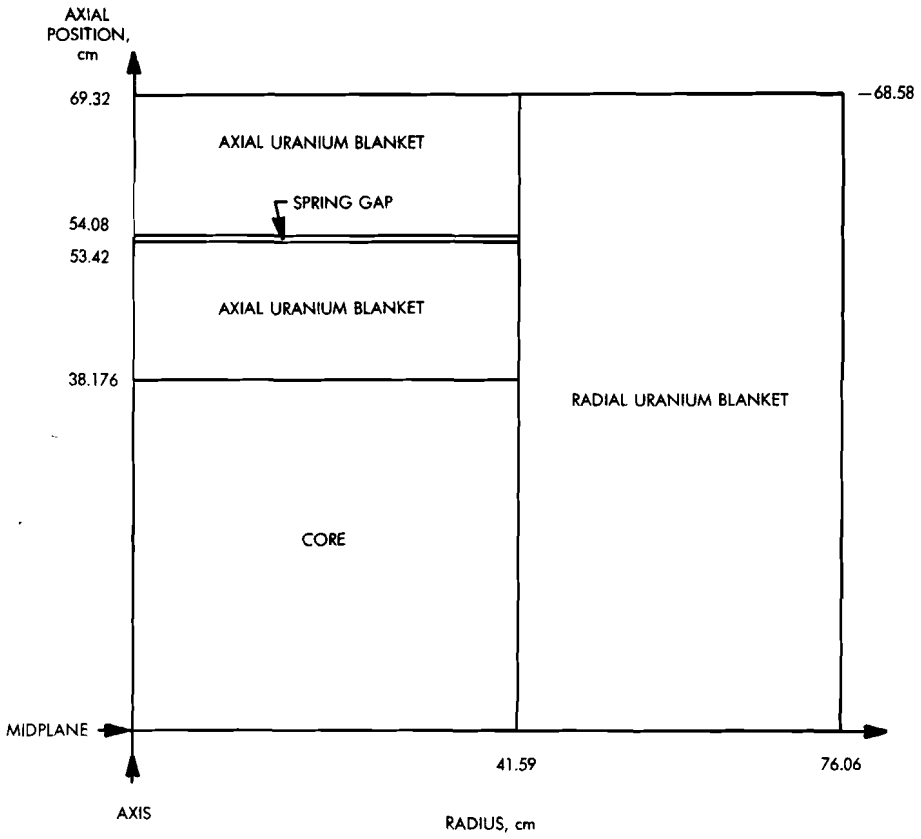

Figure 4. Critical Geometry for Heterogeneous Core Assembly 48 Represented as Circular Cylinder

FAST REACTOR BENCHMARK NO. 4

A. Benchmark Name and Type

ZEBRA-3, a 9:1 uranium/plutonium metal assembly.

B. System Description

The ZEBRA facility consists of stainless steel tubes containing reactor materials mounted vertically on a 3 meter square base plate. A pin at the lower end of each element fits into the base plate and the elements are restrained laterally by 3 steel lattice plates. The central 27 cm square of the base plate is removable so large experiments may be mounted in the reactor center. A concrete shield and steel containment vessel complete the structure.

ZEBRA-3 was a cylindrical critical assembly with a core height of 35.04 cm, an effective diameter of 46.24 cm and a core volume of 58.86 liters. The core is surrounded by a blanket of natural uranium having an axial thickness of 30.54 cm and an effective radial thickness of 34.04 cm.

The assembly has a hard spectrum with more than 80% of the neutron flux being at energies over 100 kev. The assembly is useful for testing the high energy U-238 and Pu-239 cross section data.

C. Model Description

1. One-Dimensional Model Description

A one-dimensional spherical model of ZEBRA-3 is given in Figure 1. A vacuum boundary condition should be applied to the outer reflector boundary. Atom densities for the materials in the core and reflector are given in Table 1. The standard calculational mode is an S_8 transport theory calculation using a multigroup structure composed of 26 groups, each of lethargy width equal to 0.5 and with E_{max} set at 10 MeV. The number of mesh intervals for core and reflector are 40 and 30, respectively.

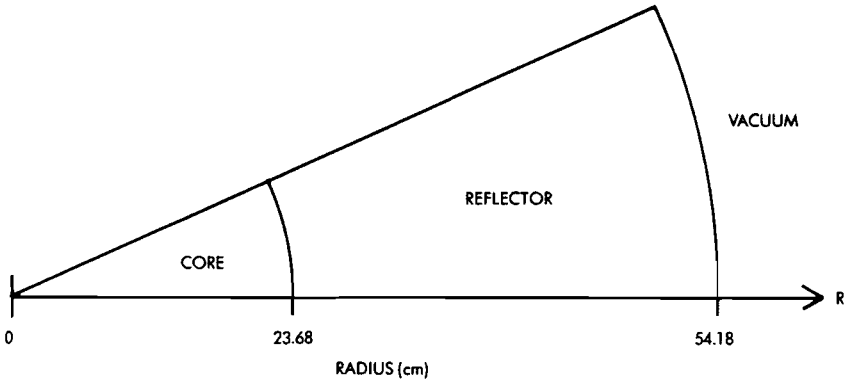

Figure 1. Spherical Model of ZEBRA-3 Assembly

2. Two-Dimensional Model Description

A two-dimensional (R-Z) cylindrical model of the ZEBRA-3 assembly is given in Figure 2. A zero return current boundary condition should be applied to the top and right side of the model; a symmetry boundary condition shouldbe applied along the model bottom. The standard calculation mode is two-dimensional diffusion theory with mesh as follows: 40 radial and axial intervals in the core; 30 intervals for the reflector thicknesses.

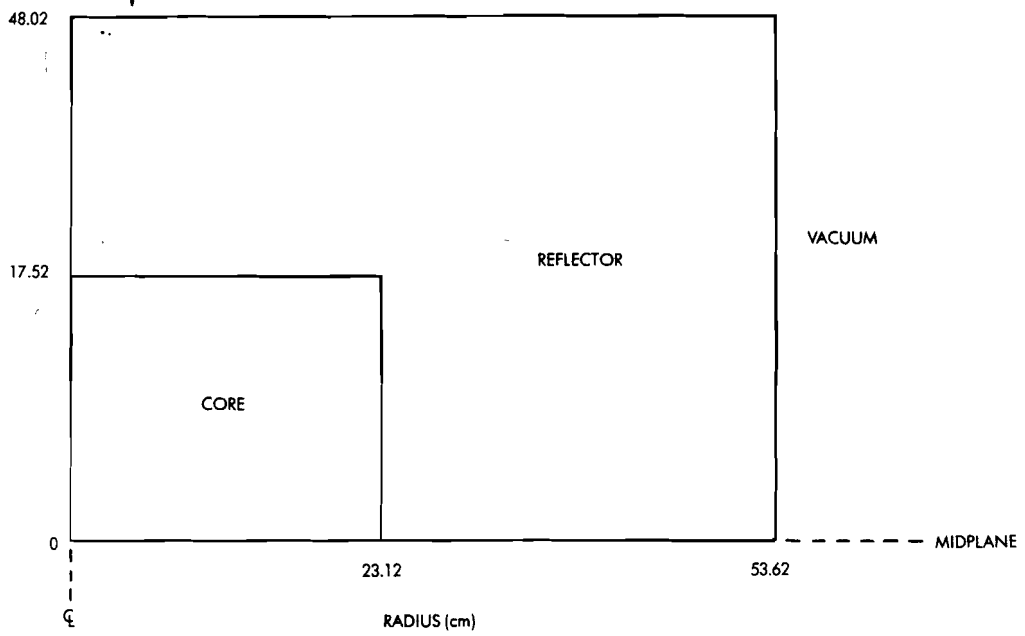

Figure 2. Two-Dimensional (R-Z) Model of ZEBRA-3 Assembly

Table 1.

ZEBRA-3 Region Compositions*

(Atoms/Barn-cm)

Material	Core	Reflector
Pu-239	0.003466	-
Pu-240	0.0001834	-
Pu-241	0.0000127**	-
U-235	0.0002264	0.000298
U-238	0.031775	0.041269
Cu	0.0043702	0.000004
Fe	0.004578	0.003323
C	0.000042	0.000042
Cr	0.000864	0.000864
Mo	0.000008	0.000008
Mn	0.000064	0.000064
Ni	0.000483	0.000483
Aℓ	0.000019	0.000019
Ti	0.000016	0.000016
Si	0.000054	0.000054
V	0.000005	0.000005

*Revised by R. W. Smith 11/70

**As of Jan./Feb. 1965, $T_{1/2}$ = 13.2 years.

D. Experimental Data

1. Experimental Critical Mass	80.1±0.2 Kg (Pu-239 + Pu-241)
Corrections for Edge Irregularities	-1.6±0.1
Finite Plate Thickness (fuel + diluent)	+2.9* ±0.8
Homogeneous Cylinder Critical Mass	81.4±0.9 Kg (Pu-239 + Pu-241)
	81.0 Kg Pu-239
	0.4 Kg Pu-241
Experimental Eigenvalue	1.000±0.003

2. Experimental Spectral Indices at Core Center Relative to σ_f U-235

σ_f (U-238) = 0.0461±0.0008

σ_f (U-233) = 1.542±0.019

σ_f (U-234) = 0.346±0.009

σ_f (U-236) = 0.099±0.005

σ_f (Pu-239) = 1.190±0.014

σ_f (Pu-240) = 0.373±0.005

σ_f (Np-237) = 0.353±0.004

*This value is the mean of the measured and calculated value: (measured 2.5 Kg; calculated 3.3 Kg)

3. Material Worths at Core Center

Material	Reactivity Coefficient (10^{-5} $\Delta k/k$/mole)
U-235	197±4
Pu-239	318±8
U-238	-9.95±0.48
B-10	-105±5
B	-26.7±0.6
Ta	-30±1
Li-6	-85±4
Au	-26±1
Cu	-6.4±0.3
C	-3.8±0.2
Na	-2.8±0.3
Aℓ	-3.4±0.4
Pb	-3.9±0.4
H	-32±1

The reactivity coefficients given above are values for effective zero size samples as quoted in Reference 1. The conversion from in-hours to $\Delta k/k$ for ZEBRA-3 is given as 860 Ih = 0.01 $\Delta k/k$.

F. Comments and Documentation

Experimental information on the ZEBRA-3 assembly is detailed in AEEW-R-461.[1] The experimental critical mass was 80.1±0.2 Kg (Pu-239 + Pu-241). Corrections for edge irregularities and heterogeneity effects were -1.6±0.1 and +2.9±0.8 Kg (Pu-239 + Pu-241), respectively, resulting in a homogeneous cylinder critical mass of 81.0 Kg Pu-239 + 0.4 Kg Pu-241. This critical mass for the equivalent homogeneous cylinder was obtained from the measured values by allowing for partially inserted control rods and counter holes as well as irregular edge and heterogeneity effects.

Applying a shape factor of 0.944±-.005 gives a homogeneous spherical critical mass of 76.8±1.0 Kg (Pu-239 + Pu-241), or 76.4 Kg Pu-239 and 0.4 Kg Pu-241. The corresponding critical sphere radius is 23.68±0.12 cm.

The correction to the S_8 eigenvalue result to extrapolate to an "S_∞" value is estimated to be -0.001. For example, if k_{eff} (S_8) is 1.003, then k_{eff} (S_∞) would be 1.002.

REFERENCES

1. J. Adamson, et al., "The Third Core of ZEBRA", AEEW-R-461 (1965).
2. Private Communication, R. W. Smith (AEEW) to H. Alter (11/70).

FAST REACTOR BENCHMARK NO. 5

A. Benchmark Name and Type:

GODIVA, a bare sphere of enriched uranium.

B. System Description

GODIVA, as a bare sphere of enriched uranium metal, is especially suited for testing ^{235}U and ^{238}U cross sections in the fission source energy range. The single-region, simple geometry and uniform composition conveniently facilitate calculational testing.

C. Model Description

The spherical homogeneous model has a core radius of 8.741 cm and the following composition:[1]

Isotope	Density, nuclei/b-cm
^{235}U	0.04500
^{238}U	0.002498
^{234}U	0.000492

The recommended mode of calculation is one-dimensional transport theory, S_{16}, with 40 mesh intervals in the core, a vacuum boundary condition at the core boundary (8.741 cm) and a 26 energy group structure with half-group structure with half-lethargy unit widths and an upper energy of 10 MeV.

D. Experimental Data

1. Measured Eigenvalue: $k = 1.000 \pm 0.001$

2. Spectral Indices at Core Center

a. Central Fission Ratios[3]

$\sigma_f(^{238}U)/\sigma_f(^{235}U)$	0.1647 ± 0.0018
$\sigma_f(^{233}U)/\sigma_f(^{235}U)$	1.59 ± 0.03
$\sigma_f(^{237}Np)/\sigma_f(^{235}U)$	0.837 ± 0.013
$\sigma_f(^{239}Pu)/\sigma_f(^{235}U)$	1.402 ± 0.025

b. Central Activation Ratios[3]

Isotope	$\sigma_{n,\gamma}/\sigma_f$ (^{235}U)	Thermal Normalization Value of $\sigma_{n,\gamma}$ barns
^{55}Mn	0.0027 ± 0.0002	13.3 ± 0.2
^{59}Co	0.038 ± 0.003	19.9 ± 0.9
^{63}Cu	0.0117 ± 0.0006	4.5 ± 0.1
^{93}Nb	0.030 ± 0.003	1.15 ± 0.05
^{197}Au	0.100 ± 0.002	98.8 ± 0.3

3. Rossi Alpha[2]

$$\alpha = -\beta_{eff}/\ell = -(1.11 \pm 0.02) \times 10^6 \text{ sec}^{-1}$$

4. Central Reactivity Worths[4]

Material	Central Worth, 10^{-5} Δk/k/mole
H	240 ± 30
Be	47 ± 7
^{10}B	-380 ± 20
C	16 ± 2
Al	3 ± 2
Fe	-1 ± 2
Co	-4 ± 2
Ni	-30 ± 2
Cu	-12 ± 2
Au	-50 ± 2
Th	-9 ± 2
^{235}U	1010 ± 10
^{238}U	162 ± 3
^{239}Pu	1934 ± 20
^{240}Pu	1150 ± 120

5. Neutron Flux Spectrum

a. Leakage Spectrum[5]

The spectrum of neutrons emitting from the surface of the core is represented below in the 1/2 lethargy group structure (E_{max} = 10 MeV) with an arbitrary normalization to the value 18 in group 5. Uncertainties are based on counting statistics alone.

Energy Group	Lower Lethargy Limit	Relative Neutron Leakage
1	0.5	2.0 ± 0.3
2	1.0	7.8 ± 0.4
3	1.5	13.6 ± 0.5
4	2.0	16.8 ± 0.6
5	2.5	18.0 ± 0.6
6	3.0	17.5 ± 0.7
7	3.5	12.0 ± 0.7
8	4.0	7.2 ± 0.7

b. Central Spectrum Relative to ^{235}U Fission Spectrum[2b]

Deviation of the central spectrum from the ^{235}U fission spectrum is characterized by the following ratios of central high-energy spectral indices to the corresponding indices for the ^{235}U fission spectrum.

Spectral Index	Ratio of Central Value to Value for ^{235}U Fission Spectrum
$\sigma_f(^{238}U)/\sigma_{n,p}(^{31}P)$	1.018 ± 0.025
$\sigma_{n,p}(^{27}Al)/\sigma_{n,p}(^{31}P)$	1.020 ± 0.020
$\sigma_{n,p}(^{56}Fe)/\sigma_{n,p}(^{31}P)$	1.022 ± 0.025
$\sigma_{n,\alpha}(^{27}Al)/\sigma_{n,p}(^{31}P)$	1.030 ± 0.030
$\sigma_{n,2n}(^{63}Cu)/\sigma_{n,p}(^{31}P)$	1.027 ± 0.040

E. Calculated Results

Calculated results may be appended to these specifications.

F. Comments and Documentation

The composition and configuration specifications were taken from Ref. 1 which also gives the uncertainty in critical mass, at the specified composition and density, as ± 0.3%. This translates to an uncertainty in eigenvalue, at the specified composition, density, and size, of ± 0.1%.

The most accurate fission ratio values for Godiva are obtained from recent absolute ratio measurements in the Flattop and Big Ten assemblies and old double-ratio measurements connecting these to Godiva. These measurements are described below.

Measurement Location	Value	Double Ratio to Godiva	Godiva	Reference
$\sigma_f(^{238}U)/\sigma_f(^{235}U)$				
Flattop-25	0.1479(±1.5%)	1.107(±0.4%)	0.1637(±1.6%)	2c
Big Ten	0.0373(±1.7%)	4.42(±0.7%)	0.1649(±1.8%)	2d
Van de Graaff (E_n=2.43 MeV)	0.433(±1.5%)	0.383(±0.8%)	0.1658(±1.7%)	ENDF/B-IV
		Average:	0.1647(±1.1%)	

Measurement Location	Value	Double Ratio to Godiva	Godiva	Reference
σ_f (^{233} /σ_f (^{235}U)				
Flattop-25	1.572(±1.5%)	0.997(±0.3%)	1.567(±1.5)	2c
Topsy	1.65(±4%)	0.997(±0.3%)	1.645(±4%)	2e
Big Ten	1.61(±2.1%)	1.008(±0.6%)	1.623(±2.2%)	preliminary value from D.M. Gilliam (1979)
		Average:	1.590(±1.9%)	
σ_f(^{237}Np)σ_f(^{235}U)				
Topsy	0.760(±4%)	1.094(±0.7%)	0.831(±4%)	2e
Big Ten	0.317(±2.2%)	2.649(±1.0%)	0.840(±2.4%)	2d
Van de Graaff	1.328(±2%)	0.629(±1.2%)	0.836(±2.3%)	ENDF/B-IV
		Average:	0.837(±1.6%)	
σ_f(^{239}Pu)/σ_f(^{235}U)				
Flattop-25	1.349(±1.5%)	1.022(±0.3%)	1.379(±1.5%)	2c
Topsy	1.42(±4%)	1.022(±0.3%)	1.451(±4%)	2e
Big Ten	1.198(±1.5%)	1.186(±0.7%)	1.421(±1.7%)	2d
		Average:	1.402(±1.8%)	

The central activation cross section ratios were obtained from double ratio measurements, connecting the thermal column of the LASL water boiler to the center of Godiva, and literature values for the thermal cross sections. The data for the central activation cross sections were reported in Ref. 3. Subsequently, the thermal normalization values, and consequently the activation cross setions, have been updated by LASL.

The measured central reactivity worths were taken from Ref. 4. Corrections for sample size effects have been reevaluated by means of 50 group transport calculations based on ENDF/B-IV. The conversion from dollars/mole to $(\Delta k/k)$/mole uses the factor $\beta_{eff} = 0.00645$, (the surface mass increment between delayed and prompt critical gave $\beta_{eff} = 0.00647$), the central void coefficient gave $\beta_{eff} = 0.00644$, and ENDF/B-IV delayed neutron data gave $\beta_{eff} = 0.0063_4$) .

The data listed for the leakage spectrum were derived from Ref. 5, A finer energy mesh representation for the spectrum is given in this reference along with statistical uncertainties.

REFERENCES

1. G. E. Hansen and H. C. Paxton, "Reevaluated Critical Specifications of Some Los Alamos Fast-Neutron Systems," Los Alamos Scientific Laboratory report LA-4208 ((1969).

2. (a) G. E. Hansen "Status of Computational and Experimental Correlations for Los Alamos Fast Neutron Critical Assemblies," Proc. Seminar Physics of Fast and Intermediate Reactors, Vienna, August 3-11, 1961 (IAEA, Vienna, 1962) Vol. I, pp. 445-455. (b) J. A. Grundl and G. E. Hansen, "Measurement of Average Cross-Section Ratios in Fundamental Fast-Neutron Spectra," Proc. Paris Conf. Nuclear Data for Reactors (IAEA, Vienna, 1967) Vol. I, pp. 321-336. (c) P. I. Amundson, A. M. Broomfield, W. G. Davey, and J. M. Stevenson, "An International Comparison of Fission Detector Standards," Proc. Intern. Conf. Fast Critical Experiments and Their Analysis, Argonne, October 10-13, 1966 (Argonne National Laboratory report ANL-7320) pp. 679-687. (d) D. M. Gilliam, "Integral Measurement Results in Standard Fields," Proc. Intern. Specialist's Symposium Neutron Standards and Applications, Gaithersburg, March 28-31, 1977 (NBS Special Publication 493, 1977) pp. 293-303. (e) G. A. Linenberger and L. L. Lowry, "Neutron Detector Traverses in the Topsy and Godiva Critical Assemblies," Los Alamos Scientific Laboratory report LA-1653 (1953).

3. C. E. Byers, "Cross Sections of Various Materials in the Godiva and Jezebel Critical Assemblies," Nucl. Sci. Eng. 8, 608-614 (1960).

4. L. B. Engle, G.E. Hansen, and H.C. Paxton, "Reactivity Contributions of Various Materials in Topsy, Godiva, and Jezebel," Nucl. Sci. Eng. 8, 543-569 (1960).

5. L. Stewart, "Leakage Neutron Spectrum from a Bare Pu-239 Critical Assembly," Nucl. Sci. Eng. 8, 595-597 (1960).

FAST REACTOR BENCHMARK NO. 6

A. Benchmark Name and Type

VERA-1B, an enriched uranium-plus-graphite system.

B. System Description

VERA-1B is a cylindrically shaped critical assembly fueled with enriched uranium and diluted with graphite. The assembly core was 27.2 cm in height and the effective core diameter was 38.1 cm. The assembly core was surrounded by a blanket of natural uranium and stainless steel. VERA-1B was designed to explore the accuracy of U-235 neutron cross section data.

C. Model Description

1. One-Dimensional Model Description

A one-dimensional spherical model of VERA-1B is given in Figure 1. A vacuum boundary condition should be applied at the outer reflector boundary. Material atom densities for the core and reflector are given in Table 1.

The standard calculation mode is an S_8 transport theory calculation using a multigroup structure composed of 26 groups, each of lethargy width equal to 0.5 and with E_{max} set at 10 MeV. Forty mesh intervals are used for both core and reflector regions.

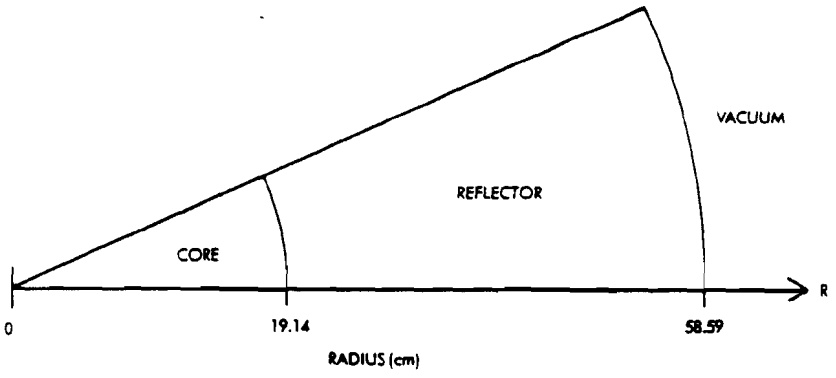

Figure 1. Spherical Model of VERA-1B Assembly

Table 1.

VERA-1B Region Compositions

(Atoms/Barn-cm)

Material	Core	Reflector*	
		(a)	(b)
U-235	0.007349	0.00025	0.00026
U-236	0.000014	-	-
U-234	0.000092	-	-
U-238	0.000455	0.03440	0.03610
C	0.057540	-	-
H	0.000058	-	-
Fe	0.006283	0.006464	0.006582
Cr	0.001635	0.001682	0.001713
Ni	0.000689	0.000708	0.000721

*Use Composition (a) in calculations

(Revised 9-78)

2. Two-Dimensional Model Description

A two-dimensional (R-Z) cylindrical model of the VERA-1B assembly is given in Figure 2. Zero return current boundary conditions should be applied to the top and right side of the model; a symmetry boundary condition should be applied along the model bottom. The suggested calculational mode is two dimensional diffusion theory with 40 mesh intervals for the radial and axial core dimensions and 40 mesh intervals for the reflector thickness.

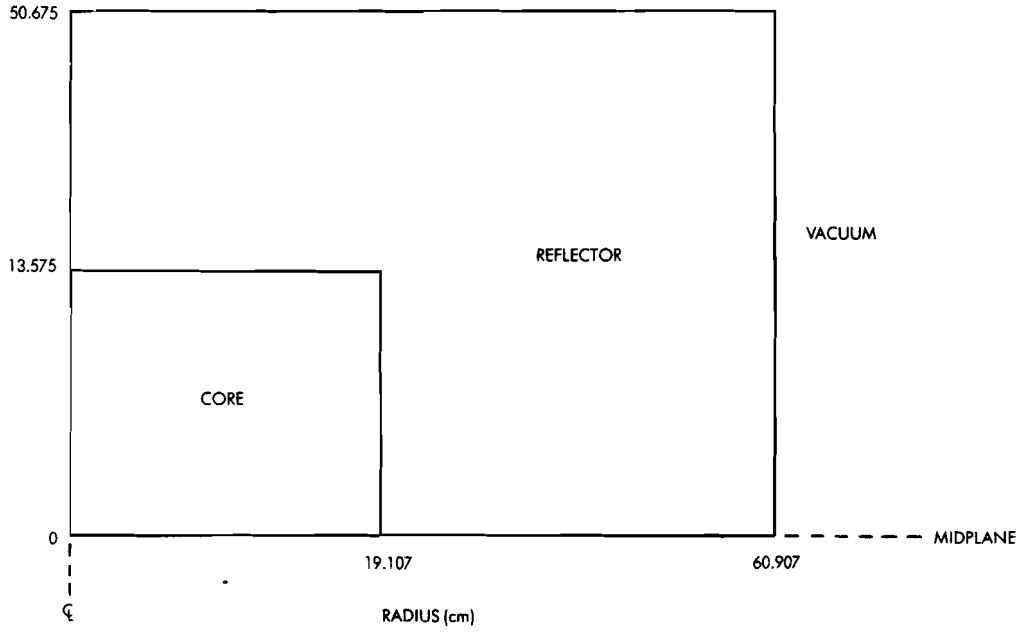

Figure 2. Two-Dimensional (R-Z) Model of VERA-1B Assembly

D. Experimental Data

1. Experimental Critical Mass 86.3±0.15 Kg U-235

Corrections for Edge Irregularities	-0.6±0.2
Finite Fuel Plate Thickness	+3.6±0.4
Homogeneous Cylinder Critical Mass	89.3±0.4 Kg U-235
Experimental eigenvalue	1.0000±0.0028

2. Experimental Spectral Indices at Core Center Relative to σ_f U-235

σ_f (U-238) = 0.0665±0.0010
σ_f (U-233) = 1.433±0.047
σ_f (U-236) = 0.134±0.010
σ_f (Pu-239) = 1.070±0.026
σ_f (Pu-240) = 0.399±0.032
σ_f (Np-237) = 0.38±0.012
σ_c (U-238) = 0.131±0.006 (cell average)
= 0.126±0.006 (average over U-238 in cell)

3. Material Worths at Core Center

Material	Reactivity Coefficient 10^{-5} Δk/k/mole
U-235	221±3
U-238	7.5±0.3
Pu-239	387±5
U-233	378±5
Np-237	28±3
B-10	-237±50
Au	-26±1
Stainless Steel	2.1±0.3
Aℓ	3.5±0.4
Na	13±1
C	5.95±0.12
H	90±2

Sample size corrections were made using experimental worth vs. size and/or S_n calculations. Errors quoted do not include those due to delayed neutron data. The conversion from inhours to $\Delta k/k$ is 416 Ih = $0.01 \Delta k/k$.

4. Rossi Alpha

At delayed critical, $\alpha = -6.9 \times 10^4$ sec^{-1}. Extrapolation to $\alpha = 0$ gave 336±10 inhours per dollar.

F. Comments and Documentation

In VERA-1B a figure of 95±15 p.p.m. of hydrogen in graphite[1] has been suggested to allow for possible moisture content in the graphite. The effect of this moisture on k_{eff} for VERA-1B is about 0.15%. This moisture content has not been included in the core composition data for VERA-1B.

Details and experimental results of the VERA-1B experiments have been described by McTaggart.[2] The experimental critical mass is 86.3±0.15 Kg U-235. Corrections for edge irregularities (-0.6±0.2) and for finite fuel plate thickness (+3.6±0.4) produce a homogeneous cylindrical critical mass of 89.3±0.4. This critical mass for the equivalent homogeneous cylinder was obtained from the measured values by allowing for partially inserted control rods and counter holes as well as irregular edge and heterogeneity effects.

Applying a shape factor of 0.943 produces a homogeneous spherical critical mass of 84.2±0.6 Kg U-235 with the radius of the critical sphere equal to 19.14±0.05 cm.

The correction to the S_8 eigenvalue to extrapolate to an "S_∞" eigenvalue is estimated to be -0.001. For example, if the k_{eff} (S_8) result was 1.0000, then the k_{eff} (S_∞) result would be 0.9990.

REFERENCES

1. Private communication, R. W. Smith (UKAEA) to H. Alter, Nov. 1970.

2. M. H. McTaggart, et al, "Interim Report on Uranium Fueled VERA Reactor Experiments", AWRE-R5/66 (1966).

FAST REACTOR BENCHMARK NO. 7

A. Name and Type: ZPR-III 6F, a dilute ∿ 1:1 fertile to fissile U system.

B. System Description:

Several early assemblies on ZPR-III (6F, 1B, 2, 2B, 5, and 13) used a core composition with a U-238 to U-235 ratio of about 1:1. The reflector of these assemblies was composed mostly of U-238.

Reasons for creating a benchmark to represent these assemblies are as follows: 1) The measurements on all of the source assemblies form an extensive set of experimental results which represents a relatively simple system; 2) The 1:1 fertile to fissile ratio provides an important interval in the range of such ratios being tested by the benchmark program; 3) And it provides an opportunity to test the U-235 and U-238 cross section sensitivities in the intermediate spectrum region.

C. Model Description:

1. One-Dimensional Model (sphere)

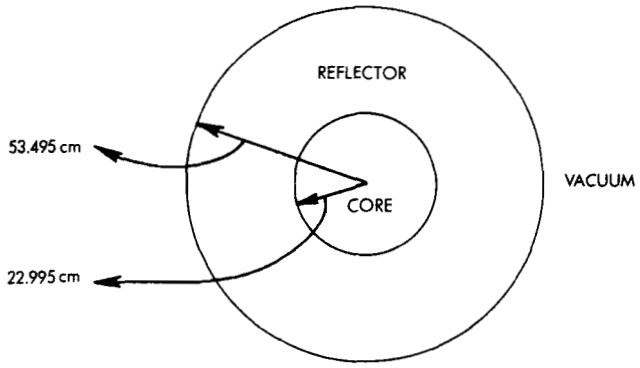

Suggestions:

Code..... 1-D transport theory with S_4.

Mesh..... 40 intervals in the core, 30 in the reflector.

2. Two-Dimensional Model (cylinder)

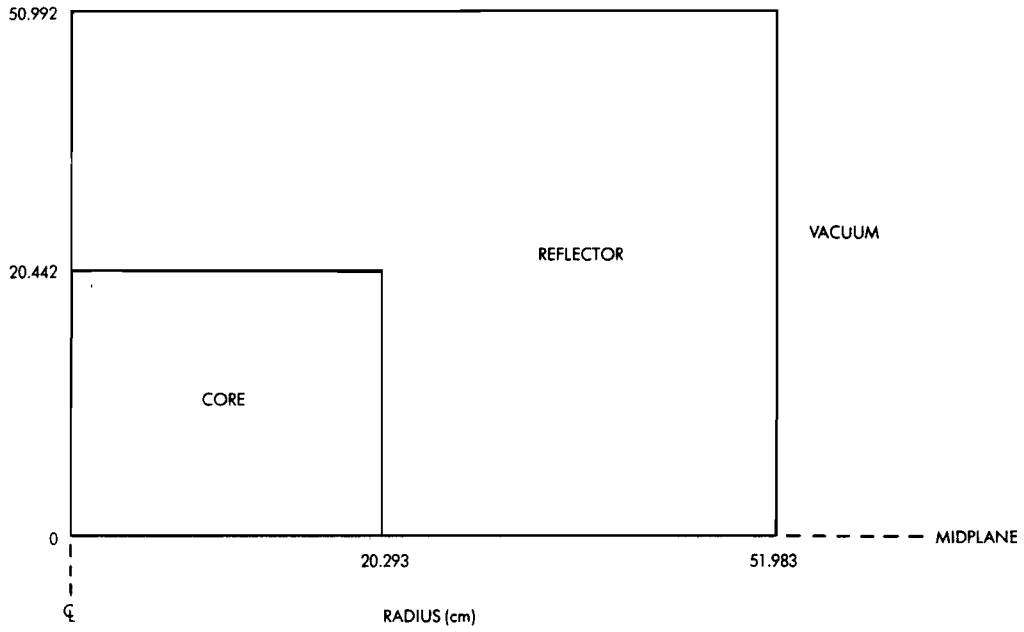

Suggestions:

Code..... 2-D diffusion theory

Mesh..... 40 radial intervals, core

40 axial intervals, core

30 radial intervals, radial reflector

30 axial intervals, axial reflector

3. Atom Densities

Material	Density, 10^{24} atoms/cc	
	Core	Reflector
U-235	0.006727	0.000089
U-238	0.007576[a]	0.040026
U-234	0.000069	- - -
Al[b]	0.019019	0.001359
Fe	0.007712	0.004539
Cr	0.001918	0.001129
Ni	0.000839	0.000494
Mn	0.000080	0.000047

a. Includes 0.000029 for U-236.

b. Includes atom density for Si in steel.

4. Techniques

All calcualtions should be performed with appropriately resonance-shielded cross sections. A suggested multigroup structure is 26 half-lethargy width groups with E_{max} = 10 MeV.

D. Experimental Data: (all errors are one standard deviation)

1. Eigenvalue = 1.0000 ± 0.0015

2. Central Spectral Indices

σ_f (U-238) / σ_f (U-235) = 0.078 ± 0.002

σ_f (U-234) / σ_f (U-235) = 0.451 ± 0.020

σ_f (U-233) / σ_f (U-235) = 1.53 ± 0.03

σ_f (Pu-239)/ σ_f (U-235) = 1.22 ± 0.03

σ_f (Pu-240)/ σ_f (U-235) = 0.53 ± 0.02

$\sigma_{n,\gamma}$ (U-238) / σ_f (U-235) = 0.104 ± 0.003

3. Material Worths at Core Center

Material	Reactivity Coeff. 10^{-5} Δk/k/mole[a]	Material	Reactivity Coeff. 10^{-5} Δk/k/mole[a]
U-235[b]	175 ± 5	Fe	-0.9 ± 0.3
U-238	1.5 ± 0.5	Cr	-0.55 ± 0.19
Pu(4.5%240)[b]	251 ± 12	Ni	-1.7 ± 0.5
U-233[b]	244 ± 24	Mn	-0.65 ± 0.24
Th	-12 ± 2	V	+1.2 ± 0.4
B-10[b]	-86 ± 5	Nb	-5.8 ± 1.2
Hf	-14 ± 5	Al	+0.23 ± 0.35
Ta	-17 ± 3	Na	+3.2 ± 0.9
W	-7.4 ± 1.6	C	+2.8 ± 1.2
Mo	-3.6 ± 0.6	Be	+4.9 ± 1.6
Zr	-0.1 ± 0.2	H	+56 ± 23

a. Derived from worths in inhours using calculated factor of 430 Ih/%k.

b. Approximately corrected for sample-size effects.

4. Rossi Alpha at Delayed Critical = -9.85×10^{4} sec^{-1}

E. Comments and Documentation:

The specifications for the 1-D model were derived from the 6F critical mass while the 2-D model was based on Assembly 2. Large probable errors have been assigned to the reactivity coefficients to cover the possible discrepancies between the measurements (with massive samples) and "zero-

size" coefficients which would be comparable to perturbation theory. The primary information source has been internal ZPR-III memos written during the conduct of these assemblies. Some results have been published, as by Long[1], but there may be differences from results quoted here because of later-established corrections to the critical mass, reaction ratios, and material worths, or from using more accurate composition breakdowns. A more recent reference[2] contains a convenient compilation of all the pertinent experimental details and measurements for these source assemblies.

According to Baker[3], for Assembly 6F

$$k_{eff}\ (S_4) - k_{eff}\ (\text{diffusion theory}) = 0.023$$

and

$$k_{eff}\ (S_\infty) - k_{eff}\ (S_4) = -.023/6 = -.0038.$$

Thus, for example, if a 1-D diffusion theory calculation gave an eigenvalue of .9900, the corrected eigenvalue would be .9900 + .023 (corrected to S_4) -.0038 (corrected to S_∞) = 1.0092.

References:

1. J. K. Long et al., "Fast Neutron Power Reactor Studies with ZPR-III," Proc. 2nd Int. Conf. on Peaceful Uses of Atomic Energy, Vol. 12, p. 119 (1958).

2. P. F. Palmedo, editor, "Compilation of Fast Reactor Experiments," BNL-15746, Brookhaven National Laboratory, Upton, New York, June 1, 1971.

3. A. R. Baker, "Comparative Studies of the Criticality of Fast Critical Assemblies," ANL-7320, Argonne National Laboratory, Argonne, Illinois, October 1966.

FAST REACTOR BENCHMARK NO. 8

A. Name and Type: ZPR-III 11, an ∿ 7:1 fertile to fissile uranium metal system.

B. System Description:

Several fast reactor experiments (ZPR-III Assembly 11, ZPR-III Assembly 22, ZEBRA Core 1, and ZPR-6 Assembly 1) were all cylindrical critical assemblies constructed with very nearly identical core compositions. The cores were fueled with uranium metal such that the ratio of U-238 to U-235 was ∿ 7:1. The reflectors were composed mostly of U-238.

Reasons for creating a benchmark to represent these assemblies are as follows: 1) the measurements on all of the source assemblies form a rather extensive set of experimental results which represents a relatively simple system; 2) the 7:1 fertile to fissile ratio provides an important interval in the range of this ratio being tested by the benchmark program; and 3) it provides an opportunity to test the U-235 and U-238 cross section sensitivities in the soft spectrum region.

C. Model Description:

1. One-Dimensional Model (sphere)

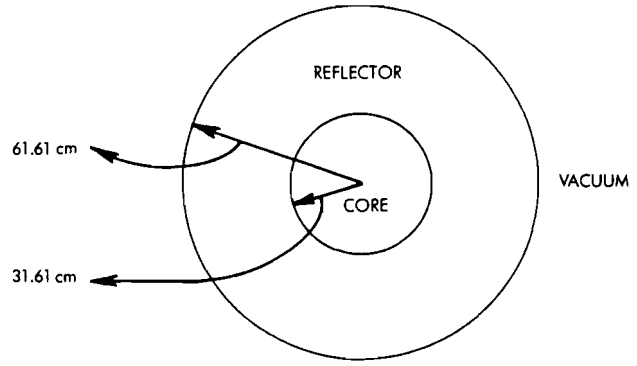

Suggestions:

Code..... 1-D transport theory with S_4

Mesh..... 30 intervals in the core, 20 in the reflector.

2. Two-Dimensional Model (cylinder)

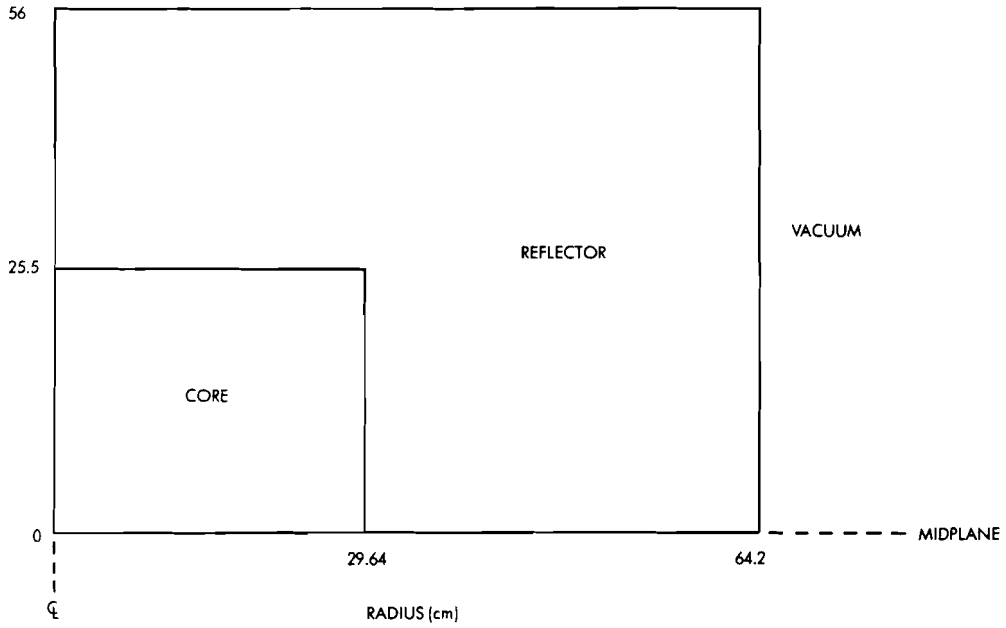

Suggestions:

Code..... 2-D diffusion theory

Mesh..... 30 radial intervals, core

30 axial intervals, core

20 radial intervals, reflector

20 axial intervals, reflector

3. Atom Densities

Material	Density, 10^{24} atoms/cc	
	Core	Reflector
U-235	0.004567	0.000089
U-238	0.034392*	0.040025
U-234	0.000046	- - -
Fe	0.005681	0.004925
Cr	0.001486	0.001196
Ni	0.000718	0.000536
Mn	0.00208	0.000111

*Includes 0.000019 for U-236.

4. Techniques

All calculations should be performed with appropriately resonance-shielded cross sections. A suggested multigroup structure is 26 half-lethargy width groups with E_{max} = 10 MeV.

D. Experimental Data: (all errors are one standard deviation)

1. Eigenvalue = 1.0000 ± 0.0025

2. Spectral Indices at Core Center

σ_f (U-238) / σ_f (U-235) = 0.038 ± 0.001

σ_f (U-234) / σ_f (U-235) = 0.31 ± 0.03[a]

σ_f (U-233) / σ_f (U-235) = 1.52 ± 0.02

σ_f (Pu-239)/ σ_f (U-235) = 1.19 ± 0.02

σ_f (Pu-240)/ σ_f (U-235) = 0.34 ± 0.02

σ_f (U-236) / σ_f (U-235) = 0.12 ± 0.02[b]

σ_f (Np-237)/ σ_f (U-235) = 0.33 ± 0.02[b]

$\sigma_{n,\gamma}$ (U-238) / σ_f (U-235) = 0.112 ± 0.005[c]

a. Measured ratio plus 5% wall-effect correction

b. Measured in ZEBRA Core 1

c. For Assembly 22, from ZPR-3 internal memo.

3. Material Worths at Core Center

Material	Reactivity Coefficient 10^{-5} $\Delta k/k/mole^a$	Material	Reactivity Coefficient, 10^{-5} $\Delta k/k/mole^a$
U-235[b]	123 ± 3	Fe	-1.7 ± 0.1
U-238	-6.6 ± 0.2	Cr	-1.7 ± 0.1
U-233	221 ± 4	Ni	-2.4 ± 0.1
Pu-239[b]	209 ± 5	Na	-0.7 ± 0.1
B-10[b]	-72 ± 2	Al	-1.0 ± 0.1
Ta	-19.6 ± 0.6	O	-0.87 ± 0.15
Mo	-5.1 ± 0.2	C	-0.85 ± 0.13
Mn	-1.8 ± 0.1		

a. Derived from measurements in inhours using conversion of 470 inhours per % $\Delta k/k$.

b. Approximately corrected for sample-size effects.

4. Rossi Alpha at Delayed Critical

$\alpha = -10.4 \pm 0.3 \times 10^4$ sec^{-1}.

E. Comments and Documentation:

The 1-D and 2-D models are based on the Assembly 11 composition and a heterogeneous critical mass of 237.4 kg U-235, (adjusted for edge irregularities and the interface-gap effect) as quoted by Davey[1]. A heterogeneity advantage of +0.8 ±0.2% k, based on fuel-bunching experiments in all the cited assemblies, was applied to derive the homogeneous critical size of the cylinder. For the sphere size, a

calculated shape factor of 0.94[1] was utilized. Except as noted, central spectral indices were taken from a report by Davey[2]. The Zebra values cited are from a report by Ingram[3]; this Zebra report also gives measured Rossi Alpha values. Material worths at the core center were derived from internal ZPR-3 and ZPR-6 memos and also from the UKAEA reports on measurements in Zebra[3,4]. Data from Zebra investigations into sample-size effects were used to correct some reactivity coefficients to values comparable to perturbation theory. A more recent reference[5] contains a convenient compilation of all the pertinent experimental details and measurements for the ZPR source assemblies.

According to Baker[6], for Assembly 11,

$$k_{eff}\ (S_4) - k_{eff}\ (\text{diffusion theory}) = 0.008$$

and

$$k_{eff}\ (S_{oo}) - k_{eff}\ (S_4) = -.008/6 = -.0013.$$

Thus, for example, if a 1-D diffusion theory calculation gave an eigenvalue of .9900, the corrected eigenvalue would be .9900 + .008 (corrected to S_4) - .0013 (corrected to S_{oo}) = .9977.

References:

1. W. G. Davey, "k Calculations for 22 ZPR-3 Fast Reactor Assemblies Using ANL Cross Section Set 635," ANL-6570 (May 1962).

2. W. G. Davey and P. I. Amundson, "A Re-evaluation of Fission Ratios Measured in ZPR-3 Critical Assemblies," ANL-6941 (October 1964).

3. G. Ingram et al., "The First Core of Zebra," AEEW-R315 (1963).

4. G. Ingram et al., "Central Perturbation Cross Sections in Zebra Cores 1 and 2," AEEW-R373 (1964).

5. P. F. Palmedo, editor, "Compilation of Fast Reactor Experiments," BNL-15746, Brookhaven National Laboratory, Upton, New York, June 1, 1971.

6. A. R. Baker, "Comparative Studies of the Criticality of Fast Critical Assemblies," ANL-7320, Argone National Laboratory, Argonne, Illinois, October 1966.

FAST REACTOR BENCHMARK NO. 9

A. Benchmark Name and Type

ZPR-III Assembly 12, a 4:1 uranium-graphite system, source experiment.

B. System Description

ZPR-III Assembly 12 was designed as a fast reactor benchmark source experiment on a 4:1 uranium-graphite system. The graphite was included to produce the softer spectra characteristic of larger power reactors. The core was approximately cylindrical composed from a repetition of a one-drawer unit cell. A blanket, consisting primarily of depleted uranium, surrounded the core. The polonium-beryllium neutron sources were removed before measurements were made.

C.1 One-Dimensional Model Description

A one-dimensional spherical model of ZPR-III Assembly 12 is shown in Figure 1, including model dimensions and suggested mesh. Zero return current boundary conditions should be applied at the outer boundary. The atom densities in both regions (atoms/barn-cm) are given in Table I. S_4 transport theory calculations are suggested in any suitable fast reactor energy group structure, but with groups no coarser than 0.5 lethargy width down to a lethargy of 12.5. The estimated uncertainty in k_{eff} ascribable to the model is $\Delta k/k = \pm 0.0023$.

C.2 Two-Dimensional Model Description

A two-dimensional (R-Z) model of ZPR-III Assembly 12 is shown in Figure 2, including model dimensions and suggested mesh. Zero return current boundary conditions are to be applied along the top and right sides; a symmetry boundary condition should be applied along the bottom. The atom densities in both regions (atoms/barn-cm) are given in Table I. Diffusion theory is suggested with cross sections in any suitable fast

reactor energy-group structure.* The estimated uncertainty in k_{eff} ascribable to the model $\Delta k/k = 0.0015$.

D. Experimental Data

1. Measured $k_{eff} = 1.0000$, uncertainty unknown

2. Experimental spectral indices at the core center, relative to σ_f (U-235) are as follows:

σ_f (U-238) = 0.047 ± 0.002
σ_f (U-234) = 0.305 ± 0.012
σ_f (U-233) = 1.48 ± 0.03
σ_f (Pu-239) = 1.12 ± 0.02
$\sigma_{n,\gamma}$ (U-238) = 0.123 ± 0.005

3. Material worths at the core center are as follows:

Material	Reactivity Coefficient 10^{-5} $\Delta k/k$/mole
U-235**	157±.5
U-238	-6.7±1.0
Plutonium**(4.5% Pu-240)	244±7
U-233**	269±7
Ta**	-31±1
Ru**	-16±1
Nb	-10±1
Mo**	-7±0.5
Ni	-2.7±0.5
Fe	-1.5±0.4
Al	-0.4±0.1
C	2.0±0.3

* If the two-dimensional problem is run with a group structure that contains groups broader than 0.5 lethargy, these cross sections should be generated by regionwise collapsing, using representative spectra for each of the regions i.e., Figure 2, from a structure that has no groups greater than 0.5 lethargy width down to a lethargy of 12.5

** Approximately corrected for sample size effects.

4. Rossi Alpha at delayed critical = $-(6.84\pm0.20)\times10^{4}\,sec^{-1}$.

F. Comments and Documentation

The primary source of information for this benchmark has been one internal ZPR-III memo giving details and results of experiments on Assembly 12. Much of the data have been reported by Long[1]; however, some of the originally published values have been adjusted with later determined corrections, including heterogeneity effects on critical mass and chamber wall effects on fission ratios. The reactivity coefficients listed have been assigned high uncertainties because of the large sample sizes used.

The eigenvalue for the one-dimensional model from the prescribed S_4 calculations differs from a hypothetical $S_{infinity}$ eigenvalue by an estimated $\Delta k/k = 0.0018$.

The conversion from inhours to $\Delta k/k$ is 427 Ih = .01 $\Delta k/k$.

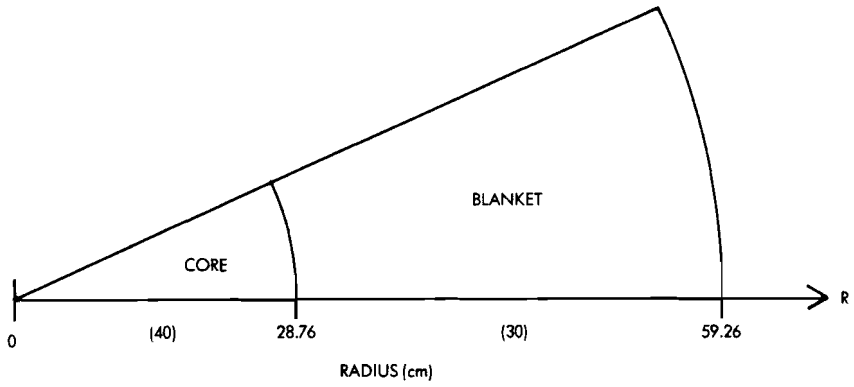

Figure 1. Spherical Model of ZPR-III Assembly 12.
Suggested Number of Mesh Intervals in ( ).

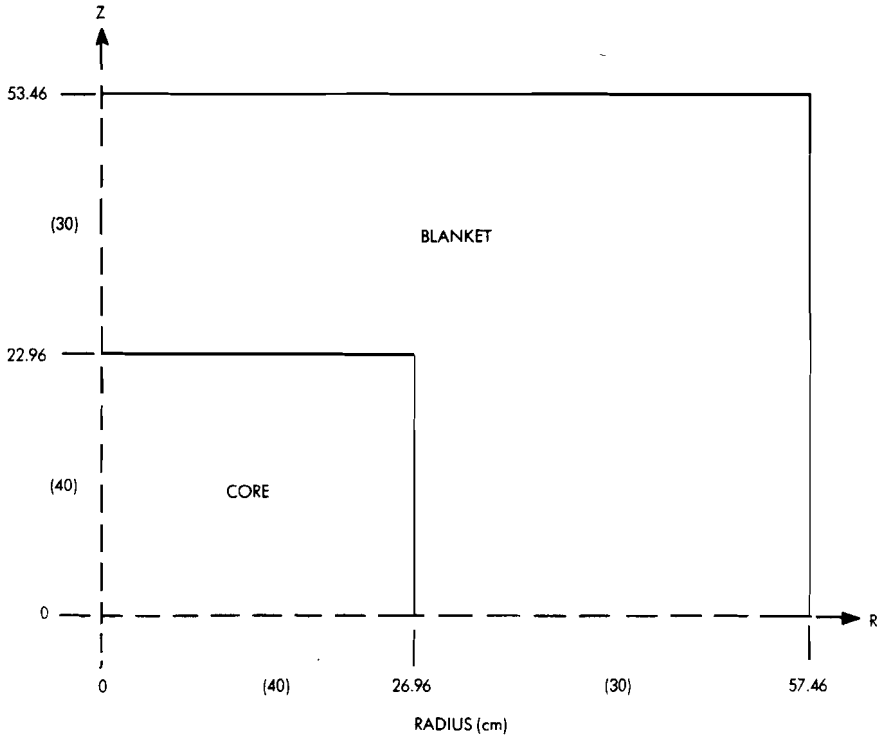

Figure 2. Two-Dimensional (R-Z) Model of ZPR-III Assembly 12.
Suggested Number of Mesh Intervals in ( ).

TABLE I

ZPR-III ASSEMBLY 12 REGION COMPOSITIONS (ATOMS/BARN-CM)

Material	Core	Blanket
U-235	0.004516	0.000089
U-238	0.016948*	0.040026
U-234	0.000046	-
C	0.026762	-
Fe	0.005704	0.004971
Cr	0.001419	0.001237
Ni	0.000621	0.000541
Mn	0.000059	0.000052
Si	0.000069	0.000060

* Including U-236.

FAST REACTOR BENCHMARK NO. 10

A. Benchmark Name and Type

ZEBRA-2, a 6:1 uranium-plus-graphite system.

B. System Description

The ZEBRA facility consists of stainless steel tubes containing reactor materials mounted vertically on a 3-meter square base plate. A pin at the lower end of each element fits into the base plate and the elements are restrained laterally by 3 steel lattice plates. The central 27 cm square of the base plate is removable so large experiments may be mounted in the reactor center. A concrete shield and steel containment vessel complete the structure.

ZEBRA Core 2 was a cylindrical critical assembly with a core height of 83.82 cm and an effective core diameter of 80.26 cm. The core is surrounded by a blanket of natural uranium having an axial thickness of 30.48 cm and an effective radial thickness of 33.26 cm. A complete detailed description of this assembly is found in the report AEEW-R410, "The Second Core of ZEBRA", by A. M. Broomfield, et al published in 1965.

ZEBRA-2 was designed to explore the accuracy of neutron cross section data for U-235 and U-238. The core contains some graphite and has a neutron spectrum similar to that of a large power reactor.

C. Model Description

A one-dimensional spherical model of ZEBRA-2 is given in Figure 1. A vacuum boundary condition should be applied to the outer reflector boundary. Material atom densities for the core and reflector regions are given in Table 1. The standard calculational mode is an S_4 transport theory calculation using a multigroup structure composed of 26 groups, each of lethargy width equal to 0.5 and with E_{max} set to 10 MeV. The number of mesh intervals for core and reflector are 40 and 30, respectively.

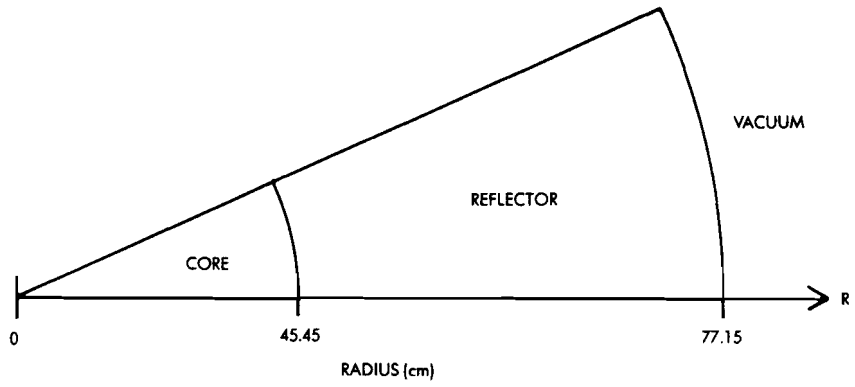

Figure 1. Spherical Model of ZEBRA-2 Assembly

2. Two-Dimensional Model Description

A two-dimensional (R-Z) cylindrical model of the ZEBRA 2 assembly is given in Figure 2. A zero return current boundary condition should be applied to the top and right side of the model; a symmetry boundary condition should be applied along the model bottom. The standard calculation mode is two-dimensional diffusion theory with mesh as follows: 40 radial and axial intervals in core; 30 intervals for the reflector thickness.

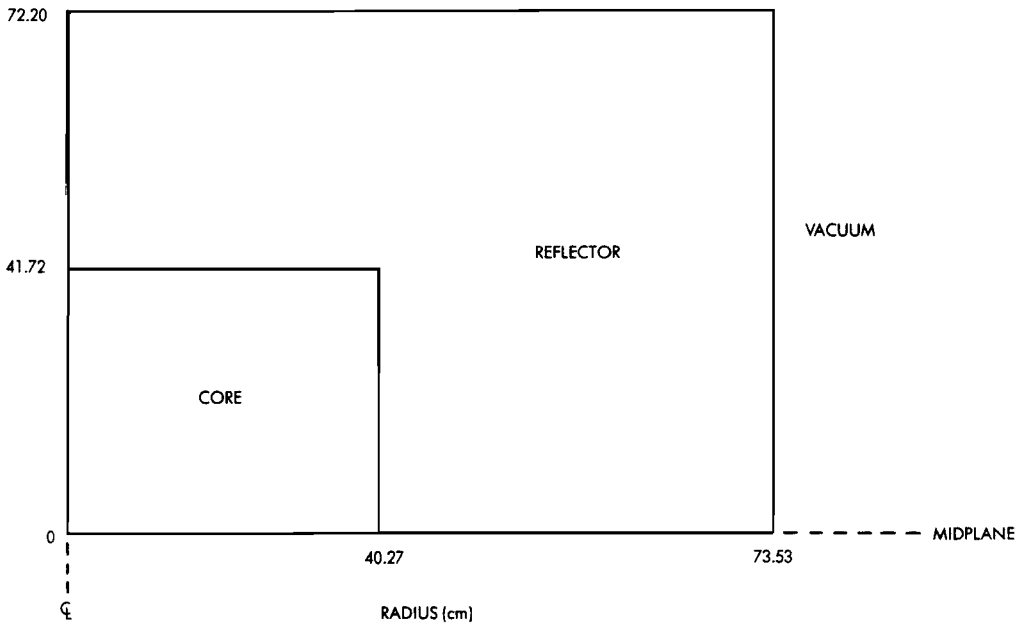

Figure 2. Two-Dimensional (R-Z) Model of ZEBRA-2 Assembly

Table 1.

ZEBRA 2 Region Compositions*

(Atoms/Barn-cm)

Material	Core	Reflector
U-235	0.002526	0.000298
U-238	0.015667	0.041269
H	0.00030876	-
O	0.0001544	-
Fe	0.0036485	0.003323
Cr	0.000864	0.000864
Cu	0.000004	0.000004
Mo	0.000008	0.000008
Mn	0.000064	0.000064
Ni	0.000483	0.000483
Aℓ	0.000019	0.000019
Ti	0.000016	0.000016
Si	0.000054	0.000054
V	0.000005	0.000005
C	0.037992	0.000042

*Revised: Private communication, R. W. Smith (AEEW) to H. Alter, 11/70

D. Experimental Data

1. Experimental Critical Mass — 418±1 Kg U-235

   Corrections for Irregularities — -2.6±0.3

   Finite Fuel Plate Thickness (Fuel + Diluent) — +3.1±6.2

   Homogeneous Cylinder Critical Mass — 418.5±6 Kg U-235

   Experimental Eigenvalue — 1.000±0.002

2. Experimental Spectral Indices at Core Center Relative to σ_f U-235

σ_f (U-238)	= 0.0320±0.0005	σ_c (U-238)	= 0.136±0.001
σ_f (U-233)	= 1.453±0.014	σ_c (Au)	= 0.298±0.015
σ_f (U-234)	= 0.153±0.016	σ_c (Mn)	= 0.026±0.002
σ_f (U-236)	= 0.093±0.014	σ_c (Ta)	= 0.401±0.040
σ_f (Pu-239)	= 0.987±0.010	σ_c (Na)	= 0.0013±0.0001
σ_f (Pu-240)	= 0.237±0.004	σ_c (B-10)	= 1.58±0.07
σ_f (Np-237)	= 0.214±0.002		

3. Material Worths at Core Center

Material	Reactivity Coefficient (10^{-5} Δk/k/mole)	Material	Reactivity Coefficient (10^{-5} Δk/k/mole)
U-235	68.4±0.7	Au	-15±1
U-238	-5.3±0.3	Cu	-1.8±0.1
Pu-239	97.3±1.2	Fe	-0.6±0.1
Pu-240	22±4	Cr	-0.6±0.1
B-10	-94±3	Ni	-1.2±0.1
B	-20±1	Mn	-0.85±0.10
Li-6	-39±2	Na	0.14±0.10
Li	-4.2±0.4	Aℓ	-0.27±0.10
Ta	-23.2±0.4	C	0.31±0.05
Hf	-20.9±0.4	H	15±1

The reactivity coefficients given in D.3 are values for effective zero size samples as quoted in the references.[1][2] The conversion from inhours to $\Delta k/k$, as calculated by ZEBRA personnel for that assembly is 480 Ih = 0.01 $\Delta k/k$.

4. Rossi Alpha

At delayed critical, $\alpha = -2.82 \pm 0.05 \times 10^{4}$ sec^{-1}. Also extrapolation to zero alpha gave 339 inhours per dollar.

F. Comments and Documentation

ZEBRA 2 was a cylindrical critical assembly. The experimental information was detailed in report AEEW-R410.[1] Another report, AEEW-R373[2] contains results of investigations into sample size effects upon material worth measurements. Comment was received from R. W. Smith[3] regarding material composition changes in core and reflector and those revised material compositions are given in Table 1. Smith also advised that an allowance had been made for the moisture contamination of the graphite of approximately 700±200 p.p.m. hydrogen. The effect on k_{eff} is approximately 1.1% $\Delta k/k$.

The experimental critical mass was 418±1 Kg U-235. Corrections for edge irregularities and heterogeneity effects were -2.6+0.3 and +3.1±6.2 Kg U-235, respectively, resulting in homogeneous cylinder critical mass of 418.5±6 Kg U-235. Plates in the fuel elements in the ZEBRA assemblies form continuous planes perpendicular to the axis of the core. It was therefore possible to estimate corrections for heterogeneity ($\sim$ 1% in k) from infinite slab calculations. Applying a shape factor of 0.925±0.005 gives a homogeneous spherical critical mass of 387±6 Kg U-235. The corresponding critical sphere radius is 45.45±0.22 cm.

The correction to the S_4 eigenvalue result to extrapolate to an "S_∞" eigenvalue is estimated to be -0.0005. For example, if the k_{eff} (S_4) value was 1.0000, then the value for S_∞ would be 0.9995.

REFERENCES

1. A. M. Broomfield, et al., "The Second Core of ZEBRA", AEEW-R410 (1965).
2. G. Ingram, et al., "Central Perturbation Cross Sections in ZEBRA Cores 1 and 2", AEEW-R373 (1964).
3. Private Communication, R. W. Smith (AEEW) to H. Alter (11/70).

FAST REACTOR BENCHMARK NO. 11

A. Benchmark Name and Type

ZPPR Assembly 02, a Demonstration Fast Reactor Benchmark Critical

B. System Description

ZPPR Assembly 02, Loading No. 90 was designed as a fast reactor benchmark critical experiment. Its composition and neutron spectrum are typical of an LMFBR. An R-Z representation of ZPPR Assembly 02 is shown in Figure 1. The reference loading contained equal volumes in the inner and outer core zones. The inner core zone was composed from a repetition of a one-drawer unit cell; the outer core zone utilized a two-drawer cell. Both inner and outer core zones contained some partial core drawers with 1/2 inch wide void channels (for poison rods) alongside, and the inner core contained movable control drawers. The region compositions in Tables I and II are not the unit cell compositions, but include the perturbation (in sodium and steel densities) due to the void channels and control drawers.

C.1 One-Dimensional Homogeneous Model Description

A one-dimensional radial model of ZPPR Assembly 02 is shown in Figure 2, including model dimensions, boundary conditions and suggested mesh. The atom densities in each region (atoms/barn-cm) are given in Table I. The perpendicular buckling to be used in all regions and groups is 5.92×10^{-4} cm.$^{-2}$ Diffusion theory is suggested with cross sections in any suitable fast reactor energy-group structure, but with groups no coarser than 0.5 lethargy width down to a lethargy of 12.5. A heterogeneity correction of +0.0175 $\Delta k/k$ should be applied to the calculated eigenvalue, to account for flux variations in the unit cells.

C.2 Two-Dimensional Model Description

The two-dimensional (R-Z) model of ZPPR Assembly 02 is shown in Figure 1, including model dimensions and suggested mesh. Zero return current boundary conditions are to be applied on the top, bottom and right boundaries. The atom densities in each region (atoms/barn-cm) are

given in Tables I and II. Diffusion theory is suggested with cross sections in any suitable fast reactor energy group structure*. The effects of heterogeneity should be included in the generation of the multigroup cross sections for each region, using the unit-cell descriptions in paragraph C.3.

C.3 Unit-Cell Descriptions

The outer dimensions of the ZPPR matrix tubes, determined from the total lattice dimensions, are a width of 5.5245 cm and a height of 5.7839 cm. The drawers inserted into the tubes have an inside cross section of 2 inches square for the loading of the various reactor-material plates. Thus, the total cell can be represented as a 2 x 2 inch loading area of plates inside a structural box, as illustrated in Figure 3. The arrangements of the plate columns used for the Assembly 02 core and blanket cells are shown in Figure 4.

Tables III and IV give average widths and compositions for the plate columns used in the core and blanket drawers. For the canned materials (fuel, sodium, and Na_2CO_3) a nominal thickness of 0.015 in. was chosen for the steel cladding, and the remainder of column width (1/4 in. or 1/2 in.) was assumed to be occupied by the fuel, Na, or Na_2CO_3-plate core. For all of the column materials, the densities were derived assuming the assigned widths, a height of 2 in. and a length of 18.036 in. (column length plus thickness of drawer front). Table IV includes the composition for the side structure of the cell (drawer plus matrix) homogenized over the true widths of the matrix wall plus drawer side plus slack. Compositions for the upper and lower regions of the cells as indicated in Figure 3 are given in Table V: These include the drawer front and bottom, matrix, edges and ends of the claddings, and in some cases shims on the bottom of the plate loadings.

---

*If the two-dimensional problems are run with a group structure that contains groups broader than 0.5 lethargy, these cross sections should be generated by regionwise collapsing, using representative spectra for each of the regions in Figure 1, from a structure that has no groups greater than 0.5 lethargy width down to a lethargy of 12.5.

Tables III and IV include a letter designation at the top for each of the different types of material columns. For cell calculations to be used in determining heterogeneously-averaged cross sections, the overall cell for each region can be viewed as a stack of vertical columns (5.08 cm high by 5.5245 cm total width) sandwiched between horizontal upper and lower plates of structure: The cell descriptions so conceived are as follows:

1. Inner Core Cell

The plate-loading pattern for core zone 1 is shown at the top in Figure 4 using the notations for column labels as given in Tables III and IV, the vertical constituents of the cell (including the side structure of the matrix and drawers) are as follows:

L B J H J F J A J F J H J B L

Column 2 of Table V gives the upper and lower structure atom densities for these drawers (which had steel shims on the bottom).

2. Outer Core Cell

As shown in the middle of Figure 4, the outer core cell was actually a two-drawer cell with three columns of fuel (giving a 1.5 ratio of fuel density of the outer zone relative to the inner zone). For simplicity, it is represented here as two cells, A and B:

Outer core A, with upper/lower structure in column 3 of Table V,
L F J A J E J H J B J G J È J A J F L.
Outer core B, with upper/lower structure in column 4 of Table V,
L J H J F J A J F J H J B J G J L.

3. Radial Blanket Cell

The loading pattern at the bottom left in Figure 4 was that used in the front 23 in. (to the

spring gap) in each half of the Inner Radial Blanket. The column notations for these regions would thus be

L C D J H J B B D J I J L.

For the back 16 in. of the Inner Radial Blanket (beyond the spring gap in each half of the assembly) the U_3O_8 was all in the form of 1/2 in. thick plates, giving the pattern of vertical constituents as

L C D J H J C D J I J L.

The upper/lower structure composition in column 5 of Table V applies to the overall average cell (full 34-in. length in each assembly half) of the Inner Radial Blanket.

The Outer Radial Blanket contained double columns of 1/4-in.-thick sodium in place of the 1/2-in.-thick Na above, giving the pattern for the front 23 in. as

L C D J G J J G J B B D J I J L,

and for the back 11 in. as

L C D J G J J G J C D J I J L.

4. Axial Blanket Cell

As indicated in Figure 4, a two-drawer cell was used for the axial blanket regions, the difference between the two drawers being a column (1/8 in.) of steel in place of a column of Fe_2O_3. Thus for the Fe_2O_3-loaded drawer, the pattern of vertical components would be

L B J H J E B D J H J B L,

and the steel-loaded drawer pattern would be

L B J H J K B D J H J B L.

The axial blanket behind the inner core contained steel shims at the bottom of the drawers, giving a high-density upper/lower structure region as indicated in column 6 of Table V.

The last column of Table V lists the upper/lower structure composition for the cell of the axial blankets behind the outer core.

The inclusion of all these cell descriptions is not to suggest that calculations are needed for each case to generate cell-averaged cross sections for all regions, but rather to point out the variances typically encountered in the construction of the critical assemblies and to show why the region compositions differ. One cell calculation each for the radial and axial blankets, with the patterns shown at the bottom of Figure 4, should be sufficient to obtain multigroup sets for use in all blanket and reflector regions.

It should also be mentioned that the homogenized compositions of the cell descriptions cited above will not agree exactly with the average region compositions given in Tables I and II because the column densities presented in Tables III and IV are averages of several lengths of plates, whereas the different regions involved variations of column plate-length patterns. Also, as indicated earlier, the core and axial blanket regions contain void channels and extra drawer steel homogenized into their compositions.

D. Experimental Data

1. Measured Keff = 1.0000 $\pm$ .0006

2. Experimental spectral indices at the core center, relative to σ_f (U-235) are as follows:

σ_f (U-233) = 1.446 ± 0.022
σ_f (U-234) = 0.1492 ± 0.0023
σ_f (U-236) = 0.0443 ± 0.0007
σ_f (U-238 = 0.0201 ± 0.0004
σ_f (Pu-239) = 0.9372 ± 0.0142
σ_f (Pu-240) = 0.1704 ± 0.0026

3. Material worths at the core center are as follows:

Material	Reactivity Coefficient 10^{-5} $\Delta k/k/mole$
Pu-239	28.29 ± 0.19
Pu-241	38.7 ± 4.9
U-235	20.86 ± 0.48
C	-0.1348 ± 0.0093
Na	-0.1172 ± 0.0056
Ta	-9.10 ± 0.18
B10	-22.37 ± 0.41
Fe	-0.1736 ± 0.0045
Cr	-0.174 ± 0.012
Ni	-0.2755 ± 0.0095
Al	-0.160 ± 0.014
Mn	-0.414 ± 0.018
W	-1.957 ± 0.009
Mo	-1.223 ± 0.052
Nb	-1.606 ± 0.060

E. Comments and Documentation

The radial dimensions for the core zones in Figures 1 and 2 have been adjusted to give a k = unity model with equal volumes in both zones. The adjustments account for the following corrections to the as-built loading:

1. Partial insertion of control rods
2. Subcriticality at operating power
3. The gap between the halves of the reactor
4. Uniform temperature representation (22.0°C average)

There were no control drawers spiked with extra fuel in this loading and the effect of smoothing the radial outlines of the inner and outer core was estimated to be negligible.

The total adjustment to the as-built Pu-239 + Pu-241 loading to derive the k = unity model was -8.5 ± 0.9 kg; with equal volume reductions in the inner and outer core zones, this gave the core radii shown in Figures 1 and 2. The radial blanket and reflector radii were adjusted to obtain the same thicknesses as in the as-built case. Overall, the loading uncertainty is about $\pm$ 1.5 kg of Pu-239 + Pu-241 (out of 1024 kg). This gives an uncertainty for the k = unity model of about $\pm$ 0.0006 $\Delta k/k$.

For the one-dimensional homogeneous model, the perpendicular buckling was determined in a CAESAR consistent-keff calculation. CAESAR is a diffusion theory code; a consistent-keff calculation alternates one-dimensional radial, axial and zero-leakage calculations until the bucklings give the same eigenvalue as in the two-dimensional model for both the radial and axial cases. 25 energy groups were employed.

The conversion from inhours to $\Delta k/k$ is 1015.7 Ih = .01 $\Delta k/k$. The calculated model was specified by Hess (ANL) and modified by Otter (AI).

1. R. E. Palmer, et al, "ZPPR-2 Benchmark Analyses to January 1971", ZPR-TM-51 (January 20, 1971)

2. R. E. Kaiser, et al, "Experimental Evaluations of the Critical Mass for ZPPR Assembly 2", ZPR-TM-47 (January 20, 1971)

3. ZPPR Staff, "ZPPR 2 Benchmark Experimental Data to January 1971", ZPR-TM-48 (January 20, 1971)

4. Private communication A. Hess to H. Alter, "Benchmark Model for ZPPR Assembly 02", January 1971.

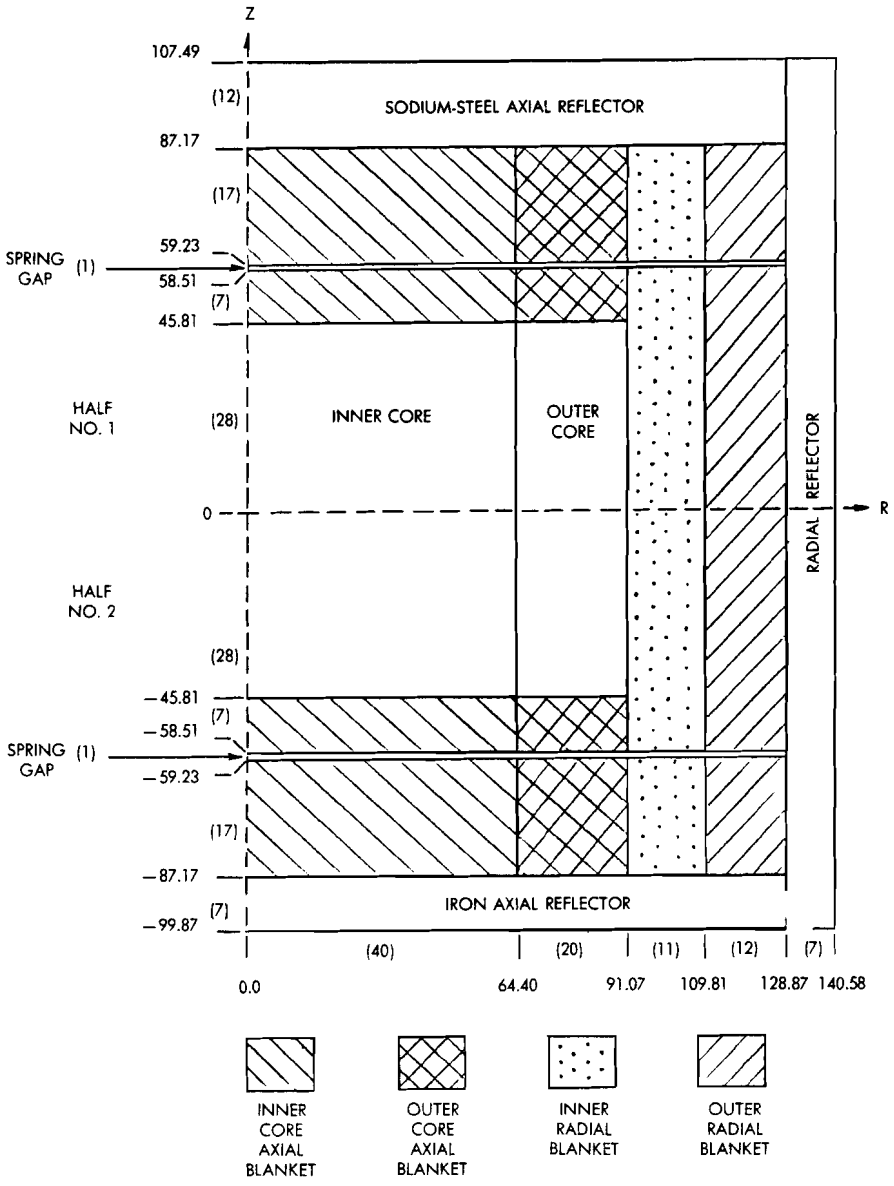

Figure 1. Benchmark Model of ZPPR Assembly 02.
Dimensions in cm; Suggested Number of Mesh Intervals in ( ).

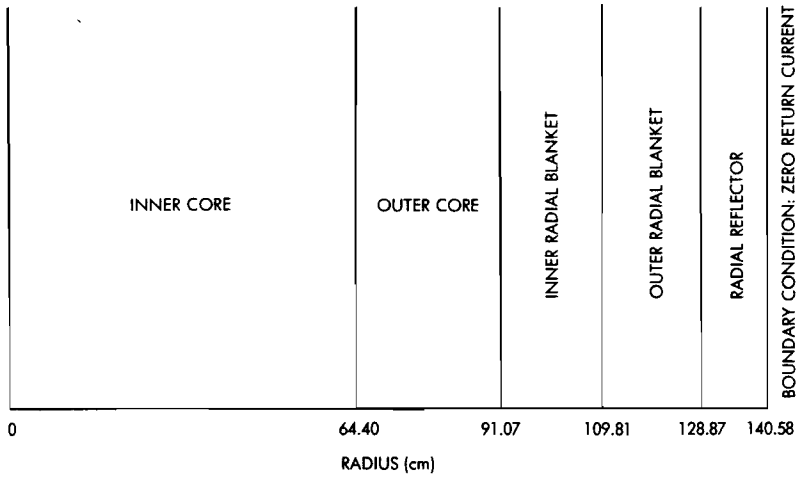

Figure 2. Radial Model of ZPPR Assembly 02.
Suggested Mesh: 40 Intervals, Inner Core; 20 Intervals Outer Core;
30 Intervals Across Inner/Outer Blankets and Reflector.

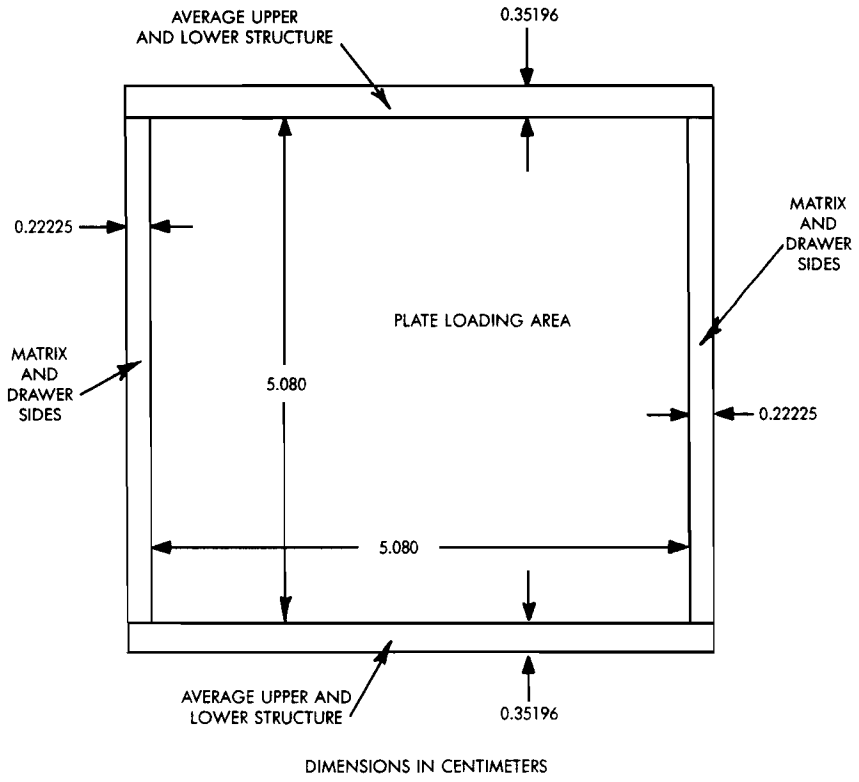

Figure 3. Geometry of ZPPR Unit-Matrix Cells

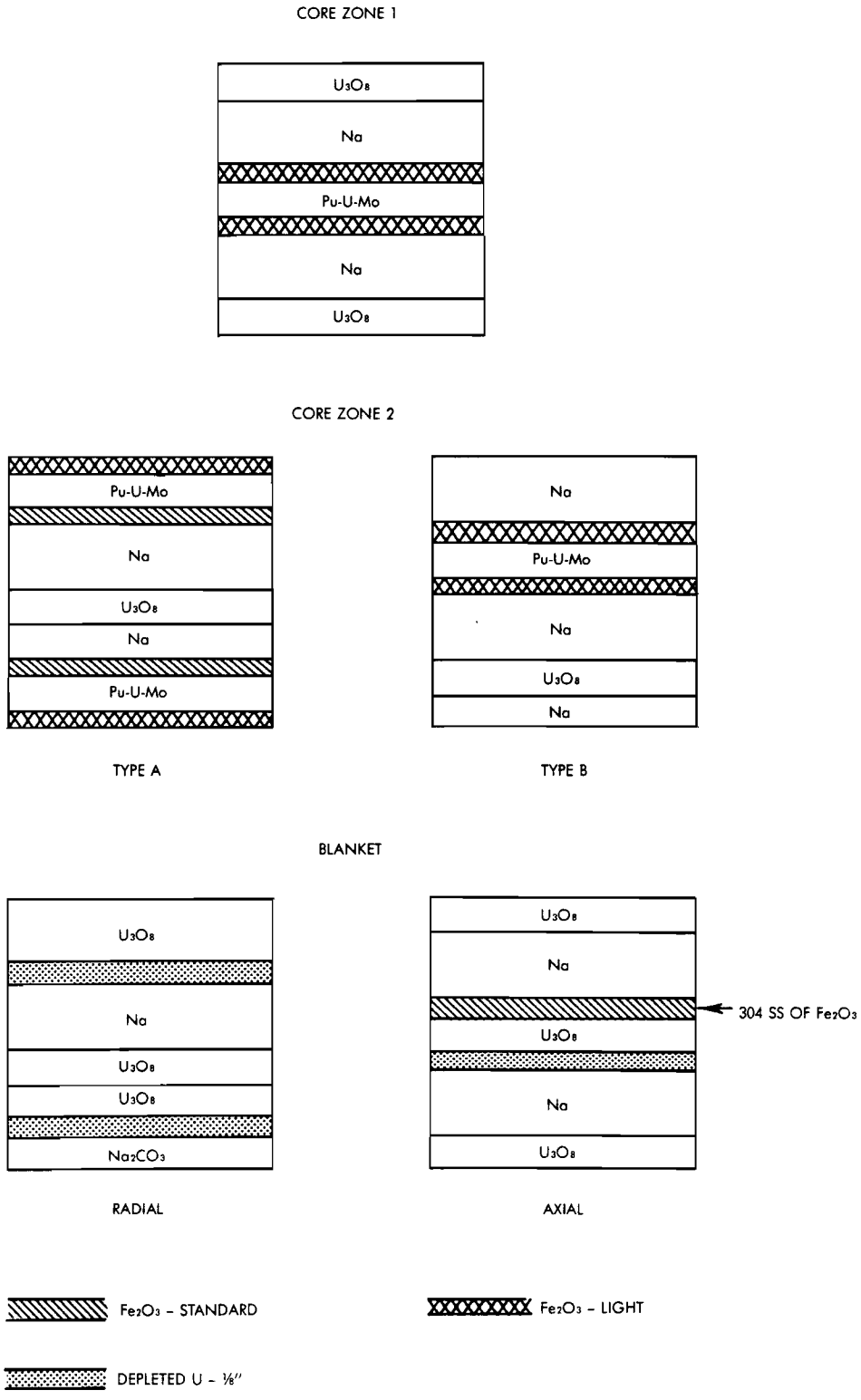

Figure 4. Cell-Loading Patterns for ZPPR Assembly 02

Table I

ZPPR Assembly 2, a Demonstration Fast Reactor Benchmark Critical
Radial Region Compositions at Axial Centerline (atoms/barn-cm)

Material	Inner Core	Outer Core	Inner Radial Blkt.	Outer Radial Blkt.	Radial Reflector
Pu 239	.0008433	.0012741			
Pu 240	.0001117	.0001687			
Pu 241	.0000153	.0000231			
Pu 242	.0000018	.0000028			
Pu 238	.0000006	.0000009			
Am 241	.0000029	.0000043			
U 235	.0000123	.0000115	.000024	.000024	
U 238	.0055549	.0051980	.011085	.011085	
C	.00003	.000023	.001013	.001013	.000558
O	.013116	.011761	.020132	.020133	
Na	.008796	.008564	.006398	.005963	
Al	.000003	.000004	.000002	.000003	
Fe	.012576	.013852	.006923	.007541	.075161
Cr	.002702	.002523	.001991	.002172	.001205
Ni	.001221	.001160	.000898	.000987	.000513
Mn	.000209	.000202	.000157	.000174	.000598
Cu	.000019	.00002	.000017	.000018	.000013
Mo	.000231	.000341	.000014	.000015	.000012
Si*	.000137	.000118	.000094	.000102	.000091
H	-	-	.000008	.000008	

*Includes minor concentrations of P and S

Table II

ZPPR Assembly 02, a Demonstration Fast Reactor Benchmark Critical

Region Compositions Off Axial Centerline (atoms/barn-cm)

Material	Axial Blanket Over Inner Core	Axial Blanket Over Outer Core	Spring Gaps	Sodium Steel Axial Reflector	Iron Axial Reflector
U 235	.000016	.000016			
U 238	.007036	.007057			
C	.000036	.000030	.000284	.000214	.000557
O	.013895	.014008			
Na	.008739	.008808		.008966	
Al	.000002	.000002	.000001	.000002	
Fe	.010751	.009355	.021133	.035713	.072271
Cr	.002835	.002418	.004393	.005347	.001639
Ni	.001275	.001095	.001503	.002412	.000706
Mn	.000230	.000205	.000279	.000611	.000623
Cu	.000017	.000017	.000030	.000017	.000014
Mo	.000014	.000014	.000023	.000014	.000013
Si*	.000150	.000119	.000182	.000305	.000114

*Includes minor concentrations of P and S

Table III. Specifications of Fuel, Fertile, and Iron Oxide Constituents of Core and Blanket Cells

Cell Component	Cores of Pu-U-Mo Alloy Plates	1/4 in. thick U_3O_8 Columns	1/2 in. thick U_3O_8 Columns	1/8 in. thick Depleted U Columns	Standard Fe_2O_3 Columns	Light Fe_2O_3 Columns
Label	A	B	C	D	E	F
Thickness (cm)	0.5588	0.6350	1.2700	0.3175	0.3175	0.3175
Atom Densities (atoms/barn-cm)						
Pu 238	.000006	- -	- -	- -	- -	- -
Pu 239	.009501	- -	- -	- -	- -	- -
Pu 240	.001258	- -	- -	- -	- -	- -
Pu 241	.000173	- -	- -	- -	- -	- -
Pu 242	.000021	- -	- -	- -	- -	- -
Am 241	.000032	- -	- -	- -	- -	- -
U 235	.000060	.000034	.000035	.000103	- -	- -
U 238	.026988	.015646	.016189	.045778	- -	- -
Mo	.002436	- -	- -	- -	- -	- -
O	- -	.041691	.042901	- -	.055404	.046632
Fe	- -	- -	- -	- -	.036869	.031735

Table IV. Specifications of Sodium, Sodium Carbonate, Cladding and Reactor-Structure Constituents of Core and Blanket Cells

Cell Component	Cores of 1/4 in. Na Columns	Cores of 1/2 in. Na Columns	Cores of 1/4 in. Na_2CO_3 Columns	Cladding of Fuel, Na and Na_2CO_3 Plates	1/8 in. thick Stainless Steel Column	Structure Side Wall, Matrix and Drawer
Label	G	H	I	J	K	L
Thickness, cm	0.5588	1.1938	0.5588	0.0381	0.3175	0.22225
Atom Densities, (atoms/barn-cm)						
Na	.022302	.023300	.022291	- -	- -	- -
C	- -	- -	.011140	- -	.000270	.000162
O	- -	- -	.033438	- -	- -	- -
Fe	- -	- -	- -	.055936	.058032	.035911
Cr	- -	- -	- -	.016276	.016146	.010303
Ni	- -	- -	- -	.008189	.007303	.004510
Mn	- -	- -	- -	.001176	.001584	.000875
Si*	- -	- -	- -	.000778	.000981	.000501
Mo	- -	- -	- -	.000043	- -	.000086
Cu	- -	- -	- -	.000093	- -	.000096
Al (H)	- -	- -	.000094	.000067	- -	- -

*Includes minor concentrations of S and P

Table V. Compositions of Upper and Lower Cell Structure

Material	Average Compositions of Upper and Lower Structural Regions [a] for Core and Blanket Cells, atoms/barn-cm					
	Cell for Inner Core	Cell for Outer Core A	Cell for Outer Core B	Cell for Inner Radial Blanket	Cell for Axial Blanket of Inner Core	Cell for Axial Blanket of Outer Core
Fe	.039436	.028733	.028801	.024899	.036611	.035240
Cr	.011337	.008237	.008268	.007141	.010693	.007347
Ni	.004960	.003643	.003482	.003128	.004703	.003259
Mn	.000860	.000680	.000683	.000551	.000814	.000621
Si*	.000607	.000335	.000338	.000330	.000580	.000332
Mo	.000054	.000050	.000055	.000060	.000059	.000059
Cu	.000072	.000074	.000074	.000065	.000068	.000068
Al	.000008	.000009	.000009	.000003	.000007	.000007
C	.000148	.000097	.000097	.000096	.000144	.000094

[a]Region dimensions as illustrated in Figure 3.

*Includes minor concentrations of P and S.

FAST REACTOR BENCHMARK NO. 12

A. ZPR-6 Assembly 7 - A Plutonium Oxide Fueled Fast Critical Assembly.

B. System Description:

The ZPR-6 consists of two halves, each a horizontal matrix of 2.2 in. square stainless steel tubes into which are loaded stainless steel drawers containing fuel and diluent materials of various types. Assembly 7 is a large (3100 liter) fast critical assembly with a soft spectrum and other characteristics representative of current LMFBR designs. It has a single fuel zone with a length-to-diameter (L/D) ratio of approximately unity; it has a simple one-draw unit cell; and it is blanketed both axially and radially with depleted uranium.[1] The assembly's spectrum characteristics, simple geometric configuration, and simple unit cell make it well suited for a benchmark assembly.

The unit cell, which is shown in Fig. 1 is identical to that of a companion benchmark assembly; ZPR-6 Assembly 6A, except that the fuel is Pu/U/Mo (28 w/o plutonium, 69.5 w/o uranium and 2.5 w/o molybdenum) rather than enriched uranium. The plutonium is 11.5 w/o ^{240}Pu. A cross sectional view of the as-built reference assembly, which had an excess reactivity of 96.2 Ih, is shown in Fig. 2 and the equivalent cylindricalized representation of the as-built system is shown in Fig. 3.

C. Model Description:

1. One-Dimensional Model: A one-dimensional model with spherical geometry has been used in the analysis of many measurements in the assembly. The spherical model was defined with reference to a two-dimensional finite cylindrical model, which will be described in Section C.2. The homogeneous spherical model was defined by first determining a blanket thickness and then searching for a core radius that gives the spherical reactor the same k_{eff} as the homogeneous two-dimensional cylinder. The blanket dimensions and compositions were defined as the weighted average of the axial and radial blanket dimensions and compositions in which the weighting was done on the basis of the relative leakages into the axial and the radial blankets (as given by the two-dimensional calculations). The resulting core radius and blanket thickness for the homogeneous spherical model were 88.16 and 33.81 cm, respectively. The appropriate compositions for use with the spherical model are given in Table I. The spherical model is expect to introduce approximately a 0.1% uncertainty in k_{eff}.

An energy group structure with 27 groups, as given in Table II, is suggested. Such a structure has sufficient detail at low energies to afford accurate computations of material worths and Doppler effects.

Because of the simplicity of the two-region, homogeneous spherical model, the macroscopic flux distributions across the

reactor may be computed with diffusion theory and a relatively coarse mesh of 2 cm should be adequate.

Central material reactivity worths and Doppler reactivity worths may be computed by perturbation tehory. If the material sample is optically thin and if the material is contained in the core, the homogeneous core cross sections for the material are appropriate to the sample. If the material sample is optically thin and, if the material is not contained in the core, then infinite dilution cross sections are appropriate for the sample.

The major flaw in the homogeneous spherical model for this geometrically simple system is in the neglect of heterogeneities in the unit cell. Sections D and F indicate the uncertainties arising from the use of homogeneous cross sections. The error in material worth or Doppler worth introduced by flux distortions depends strongly upon the nature of the sample.

2. Other More Complicated Models: A two-dimensional finite cylindrical representation of the system is closer to the physical configuration than a spherical representation. The as-built loading was thus corrected for both excess reactivity and edge smoothing. The spring gap was homogenized into the axial blanket and the radial blanket height was defined to be the same as the core plus axial blanket heights. Resulting region dimensions are given in Table III.[1]

The corresponding compositions for the zero-excess, uniform cylindrical model are given in Table IV. The "exact core region", at the center of the assembly, is simply a region in which material concentrations are known more accurately than in the rest of the core.

D. Experimental Data:

1. Measured Eigenvalues: The measured eigenvalue corresponding to the models of Section C is 1.0000 ± 0.001. Calculations indicate a 0.0166 heterogeneous-homogeneous correction[2] and a 0.0018 S_8-diffusion correction.

2. Unit-Cell Reaction Rates: Detailed unit-cell measurements of the capture and fission in ^{238}U and fission in U^{238} and ^{239}Pu were made. Activation foils of ^{238}U, ^{235}U, and ^{239}Pu were used to measure the rates within the fuel and U_3O_8 plates, such that the actual cell-averaged values of the reaction rates could be obtained. To be clear, these unit-cell reaction rate values correspond to the reactions actually taking place in the unit-cell in the assembly, and not, for example, to a cell-average defined as the value of the flux at every point in the cell multiplied by the cross section of the foil material. We use the term to refer to the flux and volume weighted reaction rates as they actually occur in the unit-cell. Hence, a per atom unit-cell reaction rate ratio is converted to the actual ratio of the number of reactions taking place in the cell simply by multiplying

the former ratio by the appropriate atom density ratio.

The details of the technique used for counting the activated foils and reducing the data to absolute reaction rates are identical with those used in Ref. 3. The absolute calibrations were made with three separate and independent techniques: (1) by absolute fission chambers with identical foils on their faces to those used in the unit-cell measurements, with the fission chambers placed in the reactor at the same spectral position; (2) by thermal irradiation of identical foils in ATSR thermal column; and (3) by absolute radiochemical analysis of some of the foils that were actually used in the unit-cell measurement. The excellent agreement among the various calibration methods made possible the small uncertainty, $1\sigma = 2\%$, in the measured reaction rate ratios.

For the plate cell environment, the unit cell in which the reaction ratios were measured differed somewhat from the "normal unit-cell" of Fig. 1. In the "experimental" unit-cell, instead of the normal 1/4 in. thick Pu/U/Mo plate, two thinner Pu/U/Mo plates were used to permit foils to be placed at the center of the fuel column so that an integration of the reaction rates through the fuel plate could be made. Each of the plates had a 0.015 in. stainless steel cladding and a 0.095 in. core thickness. The effect of this substitution for the normal fuel plate was to reduce the fuel content of the experimental unit-cell (33% less Pu-Mo, 15% less ^{238}U) and to increase

its stainless steel content by 7.5%. The measured reaction rate ratios for ^{238}U Capture-to-^{239}Pu fission, ^{238}U fission-to-^{239}Pu fission, and ^{235}U fission-to-^{239}Pu fission are given in Table V along with calculated correction factors (to be applied to the measured values) for heterogeneities.[1,2]

3. Material Worths at the Center of the Core: Central reactivity worths of several materials were measured in a small cavity with use of the radial sample changer. The uranium and plutonium samples were thin annuli clad on the outside with stainless steel. The other samples were generally unclad cylinders. The samples were held in thin-walled stainless steel sample holders and the reactivity worth of the sample was obtained by the difference in the reactivity worth (relative to void) of the sample holder between when it is empty and when it holds a sample. Further descriptions of the samples and the measurements are given in Ref. 4. Table VI gives the experimental worths of the isotopes, the weights and identifications of the samples from which they were obtained, and the calculated results.

E. Calculated Results:

The calculations described in this section were made using ENDF/B-III data and the standard one-dimensional, homogeneous spherical model of the assembly. The fundamental mode option of the SDX[5] code was used to compute homogeneous cross sections. This model yielded a multiplication constant of 0.9772 for the critical system. The addition

of the heterogeneity and transport corrections (Section D.1) gives a k_{eff} of .9956.

The calculated values for the reaction rate ratio values for the normal plate unit cell are given in Table VII.

The central worth calculations based on the homogeneous spherical model central fluxes are given in Table VII. The basic calculations used first-order perturbation theory.

F. Comments and Documentation:

To assess the limitations of the homogeneous, spherical Benchmark model the multiplication constant, reaction rate ratios and central reactivity worths were calculated with a one-dimensional spherical heterogeneous model and with a two-dimensional finite cylindrical, heterogeneous model. In this way, the errors from homogenization can be separated from the errors from the simplified geometric representation. The heterogeneous cross sections were computed with the plate unit-cell option in the SDX code, which uses equivalence theory in the narrow resonance approximation to obtain resonance cross sections and integral transport methods to obtain spatial weighting factors. The model used to represent the unit cell in these SDX problems is described in Ref. 7. For the one-dimensional model, the heterogeneous cross sections were obtained with the fundamental mode option of SDX; for the two-dimensional model, the space-dependent option was used.

The results of calculations with the three models are compared in Table VII. The one- and two-dimensional heterogeneous models are in good agreement. The difference in k_{eff} is due to both the use of fundamental mode cross sections in the spherical model and spherical model's being defined with ENDF/B-I data. From comparison of the homogeneous and heterogeneous results, heterogeneities account for a difference of about 1.7% in the multiplication constant. For the reaction rate ratios and the material worths of the homogeneous results are in surprisingly good agreement although they do show the changes in ^{10}B and ^{238}U worths expected from the spectrum difference.

For the central worth measurements, the conversion factor 1% $\Delta k/k$ = 1007 Ih was used to convert the measured periods to the desired reactivity units. The delayed neutron data of Keepin[8] were used in computing this conversion factor.

References

1. C.E. Till, L. G. LeSage, R. A. Karam, et al., "ZPR-6 Assemblies 6A and 7: Benchmark Speicifications for the Two Large Single-Core-Zone Critical Assemblies - ^{235}U-Fueled Assembly 6A and Plutonium-Fueled Assembly 7 - LMFBR Demonstration Reactor Benchmark Program", Applied Physics Division Annual Report, July 1, 1970 to June 30, 1971, 86-101, ANL-7910.

2. B. A. Zolotar, E. M. Bohn, and K. D. Dance, "Benchmark Tests and Comparisons Using ENDF/B Version III Data", Applied Physics Division Annual Report, July 1, 1971 to June 30, 1972, ANL-8010 (in press).

3. C. E. Till, J. M. Gasidlo, E. F. Groh, et al., "Null-Reactivity Measurements of Capture/Fission Ratio in ^{235}U and ^{239}Pu", Nucl. Sci. Eng. 40, 132 (1970).

4. L. G. LeSage, E. M. Bohn and J. E. Marshall, "Solium-Void and Small-Sample Reactivity Worth Measurements in ZPR-6 Assembly 7", Applied Physics Division Annual Report, July 1, 1970 to June 30, 1971, 141-154, ANL-7910.

5. W. M. Stacy, Jr., H. Henryson II, B. J. Toppel and B. A. Zolotar, "MC^2-2/SDX Development - Part II", Applied Physics Division Annual Report, July 1, 1971 to June 30, 1972, ANL-8010 (in press).

6. P. H. Kier, "Calculations of the Effects of Local Flux Distortions in Central Reactivity Worth Measurements in ZPR-6 Assembly 7", Applied Physics Division Annual Report, July 1, 1971 to June 30, 1972, ANL-8010 (in press).

7. J. E. Marshall, "The Unit-Cell Composition Model Developed for SDX Input Preparation and the Resulting Cell Speicifications for the ZPR/ZPPR Benchmark Assemblies". Applied Physics Division Annual Report, July 1, 1971 to June 30, 1972, ANL-8010 (in press).

8. G. R. Keepin, "Physics of Nuclear Kinetics", Addison-Wesley, Reading, Mass., 1965, Table 4-7.

TABLE I. Assembly 7 Spherical Model Atom Densities, atoms/barn-cm

Isotope	Core radius = 88.16 cm	Blanket thickness = 33.81 cm
^{239}Pu	0.00088672	-
^{240}Pu	0.00011944	-
^{241}Pu	0.0000133	-
^{235}U	0.0000126	0.0000856
^{238}U	0.00578036	0.0396179
Mo	0.0002357	0.0000038
Na	0.0092904	-
O	0.01398	0.000024
Fe	0.01297	0.004637
Cr	0.002709	0.001295
Ni	0.001240	0.0005635
Mn	0.000212	0.0000998

(Revised 9-78)

Table II. Specifications of 27-Group Structure

Group	ΔU	E_{upper},keV	Group	ΔU	E_{upper},keV
1	0.5	10000	14	0.5	15.034
2	0.5	6065.3	15	0.5	9.1188
3	0.5	3678.8	16	0.5	5.5308
4	0.5	2231.3	17	0.5	3.3546
5	0.5	1353.4	18	0.5	2.0347
6	0.5	820.85	19	0.5	1.2341
7	0.5	497.87	20	0.5	0.74851
8	0.5	301.97	21	0.5	0.45400
9	0.5	183.16	22	1	0.27536
10	0.5	111.09	23	1	0.10130
11	0.5	67.379	24	1	0.03727
12	0.5	40.868	25	1	0.01371
13	0.5	24.787	26	2	0.00504
			27	-	0.00068

Table III. Dimensions for the Zero-Excess Reactivity, Uniformly Loaded Cylindrical Version of ZPR-6 Assembly 7

Outer Core Radius, cm	80.30
"Exact Core" Region Radius, cm	24.34
Core Height, cm	152.56
Radial Blanket Thickness, cm	33.54
Radial Blanket Height, cm	221.10
Axial Blanket Thickness, cm	34.27
Core Volume, liters	3090

Table IV. Mean Atom Densities for the Zero-Excess Uniform Cylindrical Model of Assembly 7, atoms/barn-cm

	Exact Core	Outer Core	Axial Blanket	Radial Blanket
^{238}Pu	0.00000033	0.00000033	-	-
^{239}Pu	0.0008867	0.0008879	-	-
^{240}Pu	0.0001177	0.0001178	-	-
^{241}Pu	0.0000133	0.0000133	-	-
^{242}Pu	0.00000141	0.00000177	-	-
^{234}U	0.00000006	0.00000006	0.00000040	0.00000040
^{235}U	0.0000126	0.0000126	0.0000834	0.0000866
^{236}U	0.00000030	0.00000030	0.0000020	0.0000020
^{238}U	0.005777	0.005802	0.03859	0.04006
^{241}Am[a]	0.0000030	0.0000028	-	-
Mo	0.0002357	0.0002382	0.0000046[b]	0.0000034[b]
Na	0.0092904	0.009132	-	-
O[c]	0.01398	0.01482	0.000030[b]	0.000021[b]
Fe[d]	0.01297	0.01353	0.005652	0.004197
Cr	0.002709	0.002697	0.001579	0.0Q117
Ni	0.001240	0.001212	0.000691	0.0005082
Mn	0.000212	0.000213	0.000123	0.0000897

[a] ^{241}Pu decay to ^{241}Am corrected to 9/15/71

[b] Arising from SS304 impurities

[c] Includes ~0.005% from SS304 and Pu/U/Mo fuel impurities

[d] Includes ~0.0088% from heavy (atomic wt > Si) SS304 impurities and Pu/U/Mo fuel impurities.

Note: The number of digits in each density is a measure of the compositional precision. Nominally, the rightmost digit bounds the density according to a 2σ of 93% confidence interval.

Table V. Unit-Cell Reaction Rate Ratios in ZPR-6 Assembly 7

	Measurement (1σ = 2%)	Calculated Heterogeneity Correction Factors[a]
$^{28}c/^{49}f$	0.1400	1.023
$^{28}f/^{49}f$	0.02336	1.030
$^{25}f/^{49}f$	1.061	0.989

[a] homogeneous/heterogeneous

TABLE VI. Control Reactivity Worths Measured in a Central Cavity in ZPR-6 Assembly 7, 10^{-5} Δk/k/mole

Isotope	Isotopic Wt. in sample, gm	Sample[a] ident.	Sample-Size[b] Correction	Measured[c,d] Worth 1σ imprecision	Calculated[e] Worth
^{239}Pu	9.856	MB10	0.99	37.6 ± 0.40	47.12
^{235}U	14.702	MB21	1.01	31.10 ± 0.47	38.37
^{238}U	19.033	MB24	1.01	-2.58 ± 0.108	-2.801
^{10}B	0.1103	B(L)	1.03	-29.3 ± 0.63	-32.04
Na	17.044	NA(L2)	1.09	-0.155 ± 0.008	-0.189
Ta	18.647	TA-2		-7.739 ± 0.78	
C	33.441	C(L)		-0.1454 ± 0.0025	
Al	53.067	AL(L3)		-0.1800 ± 0.0045	
Fe	33.277	Fe-1		-0.2368 ± 0.0086	
Ni	37.916	Ni-1		-0.3770 ± 0.0108	
Cr	26.999	Cr-3		-0.2343 ± 0.0191	
Mo	43.393	Mo-1		-1.466 ± 0.010	

a. See Ref. 4 for a fuller description of samples
b. Integral transport calculation based on ENDF/B-I data and one-dimensional cylindrical representation central fluxes, see Ref. 6
c. Measured period converted to reactivity with use of conversion factor 1% Δk/k = 1007 Ih
d. Corrected for sample-size effect where given
e. FOP calculation based on ENDF/B-III data and central spherical fluxes

TABLE VII. Comparison of Calculations for Assembly 7 with Several Models

		1-Dimensional Homogeneous	1-Dimensional Heterogeneous	2-Dimensional Heterogeneous
	k_{eff}	0.9772	0.9938	0.9924
Reaction Rates	$^{28}f/^{49}f$	0.02304	0.02313	0.02316
	$^{25}f/^{49}f$	1.0962	1.1143	-
	$^{28}c/^{49}f$	0.1570	0.1530	0.1531
Central[a] Worths	^{239}Pu	47.12	47.05	47.05
	^{235}U	38.37	38.67	38.69
10^{-5} $\Delta k/k$/mole	^{238}U	-2.801	-2.990	-2.985
	^{23}Na	-0.189	-0.193	-0.190
	^{10}B	-32.04	-34.52	-34.59

a. FOP calculations not corrected for sample size effects

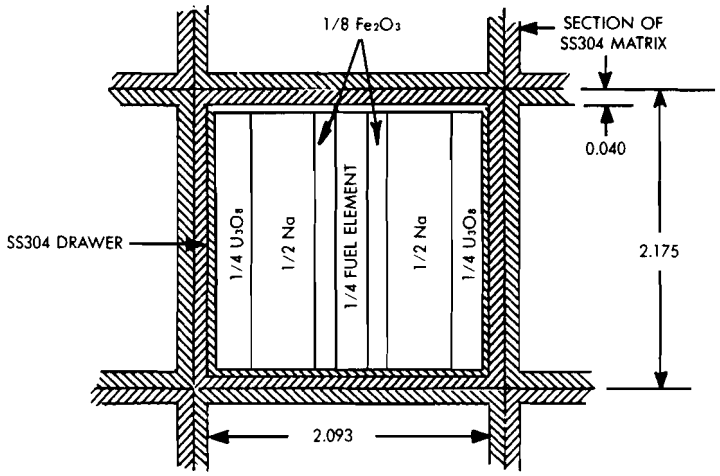

UNIT CELL FOR ASSEMBLIES 6A AND 7

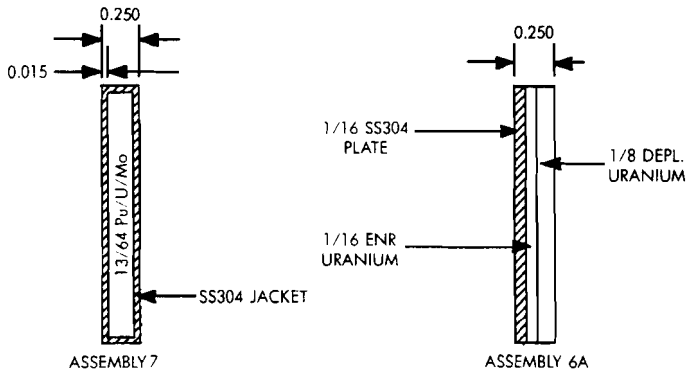

FUEL ELEMENT SPECIFICATION

ALL DIMENSIONS IN INCHES

Figure 1. Cross Section of Unit-Cell Showing Matrix and Plate Loaded Drawer, ZPR Assemblies 6A and 7, ANL-Neg. No. 116-888.

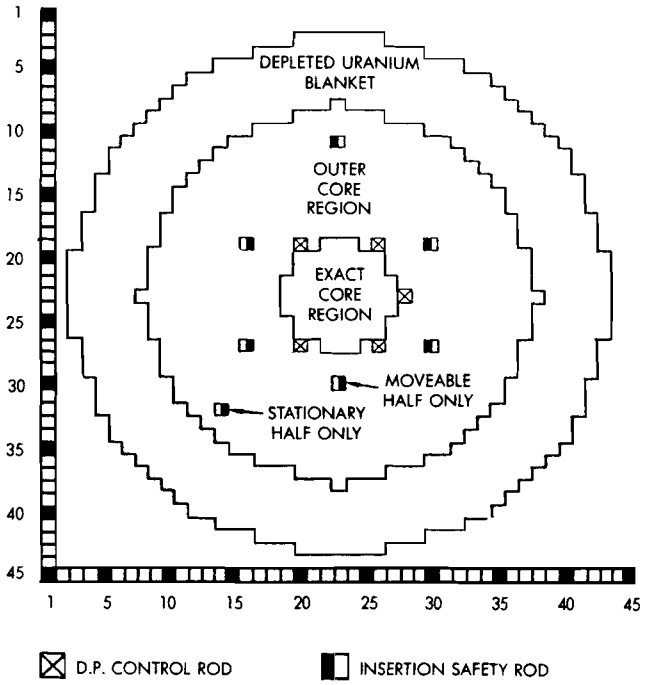

Figure 2. Radial Cross Section for the 96.2 Ih Excess Reactivity, As-Built ZPR-6 Assembly 7, ANL-Neg. No. 116-889.

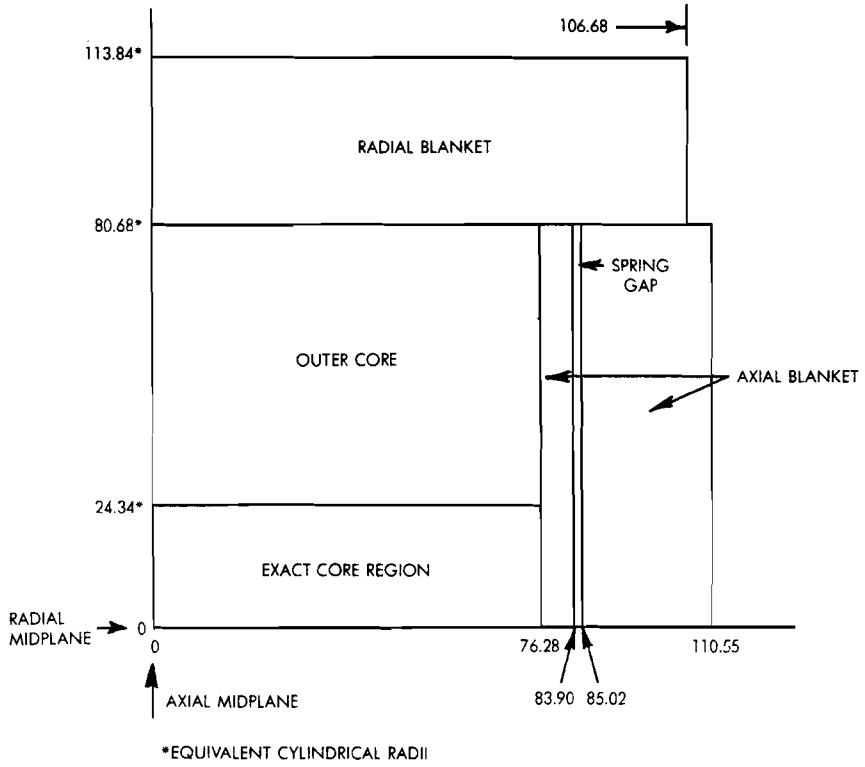

Figure 3. Axial Cross Section for the 96.2 Ih Excess Reactivity, As-Built ZPR-6 Assembly 7, ANL-Neg. No. 116-891.

FAST REACTOR BENCHMARK NO. 13

A. Benchmark Name and Type: ZPR-3-56B, and PuO_2 critical assembly with a nickel reflector.

B. System Description: This particular configuration of ZPR-3 was part of a series of critical experiments conducted to obtain data to evaluate calculational methods for the FTR. The core of assembly 56B was approximately a 615 liter cylinder fueled with Pu and U metal and UO_2 with carbonates and oxides added to simulate a PuO_2-UO_2 composition. Also, Na was added to simulate a homogenized FTR core. The reflector was composed of Ni, Na and steel.

Assembly 56B was selected for a benchmark because: 1) a rather complete set of precise measurements was performed on this relatively simple configuration; 2) this Ni reflected assembly can be compared with other Fe or U-238 reflected benchmarks; 3) and it has a relatively large PuO_2 driven core resembling the FTR.

C. Model Description:

1. One-Dimensional Model (sphere)

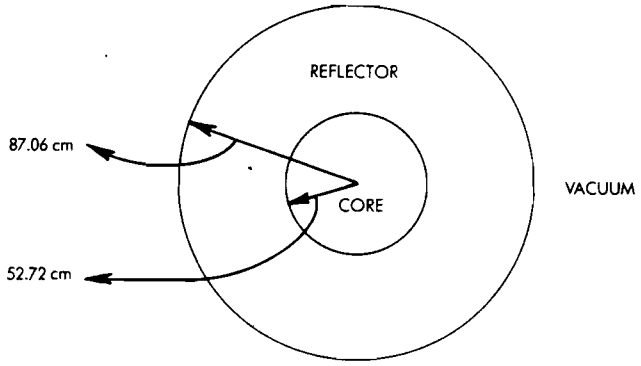

Suggestions:

Code..... 1-dimension transport theory with S_4.

Mesh..... 40 intervals in the core, 20 in the reflector.

2. Two-Dimensional Model (cylinder)

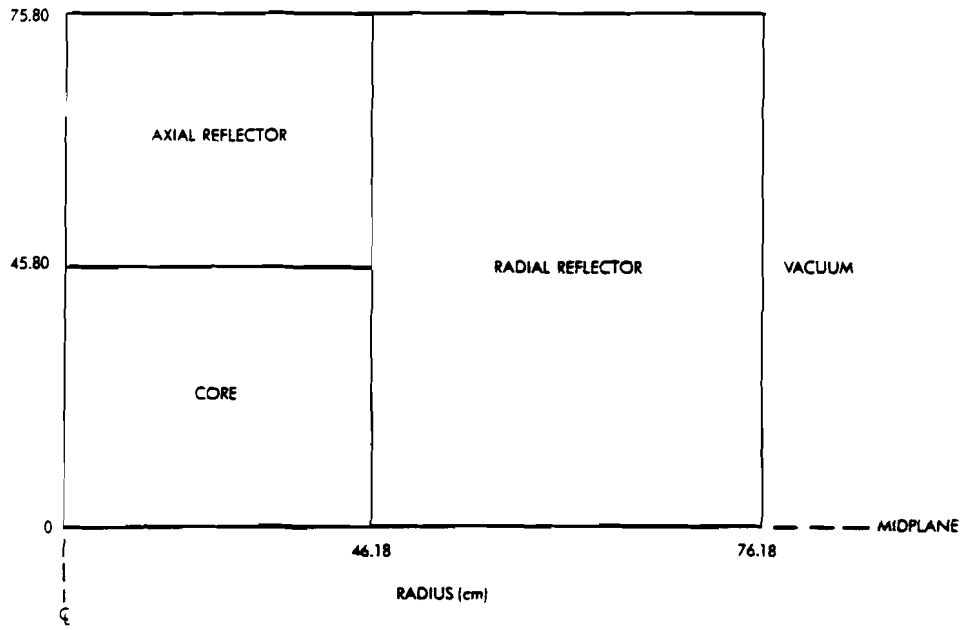

Suggestions:

Code..... 2-dimensional diffusion theory

Mesh..... 30 radial intervals, core

20 radial intervals, reflector

30 axial intervals, core

20 axial intervals, reflector

3. Atom Densities

Material	Density 10^{24} atoms/cc			
	Core	Radial Reflector	Axial Reflector	Spherical Reflector
U-235	0.000014			
U-238	0.006195			
Pu-239 & Pu-241	0.001358			
Pu-240 & Pu-242	0.000181			
O	0.015			
C	0.00103			
Na	0.008669	0.00657	0.01346	0.007879
Cr	0.0025	0.00188	0.0022	0.001941
Fe	0.0137	0.00759	0.00882	0.007824
Ni	0.00109	0.0476	0.0195	0.042261
Mo	0.000343			
Mn & Si	0.00022	0.0003	0.0003	0.0003

4. Techniques

All calculations should be performed with appropriately resonance-shielded cross sections. An acceptable multi-group structure is 26 half-lethargy width groups with E_{max} = 10 MeV.

(Revised 9-78)

D. Experimental Data: (All errors are one standard deviation)

1. Eigenvalue = 1.0000 ± .0014

2. Spectral Indices at Core Center

σ_f (U233) / σ_f (U235) = 1.478 ± 0.015

σ_f (U234) / σ_f (U235) = 0.195 ± 0.002

σ_f (U236) / σ_f (U235) = 0.0639 ± 0.0006

σ_f (U238) / σ_f (U235) = 0.0308 ± 0.0003

σ_f (Pu239) / σ_f (U235) = 1.028 ± 0.010

σ_f (Pu240) / σ_f (U235) = 0.282 ± 0.003

3. Material Worths at Core Center

Material	Reactivity Coefficient 10^{-5} Δk/k/mole
U-235	78. 3 ± 2.2
U-238	-4.95 ± 0.22
Pu-239	100.5 ± 2.0
C	-0.338 ± 0.034
Na	-0.232 ± 0.109
Cr	-0.749 ± 0.073
Fe	-0.776 ± 0.029
Ni	-1.115 ± 0.037
B10	-79.2 ± 1.1
Ta	-24.54 ± 0.91

E. Comments and Documentation:

Since central fuel worths are sensitive to core volume and composition, the 1-D and 2-D models were set up to preserve these two experimental features. However, for the sake of simplicity, materials of low density and of little importance were either omitted or combined with other homogeneous material densities.

Correction factors were obtained in the following manner:

K_{eff} (2-D diffusion) - K_{eff} (1-D diffusion) = -.0157

K_{eff} (1-D transport) - K_{eff} (1-D diffusion) = .0075

K_{eff} (heterogeneous) - K_{eff} (homogeneous) = .0102

2-D worths/1-D worths = 1.052.

The heterogeneity correction was obtained by adding the gross spatial self-shielding component (calculated using a 26-group S_{12} cell model with a homogeneous B^2 leakage) to the energy (resonance) self-shielding component (calculated using the Bell approximation).

If, for example, a 1-D transport calculation gave an eigenvalue of .9900, the corrected eigenvalue would be .9900 - .0157 (geometry correction) + .0102 (heterogeneity correction) = .9845. All 1-D central worths must be multiplied by 1.052 to account for geometric differences.

The experimental assembly 56B dimensions and compositions can be found in Reference 1, while the central indices and material worths

are given in Reference 2. The reactivity conversion parameter was calculated using the delayed neutron data of Masters (Reference 3) and found to be 1.13×10^{5} $\Delta k/Ih$. The material worth values listed have been corrected for estimated sample size and composition effects.

References:

1. ANL-7561, Reactor Development Program Progress Report, March 1969, pages 8-15.

2. ANL-7577, Reactor Development Program Progress Report, April-May 1969, pages 17-35.

3. C. F. Masters et al, "The Measurement of Absolute Delayed-Neutron Yields from 3.1 and 14.9 MeV Fission," Nucl. Sci. & Eng., 36, 202-208 (1969).

FAST REACTOR BENCHMARK NO. 14

A. Benchmark Name and Type

SEFOR Doppler Benchmark, Core I

B. System Description

The SEFOR reactor was designed to provide a Doppler measurement in an environment that is representative of an operating LMFBR, with respect to the neutron spectrum, the fuel temperature range, the reactor composition and the fuel microstructure. Standard fuel for SEFOR was mixed oxide (20% PuO_2, 80% UO_2) in which the Pu contained a minimum amount of Pu-240 ($\sim$8% of the Pu) and the U was depleted in U-235. The fuel was contained in nominal one-inch diameter rods. Several guinea pig rods, having Pu concentrations 50% greater than the standard fuel, were included. Each of the fuel rods included an expansion gap located in the core region so as to minimize the reactivity effect of fuel axial expansion; hence, the Doppler effect contributed approximately 95% of the total SEFOR power coefficient and 90% of the energy coefficient. The measured Doppler coefficient reported here excludes the fuel axial expansion component.

Control of SEFOR was provided by the vertical movement of 10 nickel slab reflectors located radially outside the reactor vessel. Fine control of the position of two of these reflectors was provided; these were calibrated and used in the measurement of reactivity.

All of the SEFOR Doppler measurements used for this benchmark problem were made with the core loaded to its full size of 648 rods. This required the use of typically, 12 to 14 B_4C rods, distributed uniformly, in place of fuel rods to maintain the excess reactivity at full power to less than 50¢.

This benchmark is for SEFOR, Core I, which contained about 6 volume percent BeO. In Core II the BeO rods were replaced with steel rods, resulting in a harder spectrum. A benchmark problem for Core II has not been specified.

C.1 One-Dimensional Spherical Model Description

A one-dimensional spherical model of SEFOR is shown in Figure 1, including model dimensions and suggested mesh. The atom densities in each region (atoms/barn-cm) are given in Table I. A zero return current boundary condition should be applied at the outer boundary. Diffusion theory is suggested with cross sections in any suitable fast reactor energy-group structure, but with groups no coarser than 0.5 lethargy width down to a lethargy of 12.5. Correction factors to be made to the calculated values of k_{eff} and the Doppler coefficient are given in Section E.

Although this spherical model does not provide a very accurate description of SEFOR, it does give a computed Doppler coefficient within 2% and k_{eff} within 0.5% of that computed for the two-dimensional model (Section C.3), without the requirement of group-dependent bucklings.

C.2 One-Dimensional Axial Model Description

A one-dimensional axial model of SEFOR is shown in Figure 2, including model dimensions, suggested mesh and the composition number assigned to each region. The atom densities in each composition (atoms/barn-cm) are given in Table III. Zero return current boundary conditions should be applied at both boundaries. The set of group-dependent bucklings in Table II was found to give the Doppler coefficient within 2% and the k_{eff} within 0.5% of that computed for the two-dimensional model (Section C.3). It was not possible to find a constant buckling which produced both Doppler coefficient and k_{eff} values near to the two-dimensional results. Diffusion theory is suggested, with cross sections in any suitable fast reactor energy-group structure, but with groups no coarser than 0.5 lethargy width down to a lethargy of 12.5. Correction factors to be made to the calculated values are given in Section E.

C.3 Two-Dimensional Model Description

A two dimensional(R-Z) model of SEFOR is shown in Figure 3, including model dimensions, suggested mesh and composition number for each region. The atom densities in each composition (atoms/barn-cm) are given in Table III. Zero return current boundary conditions are to be applied on the top, right and bottom boundaries. Diffusion theory is suggested with cross sections in any suitable fast reactor energy-group structure.* Correction factor to be made to the calculated values are given in Section E.

C.4 Doppler Calculation Model

The isothermal Doppler coefficient should be computed in the following way:

$$T \frac{dk}{dT} = \frac{k_2 - k_1}{\ell n \frac{T_2}{T_1}} = \frac{k_2 - k_1}{0.7006}$$

where

T_1 = 677°K (760°F), average fuel temperatures at zero power,
T_2 = 1365° K (2000°F), average fuel temperature at 20 MW,
k_1 = neutron multiplication factor with the fuel at T_1,
k_2 = neutron multiplication factor with the fuel at T_2.

It is suggested that a neutronics calculation be performed for the fuel at T_1, and that the value of $(k_2 - k_1)$ be obtained with first-order perturbation theory.

* If the two-dimensional problems are run with a group structure that contains groups broader than 0.5 lethargy, these cross sections should be generated by regionwise collapsing, using representative spectra for each of the regions in Figure 3, from a structure that has no groups greater than 0.5 lethargy width down to a lethargy of 12.5.

C.5 Cell Model Descriptions

Before comparing with experimental values for the Doppler coefficient and k_{eff}, the results of calculations with any of the three reactor models above must be corrected for effects not included in the models. These correction factors have been pre-calculated and are given in Section E. However, those computing this benchmark problem are encouraged to calculate their own correction factors. Descriptions of the fuel subassembly and B-10 cell are given below.

a. Fuel Subassembly.

Figure 4 shows a cross section of the fuel subassembly in the SEFOR core. This may be used, together with Composition 7 in Table III, (by computing volume fractions) to define a fuel cell for the calculation of heterogeneity effects. The fuel is mixed UO_2 - PuO_2. The 10 mil gap indicated in Figure 4, outside the channel wall, is sodium filled, so the value of 3.16 cm defines the effective cell outer dimension. Dimensions given in Figure 4 are for 70°F. Expansion to 350°F, to be consistent with Table III, will slightly increase the effective outer cell dimension, but will not change the material volume fractions.

b. B-10 Cell.

The benchmark problem contains 12 B_4C rods, essentially spaced evenly throughout the core. The B_4C rods replace fuel rods and are of the same diameter. A radial cell is defined by a single B_4C rod, surrounded by 1/12 of the core (Composition 7), homogeneously mixed.

D. Experimental Data

1. Measured $k_{eff} = 1.0000$
2. Isothermal Doppler coefficient [3] $= T \frac{dk}{dT} = -0.0080 \pm 0.0010$

The Doppler measurements were made by determining the reactivity change in SEFOR as the power was increased from a nominal zero power to full power of 20 MW, while holding the coolant temperature constant.[2] The reactivity change was determined from the positions of calibrated reflector control rods.

Components of the reactivity change due to thermal expansion were computed and subtracted from the total to arrive at the Doppler component. (The Doppler component is >90% of the total.) Then measured and computed fuel temperatures and temperature distributions were used to obtain an equivalent, full-core, isothermal Doppler coefficient. The standard deviation of ±0.0010 includes the effects of uncertainties in other reactivity components and in fuel temperatures and temperature distributions. The measured Doppler coefficient of -0.0080 has been substantiated with both sub-prompt and super-prompt transient measurements made at several initial power levels between 0 and 10 MW, and the uncertainty has been reduced from ±0.0014 due to the transient measurements.

E. Computed Correction Factors

The correction factors in Table IV are defined as the absolute changes which should be made to the computed U-238 Doppler coefficient and to k_{eff}. For example, a computed Doppler coefficient $T \frac{dk}{dT}$ of -0.0075 would be corrected for resonance heterogeneity to -0.0080, since this correction factor is -0.00050. The correction factors were obtained as follows.

a. Resonance Heterogeneity.

A Bell-approximation correction was made to the microscopic cross sections for a radial cell defined by a fuel pin surrounded by 1/6 of the non-fuel subassembly materials, homogenized.

b. Subassembly Heterogeneity.

The effect of coarse-group flux variations across the subassembly (Figure 4) was computed for a radial cell model of the subassembly, with the BeO rod at the center.

c. B-10 Heterogeneity.

The effect of coarse-group flux variations about a B_4C pin was computed for a radial cell model defined by one B_4C pin surrounded by 1/12 of the core.

d. Reactor Expansion.

This correction factor is due to the effect of expanding the reactor from the dimensions given in Figure 3, for 350°F, to the isothermal temperature of 760°F. Although the average fuel temperature was greater than 760°F during the measurements, the SEFOR design minimizes the fuel expansion effect, and a correction for this in the basic problem was not necessary. (Both the measured and calculated Doppler coefficient exclude the fuel expansion effect.)

e. Control Effect.

The atom densities in Table III for composition 13 assume that 1.25 sections of reflector control were lowered and the void uniformly distributed. Since 1.56 sections of lowered reflector is a better description of the zero power condition, this correction accounts for both the difference in the number of sections lowered and the substantial heterogeneity effect of a single reflector.

f. Non-cylinder Effect.

This factor corrects for the irregularity of the core radial boundary. The value given here was computed earlier and reported in Reference 1.

g. Diffusion Theory Error.

This error was computed by comparison of the diffusion theory results from the spherical model with the extrapolation to S_∞ from spherical calculations in S_4, S_6, S_8 and S_{12}. It has been estimated that the inclusion of the anisotropic scattering effect using S_n-P_ℓ calculations will reduce k_{eff} by 0.001 over that obtained using S_n with transport-corrected P_o cross sections, but this has not been verified by direct computation.

F. Comments and Documentation

The one-dimensional spherical model was derived as follows.

Region 1. The volume of this region was chosen to be equal to the volume of the portions of Compositions 2 and 3 in Figure 4 which lie

within the core ($41.800 \leq Z \leq 132.957$ cm). The composition of the region is the appropriate volume-weighted average of compositions 2 and 3 (Table III).

Region 2. The composition of this region is the volume-weighted average of compositions 6, 7 and 8 (Figure 4 and Table III). The radius of the region is 51.055 cm when the volume of these regions is conserved, but was reduced to 49.75 cm for the spherical model to produce the same k_{eff} as obtained for the two-dimensional model.

Region 3. The composition of this region is the volume-weighted average of Compositions 1,3,4,5,9,10,11,12,13 and 14 with the exception of the range $41.800 \leq Z \leq 94.243$ cm for Composition 3 and the range $0 \leq Z \leq 11.800$ cm for Compositions 4, 11, 12 and 14. The thickness of this region was chosen to preserve the volume of these component regions when Region 2 had a radius of 51.055 cm; the thickness of Region 3 was not changed when the radius of Region 2 was decreased.

Region 4. The composition of this region is the volume-weighted average of the remaining material from Figure 4 and Table III. The thickness of the region was chosen the same way as used for Region 3.

The composition and geometry of the one-dimensional axial model is identical to the two-dimensional model (Figure 3) for $4.226 \leq R \leq 44.118$. The spectrum of the perpendicular bucklings for the core regions and the constant perpendicular bucklings for the regions outside of the core were taken from computed results of the two-dimensional model. The magnitude of the perpendicular bucklings for the core regions was adjusted to produce the same k_{eff} as obtained from the two-dimensional model.

The value of β_{eff} (delayed neutron fraction) used to generate $T \frac{dk}{dT}$ from reactivity measurements is 0.00327.

G. References

1. L. D. Noble, et. al., "Results of SEFOR Zero Power Experiments", General Electric Co., GEAP-13588 (March 1970).
2. L. D. Noble, et. al., "SEFOR Core I Test Results to 20 MW", General Electric Co., GEAP-13702 (March 1971).
3. D. D. Freeman, "SEFOR Experimental Results and Applications to LMFBR's", General Electric Co., GEAP-13929 (January 1973).

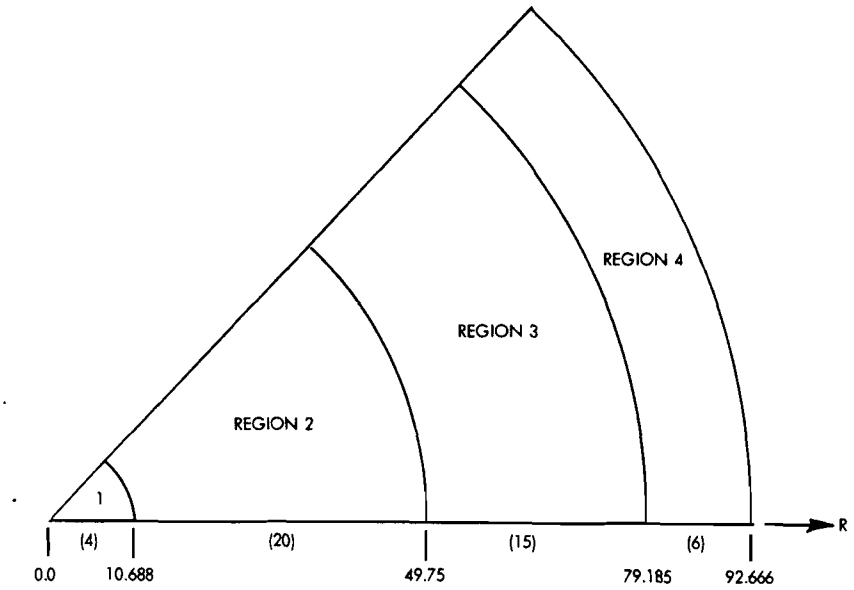

Figure 1. SEFOR Doppler Benchmark Spherical Model.
Dimensions in cm; Suggested Number of Mesh Intervals in ( ).

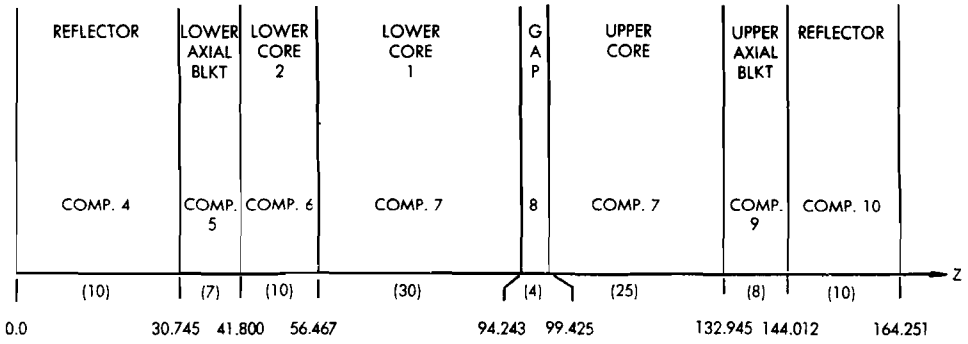

Figure 2. SEFOR Doppler Benchmark Axial One-Dimensional Model.
Dimensions in cm; Suggested Number of Mesh Intervals in ( ).

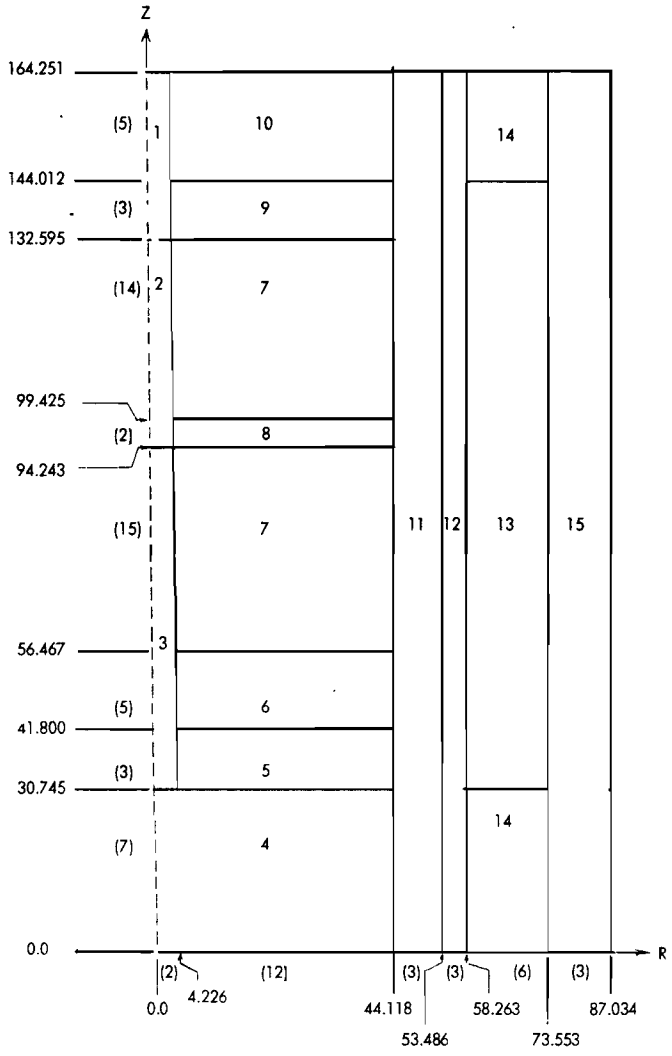

Figure 3. SEFOR Doppler Benchmark Two-Dimensional Model.
Dimensions in cm; Suggested Number of Mesh Intervals in ( ).

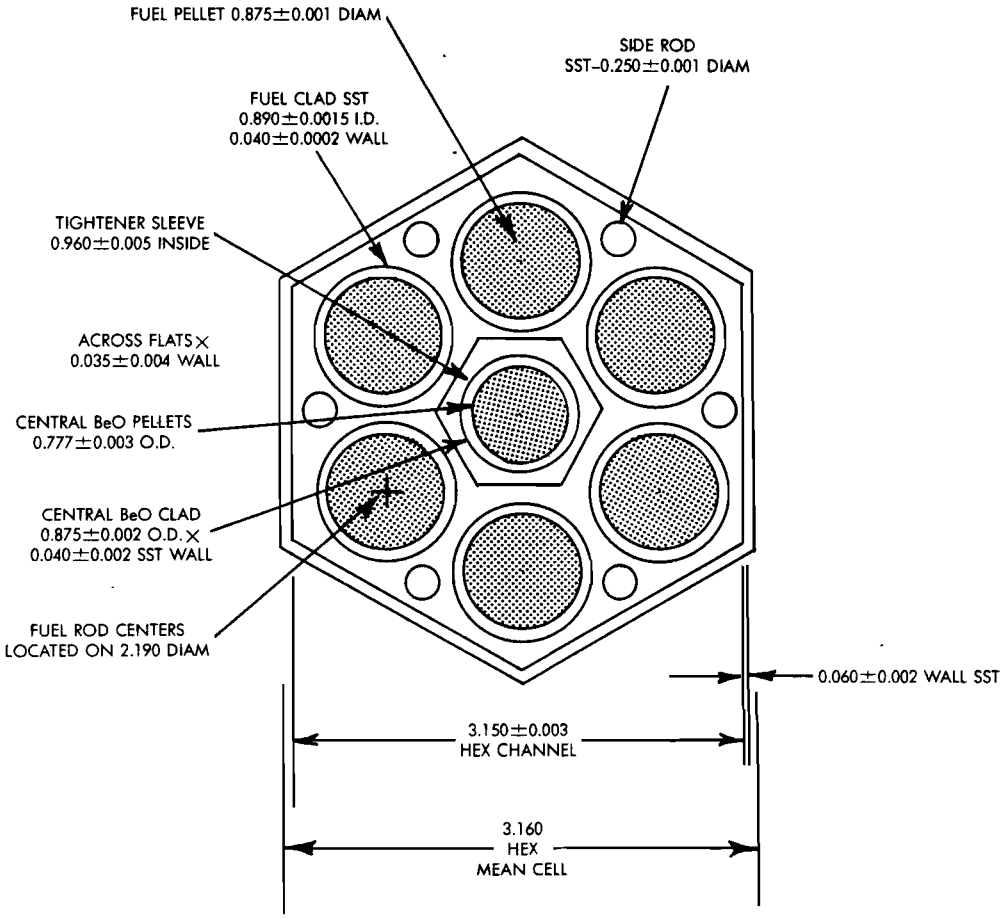

Figure 4. SEFOR Fuel Subassembly

TABLE I

SEFOR Doppler Benchmark:
Spherical Model Region Compositions (atoms/barn-cm)

Material	Region 1	Region 2	Region 3	Region 4
Fe	1.3574-2*	1.3886-2	5.8932-3	7.8587-3
Cr	3.9574-3	3.9511-3	2.8913-3	2.4623-3
Ni	2.0292-3	2.3580-3	3.0178-2	1.3315-3
Na	1.6615-2	6.8099-3	5.4493-3	1.3070-3
Be	-	3.6011-3	1.8327-5	-
O	-	2.0991-2	1.2597-4	-
Mo	-	1.1999-4	1.5605-5	-
B-10	-	6.1100-5	-	5.7684-3
B-11	-	2.4600-4	-	2.3100-2
U-235	-	1.5374-5	1.1724-7	-
U-238	-	6.9808-3	5.3438-5	-
Pu-239	-	1.5901-3	-	-
Pu-240	-	1.4355-4	-	-
Al	-	7.6770-5	-	7.2200-3
C	-	-	2.2330-3	6.5800-3

* a.bcde-n = a.bcdex10^{-n}

TABLE II

SEFOR DOPPLER BENCHMARK
AXIAL MODEL PERPENDICULAR BUCKLINGS (CM^{-2})

Lethargy Range	B_r^2 (Regions 3,4,5,6)	B_r^2 (Regions 1,8)	B_r^2 (Regions 2,7)
0 - 2	2.3-3*	1.2-3	1.4-3
2 - 4	1.8-3	1.2-3	1.4-3
4 - 6.5	1.7-3	1.2-3	1.4-3
6.5 - 9.0	1.3-3	1.2-3	1.4-3
9.0 - 10	-1.2-3	1.2-3	1.4-3
10 - ∞	-3.5-3	1.2-3	1.4-3

* a.b-n = a.bx10^{-n}

TABLE III

SEFOR DOPPLER BENCHMARK REGION COMPOSITIONS (ATOMS/BARN-CM)
FOR ONE-DIMENSIONAL AXIAL AND TWO-DIMENSIONAL MODELS

Material	Comp. 1	Comp. 2	Comp. 3	Comp. 4	Comp. 5	Comp. 6	Comp. 7	Comp. 8
Fe	1.0894-2*	7.0745-3	1.8373-2	1.4172-2	1.2837-2	1.4151-2	1.3567-2	1.7529-2
Cr	3.1760-3	2.0624-3	5.3564-3	4.4759-3	3.6373-3	4.0151-3	3.8493-3	5.1711-3
Ni	1.6285-3	1.0575-3	2.7465-3	2.3799-3	3.9552-2	2.3604-2	2.2629-3	3.6597-3
Na	1.6615-2	1.6615-2	1.6615-2	1.6900-2	6.9576-3	6.8099-3	6.8099-3	6.8099-3
Be	-	-	-	-	2.3175-4	2.6840-3	3.7769-3	3.7769-3
O	-	-	-	-	1.8660-3	2.0700-2	2.1795-2	1.0742-2
Mo	-	-	-	-	1.2014-4	1.2436-4	1.1915-4	1.1916-4
B-10	-	-	-	-	-	6.1110-5	6.1110-5	6.1110-5
B-11	-	-	-	-	-	2.4600-4	2.4600-4	2.4600-4
U-235	-	-	-	-	1.7800-6	1.5850-5	1.5850-5	7.4820-6
U-238	-	-	-	-	8.1126-4	7.1970-3	7.1970-3	3.3938-3
Pu-239	-	-	-	-	-	1.6895-3	1.6895-3	-
Pu-240	-	-	-	-	-	1.5220-4	1.5220-4	-
C	-	-	-	-	-	7.6770-5	7.6770-5	7.6770-5
Al	-	-	-	-	-	-	-	-

* a.bcde-n = a.bcdex10^{-n}

TABLE III (CONTINUED)

SEFOR DOPPLER BENCHMARK REGION COMPOSITIONS (ATOMS/BARN-CM)
FOR ONE-DIMENSIONAL AXIAL AND TWO-DIMENSIONAL MODELS

Material	Comp. 9	Comp. 10	Comp. 11	Comp. 12	Comp. 13	Comp. 14	Comp. 15
Fe	1.3748-2	1.8825-2	1.7345-2	9.4740-3	2.0489-3	9.0930-3	7.0523-3
Cr	3.9047-3	5.9192-3	5.3140-3	2.7620-3	5.9730-4	2.6590-3	2.2274-3
Ni	3.8953-2	3,1419-3	3.8328-3	1.4160-3	6.2400-2	8.3240-3	1.1843-3
Na	6.8702-3	1.3526-2	1.4842-2	-	-	-	-
Be	3.2470-4	-	-	-	-	-	-
O	1.9589-3	-	-	-	-	-	-
Mo	1.1797-4	1.2872-4	-	-	-	-	-
B-10	-	-	-	-	-	-	6.8040-3
B-11	-	-	-	-	-	-	2.7216-2
U-235	1.7800-6	-	-	-	-	-	-
U-238	8.1126-4	-	-	-	-	-	-
Pu-239	-	-	-	-	-	-	-
Pu-240	-	-	-	-	-	-	-
C	-	-	-	-	-	-	8.5149-3
Al	-	-	-	1.1790-2	2.1303-2	-	7.5555-3

* a.bcde-n = a.bcdex10^{-n}

TABLE IV

SEFOR DOPPLER BENCHMARK CORRECTION FACTORS

		$\Delta\left(T \frac{dk}{dT}\right)$	$\frac{\Delta k}{k}$
a.	Resonance Heterogeneity	-0.00050	+0.00247
b.	Subassembly Heterogeneity	-0.00009	+0.00111
c.	B-10 Heterogeneity	-0.00014	+0.00096
d.	Reactor Expansion	+0.00012	-0.00470
e.	Control Effect	∿0.0	-0.00519
f.	Non-cylinder Effect	∿0.0	-0.00300
	Total Correction to 2-D Transport Theory Results	-0.00061	-0.00835
g.	Diffusion Theory Error	-0.00004	+0.00686
	Total Correction to Diffusion Theory Results	-0.00065	-0.00149

FAST REACTOR BENCHMARK NO. 15

A. ZPR-6 Assembly 6A - A Uranium Oxide Fueled Fast Critical Assembly.

B. System Description:

The ZPR-6 consists of two halves, each a horizontal matrix of 2.2 in. square stainless steel tubes into which are loaded stainless steel drawers containing fuel and diluent materials of various types. Assembly 6A is a large (4000 liter) fast critical assembly with a soft spectrum and other characteristics representative of current LMFBR designs. It has a single fuel zone with a length-to-diameter (L/D) ratio of 0.84; it has a simple one-drawer unit cell; and it is blanketed both axially and radially with depleted uranium.[1] The assembly's spectrum characteristics, simple geometric configuration and simple unit cell make it well suited for a benchmark assembly.

The unit cell, which is shown in Fig. 1, is identical to that of a companion benchmark assembly; ZPR-6 Assembly 6A, except that the fuel is enriched uranium (5.4 w/o ^{238}U) rather than a plutonium-bearing alloy. A cross sectional view of the as-built reference assembly, which had an excess reactivity of 75.1 Ih, is shown in Fig. 2 and the equivalent cylindricalized representation of the as-built system is shown in Fig. 3.

C. Model Description:

1. One-Dimensional Model: A one-dimensional model with spherical geometry has been used in the analysis of many measurements in this assembly. The spherical model was defined with reference

to a two-dimensional finite cylindrical model, which will be described in Section C.2. The homogeneous spherical model was defined by first determining a blanket thickness and then searching for a core radius that gives the spherical reactor the same k_{eff} as the homogeneous two-dimensional cylinder. The blanket dimensions and compositions were defined as the weighted average of the axial and radial blanket dimensions and compositions in which the weighting was done on the basis of the relative leakages into the axial and radial blankets (as given by the two-dimensional calculations). The resulting core radius and blanket thickness for the homogeneous spherical model were 95.67 cm and 30.65 cm respectively. The appropriate compositions for use with the spherical model are given in Table I. The spherical model is expected to introduce approximately a 0.05% uncertainty in k_{eff}.

An energy group structure with 27 energy groups, as given in Table II, is suggested. Such a structure has sufficient detail at low energies to afford accurate computations of material worths and Doppler effects.

Because of the simplicity of the two-region, homogeneous spherical model the macroscopic flux distributions across the reactor may be computed with diffusion theory, and a relatively coarse mesh of 2 cm should be adequate.

(Revised 9-78)

Central material reactivity worths and Doppler reactivity worths may be computed by perturbation theory. If the material sample is optically thin and if the material is contained in the core, the homogeneous core cross sections for the material are appropriate to the sample. If the material sample is optically thin and if the material is not contained in the core, then infinite dilution cross sections are appropriate for the sample.

The major flaw in the homogeneous spherical model for this geometrically simple system is in the neglect of heterogeneities in the unit cell. Sections D and F indicate the uncertainties arising from the use of homogeneous cross sections. The error in material worth or Doppler worth introduced by flux distortions depends strongly upon the nature of the sample.

2. Other More Complicated Models: A two-dimensional finite cylindrical representation of the system is closer to the physical configuration than a spherical representation. The as-built loading was thus corrected for both excess reactivity and edge smoothing. The spring gap was homogenized into the axial blanket and the radial blanket height was defined to be the same as the core plus axial blanket. A portion of the outer core region was fueled with 1/8 in. thick enriched uranium fuel plates instead of the standard 1/16 in. thick plates. The reactivity effect of the difference in heterogeneities of the two types of plates was accounted for. The resulting region dimensions and compositions

for the zero-excess reactivity, uniform, two-dimensional model are given in Tables III and IV, respectively. The "exact core region", at the center of the assembly, is simply a region in which material concentrations are known more accurately than in the rest of the core.

D. Experimental Data:

1. Measured Eigenvalues: The measured eigenvalue corresponding to the models of Section C is 1.0000 ± 0.0005. Calculations indicate a 0.0073 heterogeneous-homogeneous correction.[2] The transport theory correction was not computed but it would be less than the 0.0018 effect in Assembly 7.

2. Unit-Cell Reaction Rates: Detailed unit-cell measurements of the capture and fission in ^{238}U and fission in ^{235}U were made. Activation foils of ^{238}U and ^{235}U were used to measure the rates within the fuel and U_3O_8 plates, such that the actual cell-averaged values of the reaction rates could be obtained. To be clear, these unit-cell reaction rate values correspond to the reactions actually taking place in the unit-cell in the assembly, and not, for example, to a cell-average defined as the values of the flux at every point in the cell multiplied by the cross section of the foil material. We use the term to refer to the flux and volume weighted reaction rates as they actually occur in the unit-cell. Hence, a per atom unit-cell reaction rate ratio is converted to the actual ratio of the number of reactions taking place in the cell simply by multiplying the former ratio by the appropriate atom density ratio.

The details of the technique used for counting the activated foils and reducing the data to absolute reaction rates are identical with those used in Ref. 3. The absolute calibrations were made with three separate and independent techniques: (1) by absolute fission chambers with identical foils on their faces to those used in the unit-cell measurements, with the fission chambers placed in the reactor at the same spectral position; (2) by thermal irradiation of identical foils in the ATSR thermal column; and (3) by absolute radiochemical analysis of some of the foils that were actually used in the unit-cell measurements. The excellent agreement among the various calibration methods made possible the small uncertainty, $1\sigma \tilde{=} 2\%$, in the measured reaction rate ratios. These are given in Table V along with calculated factor (to be applied to the measured value) for heterogeneities.[2]

3. Material Worths at the Center of the Core: Central reactivity worths of several materials were measured in a 2 x 2 x 1 in. cavity with use of the axial sample changer. The samples were plates that were placed in a stainless steel can. The reactivity worth of a sample was obtained from the difference in the reactivity worth (relative to void) of the empty and the sample-bearing can. Further descriptions of the measurements are given in Ref. 4. Table VI gives the experimental worths of the isotopes, their weights in the samples and the calculated results.

E. Calculated Results:

The calculations described in this section were made using ENDF/B

version III data and the standard one-dimensional, homogeneous spherical model of the assembly. The fundamental mode option of the SDX code[5] was used to compute homogeneous cross sections. This model yielded a multiplication constant of 0.9853, which is increased to 0.9926 by inclusion of the heterogeneity correction. In Table VII, are given the calculated values for the reaction rate ratios and the central material worths. First-order perturbation theory was used in the worth calculations.

F. Comments and Documentation:

To assess the limitations of the homogeneous spherical Benchmark model, the multiplication constant, reaction rate ratios and central reactivity worths were calculated also with a one-dimensional spherical heterogeneous model and a two-dimensional finite cylindrical heterogeneous model. In this way, the errors from homogenization can be separate from the errors from the simplified geometric representation. The heterogeneous cross sections were computed with the plate unit-cell option in the SDX code, which uses equivalence theory in the narrow resonance approximation to obtain spatial weighting factors. The model used to represent the unit cell in these SDX problems is described in Ref. 6. For the one-dimensional model, the heterogeneous cross sections were obtained with the fundamental mode option of SDX; for the two-dimensional model, the space-dependent option was used.

The results of the calculations with the three models are compared in Table VII. The one- and two-dimensional heterogeneous models are in good agreement. From comparison of the homogeneous and heterogeneous

results, heterogeneities account for a difference of 0.0073 in the multiplication constant. Heterogeneities do not affect appreciably the reaction rate ratios or the calculated worths of ^{239}Pu and ^{235}U but they have a 5% effect of the calculated worths of ^{238}U and ^{10}B and a large effect on the worth of sodium.

For the central worth measurements, the conversion factor, 1% $\Delta k/k$ = 449 Ih was used to convert the measured periods to the desired reactivity units. The delayed neutron data of Keepin[7] were used in computing the conversion factor.

References

1. C. E. Till, L. G. LeSage, R. A. Karam et. al., "ZPR-6 Assemblies 6A and 7: Benchmark Specifications for the Two Large Single-Core-Zone Critical Assemblies - ^{235}U-Fueled Assembly 6A and Plutonium-Fueled Assembly 7 - LMFBR Demonstration Reactor Benchmark Program," Applied Physics Division Annual Report, July 1, 1970 to June 30, 1971, 86-101, ANL-7910.

2. B. A. Zolotar, E. M. Bohn and K. D. Dance, "Benchmark Tests and Comparisons Using ENDF/B Version III Data," Applied Physics Division Annual Report, July 1, 1971 to June 30, 1972, ANL-8010 (in press).

3. C. E. Till, J. M. Gasidlo, E. F. Groh, "Null-Reactivity Measurements of Capture/Fission Ratio in ^{235}U and ^{239}Pu," Nucl. Sci. Eng. 40, 132 (1970).

4. R. A. Karam, W. R. Robinson, G. S. Stanford and G. K. Rusch, "ZPR-6 Assembly 6A, A 4000-Liter UO_2 Fast Core", Applied Physics Division Annual Report, July 1, 1969 to June 30, 1970, 175-183, ANL-7710.

5. W. M. Stacy, Jr., H. Henryson II, B. J. Toppel, and B. A. Zolotar, "MC^2-2/SDX Development - Part II," Applied Physics Division Annual Report, July 1, 1971 to June 30, 1972, ANL-8010 (in press).

6. J. E. Marshall, "The Unit-Cell Composition Model Developed for SDX Input Preparation and the Resulting Cell Specifications for the ZPR/ZPPR Benchmark Assemblies," Applied Physics Division Annual Report, July 1, 1971 to June 30, 1972, ANL-8010 (in press).

7. G. R. Keepin, "Physics of Nuclear Kinetics," Addison-Wesley, Reading, Mass., 1965, Table 4-7.

Table I Assembly 6A Spherical Model Atom Densities, atom/barn-cm

Isotope	Core	Blanket
^{235}U	0.001153	0.0000855
^{238}U	0.0058176	0.0395508
Na	0.0092904	-
O	0.01390	0.000023
Fe	0.013431	0.0044669
Ni	0.001291	0.0005407
Cr	0.002842	0.001247
Mn	0.000221	0.0000960

Table II. Specifications of 27-Group Structure

Group	ΔU	E_{upper},keV	Group	ΔU	E_{upper},keV
1	0.5	10000	14	0.5	15.034
2	0.5	6065.3	15	0.5	9.1188
3	0.5	3678.8	16	0.5	5,5308
4	0.5	2231.3	17	0.5	3,3546
5	0.5	1353.4	18	0.5	2,0347
6	0.5	820.85	19	0.5	1,2341
7	0.5	497.87	20	0.5	0.74851
8	0.5	301.97	21	0.5	0.45400
9	0.5	183.16	22	1	0.27536
10	0.5	111.09	23	1	0.10130
11	0.5	67.379	24	1	0.03727
12	0.5	40.868	25	1	0.01371
13	0.5	24.787	26	2	0.00504
			27	-	0.00068

Table III. Dimensions for the Zero-Excess Reactivity, Uniformly-Loaded Cylindrical Version of Assembly 6A

Outer core radius, cm	91.34
"Exact Core" region radius, cm	24.34
Core height, cm	152.56
Radial blanket thickness, cm	28.61
Axial blanket thickness, cm	34.22
Core Volume, liters	3999

Table IV. Atom Densities for the Zero-Excess Uniform Cylindrical Model of Assembly 6A atoms/barn-cm

	Exact Core	Outer Core	Axial Blanket	Radial Blanket
^{234}U	0.000011	0.000011	0.0000004	0.0000004
^{235}U	0.001153	0.001149	0.0000836	0.0000866
^{236}U	0.0000056	0.0000056	0.0000020	0.0000020
^{238}U	0.005801	0.005784	0.03865	0.04006
Mo	0.000011	0.000011	0.0000040[a]	0.0000034[a]
Na	0.0092904	0.009202	-	-
O[b]	0.01390	0.01474	0.000026[a]	0.000022[a]
Fe	0.01342	0.01399	0.004931	0.004197
Ni	0.001291	0.001264	0.0005977	0.0005082
Cr	0.002842	0.002841	0.001378	0.001172
Mn	0.000221	0.000222	0.000107	0.0000897

[a] Arising from SS305 impurities

[b] Includes ∿0.0088% due to heavy (atomic wt $\geq$ Si) SS304 impurities

Note: The number of digits in each density is a measure of the compositional precision. Nominally, the rightmost digit bounds the density according to a 2σ or 93% confidence interval.

Table V. Unit Cell Reaction Rate Ratios in Assembly 6A

	Measurement	Heterogeneity correction factor[a]
$^{28}f/^{25}f$	0.02411 ± 0.00072	1.016
$^{28}c/^{25}f$	0.1378 ± 0.0041	1.011

[a] calculated homogeneous/heterogeneous

Table VI. Central Reactivity Worths Measured in a Central Cavity in ZPR-6 Assembly 6A, 10^{-5} Δk/k/mole

Isotope	Isotopic wt in sample, gm	Sample-Size Correction	Measured[c,d] Worth 1σ imprecision	Calculated[e] Worth
^{239}PU	41.23	-	30.40 ± 1.06	33.16
^{235}U	4.20	-	21.86 ± 0.25	24.73
^{238}U	1151.49	1.07[a]	-1.866 ± 0.005	-2.223
^{23}Na	51.38	-	0.0082 ± 0.0021	-0.0140
^{10}B	29.29	1.60[b]	-29.28 ± 1.30	-26.09
Ta	833.69	-	-5.038 ± 0.004	
C	101.98	-	0.1033 ± 0.0005	

a. integral-transport calculation

b. by experiment

c. period/reactivity conversion factor 1% Δk/k = 449 Ih

d. corrected for sample size effect where given

e. FOP calculation based on ENDF/B-III data and homogeneous, spherical fluxes

Table VII. Comparison of Calculations with Several Models for Assembly 6A

		1-Dimensional Homogeneous	1-Dimensional Heterogeneous	2-Dimensional Heterogeneous
k_{eff}		0.9853	0.9926	0.9920
Reaction Rates	$^{28}f/^{25}f$	0.02196	0.02161	
	$^{28}c/^{25}f$	0.1434	0.1418	
Central[a] Worths, 10^{-5} $\Delta k/k/mole$	^{239}Pu	33.16	33.65	33.32
	^{235}U	24.73	25.50	25.27
	^{238}U	-2.223	-2.341	-2.317
	Na	-0.0140	-0.0343	-0.0331
	^{10}B	-26.09	-27.40	-27.12

[a] FOP Calculations not corrected for sample size effects

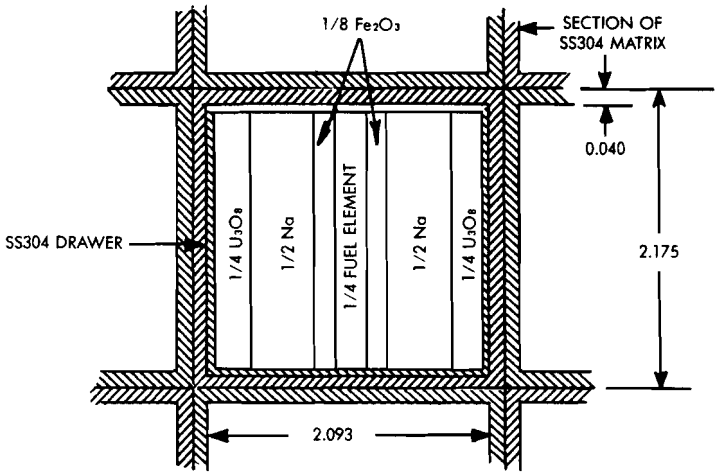

UNIT CELL FOR ASSEMBLIES 6A AND 7

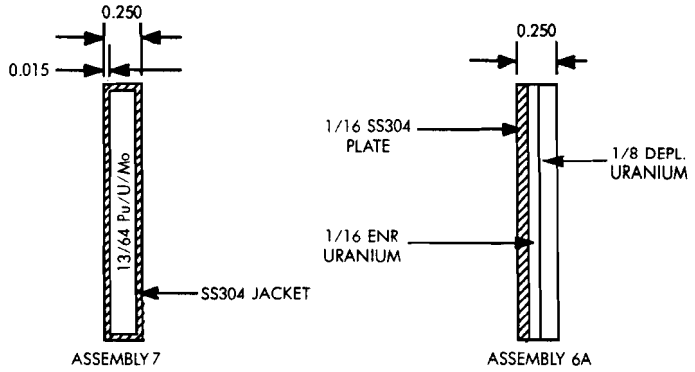

FUEL ELEMENT SPECIFICATION

ALL DIMENSIONS IN INCHES

Figure 1. Cross Section of Unit-Cell Showing Matrix and Plate Loaded Drawer, ZPR Assemblies 6A and 7, ANL-Neg. No. 116-888.

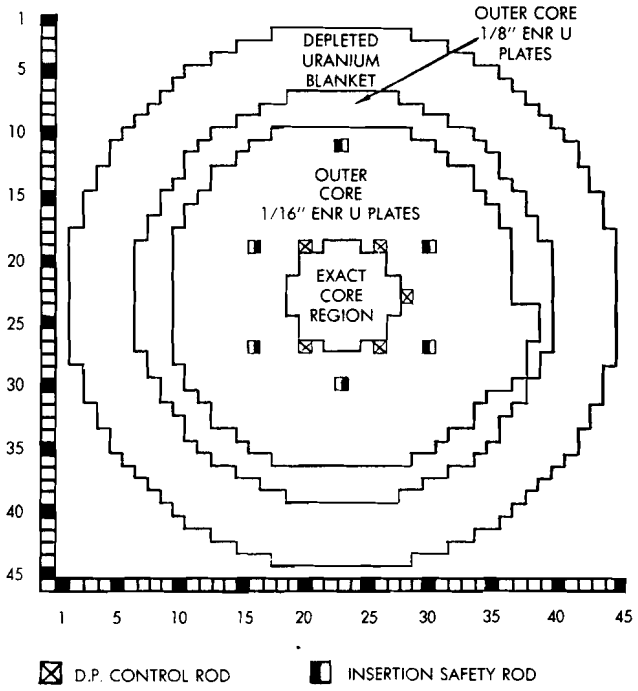

Figure 2. Radial Cross Section for 75.1 Ih Excess Reactivity, As-Built ZPR-6 Assembly 6A, ANL-Neg. No. 116-890.

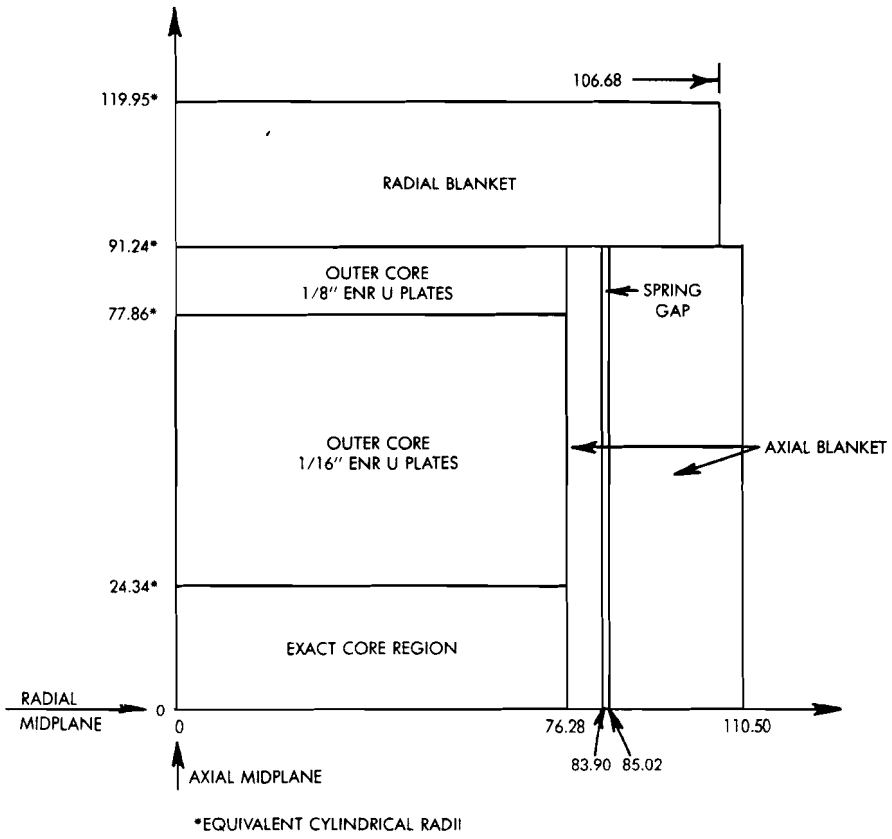

Figure 3. Axial Cross Section for 75.1 Ih Excess Reactivity, As-Built ZPR-6 Assembly 6A, ANL-Neg. No. 116-892.

Fast Reactor Benchmark No. 16

A. Benchmark Name and Type: SNEAK-Assembly 7A, a mixed oxide fuel-plus-graphite assembly.

B. System Description

Assembly 7A had a compact core with mixed oxide fuel, and a simple unit cell, which consisted of a PuO_2UO_2 platelet (0.626 cm thick) and a graphite platelet (0.313 cm thick). The core volume is about 100 liters. The $^{238}U/^{239}Pu$ ratio is about 3.0, the spectrum is hard compared to a LMFBR. In combination with assembly 7B, which has a higher ^{238}U content, the system is suitable to test the high cross sections of ^{238}U, and of ^{239}Pu.

The control rods were loaded with enriched uranium; therefore, about 10% of the critical mass was ^{235}U.

C. Model Description

C.1 One-Dimensional Model

A one-dimensional, homogeneous composition model is defined as a two-region sphere with homogeneous atom densities for the core and blanket as given in Table I. The inner core zone represents a uniform portion of the core undisturbed by the control rods and it is these inner core zone atom densities listed in Table I that are to be used in the core region of the sphere. The following dimensions apply to the spherical model:

Core Outer Radius	28.50 cm
Blanket Thickness	30.00 cm
Number of Mesh Intervals:	
Core	35
Blanket	20

The standard mode of calculation may be either diffusion theory or S_6 transport theory with a vacuum boundary condition at the outer blanket boundary and a multigroup structure composed of 26 groups, each of lethargy width equal to 0.5 and E_{MAX} set at 10 MeV.

The homogeneous spherical model was obtained as follows: A two-dimensional calculation in R-Z-geometry was carried out with the code DIXY, in 26 energy groups. The control rods were homogenized in an outer core zone ($r > 15.86$ cm). The k_{eff} obtained in this calculation was corrected for the cylindrisation, for the actual position of the control rods, and for heterogeneity effect. Then, a diffusion calculation in spherical geometry was run, assuming the composition of the "inner" core zone. The radius was iterated such that the corrected k_{eff} of the DIXY run was obtained.

C.2 Two-Dimensional Model Description

A two-dimensional, R-Z, cylindrical model is defined in Fig. 1. The full core height is 44.04 cm, the inner core zone radius is 15.86 cm, the outer core zone radius is 28.55 cm and the axial and radial blankets are 30 cm thick. The atom densities for each zone are listed in Table I. This model corresponds to a cylinder with volume equal to the actual core corrected for the 30¢ excess reactivity. The core map or lattice loading in X-Y-geometry is shown in Fig. 2.

The suggested mode of calculation is diffusion theory with a vacuum boundary condition at the outer boundaries of the blanket (top and right sides in Fig. 2) and a symmetry boundary condition along the axial and radial axes (left and bottom sides in Fig. 2). The suggested mesh structure is 30 intervals axially and radially in the core and 20 intervals in the blanket.

The following corrections should be applied to the k_{eff} as calculated in R-Z-geometry:

	$\Delta k/k$
cylindrisation	-0.0045
actual control rod position	-0.0006
heterogeneity	+0.0006
	-0.0045

The corrected k_{eff} should be compared to 1.0.

If desired, the homogenization of the control rods can be checked using the atom densities of the control rods, as given in Table 2.

D. Experimental Data

D.1 Spectral Indices at the Core Center

	Experimental value (cell averaged)	Correction for homogeneous, spherical core	Value for the equivalent homog. sphere
σ_{f8}/σ_{f5}	0.0449±3%	-0.3%	0.0448
σ_{f9}/σ_{f5}	1.023±3%	-0.7%	1.016
σ_{c8}/σ_{f5}	0.138±3%	-0.3%	0.1376

The spectral indices were measured with foils between a fuel plate and a graphite plate. Small corrections were calculated using the cell code KAPER, to obtain the cell-averaged values, which are quoted in the Table. Calculated corrections are applied to obtain the values for the equivalent homogeneous sphere.

D.2 Material Worths at the Core Center

		Reactivity Coefficient, 10^{-5} $\Delta k/k$ / mole		
Material	Sample thickness, g/cm^2	Measured	Infinitely small sample in the equivalent sphere	Hom-Het / Hom
^{235}U	0.17	189.8±3%	208.3	2.38
^{238}U	5.7	- 9.40±3%	- 11.04	7.23
^{239}Pu	0.095	+260 ±3%	287	2.69
^{240}Pu	0.12	+ 62.0 ±8%	70.4	5.15

^{10}B	0.024	-198.2 ±2%	-226	6.49
Ta	1.67	-56.2 ±2%	- 87.2	30.7
Eu_2O_3	0.165	-441 ±2%	-492	4.08
Fe	1.15	- 1.93±10%	- 2.24	1.79

For the material worth measurements, an Al frame (3.14 mm thick; average density 40%) was inserted between two normal cells at the measuring position. This Al frame was replaced by the material samples for the measurements. The value $\beta_{eff} = 0.00359$ was used to convert the data to absolute $\Delta k/k$. For analysis in a spherical model, the worths were corrected a) with the KAPER program to the worth of an infinitely small samples in a homogeneous core (see column 6), b) to the worth in the equivalent homogeneous sphere.

D.3 Additional Experiment

The material buckling of the inner core composition was measured with fission chamber traverses. The result is:

$$B_m^2 = (59.68\pm0.1)\times10^{-4}\ cm^{-2}$$

Reference

R. Böhme et al.

"Experimental Results from Two Pu-Fueled Fast Critical Assemblies" ANS Topical Meeting on New Developments in Reactor Physics and Shielding, September 12-15, 1972.

Table 1 Regional Compositions

Atom densities x 10^{-24} cm^{-3}

Isotope	Inner Core Zone	Outer Core Zone	Blanket
Al	.0000080	.0011906	
C	.0260987	.0255387	.0000135
Cr	.0022423	.0022390	.0011080
Fe	.0079713	.0079824	.0039549
Mn	.0001109	.0001178	.0000875
Mo	.0000165	.0000145	.0000100
Nb	.0000089	.0000077	.0000085
Ni	.0011664	.0011818	.0009845
O	.0218462	.0211909	
^{239}Pu	.0026374	.0023434	
^{240}Pu	.0002369	.0002105	
^{241}Pu	.0000215	.0000191	
^{242}Pu	.0000011	.0000010	
Si	.0000933	.0000932	.0000453
^{235}U	.0000586	.0002958	.0001624
^{238}U	.0079604	.0080456	.0399401

Table 2 Atom densities x 10^{-24} cm^{-3} for the Control Rods - SNEAK-7A

Isotope	Control Rod loaded with PuO_2UO_2	Control Rod loaded with Uranium
Al	.0000069	.0110350
C	.0218819	.0218280
Cr	.0029907	.0020255
Fe	.0107955	.0073807
Mn	.0001819	.0001600
Mo	.0000056	
Nb	.0000003	
Ni	.0015066	.0012258
O	.0180535	.0165945
^{239}Pu	.0021795	
^{240}Pu	.0001958	
^{241}Pu	.0000178	
^{242}Pu	.0000009	
Si	.0001248	.0000840
^{235}U	.0000484	.0022722
^{238}U	.0065783	.0090673

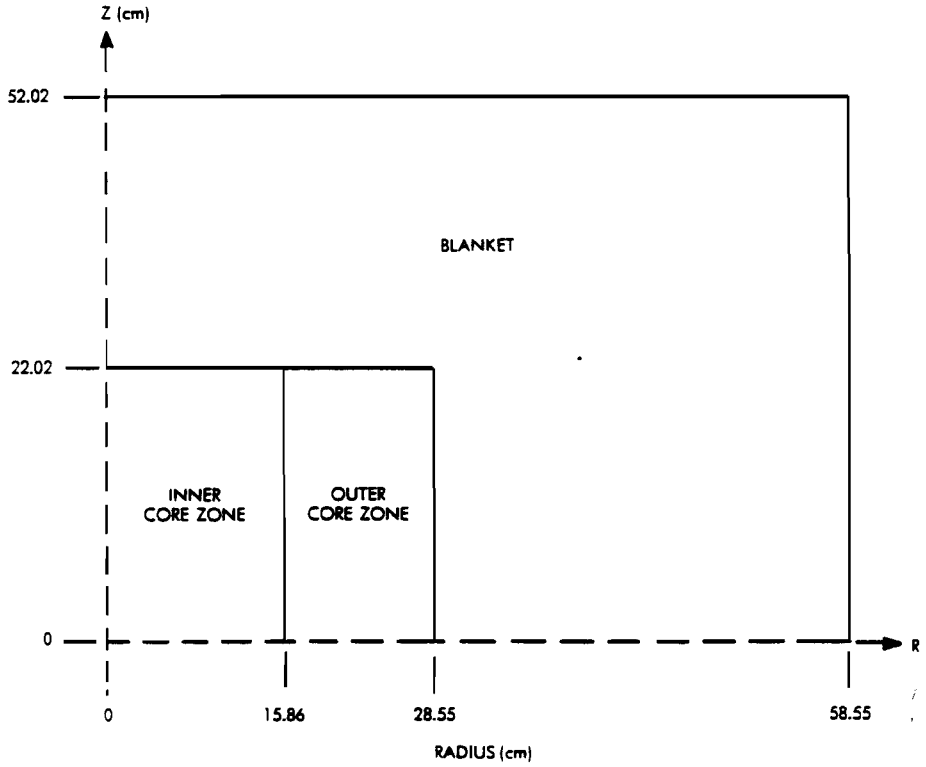

Figure 1. RZ-model for assembly SNEAK-7A.

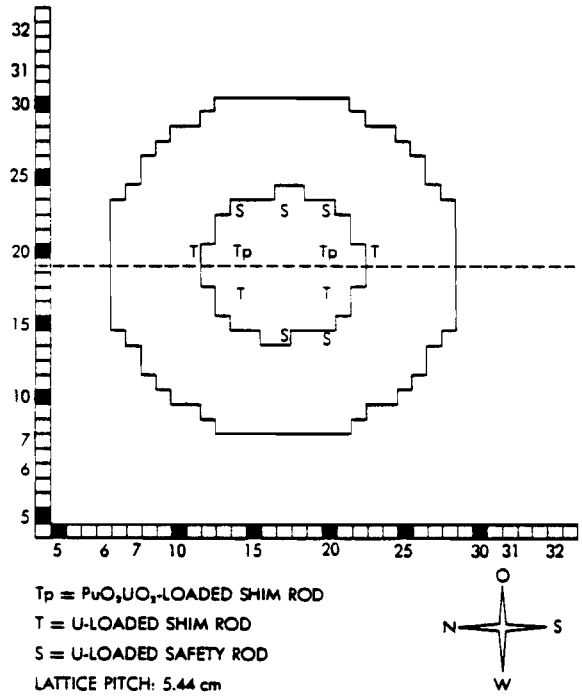

Figure 2. SNEAK-7A core map.

Fast Reactor Benchmark No. 17

A. Benchmark Name and Type: SNEAK-Assembly 7B, a mixed oxide fast critical assembly.

B. System Description

SNEAK-7B had a compact core with mixed oxide fuel, and a simple unit cell, which consists of a PuO_2UO_2 platelet (0.626 cm thick) and a $U_{nat}O_2$ platelet (0.626 cm). The core volume is about 300 liters. The $^{238}U/^{239}Pu$ ratio is about 8.0; the spectrum is harder than that of a LMFBR. In combination with assembly 7A, which has a lower ^{238}U content, the system is suitable to test the high energy cross sections of ^{238}U, and of ^{239}Pu.

The control rods were loaded with enriched uranium; therefore, about 10% of the critical mass was ^{235}U.

C. Model Description

C.1 One-Dimensional Model

A one-dimensional, homogeneous composition model is described as a two-region sphere with homogeneous atom densities for the core and blanket as given in Table I and with the following dimensions:

Core Outer Radius	40.64 cm
Blanket Thickness	30.00 cm
Number of Mesh Intervals:	
Core	45
Blanket	20

The standard mode of calculation may be either diffusion theory or S_6 transport theory with a vacuum boundary condition at the outer blanket boundary and a multigroup structure composed of 26 groups, each of lethargy width equal to 0.5 and with E_{MAX} set at 10 MeV.

The homogeneous spherical model was obtained as follows: a two dimensional calculation in R-Z-geometry was carried out with the code DIXY in 23 energy groups. The control rods were homogenized. The k_{eff} obtained in this calculation was corrected for the cylindrisation, for the actual position of the control rods, and for the heterogeneity effect. Then a diffusion calculation in spherical geometry was run, where the radius was iterated to give the k_{eff} of the DIXY run.

C.2 Two-Dimensional Model Description

A two-dimensional, R-Z, cylindrical model is defined in Fig. 1. The full core height is 70.06 cm, the core radius is 37.63 cm and the axial and radial blankets are 30 cm thick. This model corresponds to a cylinder with volume equal to the actual core corrected for the 40¢ excess reactivity. The core map or lattice loading in X-Y-geometry is shown in Fig. 2.

The suggested mode of calculation is diffusion theory with a vacuum boundary condition at the outer boundaries of the blanket (top and right sides in Fig. 2) and a symmetry boundary condition along the axial and radial axes (left and bottom sides in Fig. 2). The suggested mesh structure is 40 intervals axially and radially in the core and 20 intervals in the blanket.

The following small corrections should be applied to the k_{eff} as calculated in R-Z-geometry:

	Δk/k
cylindrisation	-0.0029
actual control rod position	+0.0000
heterogeneity	±0.0008
	-0.0021

The corrected k_{eff} should be compared to 1.0.

If desired, the homogenization of the control rods can be checked using the atom densities of the pure core cell, and of the control rods, as given in Table 2.

D. Experimental Data

D.1 Spectral Indices at the Core Center

	Experimental Value (cell averaged)	Correction for homogeneous spherical core, %	Value for the equivalent homog. sphere
σ_{f8}/σ_{f5}	0.0328±2%	+0.5	0.0330
σ_{f9}/σ_{f5}	1.014 ±2%	-0.2	1.012
σ_{c8}/σ_{f5}	0.132 ±3%	-0.6	0.1312

The spectral indices were measured with foils. The foils placed across the platelets so that they measured rates which are averages over one platelet.

Calculated corrections were applied to convert to the value for the homogeneous sphere.

D.2 Material Worths at the Core Center

Material	Sample thickness, g/cm^2	Reactivity Coefficient, 10^{-5} $\Delta k/k$ / mole: Measured	Infinitely small sample in the equivalent sphere	$\frac{Hom-Het}{Hom}$ %
^{235}U	0.17	118.9±2%	121.2	-0.8
^{238}U	5.7	- 6.38±2%	- 6.90	4.0
^{239}Pu	0.19	162.0±2%	166.9	-0.54
^{240}Pu	0.12	28.8±10%	30.8	2.12
^{10}B	0.024	- 82.8±2%	- 90.3	5.09
Ta	1.67	- 23.2±2%	- 29.8	20.1
Eu_2O_3	0.165	-164.7±3%	-174	2.23
Fe	2.30	- 1.34±5%	- 1.42	2.16

For the material worth measurements, an Al frame (3.14 mm thick, average density 40%) was inserted between two normal cells at the measuring position. This Al frame was replaced by the material samples for the measurements. The value β_{eff} = 0.00400 was used to convert the data to absolute $\Delta k/k$. For analysis in a spherical model, the worths were corrected a) with the KAPER program to the worths of infinitely small samples in a homogeneous core (correction see column 6), b) to the worths in the equivalent homogeneous sphere.

D.3 Additional Experiment

The material buckling of the core composition was measured with fission chamber traverses. The result is:

$$B_m^2 = (34.74 \pm 0.04) \times 10^{-4} \text{ cm}^{-2}$$

Reference

R. Böhme et al.
"Experimental Results from Two Pu-Fueled Fast Critical Assemblies" ANS Topical Meeting on New Developments in Reactor Physics and Shielding, September 12-15, 1972.

Table 1 Regional Compositions

Atom densities x $10^{24}/cm^3$

Isotope	Core	Blanket
Al	.0012112	
C	.0000631	.0000135
Cr	.0027560	.0011080
Fe	.0098021	.0039549
H	.0000071	
Mg	.0000095	
Mn	.0000646	.0000875
Mo	.0000184	.0000100
Nb	.0000084	.0000085
Ni	.0014594	.0009845
O	.0331936	
^{239}Pu	.0018312	
^{240}Pu	.0001645	
^{241}Pu	.0000149	
^{242}Pu	.0000007	
Si	.0001174	.0000453
^{235}U	.0002663	.0001624
^{238}U	.0145794	.0399401

Table 2 Atom Densities for the Pure Core Material and the Control Rods

Atom Densities $x10^{-24}/cm^3$

Isotope	Pure Core Material	Control Rods
Al	.0000120	.0165823
C	.0000659	.0000264
Cr	.0028030	.0021535
Fe	.0099576	.0078086
H	.0000076	
Mg	.0000053	.0000631
Mn	.0000573	.0001585
Mo	.0000198	
Nb	.0000090	
Ni	.0014602	.0014496
O	.0338377	.0249366
^{239}Pu	.0019741	
^{240}Pu	.0001773	
^{241}Pu	.0000161	
^{242}Pu	.0000008	
Si	.0001197	.0000888
^{235}U	.0001063	.0023172
^{238}U	.0145684	.0147206

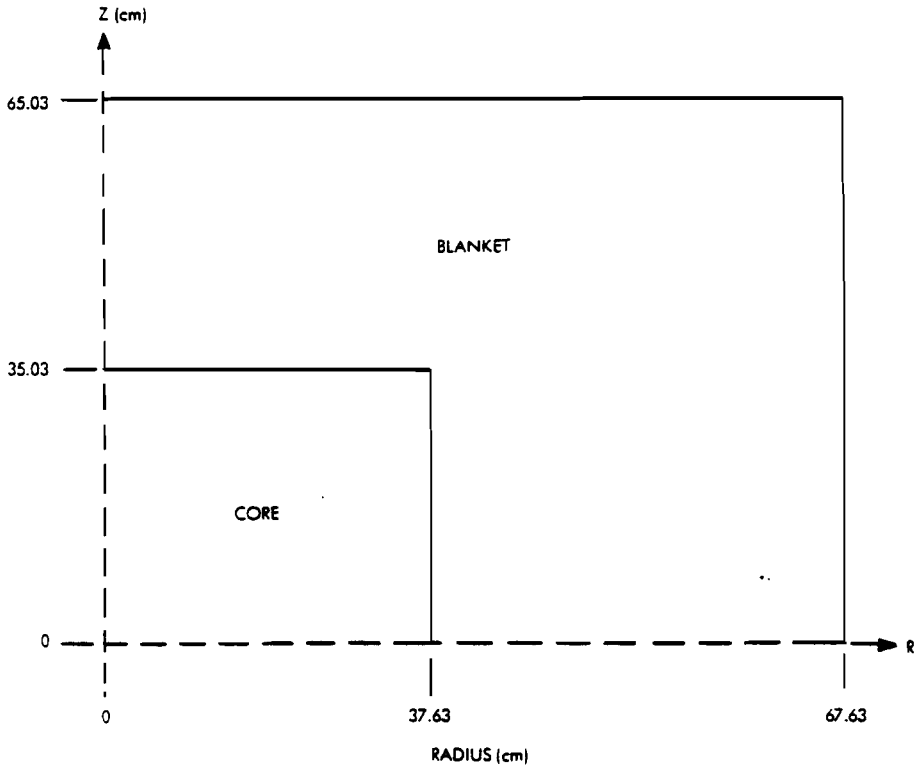

Figure 1. RZ-model for assembly SNEAK-7B.

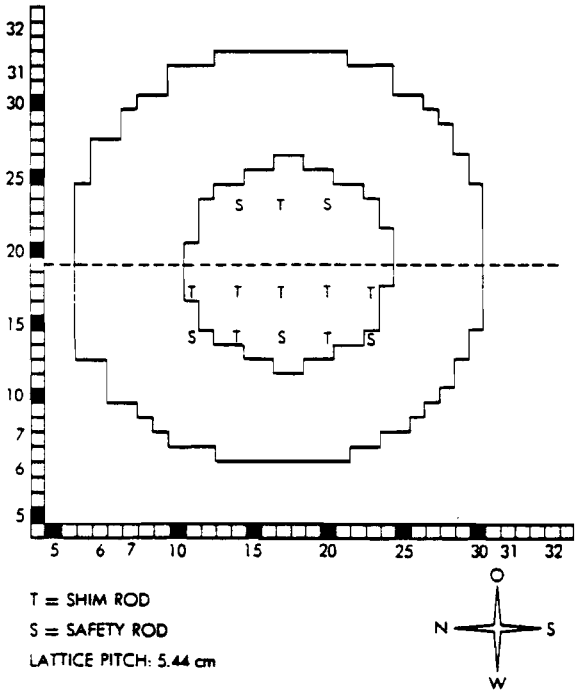

Figure 2. SNEAK-7B core map.

FAST REACTOR BENCHMARK NO. 18

A. Benchmark Name and Type

ZPR-9 Assembly 31 - a mixed (Pu, U)- fuel plus graphite fast critical assembly.

B. System Description

The ZPR-9 assembly consists of two halves, each a horizontal matrix of 5.5245 cm square stainless steel tubes into which are loaded stainless steel drawers containing fuel and diluent materials of various types. Assembly 31 is an intermediate sized (∿1000 liter) fast critical assembly with mixed (Pu, U) fuel plus carbon (graphite) and is typical of current mixed carbide-fueled LMFBR designs (Ref. 2). It has a uniform core zone with a length-to-diameter (L/D) ratio of approximately 0.77; it is blanketed both axially and radially with a uranium carbide blanket; and it is surrounded by a 15.24 cm stainless steel reflector. This assembly is the reference assembly for a study of the relative physics parameters of advanced oxide and carbide fuels. The assembly's spectrum characteristics and simple uniform geometric configuration were selected to make it a useful benchmark assembly.

The core unit cell is a two-drawer unit cell with the fuel (28 w/o plutonium, 69.5 w/o uranium, and 2.5 w/o molybdenum) columns sandwiched between carbon-depleted uranium columns or between sodium and carbon-depleted uranium columns. The plutonium is 11.6 w/o ^{240}Pu. The drawer loadings for the stationary half of the assembly are shown in Figs. 1, 2, and 3. (Material descriptors in Figs. 1-3 are: NA-sodium, UD-depleted uranium, C-graphite, SST-stainless steel, and Pu-plutonium-depleted uranium-molybdenum alloy fuel). A cross sectional view of the as-built reference assembly which had a measured excess reactivity of 48.12 Th $\pm$ 0.43 is shown in Fig. 4. The core loading had Type-1 drawers in odd-numbered columns (of the matrix) and Type-2 drawers in even-numbered columns (see Fig. 4). The equivalent R-Z representation of the as-built reference configuration is shown in Fig. 5.

C. Model Description

1. One-Dimensional Model: A one-dimensional model with spherical geometry is appropriate for many benchmark calculations. A spherical model was defined with reference to a two-dimensional finite cylindrical model (which will be described in Section C.2). The homogeneous spherical model was defined in the following manner. Equivalent thicknesses were first determined for the spherical layers of blanket and reflector. The blenket and reflector compositions were defined as the weighted averages of the radial and axial blankets and reflectors. Although the blanket and reflector regions each had a single uniform unit cell throughout, the mean atom densities differed slightly due to differences in plate lengths used). The weighting of these atom densities was done on the basis of the relative leakage rates (as determined by the two-dimensional calculation) into these radial and axial regions. A dimension search was then performed to obtain a core radius that produces the same k_{eff} as the homogeneous two-dimensional cylindrical model. These steps in generating the one-dimensional model are diagrammed in Fig. 6. This figure also illustrates the interrelationship of the homogeneous spherical model and the heterogeneous cylindrical model. The resultant dimensions and compositions for use with the spherical model are given in Table I.

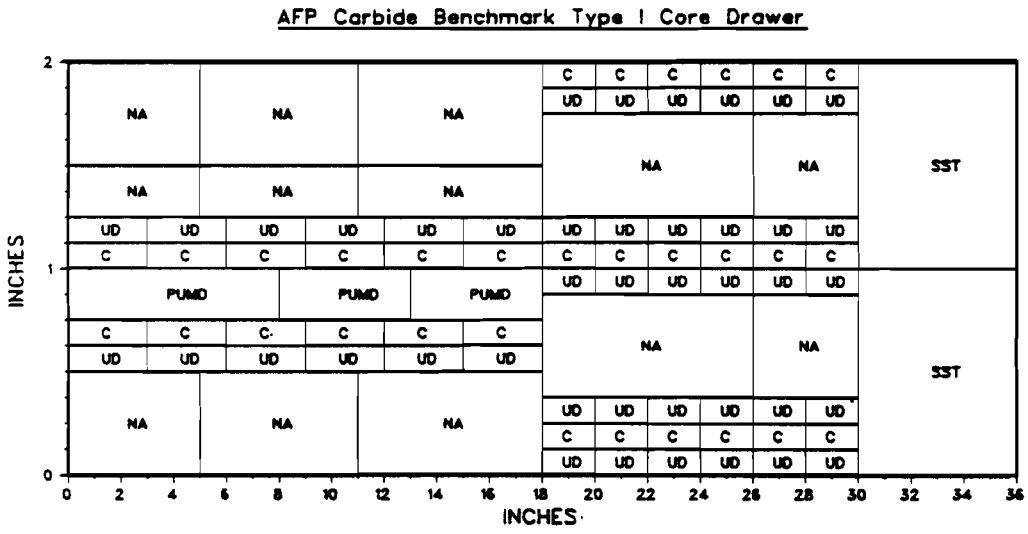

Figure 1. Type-1 core-drawer loading master.

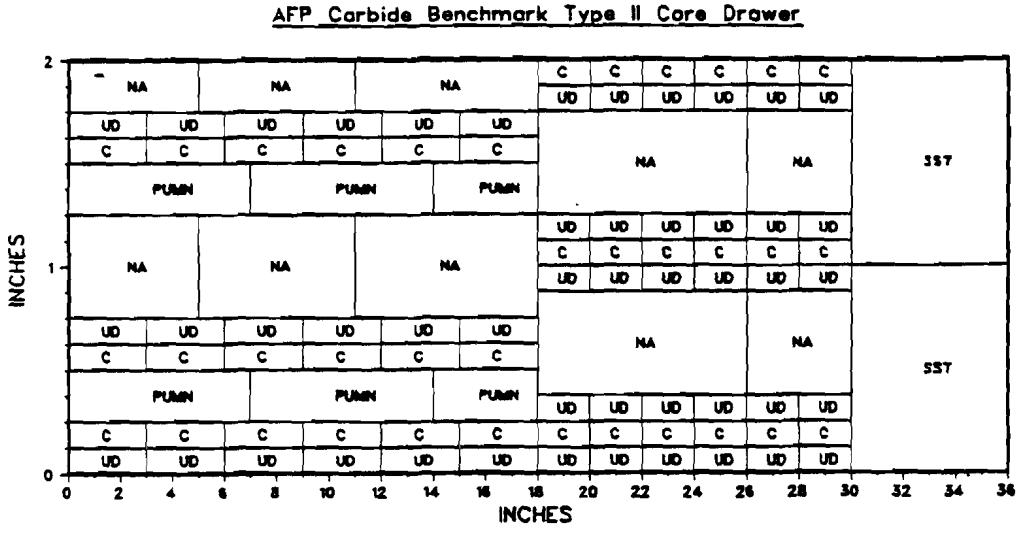

Figure 2. Type-2 core-drawer loading master.

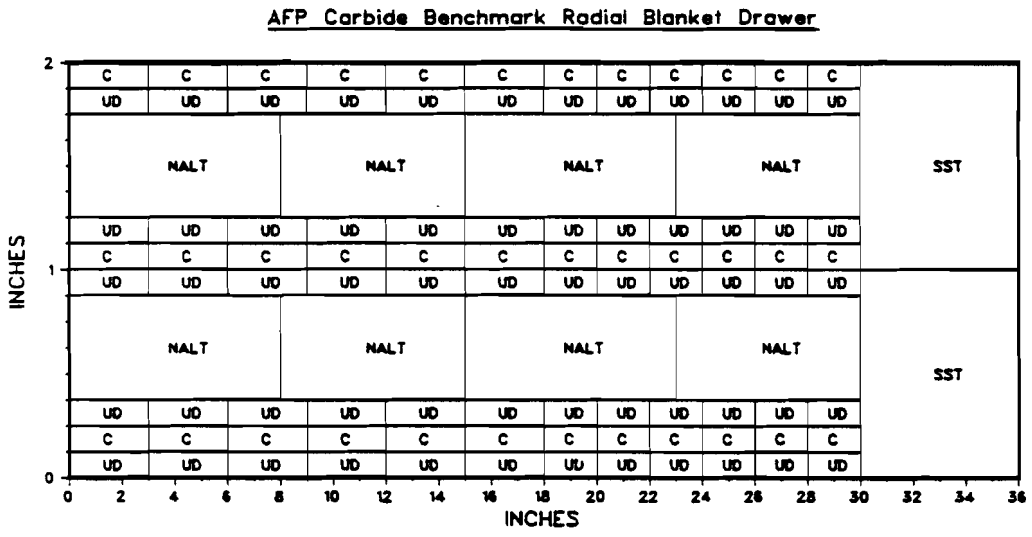

Figure 3. Radial blanket drawer loading master.

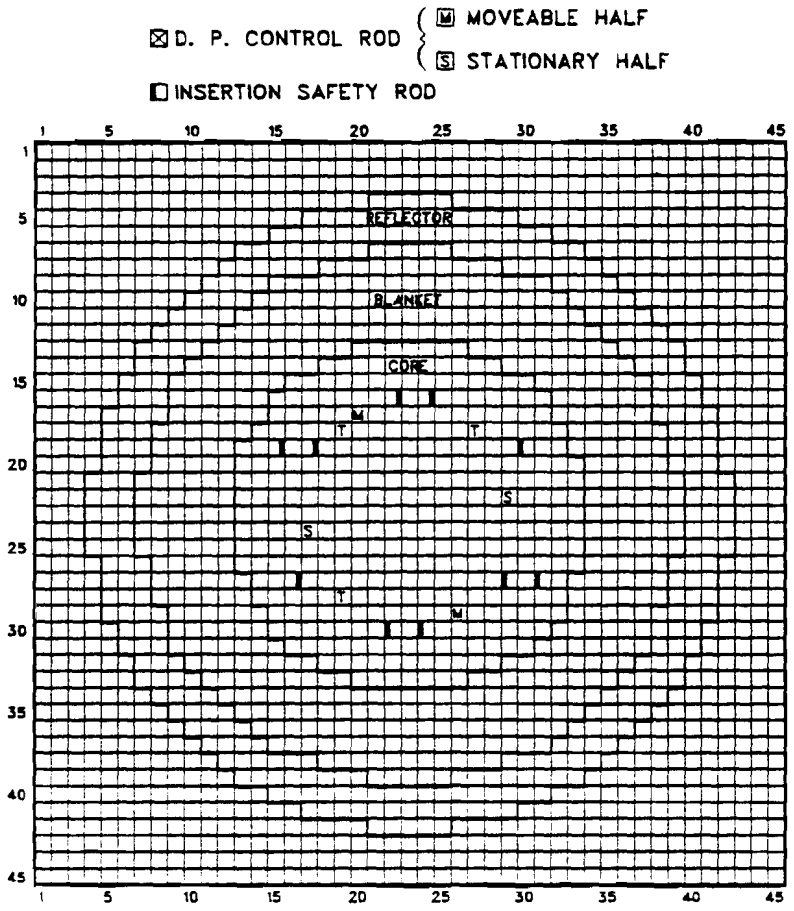

Figure 4. Reference configuration of the carbide benchmark critical assembly.

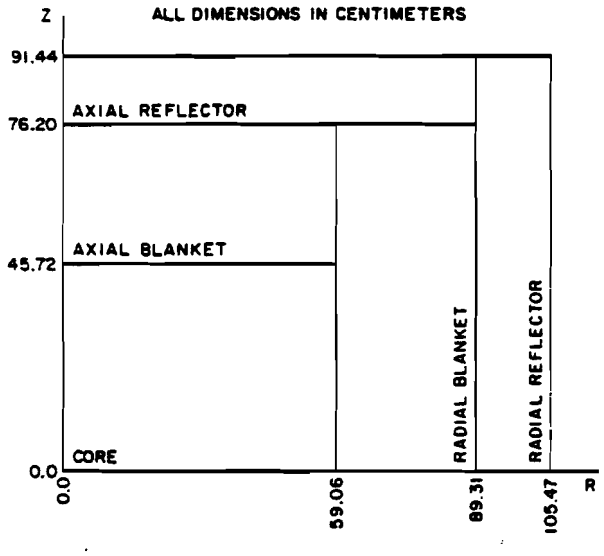

Figure 5. Carbide benchmark R-Z calculational model.

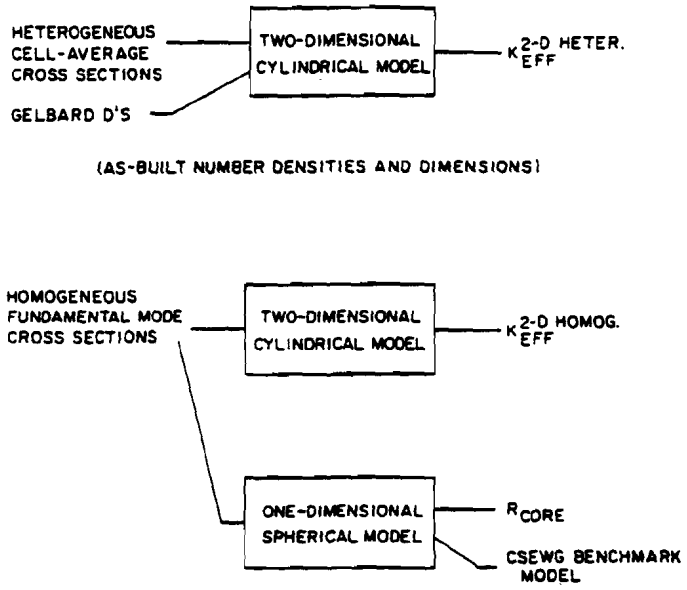

Figure 6. Generation of one-dimensional model.

TABLE I. One-Dimensional Spherical Model of the Carbide Benchmark Assembly

	Core	Blanket	Reflector
		Dimensions (cm)	
Radius	59.5054		
Thickness		22.1603	15.9200
Isotope		Mean Atom Densities (10^{21} atoms/cm^3)	
^{239}Pu	1.3320	—	—
^{240}Pu	0.1801	—	—
^{241}Pu	0.0286	—	—
^{235}U	0.0214	0.0259	—
^{238}U	9.8203	12.0936	—
Fe	10.4610	8.6259	56.5309
Ni	1.3522	1.0894	6.8174
Cr	2.9309	2.4083	15.7584
Mn	0.2301	0.1866	1.3457
Mo	0.3500	0.0097	0.0668
Na	9.0842	9.1791	—
C	10.8394	12.7930	0.2195

An energy group structure with 29 broad groups, as given in Table II, is recommended. Such a group structure has suggicient detail at low energies to afford reasonable computations of material worths and Doppler effects.

Because of the simplicity of this three-region, homogeneous spherical model, the macroscopic flux distribution across the reactor may be computed with diffusion theory. A relatively coarse mesh spacing of ∿2 cm should be adequate. This treatment should produce central real and adjoint spectra useful for benchmark data testing.

Central material reactivity worths and Doppler reactivity worths may be computed using perturbation theory. If the sample material is contained in the core and is optically thin, the homogeneous core cross sections for the material are appropriate for the sample.

The primary defect in the homogeneous spherical model for this geometrically simple system is the neglect of the heterogeneities in the unit cell. Sections D and F indicate the biases which arise from the use of homogeneous cross sections and discuss "correction factors" where appropriate. The error in material worth or Doppler worth introduced by local flux distortions depends strongly upon the nature of the sample.

2. Other More Complicated Models: A two-dimensional finite cylindrical representation of the system is closer to the physical configuration than a spherical representation. The R-Z representation of the as-built critical assembly is shown in Fig. 5. Region dimensions are given in Table III. Mean atom densities to be used with the two-dimensional cylindrical model are given in Table IV.

D. Experimental Data

1. Measured Eigenvalue: The measured eigenvalue corresponding to the models of Section C is 1.000 ± 0.0015. It may be noted the measured excess reactivity (48.12 ± 0.43 Ih) of the as-built reference configuration which has not been adjusted into this benchmark model corresponds to a very small change in eigenvalue (∿0.0005 δk). Calculations indicate a heterogeneity correction factor (discussed further in Section E) of +0.01276 δk. This heterogeneity correction includes plate heterogeneity, streaming, and transport effects.

2. Unit-Cell Reaction Rates: Cell-averaged reaction rates for ^{239}Pu (n,f), ^{235}U (n,f), ^{238}U (n,f), and ^{238}U (n,γ) were measured at the core center. Cell-averaged rates were obtained with detailed foil mappings through the unit cell. Details of these measuring techniques are given in Ref. 3 . The measured reaction rate ratios relative to ^{239}Pu-fission are given in Table V. Also shown in Table V are calculated correction factors (to be applied to the calculated values) to account for the geometry and homogeneity of the one-dimensional spherical model. These correction factors are discussed further in Section E.

3. Conversion Ratio at the Center of the Core: The measured central core conversion ratio was 0.734 ± 0.028 (Ref. 4). The components of this value are given in Table VI as well as calculated results and correction factors. Note the definition (as given in Table VI) includes only production in ^{238}U and destruction of ^{239}Pu, which is the principal component of the overall conversion ratio.

TABLE II. Specification of 29 Broad Group Energy Structure

Group	Δ(lethargy)	E_{upper}, eV	Group	Δ(lethargy)	E_{upper}, eV
1	0.35	1.4191(7)	16	0.50	9.1188(3)
2	0.50	1.0000(7)	17	0.50	5.5309(3)
3	0.50	6.0653(6)	18	0.50	3.3546(3)
4	0.50	3.6788(6)	19	0.50	2.0347(3)
5	0.50	2.2313(6)	20	0.50	1.2341(3)
6	0.50	1.3534(6)	21	0.50	7.4852(2)
7	0.50	8.2085(5)	22	0.50	4.5400(2)
8	0.50	4.9787(5)	23	1.00	2.7536(2)
9	0.50	3.0197(5)	24	1.00	1.0130(2)
10	0.50	1.8316(5)	25	1.00	3.7267(1)
11	0.50	1.1109(5)	26	1.00	1.3710(1)
12	0.50	6.7380(4)	27	1.00	5.0435(0)
13	0.50	4.0868(4)	28	1.50	1.8554(0)
14	0.50	2.4788(4)	29	∞	4.1400(-1)
15	0.50	1.5034(4)			

TABLE III. Dimensions for the Two-Dimensional Cylindrical Model of the Carbide Benchmark Assembly

Core Radius, cm	59.06
Core Height, cm	91.44
Radial Blanket Thickness, cm	30.25
Radial Blanket Height, cm	152.40
Axial Blanket Thickness, cm	30.48
Radial Reflector Thickness, cm	16.16
Radial Reflector Height, cm	210.94
Axial Reflector Thickness, cm	15.24
Core Volume, liters	1002.01

TABLE IV. Mean Atom Densities for the Two-Dimensional Model of the Carbide Benchmark Assembly, 10^{21} atoms/cm^3

Isotope	Core	Radial Blanket	Axial Blanket	Radial Reflector	Axial Reflector
^{238}Pu	0.0008	—	—	—	—
^{239}Pu	1.3320	—	—	—	—
^{240}Pu	0.1766	—	—	—	—
^{241}Pu	0.0176	—	—	—	—
^{242}Pu	0.0027	—	—	—	—
^{241}Am	0.0110	—	—	—	—
^{235}U	0.0214	0.0259	0.0259	—	—
^{238}U	9.8203	12.0969	12.0815	—	—
Fe	10.4610	8.6262	8.6249	56.6746	55.2268
Ni	1.3522	1.0894	1.0892	6.8009	6.9675
Cr	2.9309	2.4084	2.4080	15.7571	15.7707
Mn	0.2301	0.1866	0.1866	1.3289	1.4981
Mo	0.3500	0.0097	0.0097	0.0731	0.0097
Na	9.0842	9.1453	9.3053	—	—
C	10.8394	12.8410	12.6139	0.2166	0.2456

TABLE V. Cell-Averaged Reaction-Rate Ratios at the Core Center

	Measured[a]	Calculated Two-Dimensional Heterogeneous[a]	C/E	Calculated One-Dimensional Homogeneous	Model Correction Factor[b]
f^{25}/f^{49}	1.058 ± 0.014	1.0140	0.958 ± 0.013	1.0079	1.0061
f^{28}/f^{49}	0.0300 ± 0.0004	0.0288	0.960 ± 0.013	0.0288	1.0000
c^{28}/f^{49}	0.1230 ± 0.0018	0.1311	1.066 ± 0.015	0.1358	0.9654

[a] Taken from Ref. 2.

[b] Model Correction Factor $\equiv \frac{\text{Calculated Two-Dimensional Heterogeneous}}{\text{Calculated One-Dimensional Homogeneous}}$.

TABLE VI. Point Conversion Ratio at the Core Center of the Carbide Benchmark Assembly

	Measured	Calculated Two-Dimensional Heterogeneous[a]	C/E	Calculated One-Dimensional Homogeneous	Model Correction Factor[b]
c^{28}/f^{49}	0.1230 ± 0.0018	0.1311	1.066 ± 0.016	0.1358	0.9654
$(1+\alpha)^{49}$	1.236 ± 0.043	1.2202	0.987 ± 0.034	1.2243	0.9966
CR_p[c]	0.734 ± 0.028	0.7919	1.079 ± 0.041	0.8178	0.9683

[a] Taken from Ref. 3.

[b] Model Correction Factor $\equiv \frac{\text{Calculated Two-Dimensional Heterogeneous}}{\text{Calculated One-Dimensional Homogeneous}}$

[c] $CR_p \equiv \frac{^{28}N\ ^{28}c/^{49}f}{^{49}N(1+\alpha)^{49}} = \frac{(9.8203 \times 10^{21})\ ^{28}c/^{49}f}{(1.3320 \times 10^{21})\ (1+\alpha)^{49}}$

4. Material Worths at the Center of the Core: Central reactivity worths of several materials were measured in a small cavity with the use of the radial sample changer. The samples were held in thin-walled stainless steel sample holders and the reactivity worth of the sample was obtained as the difference in the reactivity worth (relative to void) of the sample holder between when it holds a sample and when it is empty. Further descriptions of the samples and the measurements are given in Ref. 5. Table VII gives the experimental worths of the isotopes as well as the calculated results and correction factors. Note that sample size correction factors have not been included.

E. Calculated Results

Two sets of calculated results are reported in these specifications of the benchmark model of ZPR-9 Assembly 31. These calculations were made using ENDF/B Version IV nuclear data, and correspond to a homogeneous treatment of the one-dimensional spherical model and a heterogeneous treatment of the two-dimensional cylindrical model. Details of the former set of calculations are included in this section; details of the latter set are given in Refs. 3-6. However, it should be noted these two-dimensional heterogeneous calculations utilized two-dimensional diffusion theory (in 29 broad groups) with cell-averaged cross sections which accounted for the plate structure of the unit cell, and Gelbard bi-directional diffusion coefficients, i.e., the treatment of heterogeneity included plate self shielding, "streaming" and transport corrections.

For the calculations of the one-dimensional spherical model, multigroup (29 b.g.) cross sections were produced by MC^2-2 for the homogeneous core and blanket compositions. For the core region the fundamental mode option was consistent P1 with a search on buckling ($k_\infty(B^2 = 0.0) = 1.23958$, $B^2_{crit} = 0.0013703$) to produce $k_{eff} = 1$. For the blanket region the consistent P1 option with zero buckling ($k_\infty(B^2 = 0.0) = 0.32520$) was used with an external ^{239}Pu fission spectra source. Cross sections generated for the blanket region were used in the reflector region.

This one-dimensional, homogeneous spherical model yielded (by definition) a multiplication constant of 0.97574. The addition of the heterogeneity correction (+0.01276 δk, which includes plate heterogeneity, streaming, and transport effects) gives a k_{eff} of 0.98850.

The calculated values for the central reaction rate ratios are summarized in Table VIII.

The central worth calculations based on the homogeneous spherical model central fluxes are summarized in Table VIII. The basic calculations used first-order perturbation theory.

F. Comments and Documentation

Details of the ZPR-9 Assembly 31 Carbide Benchmark Program are given in Ref. 1-7. These documents include discussion of the experimental program (techniques and measured values) and the concurrent analysis (methods and calculated values) for this assembly. They also provide additional references for further information on both experimental and calculational methods. The

TABLE VII. Material Reactivity Worths at the Core Center of the Carbide Benchmark Assembly

Isotope or Element	Measured[a,b] Ih/kg	Measured[a,b] $\delta k/k/10^{24}$ atoms	Conversion Factors $kg/10^{24}$ atoms	Conversion Factors Ih/%$\delta k/k$	Calculated Two-Dimensional Heterogeneous[a] Ih/kg	Calculated Two-Dimensional Heterogeneous[a] $\delta k/k/10^{24}$ atoms	C/E	Calculated One-Dimensional Homogeneous[a] $\delta k/k/10^{24}$ atoms	Model Correction Factor[c]
^{239}Pu	268.66 ± 2.81	1.1561(-3)	0.39693	922.37	319.78	1.3761(-3)	1.19	1.4689(-3)	0.9369
^{240}Pu	37.58 ± 0.80	1.6240(-4)	0.39859	922.37	48.33	2.0885(-4)	1.29	2.4119(-3)	0.8659
^{241}Pu	395.13 ± 42.9	1.7146(-3)	0.40026	922.37	442.09	1.9184(-3)	1.12	---	---
^{233}U	347.32 ± 4.71	1.4571(-3)	0.38695	922.37	408.24	1.7126(-3)	1.18	---	---
^{235}U	202.34 ± 1.96	8.5615(-4)	0.39029	922.37	245.24	1.0377(-3)	1.21	1.0967(-3)	0.9461
^{238}U	-14.41 ± 0.55	-6.1752(-5)	0.39527	922.37	-15.09	-6.4666(-5)	1.05	-6.4837(-5)	0.9974
^{10}B	-3988.0 ± 67.2	-7.1884(-4)	0.016626	922.37	-4114.9	-7.4172(-4)	1.03	-7.4834(-4)	0.9912
^{6}Li	-2841.6 ± 52.6	-3.0770(-4)	0.009988	922.37	-3248.5	-3.5176(-4)	1.14	---	---
C	-32.66 ± 0.84	-7.0617(-6)	0.019943	922.37	-51.87	-1.1215(-5)	1.59	-1.2398(-5)	0.9046
Na	-14.96 ± 1.08	-6.1913(-6)	0.038173	922.37	-21.09	-8.7283(-6)	1.41	-9.0559(-6)	0.9638
Al	-15.57 ± 1.69	-7.5626(-6)	0.044801	922.37	-18.75	-9.1071(-6)	1.20	---	---

[a] Taken from Ref. 4.

[b] The sample worths were reported for samples of smallest (available) mass, and no sample size effect corrections have been made.

[c] Model Correction Factor $\equiv \frac{\text{Calculated Two-Dimensional Heterogeneous } (\delta k/k/10^{24} \text{ atoms})}{\text{Calculated One-Dimensional Homogeneous } (\delta k/k/10^{24} \text{ atoms})}$

Note this correction factor does not include any difference in calculated reactivity conversion factor between the one- and two-dimensional models. (1% $\delta k/k$ was calculated to be 905.11 Ih in the one-dimensional homogeneous model.) This correction factor is appropriate in comparing the reactivity worths obtained with the homogeneous one-dimensional spherical model with the experimental values in units of $\delta k/k/10^{24}$ atoms.

TABLE VII. Comparison of Calculations with a Two-Dimensional Heterogeneous and a One-Dimensional Homogeneous Model for ZPR-9 Assembly 31

		One-Dimensional Homogeneous	Two-Dimensional Heterogeneous
k_{eff}		0.97574	0.98850
Central Reaction Rate Rate Ratios	f^{25}/f^{49}	1.0079	1.0140
	f^{28}/f^{49}	0.0288	0.0288
	c^{28}/f^{49}	0.1358	0.1311
Central Material Worths, $\delta k/k/10^{24}$ atoms[a]	^{239}Pu	1.4689(-3)	1.3761(-3)
	^{240}Pu	2.4119(-3)	2.0885(-4)
	^{235}U	1.0967(-3)	1.0377(-3)
	^{238}U	-6.4837(-5)	-6.4666(-5)
	^{10}B	-7.4834(-4)	-7.4172(-4)
	C	-1.2398(-5)	-1.1215(-5)
	Na	-9.0559(-6)	-8.7283(-6)

[a]First-order perturbation calculations which do not include corrections for sample size effects.

limitations of the homogeneous, spherical benchmark model can be assessed by comparison of the calculated results obtained with this simplified model with the calculated results obtained with the heterogeneous, cylindrical model. Correction factors to account for these differences have been given herein. Previous experience has indicated these corrections are not too sensitive to typical data adjustments Ref. 7.

For the central worth measurements, the reactivity conversion factor 1% $\delta k/k$ = 922.37 Ih was used to convert the experimentally measured periods to the desired reactivity units. The revised delayed neutron data of ENDF/B Version IV were used in computing this factor.

REFERENCES

1. R. D. McKnight, "Benchmark Specifications in CSEWG Format for ZPR-9 Assembly 31, The Advanced Fuels Program Carbide Benchmark Critical Assembly," ZPR-TM-281, June 13, 1977.

2. L. G. LeSage, E. M. Bohn, D. C. Wade and R. B. Pond, "Program Description—Advanced Fuels Critical Experiments on ZPR-9," ZPR-TM-256, November 10, 1976 (see also ZPR-TM-275).

3. J. A. Morman, I. K. Olson, and W. R. Robinson, "Reaction Rate Measurements in the Carbide Benchmark Assembly of the Advanced Fuels Program," ZPR-TM-299, November 28, 1977.

4. M. M. Bretscher and I. K. Olson, "Measurement of Absorption-to-Fission Ratios and the Central Core Conversion Ratio in the Carbide Benchmark Assembly of the ZPR-9 Advanced Fuels Program," ZPR-TM-296, November 11, 1977 (see also ZPR-TM-309).

5. R. G. Bucher, D. M. Smith, and R. Nepomechie, "Small-sample Reactivity-worth Measurements in Advanced Fuels Program," ANL-RDP-63 (September, 1977), also to be issued as ZPR-TM report.

6. R. W. Schaefer and D. C. Wade, "The Advanced Fuels Critical Experiments Program; Calculational Models and Results," ZPR-TM-307, February 9, 1978.

7. R. D. McKnight, "Benchmark Testing Using ENDF/B-III and -IV," Nucl. Sci. Eng., 62, 309-330 (1977).

FAST REACTOR BENCHMARK NO. 19

A. Benchmark Name and Type

JEZEBEL-23, a bare sphere of U(98.13 at. % ^{233}U)

B. Systems Description

JEZEBEL-23 as a bare sphere of U(98.13 at. % ^{233}U) metal, is especially suited for testing ^{233}U cross sections in the fission source energy range. The single-region, simple geometry and uniform composition facilitate calculational testing.

C. Model Description

The spherical homogeneous model has a core radius of 5.983 cm and the following composition.[1]

Isotope	Density, nuclei/b-cm
^{233}U	0.04671
^{234}U	0.00059
^{235}U	0.00001
^{238}U	0.00029

The recommended mode of calculation is one-dimensional transport theory, S_{16}, with 40 mesh intervals in the core, a vacuum boundary condition at the core boundary (5.983 cm) and a 26 energy group structure with half-lethargy unit widths and an upper energy of 10 MeV.

D. Experimental Data

1. Measured Eigenvalue: $k = 1.000 \pm 0.001$

2. Spectral Indices at Core Center

a. Central Fission Ratios[2]

$\sigma_f(^{238}U) / \sigma_f(^{235}U) = 0.2131 \pm 0.0023$

$\sigma_f(^{237}Np) / \sigma_f(^{235}U) = 0.977 \pm 0.016$

3. Rossi Alpha[2]

$\alpha = -\beta_{eff} / \ell = -(1.00 \pm 0.01) \times 10^6 \text{ sec}^{-1}$

4. Central Reactivity Coefficients

Essentially only central void coefficient: its value 4.35 (±1%) cents/g implies $\beta_{eff} = 0.00289$ versus 0.00288 (±1.2%) implied by the surface mass increment between delayed and prompt critical and 0.00286 implied by ENDF/B-IV delayed neutron data.

5. Neutron Flux Spectrum

a. Leakage Spectrum[5]

The spectrum of neutrons emitting from the surface of the core is represented below in the 1/2 lethargy group structure (E_{max} = 10 MeV) with an arbitrary normalization to 18 in group 4. Uncertainties are based on counting statistics alone.

Energy Group	Lower Lethargy Limit	Relative Neutron Leakage
1	0.5	2.3 ± 0.4
2	1.0	11.0 ± 0.6
3	1.5	17.8 ± 0.7
4	2.0	18.0 ± 0.8
5	2.5	17.0 ± 0.8
6	3.0	13.8 ± 0.8
7	3.5	12.1 ± 0.9

b. Central Spectrum Relative to ^{233}U Fission Spectrum [2b]

Deviation of the central spectrum from the ^{233}U fission spectrum is characterized by the following ratios of central high-energy spectral indices to the corresponding indices for the ^{233}U fission spectrum.

Spectral Index	Ratio of Central Value to Value for ^{233}U Fission Spectrum
$\sigma_f(^{238}U) / \sigma_{n,p}(^{31}P)$	1.026 ± 0.020
$\sigma_{n,p}(^{27}Al) / \sigma_{n,p}(^{31}P)$	1.013 ± 0.017
$\sigma_{n,p}(^{56}Fe) / \sigma_{n,p}(^{31}P)$	1.021 ± 0.020
$\sigma_{n,}(^{27}Al) / \sigma_{n,p}(^{31}P)$	1.029 ± 0.025
$\sigma_{n,2n}(^{63}Cu) / \sigma_{n,p}(^{31}P)$	1.011 ± 0.030

E. Calculated Results

Calculated results may be appended to these specifications.

F. Comments and Documentation

The composition and configuration specifications were taken from Ref. 1 which also gives the uncertainty in critical mass, at the specified composition and density, as ± 0.4%.

This translates to an uncertainty in eigenvalue, at the specified composition, density, and size, of ± 0.1%.

The most accurate fission ratios for Jezebel are obtained from recent absolute-ratio measurements in Flattop-25 and Big Ten and double-ratio measurements connecting these to Jezebel-23. These measurements are described below.

Measurement Location	Value	Double Ratio to Jezebel-23	Jezebel-23	Reference
$\sigma_f(^{238}U)$ $\sigma_f(^{235}U)$				
Flattop-25	0.1479(±1.5%)	1.432(±0.6%)	0.2118(±1.6%)	2c
Big Ten	0.373(±1.7%)	5.714(±0.8%)	0.2131(±1.9%	2d
Van de Graff	0.433(±1.5%)	0.4955(±0.9%	0.2146(±1.7%)	ENDF/B-IV
(E_n = 2.43 MeV)				
		Average:	0.2131(±1.1%)	
$\sigma_f(^{237}Np)$ / $\sigma_f(^{235}u)$				
Topsy	0.760(±4%)	1.278(±0.5%)	0.971(±4.0%)	2e
Big Ten	0.317(±2.2%)	3.094(±0.9%)	0.981(±2.4%)	2d
Van de Graaff	1.328(±2%)	0.735(±1.1%)	0.976(±2.3%)	ENDF/B-IV
(E_n = 2.43 MeV)				
		Average:	0.977(±1.6%)	

Reactivity-coefficient measurements were curtailed because of intense gamma radiation.

The data listed for leakage spectrum were derived from Ref. 3. A finer energy representation for the spectrum is given in this reference along with statistical uncertainties.

REFERENCES

1. G. E. Hansen and H. C. Paxton, "Reevaluated Critical Specifications of Some Los Alamos Fast-Neutron Systems," Los Alamos Scientific Laboratory report LA-4208 (1969).
2. (a) G.E. Hansen, "Status of Computational and Experimental Correlations for Los Alamos Fast Neutron Critical Assemblies," Proc. Seminar Physics of Fast and Intermediate Reactors, Vienna, August 3-11, 1961 (IAEA, Vienna, 1962) Vol. I, pp 445-455. (b) J. A. Grundl and G. E. Hansen, "Measurement of Average Cross Section Ratios in Fundamental Fast-Neutron Spectra, "Proc. Paris Conf. Nuclear Data for Reactors (IAEA, Vienna, 1967) Vol. I, pp 321-336. (c) P. I. Amundson, A. M. Broomfield, W. G. Davey, and J. M. Stevenson, "An International Comparison of Fission Detector Standards, "Proc. Intern. Conf. Fast Critical Experiments and Their Analysis, Argonne, October 10-13, 1966 (Argonne National Laboratory report ANL-7320) pp 679-687. (d) D. M. Gilliam, "Integral Measurement Results in Standard Fields,"Proc. Intern. Specialist's Symposium Neutron Standards and Applications, Gaithersburg, March 28-31, 1977 (NBS Special Publication 493, 1977) pp 293-303. (e) G.A. Linenberger and L. L. Lowry, "Neutron Detector Traverses in the Topsy and Godiva Critical Assemblies," Los Alamos Scientific Laboratory report LA-1653 (1953).

3. L. E. Bobisud, "Leakage Spectrum of ^{233}U Critical Assembly," Los Alamos Scientific Laboratory report LAMS-2755 (1962).

FAST REACTOR BENCHMARK NO. 20

A. Benchmark Name and Type

BIG TEN, a reflected cylinder of uranium contianing 10% ^{235}U.

B. System Description

BIG TEN is a cylindrical system consisting of a uranium-metal core, averaging 10 wt% ^{235}U, reflected by depleted-uranium metal. The core has a homogeneous axial region surrounded by interleaved plates of highly enriched uranium and natural uranium such that the average ^{235}U content is uniform.

C. Model Description[1]

1. Composition

Isotope	Core	Reflector
^{234}U nuclei/b-cm	0.00005	0.00000
^{235}U nuclei/b-cm	0.00484	0.00010
^{238}U nuclei/b-cm	0.04268	0.04797

2. One-Dimensional Model

An equivalent spherical system with core radius 30.48 cm and reflector radius 45.72 cm; $k_{eff} = 0.996 \pm 0.003$.

The suggested computational mode is one-dimensional transport theory, with 40 mesh intervals in the core, 20 in the reflector, a vacuum boundary at the reflector surface, and 70 energy groups with one-quarter lethargy widths and an upper energy of 10 MeV.

3. Two-Dimensional Model

A cylindrical system with core radius 26.67 and half-length 27.94 cm, and reflector radius 41.91 cm and half-length 48.26 cm; k_{eff} = 0.996 ± 0.002.

The suggested computational mode is two-dimensional transport theory with 40 mesh intervals on both core radius and half-length, 20 radial intervals on the axial reflector, a vacuum boundary at the reflector surface, and 70 energy groups with one-quarter lethargy widths and an upper energy of 10 MeV.

D. Experimental Data

1. Spectral Indices at Core Center[2]

a. Central Fission and Capture Ratios

$\sigma_f(^{238}U) / \sigma_f(^{235}U)$	0.0373 ± 0.0004
$\sigma_f(^{237}Np) / \sigma_f(^{235}U)$	0.316 ± 0.005
$\sigma_f(^{239}Pu) / \sigma_f(^{235}U)$	1.185 ± 0.020
$\sigma_f(^{233}U) / \sigma_f(^{235}U)$	1.580 ± 0.030
$\sigma_{n,\gamma}(^{238}U) / \sigma_f(^{235}U)$[1]	0.110 ± 0.003

b. Central Reaction-Rate Ratios[3]

Reaction, R	$\sigma_R / \sigma_f(^{235}U)$
$^{6}Li(n,He)^{4}$	0.71 ± 0.01
$^{10}B(n,He)^{4}$	1.011 ± 0.014
$^{27}Al(n,\alpha)^{24}Na$	0.000078 ± 0.000002
$^{45}Sc(n,\gamma)^{46}Sc$	0.0132 ± 0.0003
$^{46}Ti(n,p)^{46}Sc$	0.00130 ± 0.00003
$^{47}Ti(n,p)^{48}Sc$	0.00215 ± 0.00009
$^{48}Ti(n,p)^{48}Sc$	0.000036 ± 0.000001
$^{54}Fe(n,p)^{54}Mn$	0.0090 ± 0.0003
$^{58}Fe(n,\gamma)^{59}Fe$	0.0031 ± 0.0001
$^{58}Ni(n,p)^{58}Co$	0.0123 ± 0.0002
$^{59}Co(n,\gamma)^{60}Co$	0.0095 ± 0.0002
$^{63}Cu(n,\gamma)^{64}Cu$	0.0164 ± 0.0010
$^{115}In(n,n')^{115m}In$	0.0271 ± 0.0006
$^{197}Au(n,\gamma)^{197}Au$	0.167 ± 0.003

2. Rossi Alpha [1]

$$\alpha = \beta_{eff} / \ell = -(1.17 \pm 0.01) \times 10^{5} \text{ sec}^{-1}$$

3. Central Reactivity Worths[1]

Material	Central Worth, 10^{-5} Δk/k/mol
H	-13 ± 2
^{6}Li	-56 ± 1
^{7}Li	-1.4 ± 0.2
Be	-1.66 ± 0.04
^{10}B	-73.9 ± 0.3
^{11}B	-1.9 ± 0.1
C	-1.45 ± 0.04
O	-1.09 ± 0.07
Al	1.36 ± 0.05
Fe	-2.61 ± 0.07
In	-20.1 ± 0.3
Au	-17.7 ± 0.2
^{232}Th	- 15 ± 1
^{233}U	249 ± 2
^{235}U	144 ± 1
^{238}U	-7.53 ± 0.07
^{237}Np	15.8 ± 0.9
^{238}Pu	157 ± 4
^{239}Pu	239 ± 1

4. Central Neutron Flux Spectrum[5]

Energy Group	Lower Lethargy Limit	Group Flux (%)
1	0.5	----
2	1.0	1.7
3	1.5	3.3
4	2.0	4.0
5	2.5	8.1
6	3.0	15.7
7	3.5	19.1
8	4.0	16.3
9	4.5	13.8
10	5.0	8.0
11	5.5	4.1
12	6.0	2.5
13	6.5	1.5
14	7.0	0.9
15	7.5	0.5
16	8.0	----

E. Calculated Results

Calculated results may be appended of these specifications.

F. Comments and Documentation

A detailed model that includes description of interleaved plates in the outer portion of the core appears in Ref. 1. As noted there, with n = 8 quadrature, this added detail has no influence on the transport-computed eigenvalue.

The homogeneous portion of the core effectively isolates axial measurements from effects of heterogeneity in the surrounding structure.

The composition, configuration specifications, Rossi-α, and central reactivity worths are taken from Ref. 1.

The most accurate fission ratios for Big Ten are obtained by combining absolute-ratio measurements in Flattop-25 and in big Ten and double-ratio measurements connecting these assemblies. These measurements are described below.

Measurement Location	Value	Double Ratio to Big Ten	Big Ten	Reference
$\sigma_f(^{238}U) / \sigma_f(^{235}U)$				
Big Ten	0.0373(±1.5%)	1	0.0373(±1.5%)	2d
Flattop-25	0.1479(±1.5%)	0.2506(±0.6%)	0.0371(±1.6%)	2c
Van de Graff	0.433 (±1.5%)	0.0867(±0.9%)	0.0375(±1.7%)	ENDF/B-IV
(E_n = 2.43 MeV				
		Average:	0.0373(±1.0%)	
$\sigma_f(^{237}Np) / \sigma_f(^{235}U)$				
Big Ten	0.317(±2.2%)	1	0.317(±2.2%)	2d
Topsy	0.760(±4%)	0.413 (±0.7%)	0.314(±4.1%)	2e
Van de Graaff	1.328(±2.0%)	0.2375(±1.0%)	0.315(±2.2%)	ENDF/B-IV
(E_n = 2.43 MeV)				
		Average:	0.316(±1.5%)	

Measurement Location	Value	Double Ratio to Big Ten	Big Ten	Reference
$\sigma_f(^{233}U) / \sigma_f(^{235}U)$				
Big Ten	1.61 (±2.1%)	1	1.61 (±2.1%)	Prelim. value by D. Gilliam (1979)
Flattop-25	1.572(±1.5%)	0.989 (±0.5%)	1.555 (±1.6%)	2c
Topsy	1.65 (±4%)	0.989 (±0.5%)	1.632 (±4.0%)	2e
		Average:	1.580 (±1.9%)	
$\sigma_f(^{239}Pu) / \sigma_f(^{235}U)$				
Big Ten	1.198(±1.5%)	1	1.198 (±1.5%)	2d
Flattop-25	1.349(±1.5%)	0.862(±0.6%)	1.163 (±1.6%)	2c
Topsy	1.42 (±4%)	0.862(±0.6%)	1.224 (±4.0%)	2e
		Average:	1.185 (±1.7%)	

The tabulated central reaction-rate ratios are the "Interlaboratory Reaction Rate" (ILRR) values from Ref. 3, with the exception of $^{6}Li(n,He)$ and $^{10}Be(n,He)$ from Ref.4

The central neutron flux spectrum is derived from results of ^{6}Li spectrometry in Ref. 5. Result of less extensive Proton-recoil spectrometry are reported in Ref. 1

REFERENCES

1. G. E. Hansen and H. C. Paxton, "A Critical Assembly of Urranium Enriched to 10% in Uranium-235," Nucl. Sci. Eng. 72, 230 (November 1979).

2. (a) G.E. Hansen, "Status of Computational and Experimental Correlations for Los Alamos Fast Neutron Critical Assemblies," Proc. Seminar Physics of Fast and Intermediate Reactors, Vienna, August 3-11, 1961 (IAEA, Vienna, 1962) Vol. I, pp 445-455. (b) J. A. Grundl and G. E. Hansen, "Measurement of Average Cross Section Ratios in Fundamental Fast-Neutron Spectra, "Proc. Paris Conf. Nuclear Data for Reactors (IAEA, Vienna, 1967) Vol. I, pp 321-336. (c) P. I. Amundson, A. M. Broomfield, W. G. Davey, and J. M. Stevenson, "An International Comparison of Fission Detector Standards, "Proc. Intern. Conf. Fast Critical Experiments and Their Analysis, Argonne, October 10-13, 1966 (Argonne National Laboratory report ANL-7320) pp 679-687. (d) D. M. Gilliam, "Integral Measurement Results in Standard Fields,"Proc. Intern. Specialist's Symposium Neutron Standards and Applications, Gaithersburg, March 28-31, 1977 (NBS Special Publication 493, 1977) pp 293-303. (e) G.A. Linenberger and L. L. Lowry, "Neutron Detector Traverses in the Topsy and Godiva Critical Assemblies," Los Alamos Scientific Laboratory report LA-1653 (1953).

3. R. C. Greenwood, R. G. Helmer, J. W. Rogers, R. J. Popek, R. R. Heinrich, N. D. Dudey, L. S. Kellogg, and W. H. Zimmer, "Radiometric Reacton Rate Measurements in CFRMF and Big-10," Proc. 2nd ASTM-Euratom Symposium Reactor Dosimetry: Dosimetry methods for Fuels, Cladding, and Structural Materials, Palo Alto, October 3-7, 1977 (NUREG/CP-0004) Vol. 3, 1207-1221.

4. Harry Farrar IV, "Integral (n,α) Cross Sections by Helium Measurement," Interlaboratory Reaction Rate Program 11th Progress Report, November 1975 through October 1976, Hanford Engineering Development Laboratory Report HEDL-TME 77-34 (1978).

5. G. E. Hansen, G. De Leeuw-Girts, and S. De Leeuw, "Big-10 Neutron Spectrometry, Proc. 3rd ASTM-Euratom Symposium Reactor Dosimetry, Ispra (Varese), Italy, October 1-5, 1979.

FAST REACTOR BENCHMARK NO. 21

A. Benchmark Name and Type

JEZEBEL-PU(20.1), a bare sphere of plutonium with 20.1% ^{240}Pu.

B. Systems Description

JEZEBEL-PU(20.1) is a bare sphere of plutonium metal containing 20.1% ^{240}Pu. In supplementing JEZEBEL (F1), it provides information for testing ^{240}Pu cross sections in the fission source energy range.

C. Model Description

The spherical homogeneous model has a core radius of 6.65985 cm and the following composition.[1]

Isotope	Density, nuclei/b-cm
^{239}Pu	0.029946
^{240}Pu	0.007887
^{241}Pu	0.001203
^{242}Pu	0.000145
Ga	0.001372

The recommended mode of calculation is one-dimensional transport theory, S_{16}, with 40 mesh intervals, a vacuum boundary at the surface, and a 26 energy group structure with half-lethargy unit widths and an upper energy of 10 MeV.

D. Experimental Data

1. Measured Eigenvalue: $k = 1.000 \pm 0.002$.[1]

2. Spectral Indices at Core Center[2]

$\sigma_f(^{238}U) / \sigma_f(^{235}U)$	0.206 ± 0.003
$\sigma_f(^{237}Np) / \sigma_f(^{235}U)$	0.92 ± 0.02

3. Central Reactivity Worth Ratios

$^{238}Pu/^{235}U$	2.01 ± 0.12[3,4]
$^{239}Pu/^{235}U$	1.99 ± 0.07 [3]
$^{244}Cm/^{235}U$	1.82 ± 0.10 [3]

E. Calculated Results

Calculated results may be appended to these specifications.

F. Comments and Documentation

The uncertainty in critical mass from Ref. 1, ± 0.8% translates to the eigenvalue uncertainty of ± 0.002.

The most accurate fission ratios for Jezebel-Pu(20.1) are obtained from recent absolute-ratio measurements in Flattop-25 and Big Ten and double-ratio measurements connecting these to Jezebel-Pu (20.1). These measurements are described below.

Measurement Location	Value	Double Ratio to Jezebel-Pu(20.1)	Jezebel-Pu(20.1)	Reference
$\sigma_f(^{238}U) / \sigma_f(^{235}U)$				
Flattop-25	0.1479(±1.5%)	1.388(±0.9%)	0.2053(±1.7%)	2c
Big Ten	0.0373(±1.5%)	5.54(±1.1%)	0.2066(±1.9%)	2d
Van de Graff (E_n = 2.43 MeV	0.433 (±1.5%)	0.480(±1.1%)	0.2078(±1.9%)	ENDF/B-IV
		Average:	0.2065(±1.2%)	
$\sigma_f(^{237}Np) / \sigma_f(^{235}U)$				
Big Ten	0.317(±2.2%)	2.906(±1.1%)	0.921(±2.5%)	2d
Van de Graaff (E_n = 2.43 MeV)	1.328(±2.0%)	0.690(±1.3%)	0.916(±2.4%)	ENDF/B-IV
Topsy	0.760(±4%)	1.200(±0.8%)	0.912(±4.1%)	2e
		Average:	0.917(±1.7%)	

Measurements were curtailed because of the limited period during which the assembly was available. In particular, there was no measurement of Rossi-α, of reactivity worth except the listed ratios, or of leakage spectrum.

REFERENCES

1. G. E. Hansen and H. C. Paxton, "Reevaluated Critical Specifications of Some Los Alamos Fast-Neutron Systems," Los Alamos Scientific Laboratory report LA-4208 (1969).

2. (a) G.E. Hansen, "Status of Computational and Experimental Correlations for Los Alamos Fast Neutron Critical Assemblies," Proc. Seminar Physics of Fast and Intermediate Reactors, Vienna, August 3-11, 1961 (IAEA, Vienna, 1962) Vol. I, pp 445-455. (b) J. A. Grundl and G. E. Hansen, "Measurement of Average Cross Section Ratios in Fundamental Fast-Neutron Spectra, "Proc. Paris Conf. Nuclear Data for Reactors (IAEA, Vienna, 1967) Vol. I, pp 321-336. (c) P. I. Amundson, A. M. Broomfield, W. G. Davey, and J. M. Stevenson, "An International Comparison of Fission Detector Standards, "Proc. Intern. Conf. Fast Critical Experiments and Their Analysis, Argonne, October 10-13, 1966 (Argonne National Laboratory report ANL-7320) pp 679-687. (d) D. M. Gilliam, "Integral Measurement Results in Standard Fields,"Proc. Intern. Specialist's Symposium Neutron Standards and Applications, Gaithersburg, March 28-31, 1977 (NBS Special Publication 493, 1977) pp 293-303. (e) G.A. Linenberger and L. L. Lowry, "Neutron Detector Traverses in the Topsy and Godiva Critical Assemblies," Los Alamos Scientific Laboratory report LA-1653 (1953).

3 D. M. Barton, "Central Reactivity Contributions of ^{244}Cm, ^{239}Pu, and ^{235}U in a Bare Critical Assembly of Plutonium Metal," Nucl. Sci. Eng. 33, 51-55 (1968).

4. W. F. Stubbins, D. M. Barton, and F. D. Lonadier, "The Neutron-Production Cross Section of ^{238}Pu in a Fast Spectrum," Nucl. Sci. Eng. 25. 377-382 (1966).

FAST REACTOR BENCHMARK NO. 22

A. Benchmark Name and Type

FLATTOP-25, a reflected sphere of enriched uranium.

B. System Description

FLATTOP-25 is a spherical metallic system consisting of a highly enriched uranium core in a thick natural uranium reflector. In supplementing GODIVA (F5), it emphasizes ^{238}U transport in the fission-source energy range.

C. Model Description

The spherical model is a core of radius 6.116 cm, surrounded intimately by a reflector of radius 24.13 cm, and has the following compositions.[1]

Isotope	Core	Reflector
^{234}U nuclei/b-cm	0.00049	0.00000
^{235}U nuclei/b-cm	0.04449	0.00034
^{238}U nuclei/b-cm	0.00270	0.04774

The recommended mode of calculation is one-dimensional transport theory. S_{16}, with 30 mesh intervals in the core, 30 in the reflector, a vacuum boundary at the reflector surface, and a 26 energy group structure with one-half lethargy unit widths and an upper energy of 10 MeV.

D. Experimental Data

1. Measured Eigenvalue: $k = 1.000 \pm 0.001$. [1]

2. Spectral Indices at Core Center[2]

$\sigma_f(^{233}U) / \sigma_f(^{235}U)$	0.160 ± 0.003[2]
$\sigma_f(^{238}U) / \sigma_f(^{235}U)$	0.149 ± 0.002[3]
$\sigma_f(^{237}Np) / \sigma_f(^{235}U)$	0.76 ± 0.01[3]
$\sigma_f(^{239}Pu) / \sigma_f(^{235}U)$	1.37 ± 0.02[3]

3. Rossi Alpha[3a]

$$\alpha = \beta_{eff} / \ell = -(0.38 \pm 0.01) \times 10^6 \text{sec}^{-1}$$

4. Central Reactivity Worths[4]

Isotope	Central Worth, 10^{-5} k/k/g-atom
^{233}U [5]	2320 ± 30
^{235}U	1330 ± 20
^{238}U [5]	171 ± 6
^{237}Np	1140 ± 20
^{238}Pu	2250 ± 30
^{239}Pu	2530 ± 20
^{242}Pu	1200 ± 30
^{241}Am	1350 ± 10

5. Central Neutron Flux Spectrum[3]

Deviation of the central spectrum from the ^{235}U fission spectrum is characterized by the following ratios of central high-energy spectral indices to the corresponding indices for the ^{235}U fission spectrum.

Spectral Index	Ratio of Central Value To value for ^{235}U Fission Spectrum
$\sigma_f(^{238}U) / \sigma_{n,p}(^{31}P)$	1.022 0.021
$\sigma_{n,p}(^{27}Al) / \sigma_{n,p}(^{31}P)$	1.014 ± 0.015
$\sigma_{n,p}(^{56}Fe) / \sigma_{n,p}(^{31}P)$	1.009 ± 0.020
$\sigma_{n,}(^{27}Al) / \sigma_{n,p}(^{31}P)$	1.025 ± 0.026
$\sigma_{n,2n}(^{63}Cu) / \sigma_{n,p}(^{31}P)$	1.027 ± 0.032

E. Calculated Results

Calculated results may be appended to these specifications.

F. Comments and Documentation

The model, with close fitting reflector, is corrected for a 0.10- to 0.13-cm gap between the core and reflector. The influence on Rossi-α is negligible.

The uncertainty in critical mass from Ref. 1, ± 0.04 kg, translates to the eigenvalue uncertainty of ±0.001.

The most accurate fission ratios for Flattop-25 are obtained by combining absolute-ratio measurements in Flattop-25 and Big Ten and double-ratio measurements connecting these assemblies. These measurements are described below.

Measurement Location	Value	Double Ratio to Flattop-25	Flattop-25	Reference
$\sigma_f(^{238}U) / \sigma_f(^{235}U)$				
Flattop-25	0.1479(±1.5%)	1	0.1479(±1.5%)	3c
Big Ten	0.0373(±1.5%)	3.99 (±0.6%)	0.1488(±1.8%)	3d
Van de Graaff	0.433(±1.5%)	0.346(±0.7%)	0.1498(±1.7%)	ENDF/B-IV
(E_n = 2.43 MeV)				
		Average:	0.1488(±1.0%)	
$\sigma_f(^{237}Np) / \sigma_f(^{235}U)$				
Big Ten	0.317(±2.2%)	2.42 (±0.7%)	0.767(±2.3%)	3d
Van de Graaff	1.328(±2.0%)	0.575(±1.0%)	0.764(±2.2%)	ENDFB-IV
(E_n = 2.43 MeV)				
Topsy	0.760 (±4%)	1	0.760(±4%)	3e
		Average:	0.765(±1.5%)	
$\sigma_f(^{233}U) / \sigma_f(^{235}U)$				
Flattop-25	1.572 (±1.5%)	1	1.572 (±1.6%)	3c
Topsy	1.65 (±4%)	1	1.65 (±4%)	3e
Big Ten	1.61 (±2.1%)	1.011(±0.5%)	1.628 (±2.2%)	Prelim. value from D. Gilliam
		Average:	1.595 (±1.9%)	

Measurement Location	Value	Double Ratio to Flattop-25	Flattop-25	Reference
$\sigma_f(^{239}Pu) / \sigma_f(^{235}U)$				
Flattop-25	1.349 (±1.5%)	1	1.349 (±1.5%)	3c
Big Ten	1.198 (±1.5%)	1.160 (±0.6%)	1.390 (±1.6%)	3d
Topsy	1.42 (±.4%)	1	1.42 (±7%)	3e
		Average:	1.372 (±1.7%)	

The reactivity worths of ^{233}U and ^{238}U were measured in Topsy, a similar assembly that crudely approximated spherical geometry. Reactivity worths of many nonfissionable materials in Topsy are reported in Ref. 5.

REFERENCES

1. G. E. Hansen and H. C. Paxton, "Reevaluated Critical Specifications of Some Los Alamos Fast-Neutron Systems," Los Alamos Scientific Laboratory report LA-4208 (1969).

2. D. M. Gilliam, private communication.

3. (a) G.E. Hansen, "Status of Computational and Experimental Correlations for Los Alamos Fast Neutron Critical Assemblies," Proc. Seminar Physics of Fast and Intermediate Reactors, Vienna, August 3-11, 1961 (IAEA, Vienna, 1962) Vol. I, pp 445-455. (b) J. A. Grundl and G. E. Hansen, "Measurement of Average Cross Section Ratios in Fundamental Fast-Neutron Spectra, "Proc. Paris Conf. Nuclear Data for Reactors (IAEA, Vienna, 1967) Vol. I, pp 321-336.

(c) P. I. Amundson, A. M. Broomfield, W. G. Davey, and J. M. Stevenson, "An International Comparison of Fission Detector Standards, "Proc. Intern. Conf. Fast Critical Experiments and Their Analysis, Argonne, October 10-13, 1966 (Argonne National Laboratory report ANL-7320) pp 679-687. (d) D. M. Gilliam, "Integral Measurement Results in Standard Fields,"Proc. Intern. Specialist's Symposium Neutron Standards and Applications, Gaithersburg, March 28-31, 1977 (NBS Special Publication 493, 1977) pp 293-303. (e) G.A. Linenberger and L. L. Lowry, "Neutron Detector Traverses in the Topsy and Godiva Critical Assemblies," Los Alamos Scientific Laboratory report LA-1653 (1953).

4. G. E. Hansen, private communication.

5. L. B. Engle, G. E. Hansen, and H. C. Paxton, "Reactivity Contributions of Various Materials in Topsy, Godiva, and Jexebel, "Nucl. Sci. Eng. 8, 543-569 (1960).

FAST REACTOR BENCHMARK NO. 23

A. Benchmark Name and Type

FLATTOP-PU, a reflected plutonium sphere.

B. System Description

FLATTOP-PU is a spherical metallic system consisting of a plutonium (4.5% ^{240}Pu) core in a thick natural uranium reflector. In supplementing JEZEBEL (F1), it emphasizes ^{238}U transport in the fission-source energy range.

C. Model Description

The spherical model is a core of radius 4.533 cm, surrounded intimately by a reflector of radius 24.13 cm, and has the following compositions.[1]

Isotope	Core	Reflector
^{239}Pu nuclei/b-cm	0.03674	—
^{240}Pu nuclei/b-cm	0.00186	—
^{241}Pu nuclei/b-cm	0.00012	—
Ga nuclei/b-cm	0.00138	—
^{235}U nuclei/b-cm	—	0.00034
^{238}U nuclei/b-cm	—	0.04774

The recommended mode of calculation is one-dimensional transport theory. S_{16}, with 30 mesh intervals in the core, 30 in the reflector, a vacuum boundary at the reflector surface, and a 26 energy group structure with one-half lethargy unit widths and an upper energy of 10 MeV.

D. Experimental Data

1. Measured Eigenvalue: $k = 1.000 \pm 0.001_4$. [1]

2. Spectral Indices at Core Center[2]

$\sigma_f(^{238}U)/\sigma_f(^{235}U)$	0.180 ± 0.003
$\sigma_f(^{237}Np)/\sigma_f(^{235}U)$	0.84 ± 0.01

3. Rossi Alpha[2a]

$$\alpha = -\beta_{eff}/\ell = -(0.214 \pm 0.005) \times 10^6 \text{ sec}^{-1}$$

4. Central Reactivity Worths[3]

Isotope	Central Worth, 10^{-5} k/k/g-atom
^{235}U	2380 ± 30
^{238}U	145 ± 4
^{237}Np	2220 ± 30
^{238}Pu	4090 ± 60
^{239}Pu	4520 ± 20
^{242}Pu	2240 ± 40
^{241}Am	2800 ± 20

6. Central Neutron Flux Spectrum[2]

Deviation of the central spectrum from the ^{239}Pu fission spectrum is characterized by the following ratios of central high-energy spectral indices to the corresponding indices for the ^{239}Pu fission spectrum.

Spectral Index	Ratio of Central Value To value for ^{239}Pu Fission Spectrum
$\sigma_f(^{238}U)/\sigma_{n,p}(^{31}P)$	1.015 ± 0.020
$\sigma_{n,p}(^{27}Al)/\sigma_{n,p}(^{31}P)$	1.016 ± 0.018
$\sigma_{n,p}(^{56}Fe)/\sigma_{n,p}(^{31}P)$	1.033 ± 0.021
$\sigma_{n,\alpha}(^{27}Al)/\sigma_{n,p}(^{31}P$	1.043 ± 0.24
$\sigma_{n,2n}(^{63}Cu)/\sigma_{n,p}(^{31}P)$	1.038 ± 0.032

E. Calculated Results

Calculated results may be appended to these specifications.

F. Comments and Documentation

The model, with close fitting reflector, is corrected for a 0.10- to 0.13-cm gap between the core and reflector. The influence on Rossi-α is negligible.

The uncertainty in critical mass from Ref. 1, ± 0.03 kg, translates to the eigenvalue uncertainty of $\pm 0.001_4$.

The most accurate fission ratios for Flattop-Pu are obtained from recent absolute-ratio measurements in Flattop-25 and Big Ten and double-ratio measurements connecting these to Flattop-Pu. These measurements are described below.

Measurement Location	Value	Double Ratio to Flattop-Pu	Flattop-Pu	Referer
$\sigma_f(^{238}U)/\sigma_f(^{235}U)$				
Flattop-25	0.1479(±1.5%)	1.207(±0.4%)	0.1785(±1.6%)	2c
Big Ten	0.0373(±1.5%)	4.816(±0.7%)	0.1769(±1.7%)	2d
Van de Graaff	0.433(±1.5%)	4.176(±0.8%)	0.1808(±1.7%)	ENDF/B-IV
(E_n = 2.43 MeV)		Average:	0.1796(±1.0%)	
$\sigma_f(^{237}Np)/\sigma_f(^{235}U)$				
Topsy	0.760(±4%)	1.101(±0.5%)	0.837(±4%)	2e
Big Ten	0.317(±2.2%)	2.866(±0.9%)	0.845(±2.4%)	2d
Van de Graaff	1.328(±2%)	0.633(±1.1%)	0.841(±2.3%)	ENDFB-IV
(E_n = 2.43 MeV)		Average:	0.842(±1.6%)	

REFERENCES

1. G.E. Hansen and H.C.Paxton, "Reevaluated Critical Specifications of Some Los Alamos Fast-Neutron Systems," Los Alamos Scientific Laboratory report LA-4208 (1969).

2. (a) G.E. Hansen, "Status of Computational and Experimental Correlations for Los Alamos Fast Neutron Critical Assemblies," Proc. Seminar Physics of Fast and Intermediate Reactors, Vienna, August 3-11, 1961 (IAEA, Vienna, 1962) Vol. I, pp. 445-455. (b) J.A. Grundl and G.E. Hansen, "Measurement of Average Cross-Section Ratios in Fundamental Fast-Neutron Spectra," Proc. Paris Conf. Nuclear Data for Reactors (IAEA, Vienna, 1967) Vol. I, pp. 321-336. (c) P.I. Amundson, A.M. Broomfield, W.G. Davey, and J.M. Stevenson, "An International Comparison of Fission Detector Standards," Proc. Intern. Conf. Fast Critical Experiments and Their Analysis, Argonne, October 10-13, 1966 (Argonne National Laboratory report ANL-7320) pp. 679-687. (d) D.M. Gilliam, "Integral Measurement Results in Standard Fields," Proc. Intern. Specialists' Symposium Neutron Standards and Applications, Gaithersburg, March 28-31, 1977 (NBS Special Publications 493, 1977) pp. 293-303. (e) G.A. Linenberger and L.L. Lowry, "Neutron Detector Traverses in the Topsy and Godiva Critical Assemblies," Los Alamos Scientific Laboratory report LA-1653 (1953).

3. G.E. Hanson, private communication.

FAST REACTOR BENCHMARK NO. 24

A. Benchmark Name and Type

FLATTOP-23, a reflected ^{233}U sphere.

B. System Description

FLATTOP-23 is a spherical metallic system consisting of a ^{233}U (98.13%) core in a thick natural uranium reflector, with 0.218-cm gap between core and reflector. In supplementing JEZEBEL-23 (F19), it emphasizes ^{238}U transport in the fission-source energy range.

C. Model Description

The spherical model is a core of radius 4.317 cm, centered in a reflector of 4.610-cm inner radius and 24.13-cm outer radius, and has the following compositions.[1]

Isotope	Core	Reflector
^{233}U nuclei/b-cm	0.04671	-
^{234}U nuclei/b-cm	0.00059	-
^{235}U nuclei/b-cm	0.00001	0.00034
^{238}U nuclei/b-cm	0.00028	0.04774

The recommended mode of calculation is one-dimensional transport theory, S_{16} with 30 mesh intervals in the core, 2 in the gap, 30 in the reflector, a vacuum boundary at the outer reflector surface, and a 26 energy group structure with one-half lethargy unit widths and an upper energy of 10 MeV.

D. Experimental Data

1. Measured Eigenvalue: $k = 1.000 \pm 0.001_4$.[2]

2. Spectral Indices at Core Center[3]

$\sigma_f(^{238}U/\sigma_f(^{235}U)$	0.191± 0.003
$\sigma_f(^{237}Np)/\sigma_f(^{235}U)$	0.89 ± 0.01

3. Rossi Alpha[3a]

$$\alpha = -\beta_{eff}/\ell = -(0.267 \pm 0.005) \times 10^6 \text{ sec}^{-1}$$

4. Central Reactivity Worth [1]

The central void coefficient is 4010 ± 30 in units of 10^{-5} $\Delta k/k/g\text{-atom}$

E. Calculated Results

Calculated results may be appended to these specifications.

F. Comments and Documentation

The critical mass, corrected to a close-fitting reflector of the same outer radius, is given in Ref. 2.

The uncertainty in critical mass from Ref. 2, ± 0.03 kg in 5.74 kg, translates to the eigenvalue uncertainty of ± 0.001_4.

The most accurate fission ratios for FLATTOP-23 are obtained from recent absolute-ratio measurements in FLATTOP-25 and Big Ten and double-ratio measurements connecting these to FLATTOP-23. These measurements are described below.

Measurement Location	Value	Double Ratio to Flattop-23	Flattop-23	Reference
$\sigma_f(^{238}U)$ $\sigma_f(^{235}U)$				
Flattop-25	0.1479(±1.5%)	1.282(±0.4%)	0.1896(±1.6%)	3c
Big Ten	0.0373(±1.5%)	5.12%(±0.7%)	0.1908(±1.7%)	3d
Van de Graaff	0.433(±1.5%0)	0.444(±0.8%)	0.1921(±1.7%)	ENDF/B-IV
(E_n = 2.43 MeV)		Average:	0.1908(±1.0%)	
$\sigma_f(^{237}Np)/\sigma_f(^{235}U)$				
Topsy	0.760(±4%)	1.166(±0.5%)	0.886(±4%)	3e
Big Ten	0.317(±2.2%)	2.823(±0.9%)	0.895(±2.4%)	3d
Van de Graaff	1.328(±2%)	0.671(±1.1%)	0.891(±2.3%)	ENDF/B-IV
(E_n = 2.43 MeV)		Average:	0.892(±1.6%)	

Reactivity-worth measurements were curtailed because of intense gamma radiation.

REFERENCES

1. G.E. Hansen, private communication.

2. G.E. Hansen and H.C. Paxton, "Reevaluated Critical Specifications of Some Los Alamos Fast-Neutron systems," Los Alamos Scientific Laboratory report LA-4208 (1969)

3. (a) G.E. Hansen, "Status of Computational and Experimental Correlations for Los Alamos Fast Neutron Critical Assemblies," Proc. Seminar Physics of Fast and Intermediate Reactors, Vienna, August 3-11, 1961 (IAEA, Vienna, 1962) Vol. I, pp. 445-455. (b) J.A. Grundl and G.E. Hansen, "Measurement of Average Cross-Section Ratios in Fundamental Fast-Neutron Spectra," Proc. Paris Conf. Nuclear Data for Reactors (IAEA, Vienna, 1967) Vol. I, pp. 321-336. (c) P.I. Amundson, A.M. Broomfield, W.G. Davey, and J.M. Stevenson, "An International Comparison of Fission Detector Standards," Proc. Intern. Conf. Fast Critical Experiments and Their Analysis, Argonne, October 10-13, 1966 (Argonne National Laboratory report ANL-7320 pp. 679-687. (d) D.M. Gilliam, "Integral Measurement Results in Standard Fields," Proc. Intern. Specialist's Symposium Neutron Standards and Applications, Gaithersburg, March 28-31, 1977 (NBS Special Publication 493, 1977) pp. 293-303. (e) G.A. Linenberger and L.L. Lowry, "Neutron Detector Traverses in the Topsy and Godiva Critical Assemblies," Los Alamos Scientific Laboratory report LA-1653 (1953).

FAST REACTOR BENCHMARK NO. 25

A. Benchmark Name and Type

THOR, a thorium-reflected Pu sphere.

B. System Description

THOR consists of a sphere of plutonium (5.1% ^{240}Pu) metal centered in a close-fitting 53.3-cm equilateral cylinder of thorium metal. In supplementing JEZEBEL (Fl), it emphasizes ^{232}Th transport in the fission-source energy range.

C. Model Description[1]

The equivalent spherical model is a core of radius 5.310 cm centered in a reflector of 5.310-cm inner radius and 29.88-cm outer radius, and has the following compositions:

Isotope	Core	Reflector
^{239}Pu nuclei/b-cm	0.03618	—
^{240}Pu nuclei/b-cm	0.00194	—
Ga nuclei/b-cm	0.00133	—
^{232}Th nuclei/b-cm	-	0.03005

The recommended mode of calculation is one-dimensional transport theory, S_{16} with 30 mesh intervals in the core, 30 in the reflector, a vacuum boundary at the outer reflector surface, and a 26 energy group structure with one-half lethargy unit widths and an upper energy of 10 MeV.

D. Experimental Data[1]

1. Measured Eigenvalue: $k = 1.000 \pm 0.001$

2. Spectral Indices at Core Center

a. Fission Ratios

$\sigma_f(^{238}U)/\sigma_f(^{235}U)$	0.195 ± 0.003
$\sigma_f(^{237}Np)/\sigma_f(^{235}U)$	0.92 ± 0.02
$\sigma_f(^{232}Th)/\sigma_f(^{238}U)$	0.26 ± 0.01 at all radii

b. Other Reaction Ratios

$\sigma_{n,\gamma}(^{238}U)/\sigma_f(^{235}U)$	0.083 ± 0.003
$\sigma_{n,2n}(^{238}U)/\sigma_f(^{238}U)$	0.053 ± 0.003
$\sigma_{n,\gamma}(^{232}Th)/\sigma_{n,\gamma}(^{238}U)$	1.20 ± 0.06 at all radii
$\sigma_{n,2n}(^{232}Th)/\sigma_{n,2n}(^{238}U)$	1.04 ± 0.03 at all radii

3. Rossi Alpha

$$\alpha - \beta_{eff}/\ell = -(0.19_7 \pm 0.01) \times 10^6 \text{sec}^{-1}$$

4. Central Reactivity Worth

The central void coefficient is 15.5±03 dollars/g-atom Pu.

E. Calculated Results

Calculated results may be appended to these specifications.

F. Comments and Documentation

The effective spherical equivalent of the cylindrical thorium reflector, 29.88-cm radius, was based on the inverse fourth-power dependence of reflector worth per unit volume. Insensitivity of k to radius in this region is indicated by calculations with ENDF/B-IV cross sections that give a 0.04% increase in k when increasing radius from 29.88 cm to 30.53 cm, the radius that preserves thorium mass.

The uncertainty in eigenvalue is based on the ±0.017 kg uncertainty in critical mass from Ref. 1, with additional allowance for uncertainty in conversion to the equivalent spherical system.

The uncertainties for the first two fission ratios are typical of 4-barrel chamber measurements.

The uncertainty for Rossi alpha is estimated from Fig. 7 of Ref. 1.

The uncertainty for central void coefficient is about twice the value obtained in assemblies with a more lengthy history. There is insufficient experimental information for conversion from dollars/g-atom to absolute units.

REFERENCE

1. G.E. Hansen and H.C. Paxton, "THOR, A Thorium-Reflected Plutonium-Metal Critical Assembly," Nucl. Sci. Eng. 71, 287-293 (1979).

CROSS SECTION EVALUATION WORKING GROUP
THERMAL REACTOR BENCHMARK COMPILATION

June 1974

CSEWG Data Testing Subcommittee
Thermal Data Testing Group

THERMAL REACTOR BENCHMARK CONTENTS

I. INTRODUCTION

II. THERMAL REACTOR BENCHMARKS

1. ORNL-1
2. ORNL-2
3. ORNL-3
4. ORNL-4
5. ORNL-10
6. TRX-1 (Revised)
7. TRX-2 (Revised)
8. TRX-3 (Revised)
9. TRX-4 (Revised)
10. MIT-4
11. MIT-5
12. MIT-6
13. PNL-1
14. PNL-2
15. PNL-3
16. PNL-4
17. PNL-5
18. BAPL-UO_2-1
19. BAPL-UO_2-2
20. BAPL-UO_2-3
21. BAPL-THO_2-1 (Revised)
22. BNL-THO_2-2 (Revised)
23. BNL-THO_2-3 (Revised)
24. PNL-6
25. PNL-7
26. PNL-8
27. PNL-9
28. PNL-10
29. PNL-11
30. PNL-12
31. PNL-30
32. PNL-31
33. PNL-32
34. PNL-33
35. PNL-34
36. PNL-35

I. Introduction

The validation of nuclear data files in the calculation of thermal reactor benchmarks is an important objective of CSEWG. At this time no special introductory material has been written for the thermal reactor benchmarks but much of the introductory material for the section on Fast Benchmarks is appropriate.

THERMAL REACTOR BENCHMARKS NOS. 1-5

A. Benchmark Name and Type: ORNL-1 through ORNL-4, ORNL-10, unreflected spheres of ^{235}U.

B. System Description

This series of benchmarks consists of five unreflected spheres of ^{235}U (as uranyl nitrate) in H_2O, three of them poisoned with boron. Critical compositions and volumes were determined. These benchmarks are useful for testing H_2O fast scattering data, the ^{235}U and thermal absorption of hydrogen.

C. Model Description

Benchmarks ORNL-1 through ORNL-4 are of radius 34.595 cm; ORNL-10 has radius 61.011 cm.

	Concentration, 10^{24} atoms/cm^3				
Material	ORNL-1	ORNL-2	ORNL-3	ORNL-4	ORNL-10
^{10}B	0.0	1.0286×10^{-6}	2.0571×10^{-6}	2.5318×10^{-6}	0.0
H	0.066228	0.066148	0.066070	0.066028	0.066394
O	0.033736	0.033800	0.033865	0.033902	0.033592
N	1.869×10^{-4}	2.129×10^{-4}	2.392×10^{-4}	2.548×10^{-4}	1.116×10^{-4}
^{234}U	5.38×10^{-7}	6.31×10^{-7}	7.16×10^{-7}	7.62×10^{-7}	4.09×10^{-7}
^{235}U	4.8066×10^{-5}	5.6206×10^{-5}	6.3944×10^{-5}	6.7959×10^{-5}	3.6185×10^{-5}
^{236}U	1.38×10^{-7}	1.63×10^{-7}	1.84×10^{-7}	1.97×10^{-7}	2.20×10^{-7}
^{238}U	2.807×10^{-6}	3.281×10^{-6}	3.734×10^{-6}	3.967×10^{-6}	1.985×10^{-6}

It is suggested that the multiplication factor be calculated with multigroup $S_n (n \geq 4)$ or equivalent P_ℓ theory.

The measured k values (Ref. 1) and "corrected" experimental k values (Ref. 2) are shown below. The corrections were evaluated by Staub et al. to account for newer β values, the thin aluminum shells, distortion of the spherical shape, fill tubes and room return.

D. Experimental Data

	Measured k	Corrected Measured k
ORNL- 1	1.00118	1.00026
2	1.00073	.99975
3	1.00090	.99994
4	1.00028	.99924
10	1.00129	1.00031

E. Comments and Documentation

The experiments are described in Ref. 1. The experimental k values are for a sphere without container. Reference 2 presents a detailed analysis of these systems including a discussion of cross section sensitivities and uncertainties in the analysis, both systematic and random.

References:

1. R. Gwin and D. W. Magnuson, "Eta of ^{233}U and ^{235}U for Critical Experiments," Nucl. Sci. Eng. 12, 364 (1962).
2. A. Staub et al., "Analysis of a Set of Critical Homogeneous U-H_2O Spheres," Nucl. Sci. Eng. 34, 263 (1968).

THERMAL REACTOR BENCHMARKS NOS. 6-9

A. Benchmark Name and Type: TRX-1 through TRX-4, H_2O-moderated uranium lattices.

B. System Description

These benchmarks are H_2O moderated lattices of slightly enriched (1.3%) uranium rods with diameters of .4915 cm in a triangular pattern. Measured lattice parameters include ρ^{28}, δ^{25}, δ^{28}, and C*; B^2 was measured for TRX-1 and TRX-2, but not for TRX-3 and TRX-4 which are two-region lattices.

These lattices directly test the U235 resonance fission integral and thermal fission cross section. They also test U238 shielded resonance capture and the thermal capture cross section. They are sensitive to the U238 fast fission cross section, U238 inelastic scattering and the U235 fission spectrum. The scattering and (thermal) absorbtion cross sections of H_2O are very important also.

C. Model Description

There are two principal methods of analysis:

- a heterogeneous infinite lattice cell calculation followed by a homogenized-core leakage calculation.
-- an explicit description of the full core in three dimensions.

1. Infinite Lattice Cell

a. Physical Properties

Region	Outer Radius, cm	Isotope	Concentration 10^{24} Atoms/cm^3
Fuel	0.4915	^{235}U	6.253×10^{-4}
		^{238}U	4.7205×10^{-2}
Void	0.5042	-	
Clad	0.5753	Al	6.025×10^{-2}
Moderator	*	^{1}H	6.676×10^{-2}
		^{16}O	3.338×10^{-2}

*Lattice spacings of 1.8060, 2.1740, 1.4412, and 2.8824 cm, respectively, for TRX-1 through TRX-4. (Triangular arrays)

b. Suggested Method of Calculation

Monte Carlo, multigroup $S_n (n \geq 4)$ or equivalent P_ℓ, or integral transport theory. An accurate treatment of resonance absorption is essential.

2. Leakage Calculation

a. To account for leakage use a homogenized multigroup B_ℓ calculation with a total buckling $B^2 = .0057$ cm^{-2} for TRX-1 and $B^2 = .005469$ cm^{-2} for TRX-2. This is not suitable for TRX-3 and TRX-4 which are two-region lattices.

b. An alternative treatment of leakage, applicable to all four lattices, is to cylinderize them and calculate radial shapes explicitly using multigroup S_n or P_ℓ theory. In all four lattices the axial buckling is .000526 cm^{-2}; all are fully reflected.

Dimensions of Cylinderized TRX Lattices

Composition	Outer Radius (cm) TRX-1	TRX-2	TRX-3	TRX-4
Homogenized test lattice cells	26.2093	27.4419	11.1467	11.8198
Water gap	-	-	12.3268	12.3268
Homogenized driver lattice cells	-	-	37.9406	42.1717
Reflector		large		

Properties of UO_2 Driver Lattice (TRX-3 and TRX-4)

Region	Outer Radius, cm	Isotope	Concentration 10^{24} Atoms/cm^3
Fuel	.4864	^{235}U	3.112×10^{-4}
		^{238}U	2.3127×10^{-2}
		^{16}O	4.6946×10^{-2}
Void	.5042	-	
Clad	.5753	Al	6.025×10^{-2}
Moderator	*	^{1}H	6.676×10^{-2}
		^{16}O	3.338×10^{-2}

*Triangular pitch lattice with spacing of 1.8060 cm.

3. Full Core Model

The actual full-core configurations and loadings were:

TRX-1: 764 fuel rods

TRX-2: 578 fuel rods

TRX-3: A hexagonal array of 169 UO_2 rods was removed from the center of the driver lattice (pitch 1.806 cm), leaving 1432 rods. A hexagonal array of 217 metal rods (pitch 1.4412 cm) was centered in the opening.

TRX-4: Every other rod of the TRX-3 inner lattice was removed, leaving 61 metal rods (pitch 2.8824 cm). 1809 UO_2 driver rods were now required.

Figures 1 and 2 show 1/3-core representations of these lattices. Slight differences from the actual core loadings are due to symmetrizing the outer boundary (for simplicity). Figure 3 shows the axial model for these lattices. The tank inner diameter is 162.56 cm.

This model neglects the following items, which are considered to be inconsequential. It has omitted the 0.635 cm-thick lucite spacer sheets located at 1/3 and 2/3 of fuel full-height. In some cases, the top lattice plate was of aluminum. In some metal-fueled lattices, the rod handles and tips were actually made of brass.

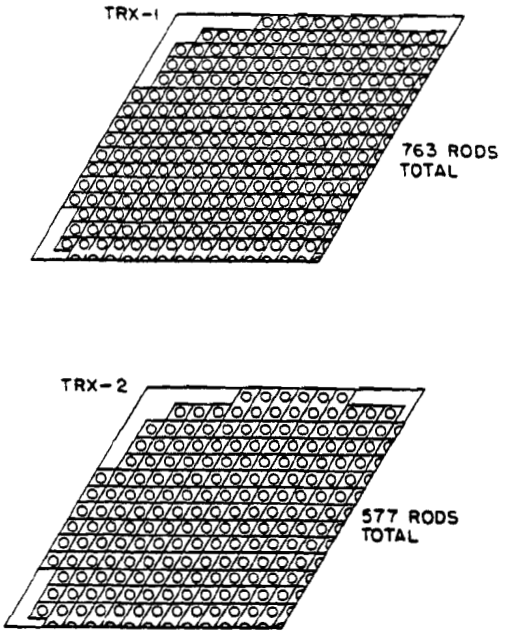

Figure 1.

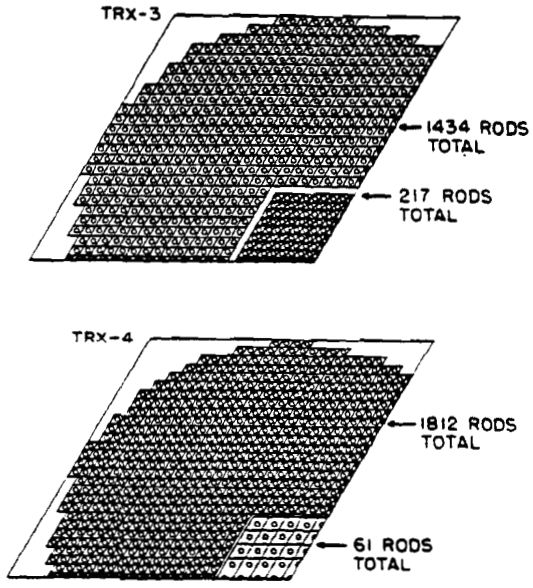

Figure 2.

AXIAL MODEL OF TRX LATTICES (SCHEMATIC)
DIMENSIONS IN CENTIMETERS

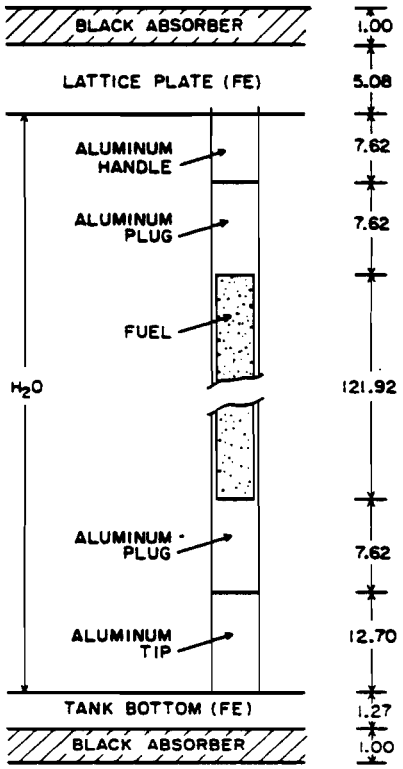

Figure 3.

D. Experimental Data

	TRX-1	TRX-2	TRX-3	TRX-4
Pitch, cm	1.8060	2.1740	1.4412	2.8824
Water/fuel vol. ratio	2.35	4.02	1.00	8.11
Number of rods	764	578	217	61
B^2, 10^{-4} cm^{-2}	57 ± 1	54.69 ± .36	-	-
ρ^{28}	1.320 ± .021	.837 ± .016	3.03 ± .05	.481 ± .011
δ^{25}	.0987 ± .0010	.0614 ± .0008	.231 ± .003	.0358 ± .0005
δ^{28}	.0946 ± .0041	.0693 ± .0035	.167 ± .008	.0482 ± .0020
C*	.797 ± .008	.647 ± .006	1.255 ± .011	.531 ± .004

Note: Parameters correspond to thermal cutoff of 0.625 eV and were measured at core center. They embody corrections obtained in Ref. 6.

ρ^{28} = ratio of epithermal-to-thermal ^{238}U captures.

δ^{25} = ratio of epithermal-to-thermal ^{235}U fissions.

δ^{28} = ratio of ^{238}U fissions to ^{235}U fissions.

C* = ratio of ^{238}U captures to ^{235}U fissions.

E. Comments and Documentation

Parameter measurements are described in Ref. 1 and 2. Measurements of thermal disadvantage factors (Ref. 3) and fast advantage factors (Ref. 4) are also available. Reference 5 shows some additional details about the lattices, fuel rods, etc. Cadmium cutoff energies and foil perturbation were given careful attention.

REFERENCES

1. J. Hardy, Jr., D. Klein and J. J. Volpe, "A Study of Physics Parameters in Several Water-Moderated Lattices of Slightly Enriched and Natural Uranium," WAPD-TM-931, March 1970.
2. J. Hardy, Jr., D. Klein and J. J. Volpe, Nucl. Sci. Eng., 40, 101 (1970).
3. J. J. Volpe, J. Hardy, Jr., and D. Klein, Nucl. Sci. Eng. 40, 116 (1970).
4. J. Hardy, Jr., D. Klein and R. Dannels, Nucl. Sci. Eng. 26, 462 (1966).
5. J. R. Brown et al., "Kinetics and Buckling Measurements in Lattices of Slightly Enriched U or UO_2 Rods in H_2O," WAPD-176 (January 1958).
6. R. Sher and S. Fiarman, "Studies of Thermal Reactor Benchmark Data Interpretation: Experimental Corrections," EPRI NP-209, October 1976.

THERMAL REACTOR BENCHMARKS NOS. 10-12

A. Benchmark Name and Type: MIT-4, MIT-5, and MIT-6, D_2O-moderated Subcritical slightly enriched uranium lattices.

B. System Description

These benchmarks consist of D_2O-moderated lattices of uranium metal rods enriched to 0.947 w/o ^{235}U. The rods were 0.983 cm in diameter and measurements were made at triangular lattice pitches of 3.81 cm, 5.715 cm, and 7.62 cm. The measured lattice parameters include B^2_m, ρ^{28}, δ^{25}, δ^{28}, and C*. These lattices are useful for testing D_2O cross section data, cross sections for thermal and epithermal ^{235}U fission, thermal and epithermal ^{238}U neutron capture, and ^{238}U fast fission.

C. System Description

1. Infinite Lattice Calculation

a. Physical Properties (Cylindrical Geometry)

		Composition	
Region	Outer Radius, Cm	Isotope	Concentrations 10^{24} atoms/cm
Fuel	0.4915	^{235}U	4.5864×10^{-4}
		^{238}U	4.7367×10^{-2}
Homogenized Clad and Air Gap	0.5703	Al	5.4806×10^{-2}
		O	4.856×10^{-5}
Moderator	*	^{1}H	3.9156×10^{-4}
		^{2}H	6.6099×10^{-2}
		O	3.3245×10^{-2}

*Lattice spacings of 3.81, 5.715, and 7.62 cm (Benchmarks MIT-4, MIT-5, and MIT-6 respectively).

b. Suggested Method of Calculation

Monte Carlo, Sn ($n \geq 4$), or integral transport theory.

An accurate treatment of resonance absorption is essential.

2. Axial Leakage Calculation

To account for leakage use the following geometrical bucklings in B_L calculations with $L \geq 1$.

Benchmark	Pitch, cm	$B^2(m^{-2})$
MIT-4	3.81	8.05
MIT-5	5.715	11.78
MIT-6	7.62	10.00

A less desirable way to account for axial leakage is to use the following critical water heights, h:

Benchmark	h,cm	λ_{tr},cm
MIT-4	108.5	3.201
MIT-5	89.42	2.969
MIT-6	97.37	2.782

These heights have been derived from measured material bucklings using

$$B^2 = \frac{(\Pi)^2}{(h+\varepsilon)^2}$$

Where the extrapolation distance, ε is determined from

$$\varepsilon = 0.71\ \lambda_{tr}$$

The values for the transport mean free path were obtained using leakage corrected integral transport theory and ENDF/B-IV cross sections.

D. Experimental Data

Parameter	Pitch, cm 3.81	5.715	7.62
B_m^2 (m^{-2})	8.05 ± .15	11.78± .11	10.00 ± .08
ρ^{28}	1.155 ± .001	0.525 ± 0.002	0.317 ± 0.002
δ^{25}	0.0865± .0016	0.0371± 0.0012	0.0222± 0.0024
δ^{28}	0.0459± .0013	0.0326± 0.0010	0.0291± 0.0018
C^*	1.007 ± .008	0.740 ± 0.007	0.647 ± 0.002

ρ^{28} = ratio of epithermal to thermal ^{238}U captures

δ^{25} = ratio of epithermal to thermal ^{235}U fissions

δ^{28} = ratio of ^{238}U fissions to ^{235}U fissions

C^* = ratio of ^{238}U captures to ^{235}U fissions

Note: Parameters correspond to an epithermal - thermal cut-off energy of 0.625 eV.

E. Comments and Documentation

The physical properties of the lattices are described in Ref. 1.
The experimental facilities are described in Ref. 2.
The measured lattice parameters are documented in Ref. 3.
The material bucklings have been altered based on quantitive consistency analysis in Ref. 4.

References

1. T. J. Thompson, et al., "Heavy Water Lattice Project Annual Report, September 30, 1966," MIT-2344-09 (1966).

2. P. F. Palmedo, et al., "Measurements of the Material Bucklings of Lattices of Natural Uranium Rods in D_2O," NYO-9660 (MITNE-13), 1962)

3. T. J. Thompson, et al., "Heavy Water Lattice Project Final Report," MIT-2344-12 (1967).

4. D. R. Finch and W. E. Graves, "Quantitative Consistency Testing of Thermal Benchmark Lattice Experiments," Trans. of ANS, 27, 888 (1977) Also DP-MS-77-33, E. I. du Pont, Savannah River Laboratory, 1977.

THERMAL REACTOR BENCHMARKS NOS. 13-17

A. Benchmark Name and Type: PNL-1 through PNL-5, unreflected plutonium spheres.

B. System Description

This series of benchmarks consists of five unreflected spheres of plutonium nitrate solutions with hydrogen/^{239}Pu atom ratios ranging from 131 to 1204. Critical volumes for the various solutions were measured. In one experiment the critical buckling was determined. These benchmarks are useful for testing H_2O scattering data, cross sections for thermal neutron capture and fission by ^{239}Pu, and the ^{239}Pu fission spectrum.

C. Model Description

PNL-1 and PNL-2 have H/^{239}Pu atom ratios of 700 and 131 respectively; each contains 4.6 wt. % ^{240}Pu and has an effective radius of 19.509 cm.

	Concentration, 10^{24} atoms/cm^3	
Material	PNL-1	PNL-2
H	.06563	.05416
O	.03456	.03977
N	6.216×10^{-4}	4.720×10^{-3}
^{239}Pu	9.373×10^{-5}	4.141×10^{-4}
^{240}Pu	4.501×10^{-6}	1.988×10^{-5}

Benchmarks PNL-3 and PNL-4 have H/^{239}Pu atom ratios of 1204 and 911 respectively; each contains 4.20 wt. % ^{240}Pu and has an effective radius of 22.70 cm.

Material	Concentration, 10^{24} atoms/cm^3 PNL-3	PNL-4
H	.06495	.06041
O	.03441	.03712
N	7.393×10^{-4}	2.775×10^{-3}
Fe	1.294×10^{-6}	1.520×10^{-6}
^{239}Pu	5.395×10^{-5}	6.633×10^{-5}
^{240}Pu	2.355×10^{-6}	2.895×10^{-6}

Benchmark PNL-5 has an effective radius of 20.1265 cm, a H/^{239}Pu atom ratio of 578 and contains 4.17 wt. % ^{240}Pu.

Material	Concentration, 10^{24} atoms/cm^3
H	.06028
O	.03710
N	2.737×10^{-3}
Fe	1.930×10^{-6}
^{239}Pu	1.043×10^{-4}
^{240}Pu	4.520×10^{-6}

It is suggested that multiplication constants k be calculated using S_n theory ($n \geq 4$) with approximately 50 mesh points per sphere. A group structure should be selected which adequately represents fast leakage phenomena as well as thermal events. Pu-240 resonance absorption is significant in these calculations.

D. Experimental Data

The compositions and dimensions specified above were experimentally derived for criticality (k = 1). A geometric buckling of 0.02182 ± 0.00015 cm^{-2} was derived for PNL-1.

F. Comments and Documentation

The experimental conditions associated with benchmarks PNL-1 and PNL-2 are given in (1). Recent calculations for these two benchmarks with ENDF/B-II data are described in (2). Reference 3 documents the experimental conditions associated with PNL-3, PNL-4, and PNL-5. In all five experiments the plutonium nitrate solutions were enclosed in stainless steel walled spheres. The effective radii quoted above in the Physical Properties Section were derived by the experimenters (1), (3) and specify critical sizes for solutions without stainless steel walls.

REFERENCES

1. R. C. Lloyd et al., "Criticality Studies with Plutonium Solutions," Nuc. Sci. and Eng. 25, 165 (1966).
2. L. E. Hansen and E. D. Clayton, "Theory-Experiment Tests Using ENDF/B Version II Cross-Section Data," Trans. Amer. Nuc. Soc. 15, 309 (June 1972).
3. F. E. Kruesi et al., "Critical Mass Studies of Plutonium Nitrate Solution," HW-24514 (1952).

THERMAL REACTOR BENCHMARKS NOS. 18-20

A. Benchmark Name and Type: BAPL-UO_2-1 through 3,H_2O moderated uranium oxide critical lattices.

B. System Description

These experiments consist of H_2O moderated critical lattices of 1.311 w% enriched uranium oxide rods (O.D. 0.9728 cm) arranged in a triangular pattern. The measured parameters include ρ^{28}, δ^{25}, δ^{28}, and B^2. Three lattices with moderator to fuel volume ratios of 1.43, 1.78 and 2.40 are specified.

C. Model Description

1. Infinite lattice calculation

a) Physical properties (cylindrical geometry)

Region	Outer Radius (cm)	Isotope	Concentration (10^{24} atoms/cm^3)
Fuel	.4864	^{235}U	3.112×10^{-4}
		^{238}U	2.3127×10^{-2}
		O	4.6946×10^{-2}
Void	.5042	--	--
Clad	.5753	Al	6.025×10^{-2}
Moderator	*	O	3.338×10^{-2}
		H	6.676×10^{-2}

*Triangular lattices with a pitch of 1.5578, 1.6523 and 1.8057 cm respectively.

b) Suggested Method of Calculation

Integral transport theory, Monte Carlo or Multigroup Sn with special treatment of the resonance region.

2. Leakage Calculation

To account for leakage a homogenized B_ℓ calculation with the following total bucklings should be used.

Lattice	Buckling $[m^{-2}]$
BAPL-UO_2-1	32.59 ± .15
BAPL-UO_2-2	35.47 ± .18
BAPL-UO_2-3	34.22 ± .13

D. Experimental Data

	BAPL-UO_2-1	BAPL-UO_2-2	BAPL-UO_2-3
Pitch, Cm	1.5578	1.6523	1.8057
Water/fuel vol. ratio	1.43	1.78	2.40
Number of rods	2173 ± 3	1755 ± 3	1575 ± 3
B^2 $[m^{-2}]$	32.59 ± .15	35.47 ± .15	34.22 ± .13
ρ^{28}	1.39 ± .01	1.12 ± .01	0.906 ± .01
δ^{25}	.084 ± .002	.068 ± .001	.052 ± .001
δ^{28}	.078 ± .004	.070 ± .004	.057 ± .003

NOTE: Measured parameters correspond to a thermal cutoff of 0.625 eV and were measured at the core center.

E. Comments and Documentation

The specifications for the lattices and the measured values were taken from reference 1 where the following identifications have been used:

BAPL-UO_2-1	OA-131-383-143
BAPL-UO_2-2	OA-131-383-178
BAPL-UO_2-3	OA-131-383-240

Reference 2 describes the original experiment. Results of an analysis using ENDF/B-IV data are given in Reference 3.

References

1. Hellens, R. L., Price, G. A. , "Reactor Physics Data for Water-Moderated Lattices of Slightly Enriched Uranium", Reactor Technology Selected Reviews, 529, 1964.
2. Brown, J. R. and Harris, D. R., et al., "Kinetic and Buckling Measurements on Lattices of Slightly Enriched Uranium and UO_2 Rods in Light Water" WAPD-176 (1958).
3. Rothenstein, W., "Thermal Reactor Lattice Analysis Using ENDF/B-IV Data with Monte Carlo Resonance Reaction Rates", BNL-20446 (1975); Nucl. Sci. Eng. 59, 337-349, (1976).

THERMAL REACTOR BENCHMARKS NOS. 21-23

A. Benchmark Name and Type: BNL-ThO_2-1 through 3, H_2O moderated Thorium oxide exponential lattices.

B. System Description

These experiments consist of H_2O moderated exponential lattices fueled by vibratory compacted particles of 3wt% $^{233}UO_2$ - 97wt%ThO_2. The fuel rods (O.D. 1.0922 cm) were clad in Zircaloy-2 and arranged in a triangular pattern in a 180 cm diameter X 180 cm deep aluminum tank erected on top of a thermal column. Measured parameters include B_m^2, ρ^{28} and the dysprosium disadvantage factor (ζ_{Dy}). Three lattices with moderator to fuel volume ratios of 1.0, 1.38 and 3.0 are specified.

These lattices are sensitive to cross sections for thermal and epithermal U233 fission, thermal and epithermal Th232 capture, and H_2O scattering.

C. Model Description

There are two principal methods of analysis:

- A heterogeneous infinite lattice cell calculation followed by a homogenized-core leakage calculation (either with the measured material B^2, or an explicit radial calculation with the measured axial B^2).

- An explicit description of the actual lattice in two dimensions with an axial leakage correction obtained from the homogenized-core description with the measured axial B^2.

It has been observed that the second method produces significantly different radial leakage than either of the homogenized-core approximations (Ref. 4).

1. Infinite Lattice Cell

a) Physical Properties

Region	Outer radius (cm)	Isotope	Concentration 10^{24} Atoms/cm^3
Fuel	0.5461	^{16}O	4.08832×10^{-2}
		^{232}Th	1.98115×10^{-2}
		^{233}U	6.1021×10^{-4}
		^{234}U	9.09×10^{-6}
		^{235}U	2.7×10^{-7}
		^{238}U	6.55×10^{-6}
		B	2.2×10^{-6}
Clad	0.63373	Zr	4.4355×10^{-2}
		Sn	5.03×10^{-4}
		Cr	7.92×10^{-5}

Region	Outer radius (cm)	Isotope	Concentration 10^{24} Atoms/cm^3
		Fe	9.58×10^{-5}
		Ni	3.51×10^{-5}
		Co	3.5×10^{-7}
		B	5.3×10^{-7}
		Cd	2.0×10^{-8}
		Hf	7.0×10^{-8}
Moderator	*	H	6.676×10^{-2}
		O	3.338×10^{-2}

*Triangular lattices with a pitch of 1.5923, 1.7188 and 2.1697 cm respectively.

b) Suggested Method of Calculation

Integral transport theory, Monte Carlo or Multigroup Sn with special treatment of the resonance region.

2. Leakage Calculation

a) To account for leakage a homogenized B_ℓ calculation with the following total material bucklings should be used.

	Buckling [m^{-2}]	Axial Relaxation Length (cm)	No. of Rods
BNL-ThO_2-1	75.88 ± 2.0	39.57	511
BNL-ThO_2-2	86.06 ± 1.3	43.58	397
BNL-ThO_2-3	85.54 ± 0.8	45.18	271

b) An alternative treatment of leakage is to cylindricize the lattice region then use Sn or P_ℓ theory with an axial buckling obtained from the relaxation length.

3. Explicit Full Core Model (Two Dimensions)

Figure 1 shows a 1/3-core 2-dimensional representation of the BNL-$Th\emptyset_2$-1 lattice. The model includes the water reflector (not shown) out to a radius of 90 cm, which coincides with the position of the tank wall. BNL-$Th\emptyset_2$-2, -3 is represented similarly except for the number of fuel rods. The outer fuel boundary is symmetricized in all cases.

The axial direction is not represented in the full-core Monte Carlo description. The correction for axial inleakage is obtained as in Section 2(b), with a negative axial buckling given by $-1/L_z^2$, where L_z is the measured axial relaxation length.

D. Experimental Data

	BNL-ThO_2-1	BNL-ThO_2-2	BNL-ThO_2-3
Pitch, cm	1.5923	1.7188	2.1697
Water/fuel vol. ratio	.997	1.384	3.0043
Number of rods	511	397	271
δ_{Dy}	1.219 ± 0.024	1.257 ± 0.024	1.325 ± 0.024
$\rho 02$	1.338 ± 0.042	.903 ± 0.038	.421 ± 0.013

Note: parameters correspond to a thermal cutoff of 0.625 eV

$\rho 02$ = ratio of epithermal to thermal captures in ^{232}Th

ζ_{Dy} = Dysprosium-164 disadvantage factor - Ratio of the activations of ^{164}Dy in the moderator to those in the fuel.

BNL-01 0.997-1.0 LATTICE

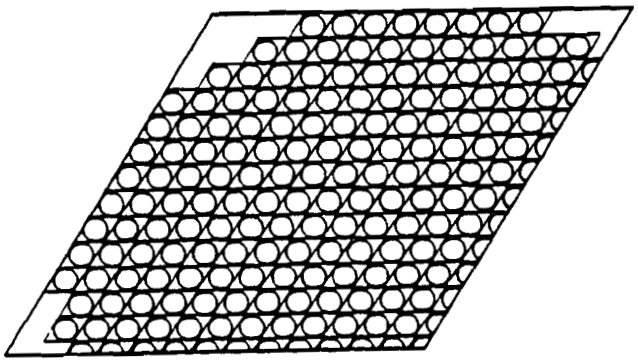

E. Comments and Documentation

The measurements are described in references 1 and 2. Reference 3 describes the analysis.

References

1. Windsor, H. H., Tunney, W. J. and Price, G. A. "Exponential Experiments with Lattices of Uranium-233 Oxide and Thorium Oxide in Light and Heavy Water." Nucl. Sci. Engr. 42 150 (1970).
2. Price, G. A. Uranium - Water Lattice Compilation Part I, BNL Exponential Assemblies, BNL-50035 (T-449) Reactor Technology - TID 45007.
3. Sehgal, B. R. "Analysis of Brookhaven ^{233}U - ^{232}Th Oxide, Light and Heavy Water Lattice Experiments" Trans. Am. Nucl. Soc. 10, 596 (1967).
4. J. J. Ullo, J. Hardy, Jr., and N. M. Steen, "Review of Thorium-U233 Cycle Thermal Reactor Benchmark Studies," BNL/EPRI Symposium on Nuclear Data Problems for Thermal Reactor Applications, May 22-24, 1978.

THERMAL REACTOR BENCHMARKS NOS. 24-30

A. Benchmark Name and Type: PNL-6 through PNL-12, homogeneous aqueous plutonium nitrate spheres and cylinders.

B. System Description

This series of benchmarks consists of seven homogeneous aqueous solutions of plutonium nitrate with hydrogen/Pu239 ratios ranging from 125 to 1067, as shown in Table 1.

Critical volumes and compositions were determined. These benchmarks are generally useful for testing H_2O scattering data, cross sections for resonance and thermal fission of Pu239 and the Pu239 fission spectrum. PNL 10 and PNL 11 have significant concentrations of Pu240, Pu241, and Pu242.

C. Model Descriptions

It is suggested that the multiplication factor be obtained using an S_N ($N > 4$), or equivalent P_ℓ, multigroup one-dimensional calculation.

A more detailed model, suitable for Monte Carlo analyses, represents the system explicitly in three dimensions with some simplification of auxiliary structure.

Specifications for these models are given separately for each assembly, along with composition data and explicit descriptions of the assemblies.

D. General Reference

U.P. Jenquin and S.R. Bierman, "Benchmark Experiments to Test Plutonium and Stainless Steel Cross Sections", NUREG/CR-0210 (PNL-2273) June 1978.

Table 1

Summary of Atomic Ratios for Benchmarks PNL-6 through PNL-12

		Pu Isotope/All Pu				
	H/Pu	Pu238	Pu239	Pu240	Pu241	Pu242
PNL-6	125	—	.9514	.0455	.0030	.0001
PNL-7	980	—	.9946	.0054	—	—
PNL-8	758	—	.9514	.0455	.0030	.0001
PNL-9	910	—	.9544	.0456	—	—
PNL-10	210	.0000	.9075	.0835	.0085	.0005
PNL-11	623	.0020	.4153	.4286	.1075	.0466
PNL-12	1067	—	.9514	.0454	.0031	.0001

Benchmark No. 24 (PNL-6)

GENERAL DESCRIPTION:

Stainless steel (type 304L) sphere, unreflected and filled with a homogeneous aqueous solution of Pu(4.57) $(NO_3)_4$ at 125H:Pu. This is a revised description of PNL-2.

DATA SOURCE:

R.C. Lloyd, Battelle Pacific Northwest Laboratories, Richland, Washington 99352.
R.C. Lloyd, C. R. Richey, E.D. Clayton, and D.R. Skeen, "Criticality Studies with Plutonium Solutions," N.S. & E. 25, 165-173, (1966).

COMPOSITION OF FUEL[a]:

Nuclide	Wt%	10^{30} Atoms/m^3
Pu-238	0.0000 ± ———	———
Pu-239	11.4689 ± 0.0572	4.1307×10^{-4}
Pu-240	0.5507 ± 0.0027	1.9752×10^{-5}
Pu-241	0.0371 ± 0.0002	1.3251×10^{-6}
Pu-242	0.0007 ± ———	2.4899×10^{-8}
N	7.6827 ± 0.0280	4.7224×10^{-3}
O	73.8935 ± 0.2561	3.9764×10^{-2}
H	6.3433 ± 0.0299	5.4182×10^{-2}
Fe	0.0231 ± 0.0001	3.5612×10^{-6}

Solution Density, kg/m^3	1429.00 ± 5.72
Plutonium Concentration, kg/m^3	172.30 ± 0.86
Excess Nitrate Concentration, Molarity	4.96 ± 0.12
H:Pu, Atom Ratio	124.8 ± 0.9

[a] Water and hydrogen ion concentration adjusted to obtain density and total nitrate reported by data source.

COMPOSTION OF EXPERIMENTAL VESSEL[b]:

Nuclide	Wt%	10^{30} Atoms/m^3
Fe	74.0	6.331×10^{-2}
Cr	18.0	1.654×10^{-2}
Ni	8.0	6.510×10^{-3}

[b] 304L Stainless Steel at 7.93 Mg/m^3.

COMPOSITION OF REFLECTOR:

None

Benchmark No. 24 (PNL-6)

DIMENSIONS OF EXPERIMENTAL VESSEL:

Inside Radius, mm	193.18 ± 0.02
Vessel Wall Thickness, mm	1.22 ± ——

DELAYED CRITICAL CONFIGURATION:

Unreflected assembly[c)]

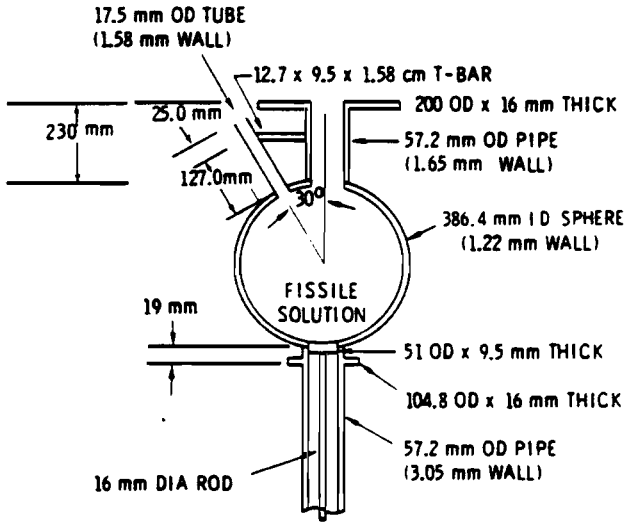

Core Temperature, K	299.8 ± 2
Room Temperature, K	297.0 ± 2

c) Experimentally determined corrections for the vessel and piping increases the spherical critical volume for this solution to 0.0311 m^3.

Reflected assembly

None

Benchmark No. 24 (PNL-6)

1) PNL-6A

Unreflected spherical plutonium nitrate solution (no vessel)

R = 19.5085 cm

Atomic number densities as shown on page T(24-30)-3.

2) PNL-6B

Spherical model. Atomic number densities as shown on page T(24-30)-3.

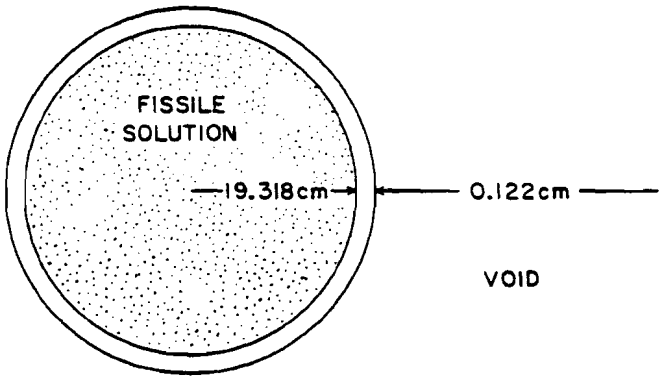

Benchmark No. 25 (PNL-7)

GENERAL DESCRIPTION:

Stainless steel (Type 347) sphere, reflected with at least 30 cm of water and filled with a homogeneous aqueous solution of Pu (0.54) $(NO_3)_4$ at 980 H:Pu.

DATA SOURCE:

F.F. Kruesi, J.O. Erkman, and D.D. Lanning, "Critical Mass Studies of Plutonium Solutions," HW-24514 DEL, p 67, 1952.

COMPOSITION OF FUEL[a]:

Nuclide	Wt%	10^{30} Atoms/m^3
Pu-238	———	———
Pu-239	2.4493 ± 0.0245	6.6004×10^{-5}
Pu-240	0.0133 ± 0.0009	3.5692×10^{-7}
Pu-241	———	———
Pu-242	———	———
N	1.6332 ± 0.0217	7.5114×10^{-4}
O	85.7193 ± 0.0746	3.4514×10^{-2}
H	10.1715 ± 0.0077	6.5006×10^{-2}
Fe	0.0134 ± 0.0002	1.5457×10^{-6}

Solution Density, kg/m^3	1069.2 ± 0.3
Plutonium Concentration, kg/m^3	26.3 ± 0.3
Excess Nitrate, Concentration, Molarity	0.806 ± 0.009
H:Pu, Atom Ratio	979.6 ± 9.9

[a] Water and hydrogen ion concentration adjusted to obtain density and total nitrate reported by data source

COMPOSITION OF EXPERIMENTAL VESSEL[b]:

Nuclide	Wt%	10^{30} Atoms/m^3
Fe	72.0	6.175×10^{-2}
Cr	18.0	1.658×10^{-2}
Ni	10.0	8.158×10^{-3}

[b] 347 Stainless Steel at 7.95 Mg/m^3

COMPOSITION OF REFLECTOR[c]:

Nuclide	Wt%	10^{30} Atoms/m^3
H	11.19	6.663×10^{-2}
O	88.81	3.332×10^{-2}

[c] Water at 299.8 ± 0.3 K

Benchmark No. 25 (PNL-7)

DIMENSIONS OF EXPERIMENTAL VESSEL:

Inside Radius of Sphere, mm	177.80 ± 1.59
Vessel Wall Thickness, mm	1.27 ± ——

DELAYED CRITICAL CONFIGURATION:

Unreflected Assembly

None

Water Reflected Assembly[d)]

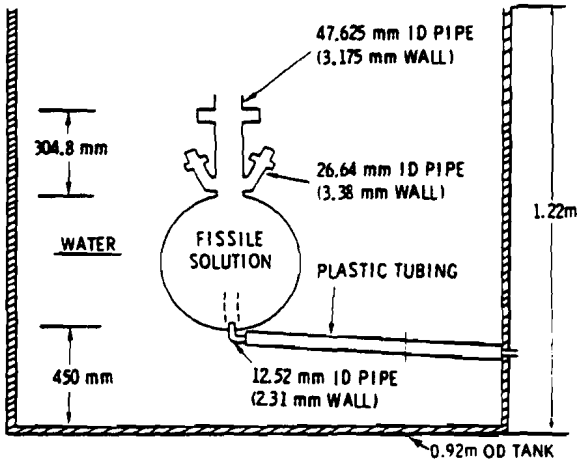

Reflector and core temperature, K	299.8 ± 0.3
Room temperature, K	297.0 ± ——

d) The vessel neck increases the critical mass by a maximum of 50 mg of Pu.

Benchmark No. 25 (PNL-7)

1) PNL-7A

Spherical Model. Atomic number densities as shown on page T(24-30)-6 except for $^{239}Pu = 6.5998 \times 10^{-5}$ and $^{240}Pu = 3.5689 \times 10^{-7}$ (in units of 10^{30} atoms/m^3).

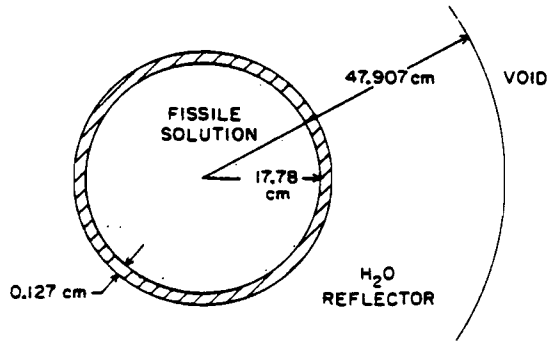

Benchmark No. 25 (PNL-7)

2) PNL-7B

Monte Carlo Model. Atomic number densities as shown on page T(24-30)-6. Atomic number densities for tank same as experimental vessel.

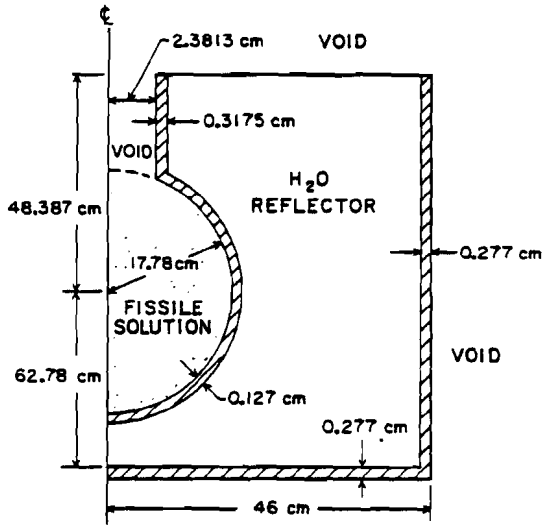

Benchmark No. 26 (PNL-8)

GENERAL DESCRIPTION:

Stainless steel (Type 304L) sphere, reflected with 6.604 mm of Type 304L steel and filled with a homogeneous aqueous solution of Pu (4.57) $(NO_3)_4$ at 758 H:Pu.

DATA SOURCE:

R.C. Lloyd, Battelle, Pacific Northwest Laboratories, Richland, Washington 99352.
R.C. Lloyd, C.R. Richey, E.D. Clayton, and D.R. Skeen, "Criticality Studies with Plutonium Solutions," N.S.&E. 25, 165-173 (1966).

COMPOSITION OF FUEL[a]:

Nuclide	Wt%	10^{30} Atoms/m^3
Pu-238	———	———
Pu-239	3.0322 ± 0.0152	8.2232×10^{-5}
Pu-240	0.1456 ± 0.0007	3.9321×10^{-6}
Pu-241	0.0098 ± ———	2.6356×10^{-7}
Pu-242	0.0002 ± ———	5.3567×10^{-9}
N	1.3856 ± 0.0754	6.4132×10^{-4}
O	85.2334 ± 0.3727	3.4536×10^{-2}
H	10.1872 ± 0.0460	6.5520×10^{-2}
Fe	0.0060 ± 0.0003	6.9650×10^{-7}

Solution Density, kg/m^3	1076.0 ± 4.3
Plutonium Concentration, kg/m^3	34.3 ± 0.2
Excess Nitrate Concentration, Molarity	0.49± 0.02
H:Pu, Atom Ratio	758.0 ± 0.2

[a] Water and hydrogen ion concentration adjusted to obtain density and total nitrate reported by data source

COMPOSITION OF EXPERIMENTAL VESSEL[b]:

Nuclide	Wt%	10^{30} Atoms/m^3
Fe	74.0	6.331×10^{-2}
Cr	18.0	1.654×10^{-2}
Ni	8.0	6.510×10^{-3}

[b] 304L Stainless Steel at 7.93 Mg/m^3

COMPOSITION OF REFLECTOR:

Same as experimental vessel.

Benchmark No. 26 (PNL-8)

DIMENSIONS OF EXPERIMENTAL VESSEL:

Inside Radius, mm	193.18 ± 0.02
Vessel Wall Thickness, mm	1.22 ± ——

DELAYED CRITICAL CONFIGURATION:

Unreflected Assembly

None

Steel Reflected Assembly

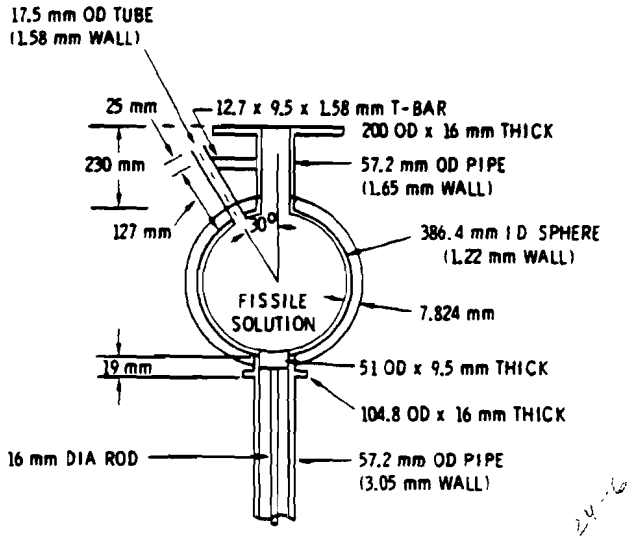

Reflector and core temperature, K	299.8 ± 2
Room Temperature, K	297.0 ± 2

Benchmark No. 26 (PNL-8)

1) PNL-8A

Spherical Model. Atomic number densities as shown on page T(24-30)-11.

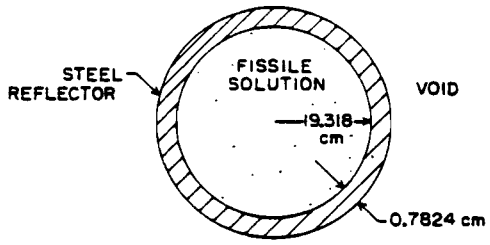

2) PNL-8B

Monte Carlo Model. Atomic number densities as shown on page T(24-30)-11.

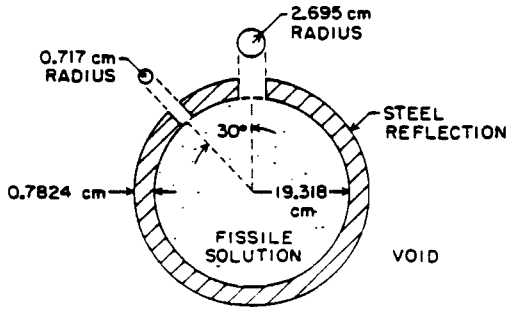

Benchmark No. 27 (PNL-9)

GENERAL DESCRIPTION:

Stainless steel (Type 304L) cylinder, unreflected and partially filled with a homogeneous aqueous solution of Pu(13.8) $(NO_3)_4$ at 910H:Pu

DATA SOURCE:

F. Abbey, P.J. Hemmings, and E.R. Woodlock, "Data Checks on Plutonium Systems", HSRC/CSC/p. 24, (UK)

J.C. Smith, (Title unknown), HSRC/CSC/p. 30 (1964) (UK)

COMPOSITION OF FUEL:

Nuclide	Wt%	10^{30} Atoms/m^3
Pu-239	2.308	6.1822×10^{-5}
Pu-240	0.369	9.8429×10^{-6}
N	1.354	6.1898×10^{-6}
O	85.703	3.4300×10^{-2}
H	10.266	6.5215×10^{-2}

Solution Density, kg/m^3	1063.3
Plutonium Concentration, kg/m^3	28.5
Excess Nitrate Concentration, Molarity	0.55
H:Pu, Atom Ratio	910

COMPOSITION OF EXPERIMENTAL VESSEL[a]:

Nuclide	Wt%	10^{30} Atoms/m^3
Fe	74.0	6.331×10^{-2}
Cr	18.0	1.654×10^{-2}
Ni	8.0	6.510×10^{-3}

[a] 304L Stainless Steel at 7930 kg/m^3

COMPOSITION OF REFLECTOR:

None

Benchmark No. 27 (PNL-9)

DIMENSIONS OF EXPERIMENTAL VESSEL:

Inside Radius, mm	227.33[a]
Inside Height, mm	b)
Side Wall Thickness, mm	1.626
End Thicknesses, mm	1.626

a) It is not clear whether the vessel radius is internal or external.

b) Not given.

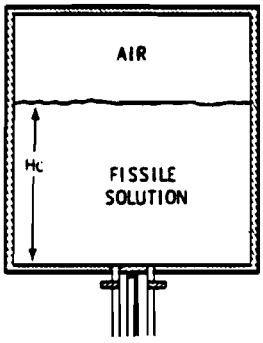

Critical height of solution, mm	364.03[c]
Reflector and core temperature, K	d)
Room temperature, K	d)

c) It is not clear whether a correction has been made for the effects of the feed pipe. The correction might amount to 2.5 mm (max.) in the critical height.

d) Not given

REFLECTED ASSEMBLY

None

Benchmark No. 27 (PNL-9)

1) PNL-9

Cylindrical Model. Atomic number densities as shown on page T(24-30)-13. Assume temperature 300°K.

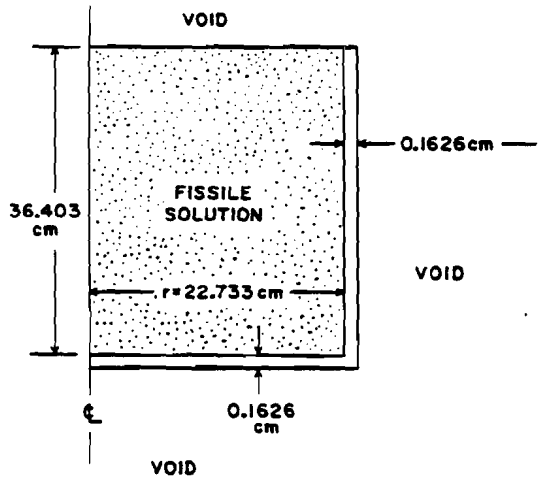

Benchmark No. 28 (PNL-10)

GENERAL DESCRIPTION:

Stainless steel (type 304L) cylinder reflected with at least 200 mm of water on sides and bottom, and partially filled with a homogeneous aqueous solution of Pu (8.4) $(NO_3)_4$ at 210 H:Pu.

DATA SOURCE:

R.C. Lloyd, E. D. Clayton, and L.E. Hansen "Criticality of Plutonium Nitrate Solution Containing Soluble Gadolinium", Nucl Sci & Engr 48, 300-304, (1972).

COMPOSITION OF FUEL:[a)]

Nuclide	Wt%	10^{30} Atoms/m^3
Pu-238	0.0004	1.2701×10^{-8}
Pu-239	8.3833	2.6508×10^{-4}
Pu-240	0.7747	2.4394×10^{-5}
Pu-241	0.0787	2.4679×10^{-6}
Pu-242	0.0045	1.4053×10^{-7}
N	4.2995	2.3202×10^{-3}
O	78.2964	3.6991×10^{-2}
H	8.1625	6.1211×10^{-2}

Solution Density, kg/m^3	1255.2
Plutonium Concentration, kg/m^3	116
Excess Nitrate, Concentration, Molarity	1.91
H:Pu, Atom Ratio	209.6

a) Water and hydrogen ion concentration adjusted to obtain density and total nitrate reported by data source.

COMPOSITION OF EXPERIMENTAL VESSEL:[b)]

Nuclide	Wt%	10^{30} Atoms/m^3
Fe	72.0	6.175×10^{-2}
Cr	18.0	1.658×10^{-2}
Ni	10.0	8.158×10^{-3}

b) 347 Stainless Steel at 7950 kg/m^3

COMPOSITION OF REFLECTOR:[c)]

Nuclide	Wt%	10^{30} Atoms/m^3
H	11.19	6.668×10^{-2}
O	88.81	3.334×10^{-2}

c) Water at 296 ± 2K

Benchmark No. 28 (PNL-10)

DIMENSIONS OF EXPERIMENTAL VESSEL:

Inside Radius, mm	305.14
Inside Height, mm	1057.3
Side Wall Thickness, mm	0.79
End Thicknesses, mm	9.5

DELAYED CRITICAL CONFIGURATION:

Unreflected Assembly

None

Water Reflected Assembly

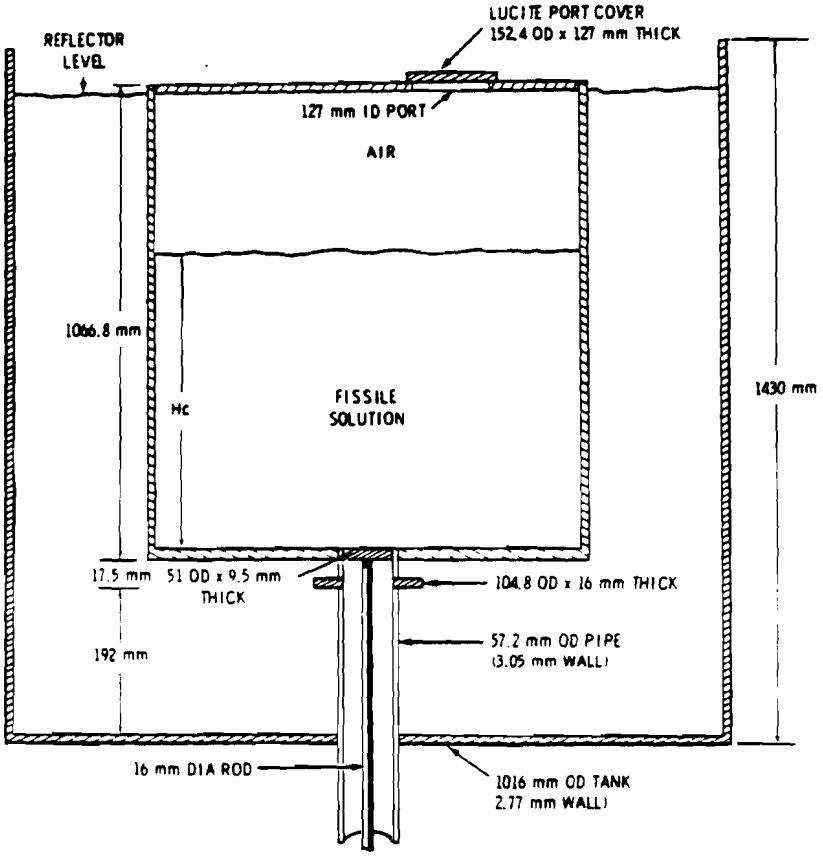

Critical height of solution, mm	154.4
Reflector and core temperature, K	296 ± 2
Room temperature, K	294 ± 2

Benchmark No. 28 (PNL-10)

1) PNL-10

Cylindrical Model. Atomic number densities as shown on page T(24-30)-16. Atomic number densities for tank same as experimental vessel. H_c=15.44 cm.

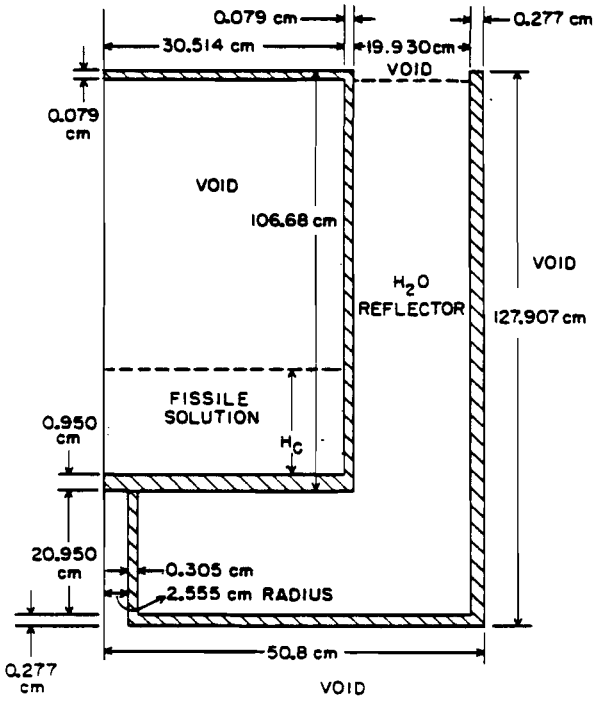

Benchmark No. 29 (PNL-11)

GENERAL DESCRIPTION:

Stainless steel (type 304L) cylinder reflected with at least 200 mm of water on sides and bottom, and partially filled with a homogeneous aqueous solution of Pu (42.9) $(NO_3)_4$ at 623 H:Pu.

DATA SOURCE:

R.C. Lloyd, Battelle, Pacific Northwest Laboratories, Richland, Washington 99352
R.C. Lloyd, and E.D. Clayton "The Criticality of High Burnup Plutonium", Nucl. Sci. & Engr. 52, 73-75 (1973).

COMPOSITION OF FUEL:[a)]

Nuclide	Wt%	10^{30}Atoms/m^3
Am-241	0.0394	1.0946×10^{-6}
Pu-238	0.0073	2.0537×10^{-7}
Pu-239	1.5114	4.2342×10^{-5}
Pu-240	1.5662	4.3694×10^{-5}
Pu-241	0.3943	1.0955×10^{-5}
Pu-242	0.1716	4.7478×10^{-6}
N	2.6918	1.2870×10^{-3}
O	84.0564	3.5184×10^{-2}
H	9.5613	6.3526×10^{-2}
Gd	0.0003	1.2776×10^{-8}

Solution Density, kg/m^3	1112.09
Plutonium, kg/m^3	40.6
Excess Nitrate, Molarity	1.46
H:Pu, Atom Ratio	623.1

a) Water and hydrogen ion concentration adjusted to obtain density and total nitrate reported by data source.

COMPOSITION OF EXPERIMENTAL VESSEL:[b)]

Nuclide	Wt%	10^{30}Atoms/m^3
Fe	74.0	6.331×10^{-2}
Cr	18.0	1.654×10^{-2}
Ni	8.0	6.510×10^{-3}

b) 304L Stainless Steel at 7930 kg/m^3

COMPOSITION OF REFLECTOR:[c)]

Nuclide	Wt%	10^{30}Atoms/m^3
H	11.19	6.668×10^{-2}
O	88.81	3.334×10^{-2}

c) Water at 296K

Benchmark No. 29 (PNL-11)

DIMENSIONS OF EXPERIMENTAL VESSEL:

Inside Radius, mm	305.14
Inside Height, mm	1057.3
Side Wall Thickness, mm	0.79
End Thicknesses, mm	9.5

DELAYED CRITICAL CONFIGURATION

Unreflected Assembly

None

Water Reflected Assembly

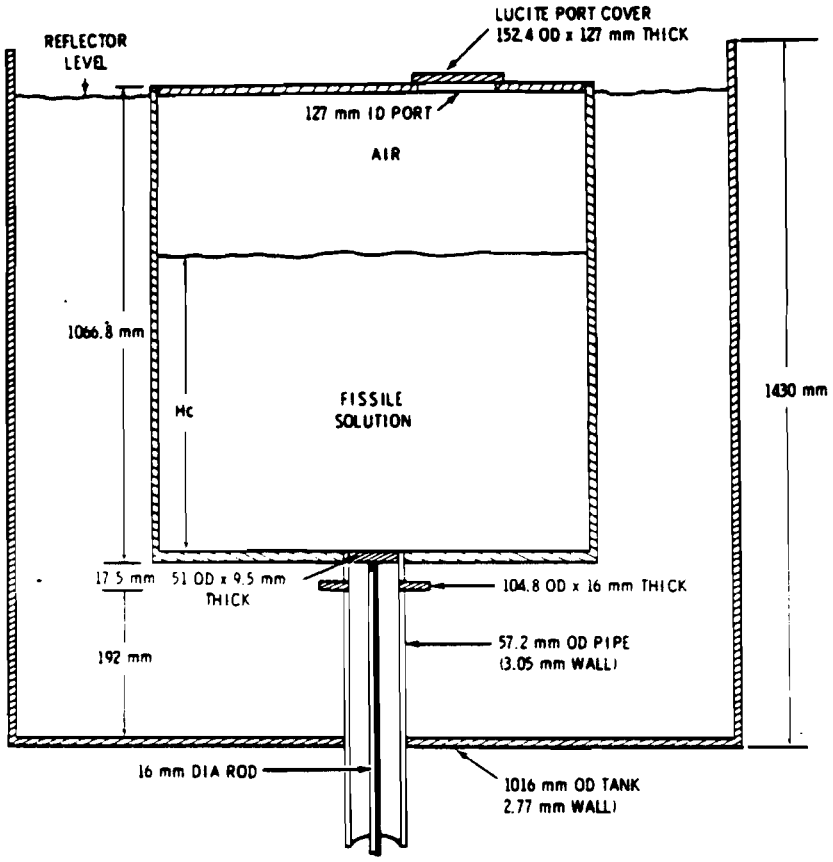

Critical height of solution, mm	809.2
Reflector and core temperature, K	296 ± 2
Room temperature, K	294 ± 2

Benchmark No. 29 (PNL-11)

1) PNL-11

Cylindrical Model. Atomic number densities as shown on page T(24-30)-19. Atomic number densities for tank same as experimental vessel. H_c=80.92 cm

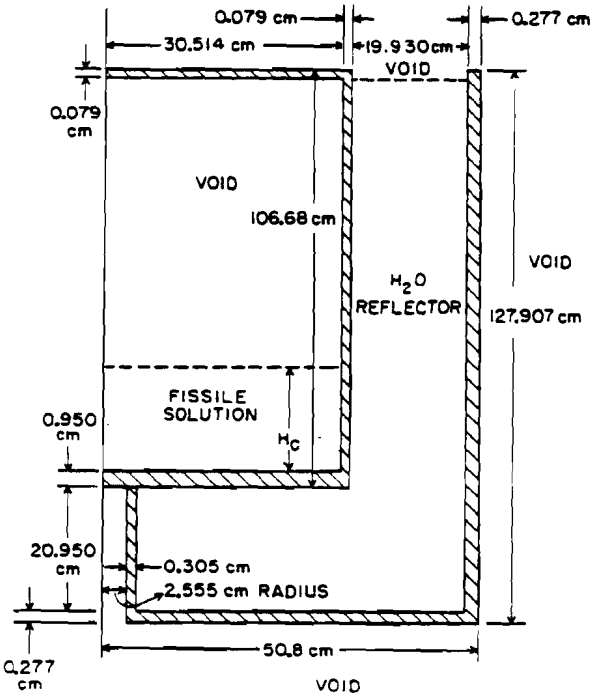

Benchmark No. 30 (PNL-12)

GENERAL DESCRIPTION:

Stainless steel sphere reflected uniformly with water. Completely filled with a homogeneous aqueous solution of Pu (4.6) $(NO_3)_4$ at 1067 H:Pu.

DATA SOURCE:

R.C. Lloyd, Battelle, Pacific Northwest Laboratories, Richland, Washington 99352
R.C. Lloyd, et al., "Criticality Studies with Plutonium Solution", Nucl Sci & Engr 25, 165-173 (1966)

COMPOSITION OF FUEL:[a)]

Nuclide	Wt%	10^{30} Atoms/m^3
Pu-239	2.190 ± 0.014	5.848×10^{-5}
Pu-240	0.105 ± 0.0007	2.79×10^{-6}
Pu-241	0.0070± 0.0001	1.9×10^{-7}
Pu-242	0.0002± 0.0001	5.0×10^{-9}
N	1.236 ± 0.0019	5.633×10^{-4}
O	86.09 ± 0.51	3.435×10^{-2}
H	10.36 ± 0.06	6.561×10^{-2}
Fe	0.0044± 0.0002	5.0×10^{-7}

Solution Density kg/m^3	1060 ± 4
Plutonium Density kg/m^3	24.4 ± 0.1
Excess Nitrate Molarity	0.53 ± 0.01
H:Pu Atom Ratio	1067 ± 7

a) Water and hydrogen ion concentration adjusted to obtain density and total nitrate reported by data source.

COMPOSITION OF EXPERIMENTAL VESSEL:[b)].

Nuclide	Wt%	10^{30} Atoms/m^3
Fe	74.0	6.331×10^{-2}
Cr	18.0	1.654×10^{-2}
Ni	8.0	6.510×10^{-3}

b) 304L Stainless Steel at 7930 kg/m^3

COMPOSITION OF REFLECTOR:[c)]

Nuclide	Wt%	10^{30} Atoms/m^3
H	11.19	6.668×10^{-2}
O	88.81	3.334×10^{-2}

c) Water at 296K

Benchmark No. 30 (PNL-12)

DIMENSIONS OF EXPERIMENTAL VESSEL:

Inside Radius of Sphere	193.18 ± 0.16mm
Vessel Wall Thickness	1.22mm

DELAYED CRITICAL CONFIGURATION:

Unreflected Assembly

None

Water Reflected Assembly[d)]

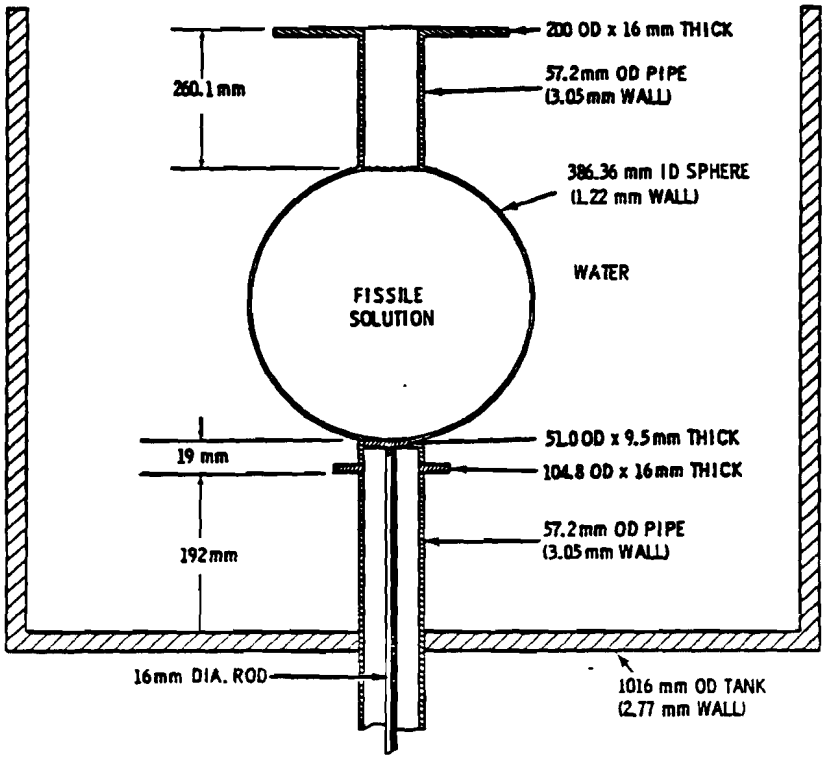

Reflector and core temperature, K	296 ± 2
Room temperature, K	294 ± 2

d) The vessel neck and the support column increase the critical volume by ~0.4% (Reference: R.C. Lloyd, et al., "Criticality Studies with Plutonium Solutions," NS&E 25, 171 (1966)

Benchmark No. 30 (PNL-12)

1) PNL-12A

Spherical Model. Atomic number densities as shown on page T(24-30)-22.

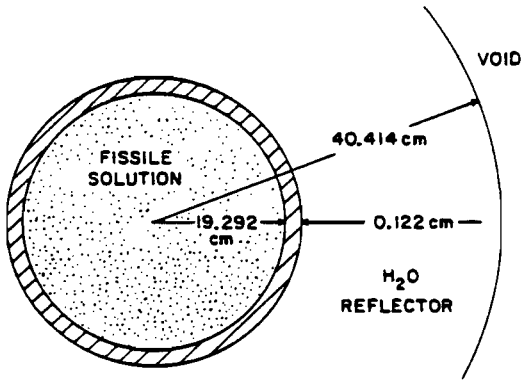

Benchmark No. 30 (PNL-12)

2) PNL-12B

Monte Carlo Model. Atomic number densities as shown on page T(24-30)-22.

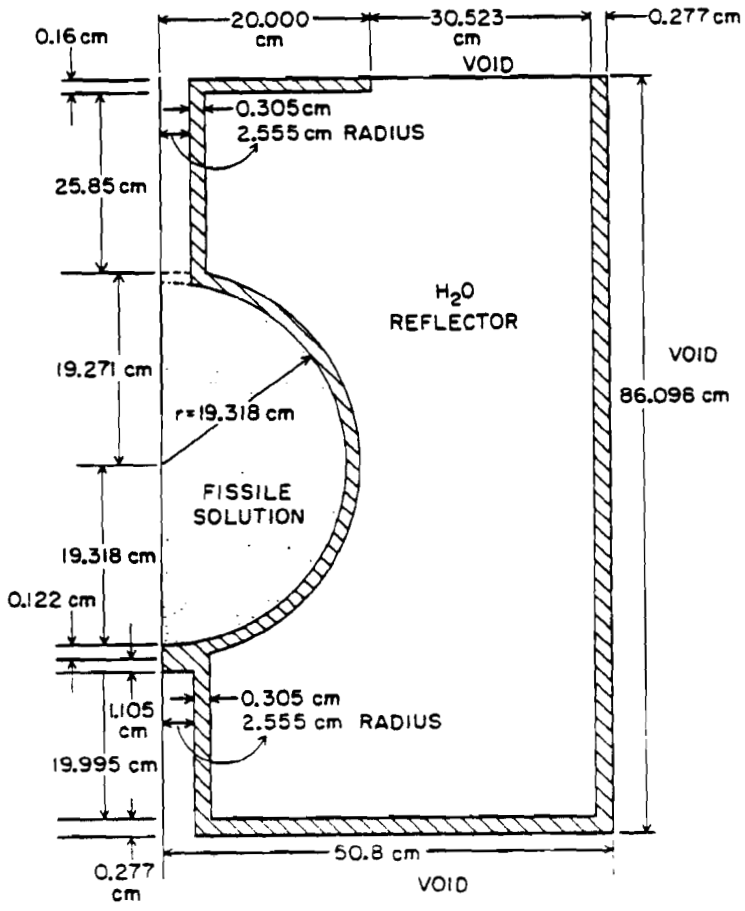

THERMAL REACTOR BENCHMARKS NOS. 31-36

(PNL-30 through PNL-35)

A. Benchmark Name and Type

PNL-30 through 35, H_2O moderated Mixed Oxide Lattices.

B. System Description

These experiments consist of H_2O moderated lattices fueled by compacted particles of UO_2 -2wt% PuO_2. The plutonium contained 8% Pu-240. The fuel rods (O.D. 1.4352cm) were clad in zircalloy and arranged in a square lattice. Critical configurations were determined for three lattice spacings, with borated and unborated moderator. Very little additional experimental data is available.

C. Model Description

A simple model (infinite square lattice cell) is defined for methods comparison purposes. In addition, a full core model is defined for calculation of k_{eff}.

1. Simple Model

An infinite square cell lattice calculation with reflecting boundary conditions is the preferred model. Alternatively a cylindrical cell can be calculated with white boundary conditions. Tables 1 and 2 give the specifications for PNL-30 through 35.

Suggested method of calculation:

Integral transport theory, Monte Carlo, or Multigroup Sn with special treatment of resonance region.

Table 1

Physical Properties of Lattice Cell

Region	Outer Radius (cm)	Isotope	Concentration 10^{24} atoms/cm^3
Fuel	.6414	^{239}Pu	3.974×10^{-4}
		^{240}Pu	3.344×10^{-5}
		^{241}Pu	1.60×10^{-6}
		^{242}Pu	1.20×10^{-7}
		^{235}U	1.504×10^{-4}
		^{238}U	2.073×10^{-2}
		O	4.401×10^{-2}
Clad	.7176	Zr	4.226×10^{-2}
Moderator	*	H	6.671×10^{-2}
		O	3.336×10^{-2}
		^{10}B	see Table 2

*Square lattices with a pitch of 1.77800, 2.20914, and 2.51447cm respectively.

T(31-36)-3

Table 2

Lattice Parameters

Lattice	Designation EPRI-196	Moderator Temperature °C	Critical No. of Rods	Lattice Spacing (cm)	Equivalent Cell Radius (cm)	^{10}B Concentration (10^{24} atoms/cm^3)	Experimental k_{excess}	Δk_{eff} for PuO_2 Particle Effects
30	U-L266	21	469	1.77800	1.00313	1.873-08	0.00017	0.0
31	U-L250	22	761	1.77800	1.00313	7.504-06	0.00006	0.0
32	U-L189	23	195	2.20914	1.24637	9.916-09	0.00028	-0.0018
33	U-L212	23	761	2.20914	1.24637	1.202-05	0.00023	-0.0018
34	U-L282	22	161	2.51447	1.41864	1.763-08	0.00077	-0.0025
35	U-L232	23	689	2.51447	1.41864	8.455-06	0.00013	0.0025

2. Full Core Model

Figure 1 shows the axial model for these lattices. They are fully reflected by water ($\geq$20cm) on the sides and bottom. The top reflector is 15.24 cm thick for assemblies 30, 31, 33, and 35. It is 5.72 cm thick for assembly 32 and 2.29 cm thick for assembly 32 and 2.29cm thick for assembly 34. Figures 2-4 show radial quarter-core representations for five of the six lattices. PNL-33 (0.87 inch pitch) has the same geometric configuration as PNL-31 (0.70 inch pitch). These cores may be represented by 1/8 core symmetry. Figure 5 shows the full core representation for PNL-32, which does not have core symmetry.

Additional atomic number densities for the full core model are given in Tables 3 and 4.

Corrections to calculated k_{eff} (Table 2) shall be used to account for PuO_2 particle effects not specified in the calculational model. These cores were slightly supercritical for the configurations specified. Experimental values of excess multiplication are given in Table 2.

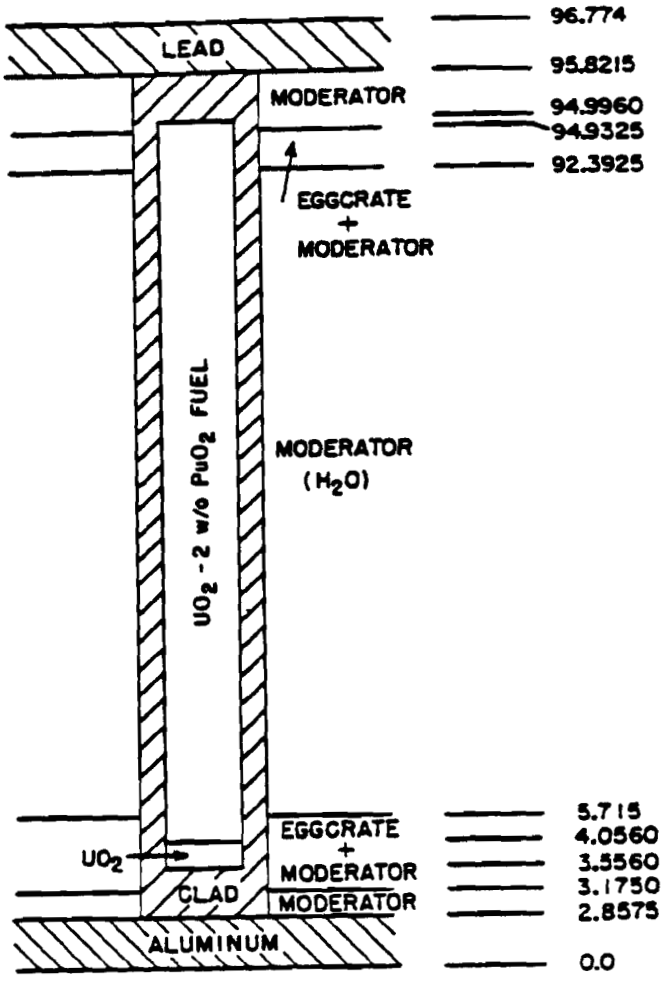

AXIAL REPRESENTATION OF PNL ASSEMBLIES
DIMENSIONS IN CENTIMETERS

Fig. 1 Axial Model

Table 3

Atomic Number Densities for Homogenized "Egg Crate" Structure plus H_2O* (see Fig. 1)

Assembly	Concentration 10^{24} atoms/cm^3			
	H	O	Al	^{10}B
PNL-30	.02226	.01114	.04014	6.255-09
PNL-31	.02226	.01114	.04014	2.506-06
PNL-32	.05660	.02830	.009137	8.417-09
PNL-33	.05660	.02830	.009137	1.020-05
PNL-34	.03755	.01878	.02634	9.924-09
PNL-35	.03755	.01878	.02634	4.760-06

*For the purpose of benchmark calculations the egg crate structure is terminated at the core boundary.

Table 4

Additional Atomic Number Densities for the Full-Core Model

UO_2 at bottom of Fuel Rod	Concentration 10^{24} atoms/cm^3
^{234}U	1.150×10^{-6}
^{235}U	1.532×10^{-4}
^{238}U	2.1123×10^{-2}
O	4.2555×10^{-2}
Al Plate	
Al	6.027×10^{-2}
Pb Shield	
Pb	3.2961×10^{-2}

PNL-34 (U-L282) 0.99 INCH PITCH
QUARTER-CORE RADIAL SLICE

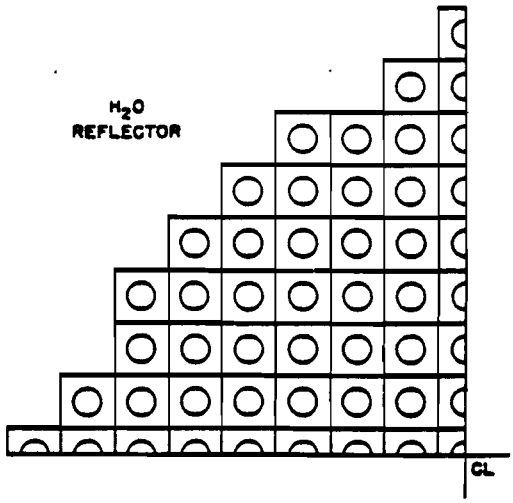

PNL-30 (U-L266) 0.70 INCH PITCH
QUARTER-CORE RADIAL SLICE

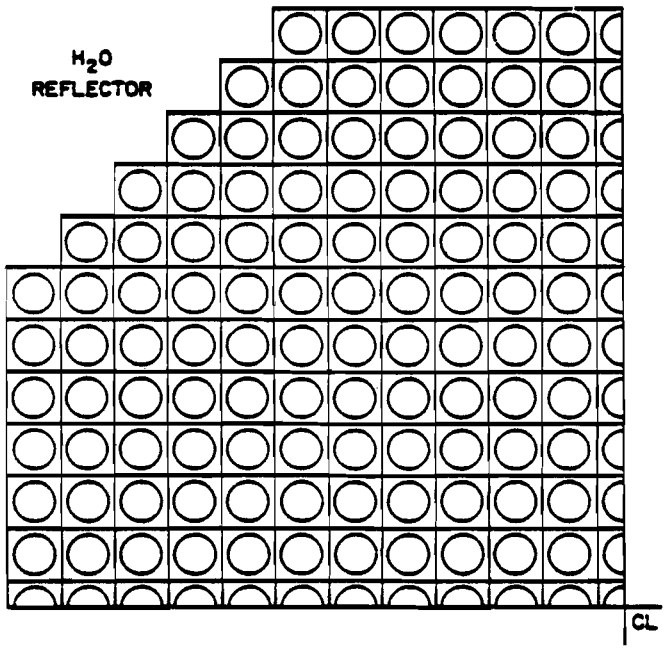

Fig. 2 PNL-30 and PNL-34

PNL-31 (U-L250) 0.70 INCH PITCH
QUARTER-CORE RADIAL SLICE

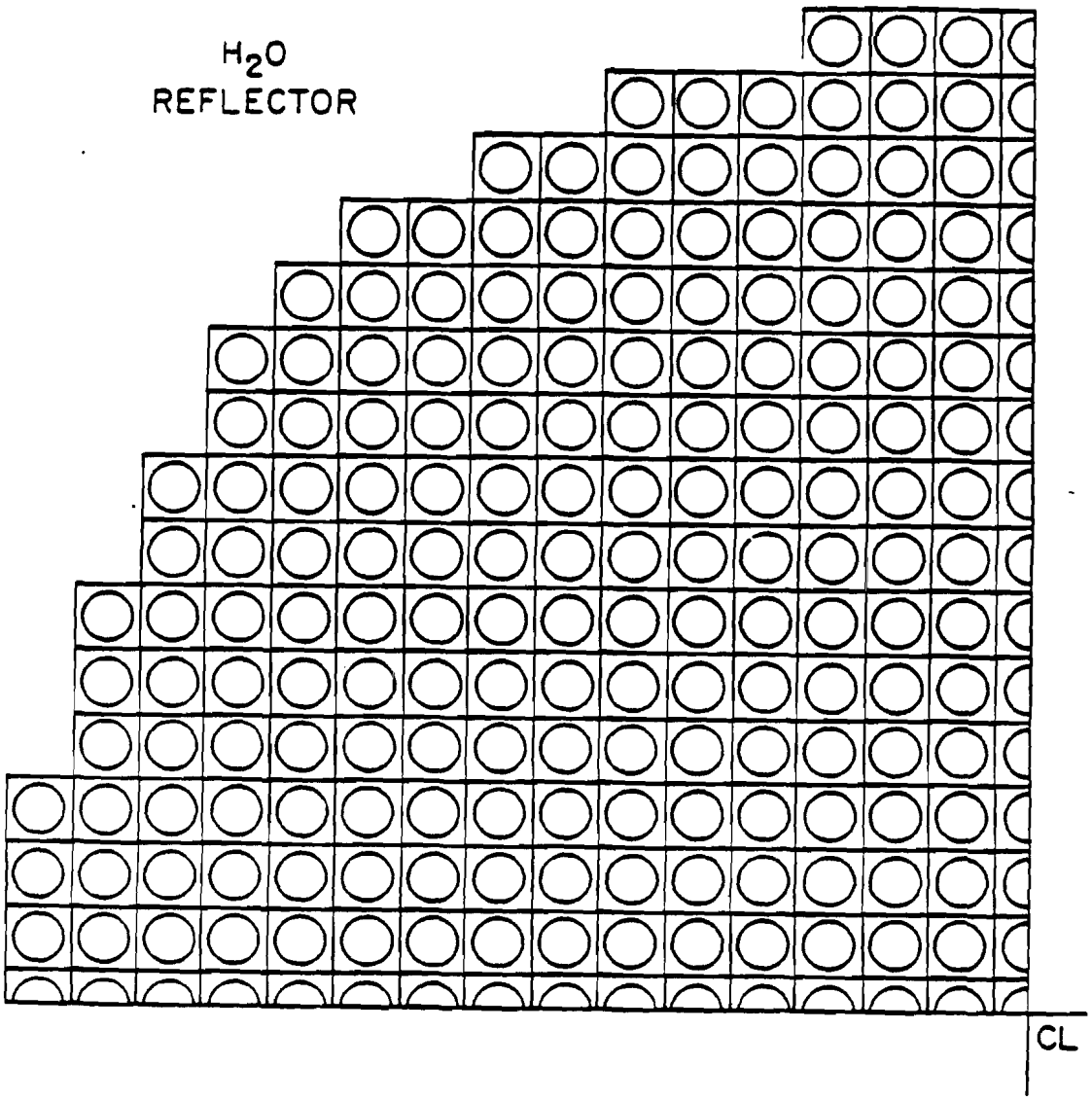

Fig. 3 PNL-31

PNL-35 (U-L232) 0.99 INCH PITCH
QUARTER-CORE RADIAL SLICE

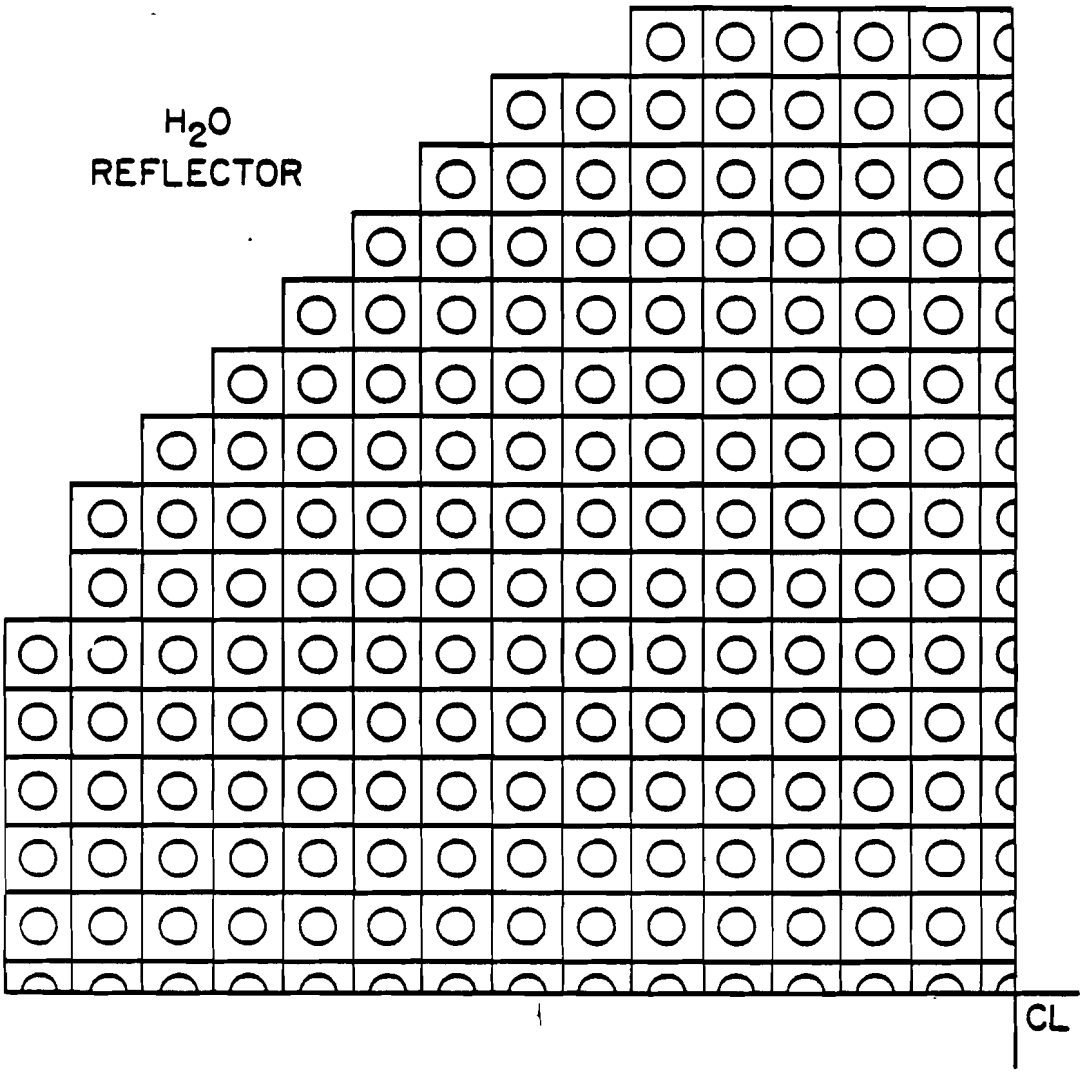

Fig. 4 PNL-35

PNL-32 (U-L189) 0.87 INCH PITCH
FULL — CORE RADIAL SLICE

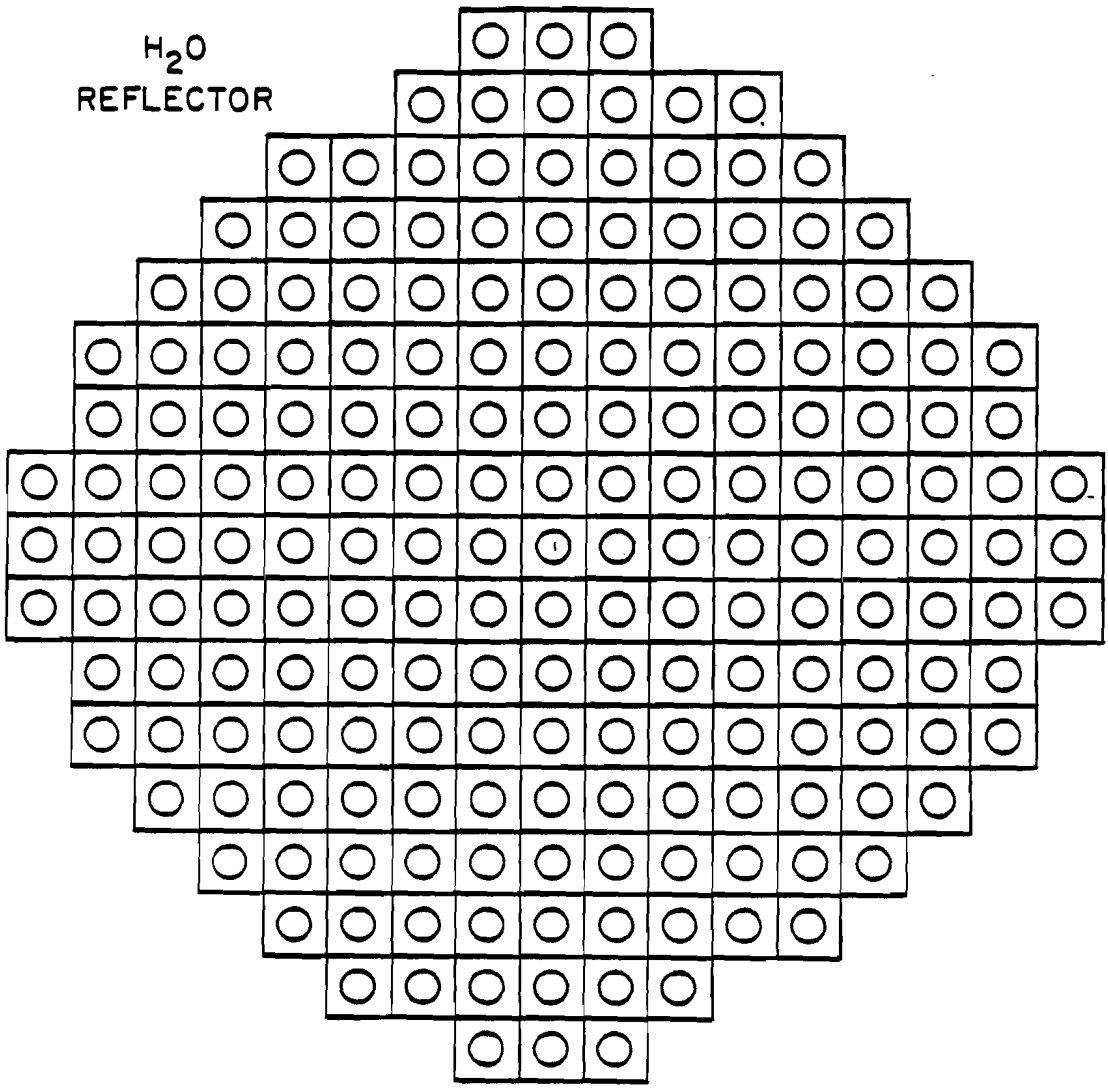

Fig. 5 PNL-32

D. Data to Report

In addition to k_{∞} and k_{eff} the following quantities should be reported:

1. Isotopic reaction rates in the following four groups for the lattice cell and the full core.

Group	E_{upper}	E_{lower}
1	10 MeV	821 keV
2	821 keV	5.53 keV
3	5.53 keV	0.625 eV
4	0.625 eV	0.00001 eV

These rates should be normalized to one neutron born of all fission.

2. Disadvantage factors $[\bar{\phi}_{fuel}/\bar{\phi}_{moderator}]$ for both the lattice cell and the full core by energy group.

3. Infinite cell or core average microscopic isotopic cross sections in four groups. These are derived from the appropriate reaction rates and fluxes (Items 1 and 2).

4. Infinite Cell Lattice Parameter

ρ_{28} = Epithermal to thermal U-238 capture rate
δ_{25} = Epithermal to thermal U-235 fission rate
δ_{28} = U-238 fission rate to U-235 fission rate
CR = U-238 capture rate to U-235 fission rate
δ_{49} = Epithermal to thermal Pu-239 fission rate
ε_{25} = U-235 fission rate to Pu-239 fission rate

References

1. U.P. Jenquin and S.R. Bierman, "Benchmark Experiments to Test Plutonium and Stainless-Steel Cross Section," NUREG/CR-0210, PNL-2273, June 1978.

2. R.I. Smith and G.J. Konzek, "Clean Critical Experiment Benchmarks for Plutonium Recycle in LWR's," EPRI-NP-196, Vol. 1, April 1976.

3. R.C. Liikala, V.O. Uotinen, and U.P. Jenquin, Nucl. Tech. 15, 272, August 1972.

4. R.Scher and S. Fiarman, "Analysis of some Uranium Oxide and Mixed-Oxide Lattice Measurements," EPRI NP-691, Feb. 1978.